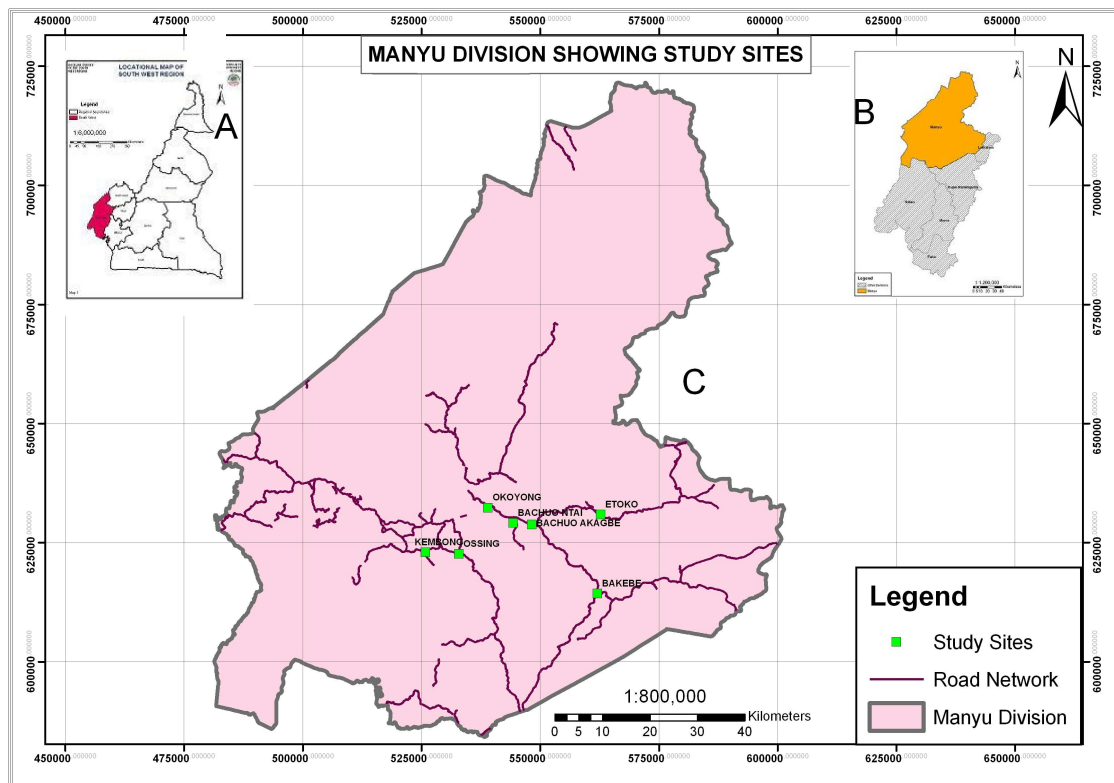


# Applied Ecology and Environmental Research

International Scientific Journal



VOLUME 9 \* NUMBER 4 \* 2011

## LEAF-WATER RELATIONS OF A NATIVE AND AN INTRODUCED GRASS SPECIES IN THE MIXED-GRASS PRAIRIE UNDER CATTLE GRAZING

DONG, X.<sup>1\*</sup> – PATTON, B.<sup>1</sup> – NYREN, P.<sup>1</sup> – LIMB, R.<sup>2</sup> – CIHACEK, L.<sup>3</sup> – KIRBY, D.<sup>4</sup> – DECKARD, E.<sup>5</sup>

<sup>1</sup>*Institution North Dakota State University, Central Grasslands Research Extension Center, Streeter, ND 58483 USA*

<sup>2</sup>*North Dakota State University, Department of Animal and Range Science, Fargo, ND 58108 USA; Present address: Oregon State University, Department of Rangeland Ecology & Management, La Grande, Oregon 97850, USA*

<sup>3</sup>*North Dakota State University, Department of Soil Science, Fargo, ND 58108 USA*

<sup>4</sup>*North Dakota State University, Department of Animal and Range Science, Fargo, ND 58108 USA; Present address: North Dakota State University, School of Natural Resource Sciences, Fargo, ND 58108 USA*

<sup>5</sup>*North Dakota State University, Department of Plant Science, Fargo, ND 58108 USA*

*\*Corresponding author  
e-mail: xuejun.dong@ndsu.edu*

(Received 8<sup>th</sup> November 2011; accepted 2<sup>nd</sup> December 2011)

**Abstract.** Both the native *Pascopyrum smithii* and introduced *Poa pratensis* are dominant plants in the mixed-grass prairie. Knowledge of leaf-water relations and water use strategies in these two grasses under animal grazing and drought is needed for understanding responses of the prairie to future climate change. We studied leaf-water relations traits of *Pascopyrum* and *Poa* by combined use of information from the pressure-volume analysis, leaf structural characteristics and leaf stomatal conductance as a function of leaf water status. Fieldwork was done in three grazed pastures and three exclosures in 2002 and 2003. With growing season drought, available soil water became lower in the grazed pastures than in the non-grazing exclosures. This had a more negative impact on leaf water status of the shallow-rooted *Poa* than the deep-rooted *Pascopyrum*. In both grasses, a significant decrease in leaf stomatal conductance occurred near the turgor loss water potentials of -2.42 MPa for *Poa* and -3.5 MPa for *Pascopyrum*, respectively. Both *Poa* and *Pascopyrum* responded to grazing with more negative osmotic potentials (and thus more concentrated cell solution) in months of peak growth. Specific leaf area and its two components, i.e., leaf density and thickness, had minimum responses to grazing for *Pascopyrum*, while in *Poa*, less dense leaves accompanied by a higher specific leaf area was observed, suggesting that long-term grazing encourages a higher potential growth rate but also a higher susceptibility to drought stress in *Poa* than in *Pascopyrum*.

**Keywords:** leaf density, leaf osmotic potential, *Pascopyrum smithii*, *Poa pratensis*, specific leaf area

### Introduction

In the Great Plains of North America, widespread dispersal of introduced plants, such as *Poa pratensis* L. and *Bromus inermis* (Rydb.) A. Love, alter plant community structure (Murphy and Grant, 2005) and challenge grassland management (DeKeyser et al., 2010). On grasslands, one major task is to understand plant water-relations and water use strategies constrained by grazing and drought (Svejcar and Christiansen, 1987a; Wraith et al., 1987; Heitschmidt et al., 1999). However, even the question of

whether animal grazing actually can alter plant water status on grasslands is still not fully answered. Although many studies had showed a positive effect of grazing on water status of the remaining plants (Archer and Detling, 1986; Svejcar and Christiansen, 1987a, 1987b; Day and Detling, 1994; Bremer et al., 2001), factors such as developmental stage of the same species, genetic differences between species (Mohammad et al., 1982; Frank, 1994), variations in rooting depths (Wraith et al., 1987; Fahnestock and Knapp, 1993; Jefferson and Cutforth, 2005), as well as grazing intensity (Fahnestock and Detling, 2000), all can influence the observed plant water status under field conditions. Under certain situations, conserved soil moisture due to the removal of green leaves by heavy grazing cannot compensate for the increased soil evaporation and/or run-off due to grazing induced bare-soil exposure (Patton and Nyren, 1998). This dictates the need for additional site- and context-specific study of leaf-water relations of grassland plants.

The specific strategies in leaf-water relations that plants employ to cope with varied biotic and abiotic stresses can be inferred (a) from the pressure-volume (PV) analysis (Turner, 1981); (b) from measuring specific leaf area (SLA) and its components: leaf density and leaf thickness (Witkowski and Lamont, 1991; Niinemets, 2001; Mojzes et al., 2003); and (c) from the relationship between leaf stomatal conductance ( $g_s$ ) and leaf water potential ( $\psi$ ) (Bittman and Simpson, 1989). While the PV traits for assaying leaf-water relations is widely used (Monson and Smith, 1982; Sinclair and Venables, 1983; Schulte and Hinckley, 1985; Parker and Colombo, 1995; Dong and Zhang, 2001; Lenz et al., 2006), the use of SLA and its two components primarily for assaying leaf-water relations is relatively less emphasized (Maxwell and Redmann, 1978; Rascio et al., 1990; Krasser and Kalapos, 2000; Niinemets, 2001). As leaf density correlates tightly with leaf elastic modulus governing leaf turgidity response to dehydration across a broad range of plants (Niinemets, 2001), its value for indicating overall cell wall rigidity, a major component dictating leaf-water relations, is apparent. Actually, SLA itself carries information of plant water status (Garnier et al., 2001; Roderick, 2001). Furthermore, the fact that the other component of SLA (leaf thickness) scales well with light (Chabot and Chabot, 1977; Nobel and Hartsock, 1981; Witkowski and Lamont, 1991) and leaf "liquid content" (Roderick et al., 2000) provides a linkage from leaf water status to photosynthetic light capturing. These two ways of characterizing leaf-water relations, namely, the PV-based and the leaf structure-based, can be used together to enable a better interpretation of the roles played by eco-physiological traits in site- and context-specific studies determining plant resource use (Smith and Knapp, 2001) and drought adaptations (Krasser and Kalapos, 2000).

We used both the PV-based and SLA-based traits to study leaf-water relations of a native grass *Pascopyrum smithii* and an introduced grass *Poa pratensis* in a mixed-grass prairie (Lura et al., 1988; Biondini et al., 1998; Patton and Nyren, 1998). Dominant in this mixed-grass prairie (Patton et al., 2007), *Pascopyrum* is excellent forage grass and fully adapted to grazing and drought (Coupland and Johnson, 1965). *Poa*, an introduced grass responding to high water/nutrient supply and frequent cutting (Jiang and Huang, 2001a), also dominates on mixed-prairies (Murphy and Grant, 2005; DeKeyser et al., 2010). The rooting depth of *Pascopyrum* may reach 2 m or deeper into soil profile (Weaver, 1926; Coupland and Johnson, 1965), while for *Poa*, roots may reach down to 40-45 cm (Gist and Smith, 1948; Peterson et al., 1979; Jiang and Huang, 2001b). These contrasts in rooting depth may depict differences in plants' access to soil moisture (Stewart et al., 2004), as well as in leaf-water relations traits (Krasser and

Kalapos, 2000). On the other hand, grazing may not only reduce plant rooting depth (Mohammad et al., 1982; Wraith et al., 1987; Rogers et al., 2005), it also encourages the development of “less expensive” leaves (Niinemets, 2001) that are thinner, less dense, but potentially more prone to drought stress (Díaz et al., 2001; Cingolani et al., 2007; Rotundo and Aguiar, 2008). Moreover, leaf structural traits of grassland plants may also exhibit a seasonal variation (Mojzes et al., 2003). Finally, while leaf  $g_s$  has been shown to decrease with the decrease of leaf  $\psi$  (Jarvis, 1976; Bittman and Simpson, 1989), and the relationship was described to be either linear (Kim and Verma, 1991) or non-linear (Abril and Hanano, 1998), the lack of relevant data on *Pascopyrum* and *Poa* limits our ability to predict the leaf gas exchange characteristics of these two species under varied water supply on the prairie.

Based on above considerations, we asked the following research questions and used relevant field data and analysis to address them. (a) Is soil water conserved under grazing compared with non-grazing control in this mixed-grass prairie? (b) What are the intrinsic differences in leaf-water relations traits between *Poa* and *Pascopyrum* growing in the mixed-grass prairie? (c) How does cattle grazing influence the leaf-water relations traits of these two species and what are the potential impacts of these influences, if any, on the performance of *Poa* and *Pascopyrum* in a changed climate?

## Materials and methods

### Site description

The study site has a continental type climate with an average Jan. temperature of  $-17^{\circ}\text{C}$  and Aug. temperature of  $20^{\circ}\text{C}$ . Mean annual precipitation is 458 mm with about 70% occurring during May to Sep. Elevation is about 587 m.

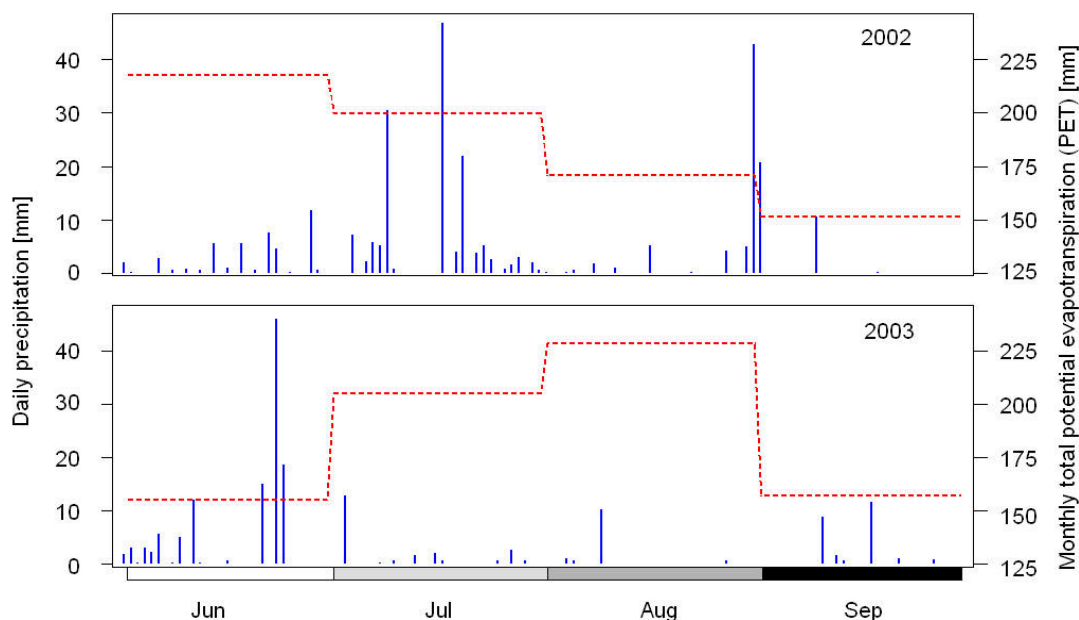


**Figure 1.** Daily precipitation (solid lines) and monthly total potential evapotranspiration (PET, dotted lines, from <http://ndawn.ndsu.nodak.edu>) at the Central Grasslands Research Extension Center (CGREC), Streeter, ND, from Jun. to Sep. in 2002 and 2003

The vegetation is dominated by grasses, with forbs contributing 20% and shrubs 2% of the peak standing crop (Lura et al, 1988). The dominant grasses include *Poa pratensis* L., *Bromus inermis* Leyss. and *Pascopyrum smithii* (Rydb.) A. Love; dominant forbs include *Aster ericoides* L., *Oligoneuron rigidum* [L.] Small var. *humile* [Porter] Nesom, *Artemisia ludoviciana* Nutt., and *Achillea millefolium* L., and the dominant shrub is *Symphoricarpos occidentalis* Hook. Field measurements were conducted in 2002 and 2003 on 3 non-grazing exclosures, the size of which ranges from 1050 to 2020 m<sup>2</sup>, and 3 grazed pastures, each about 13 ha in size and stocked at 6.8 AUM (animal unit month) ha<sup>-1</sup> since 1988 within a long-term grazing intensity study trial (Patton et al., 2007). An animal unit (AU) is defined as one mature 454 kg cow with calf or its equivalence based on an average forage consumption of 12 kg of dry matter per day. Cattle were removed from pastures when approximately 850 kg ha<sup>-1</sup> of forage remained at the end of the grazing season. Both growing seasons in 2002 and 2003 experienced drought with uneven distribution of precipitation (Fig. 1).

### ***Leaf water potential and soil water content***

Leaf  $\psi$  of *Pascopyrum* and *Poa* was measured in the early morning (one hour after sunrise) using a pressure chamber (PMS Instrument Co. Model-1000, Corvallis, Oregon USA). The distance between pastures prevented us from measuring leaf  $\psi$  from all the six pastures/exclosures that were used in SLA measurement (see below). Instead, we selected a representative exclosure and a grazed pasture for field sampling. The measurements were made 3-5 times from mid-Jun. to mid-Sep. with a replication of 6 leaves for each species-treatment combination. For each measurement period, we were not able to make the measurements at different locations within on one morning but within 3 adjacent mornings without rain interruption. Soil water content was measured once every two weeks from Jun. to Sep. using a neutron probe (Troxler 4300 Depth Moisture Gauge, Research Triangle Park, NC USA). One access tube was installed at a typical silty location (Patton et al. 2007) in each of the six pastures/exclosures. The data were converted into available water (cm of water) to the depths of 0-23 cm and 0-83 cm by subtracting soil water content at -1.5 MPa (permanent wilting point) from total soil water content for a particular soil depth. The purpose of choosing these two depth intervals is to roughly represent shallow and deep soil water reserves available to plants (Dong et al., 2010), although some roots may reach much deeper into the soil profile (Weaver, 1958; Coupland and Johnson, 1965).

### ***Leaf water potential and soil water content***

In 2002, leaf samples of *Pascopyrum* and *Poa* were collected in three grazed pastures and three exclosures. The samples were collected in four time periods, i.e., May 17-24, Jun. 17 to Jul. 8 (Jun-Jul), Aug. 1-17, and Sep. 24 to Oct. 2 (Sep) on non-rainy days. On each sampling day, leaves of the two species each were collected twice, i.e., ca. 1-2 hr. after sunrise and ca. 2-3 hr. after noon, each with 3 batches (one batch contained ca. 50-60 leaves). By sampling twice a day, we hoped to obtain specific leaf area (SLA) measurements that roughly represented diurnal average values (Garnier et al., 2001). Once severed from the plant, leaves were sealed in plastic bags, stored in a chilled cooler and transported to the laboratory in ca. 20 min. for further processing. Both senescent and immature leaves were avoided. In each of the locations (2 grazing levels

× 3 sites = 6 locations), leaf samples were obtained randomly from within an area ca. 10-15m away from a permanent soil access tube for measuring soil water (see above).

Each batch of leaves was used to measure leaf volume, leaf area and leaf dry mass. Leaf volume was measured by displacement of water in a cylinder (precision 0.05 cm<sup>3</sup>). The relative error for the volume measurement for ca. 1 g leaves (fresh mass) was estimated to be ca. 5%. To measure leaf area, leaves were laid flat (unfolding *Poa* leaves if necessary) on transparent contact paper. The image was scanned into the computer and total leaf area was calculated using image processing software SigmaScan Pro 5.0 (SPSS Inc. Chicago, IL USA). Then, leaves were removed from the contact paper and oven-dried to measure dry mass. Leaf density was calculated as leaf dry mass per unit leaf volume; leaf thickness was calculated by dividing leaf volume by leaf area, and specific leaf area (SLA) was calculated from leaf area divided by leaf dry mass.

### ***Leaf pressure-volume curves***

Due to the time-consuming nature of constructing leaf pressure-volume (PV) curves, only one grazed pasture and one enclosure were used to collect leaves of the two species (*Pascopyrum* and *Poa*) in 2003. The criteria for leaf selection were the same as that in the SLA measurement. Leaf samples from both locations were collected three times: Jun. 22 to Jul. 7 (Jun-Jul); Jul. 28 to Aug. 1 (Jul-Aug); and Sep. 6-8 (Sep). In the Jun-Jul sampling, 30 leaves of each grass species were collected from each of the two locations. In the Jul-Aug sampling, 60 leaves of each of the two species were available to be sampled; in the Sep sampling, 60 leaves of only *Pascopyrum* were collected (*Poa* leaves were not available). The leaf samples were collected in the morning from 0900 h to 1130 h local time, placed in plastic bags, stored in a chilled cooler and promptly transferred to the laboratory for further processing. In each sampling day, leaves of only one plant species from a particular location (enclosure or grazed site) were collected. About 2/3 of the leaves were subjected to saturation treatment following the procedure of Garnier et al (2001). The remaining leaves were used directly for generating a portion (and usually the drier portion) of the PV curve, using the “composite” method of Parker and Colombo (1995), in which many leaves were used to construct a single PV curve. The water-saturated leaves were placed on a bench for different time durations, allowing water loss through transpiration, and paired water potential ( $\psi$ ) and water content measurements were made according to Turner (1981). Leaf  $\psi$  was measured with a pressure chamber as described above and water content was obtained by measuring fresh and dry mass of leaves to the nearest ten thousandth of a gram. One composite PV curve (with 30 to 60 data points each) was generated for each treatment/species combination in each of the measurement periods (Jun-Jul, Jul-Aug or Sep).

### ***Leaf stomatal conductance in field conditions***

Leaf stomatal conductance ( $g_s$ ) and  $\psi$  for both *Pascopyrum* and *Poa* were measured in the field. In 2002,  $g_s$  was measured using a LI-COR 6200 Portable Photosynthesis System (LI-COR Inc., Lincoln, Nebraska USA) on six selected days (Jul. 3, Jul. 5, Aug. 27 and Sep. 4-6) in an enclosure and two grazed pastures. The days were mostly clear with the actual photosynthetically active radiation (PAR) ranging from 1030 to 1839  $\mu\text{mol photon m}^{-2}\text{s}^{-1}$ , air temperature from 28.9 to 39.6 °C, and relative humidity from 25.6 to 64.1 % for all the measurements recorded. The measurements were made once

every two hours from about 1100 h to 1800 h local time with each measurement made on four different leaves. Meanwhile, leaf  $\psi$  was measured using a pressure chamber (same as described above) on six leaves each day from about 1200 h to 1400 h local time, except in Sep. 4-6, the measurements were made once every two hours immediately following  $g_s$  measurement. In 2003,  $g_s$  was measured using a LI-COR 6400 Portable Photosynthesis System (LI-COR Inc., Lincoln, Nebraska USA) on 12 selected days (Jun. 16-19, Jul. 17, Jul. 21-23, Aug. 21-22 and Aug. 25-26) in an enclosure and two grazed pastures. The  $g_s$  measurement was made once an hour, or once every two hours, from about 1100 h to 1800 h local time. Each measurement was made under a fixed PAR of 2000  $\mu\text{mol photon m}^{-2}\text{s}^{-1}$ . Depending on ambient PAR that the leaves had been experiencing prior to the measurement, about 15-40 min was needed in order to let stomata fully acclimate to this high light condition. The leaf  $\psi$  measurement was made on six leaves using a pressure chamber each day from about 1200 h to 1400 h local time.

### **Statistical data analysis**

#### *Specific leaf area (SLA) in relation to grazing and season*

The averaged values of SLA, leaf thickness and leaf density for leaves collected from one pasture in a particular sampling period was considered as one sample. So, there were 3 replications for each grazing level in each sampling period ( $n = 3$ ). In Sep. 2002, samples for *Poa* were available from only 3 of the 6 sampling locations. These data were excluded from the statistical analysis. So the data for *Poa* presented here cover the periods of May, Jun-Jul and Aug, while the data for *Pascopyrum* cover the periods of Jun-Jul, Aug, and Sep. The ANOVA procedure of the General Linear Model (GLM) was used for the data analysis with three leaf properties, namely, SLA, leaf density and leaf thickness, considered as dependent variables, and sampling time (month) and grazing intensity as fixed factors crossed with each other. The three dependent variables were checked for normality in distribution, and leaf thickness was transformed to its natural logarithm. Post hoc comparisons of specific combinations of treatments were performed using the Tukey method with the convention of ( $P < 0.05$ ) in MINITAB 13.39 (Minitab Inc, State College, PA, USA).

#### *Specific leaf area (SLA) correlated with leaf density and leaf thickness*

We conducted correlation analysis between SLA and its two components (leaf thickness and leaf density) by pooling the original measurements from different pastures/locations and different sampling periods within a common grazing ( $n = 54$ ). The analysis was done using both the Pearson correlation procedure in MINITAB and permutation resampling according to Hesterberg et al. (2006). For the resampling analysis, the null hypothesis was: the observed correlation coefficient ( $r$ ) was purely due to spurious source and there was no causal mechanism between the two variables. The alternative hypothesis was: there existed a causal mechanism between the two variables because the observed correlation coefficient could not occur purely by chance. Using this program, we drew 2000 resamples from the measured original data (of SLA, leaf thickness and leaf density) and obtained the median of the simulated  $r$  values for the null model ( $r_0$ ), the 95% confidence interval (C.I.) for the simulated  $r$ , as well as the  $p$ -

value that the observed  $r$  occurred purely by chance. The computer simulations were conducted separately for *Pascopyrum* and *Poa* under different grazing treatments.

#### Fitting the pressure-volume curves

Because the regression analysis of the PV curves used relative water deficit ( $R_{wd}$ ) as the independent variable, measured water content data (leaf dry mass based) was converted to  $R_{wd}$  by the formula  $R_{wd} = (M_s - M_f)/(M_s - M_d)$ , where  $M_s$  is the saturated leaf mass,  $M_f$  the fresh leaf mass and  $M_d$  the oven-dried leaf mass. First, the whole data set was fitted using a single non-linear equation according to Sinclair and Venables (1983) and Schulte and Hinckley (1985):

$$\psi = \psi_{\pi,s} \left[ -e^{-aR_{wd}} + \frac{x}{x - R_{wd}} \right] \quad (\text{Eq.1})$$

where  $R_{wd}$  is the relative water deficit,  $\psi_{\pi,s}$  is the osmotic potential at full turgor,  $x$  the symplastic water fraction at full turgor and  $a$  is a constant influencing the change of pressure potential. Parameter  $x$  was not further analyzed because the estimated  $x$  values by the “composite” PV method tended to be too high to be physiologically meaningful (Parker and Colombo, 1995).

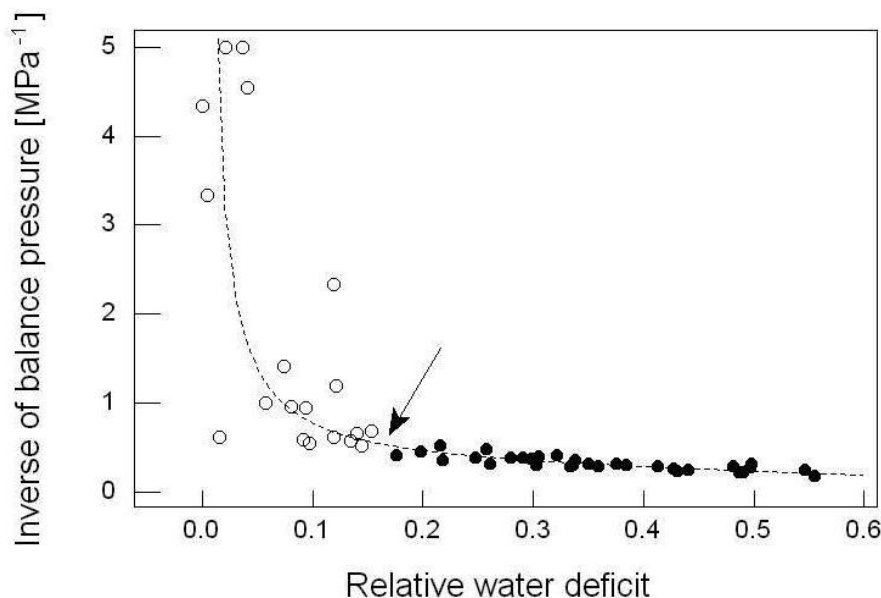


**Figure 2.** A sample pressure-volume curve for leaves of *Pascopyrum smithii* growing in an ungrazed exclosure, measured from Jul. 28 to Aug. 1, 2003. Each data point represents the measurement made on one leaf blade. First, the whole data set was fitted using a non-linear curve (dotted line). Then, by visual inspection, the data points belonging to the linear portion (solid circles) were located and fitted using a linear regression to obtain osmotic potential at full turgor (solid line). The waterpotentials at initial turgor loss point were estimated by systematically comparing the fitted linear and non-linear curves (see the main text)

By plotting the fitted Equation 1 as inverse of balance pressure ( $1/P$ ) against  $R_{wd}$  (Turner, 1981), the trend of the original data was described by a linear portion and a non-linear portion (Fig. 2). Using visual inspection, the transition point between the non-linear and the linear portions was located. Using data points from the linear portion,



a linear regression of inverse of  $P$  against  $R_{wd}$  was obtained for each PV curve according to Sinclair and Venables (1983):

$$1/P = -1/\psi_{\pi,s} + (1/\psi_{\pi,s}x)R_{wd} \quad (\text{Eq.2})$$

where all symbols are the same as in Equation 1. The recipe of linear regression analysis from Zar (1984) was used to calculate the 95% confidence intervals for the Y-intercepts of the linear part of the PV curves (Fig. 2), which was then used to compute  $\psi_{\pi,s}$ . The osmotic potential at turgor loss point ( $\psi_{tlp}$ ) was estimated by comparing the nonlinear curve (Equation 1) and the linear curve (Equation 2). In particular, the whole range of the domain of Equations 1 and 3 (see Fig. 2) was sub-divided into 200 intervals. Then, starting from the lowest  $R_{wd}$  end and moving toward the high  $R_{wd}$  end, the two curves were compared systematically. When the relative difference first fell below a pre-set criteria of 5%, the comparison stopped and the corresponding  $\psi$  was regarded as  $\psi_{tlp}$ . Similar to  $\psi_{\pi,s}$ , the 95% C.I. for  $\psi_{tlp}$  was also established according to Zar (1984); using the data points from the linear part of the PV curve (solid circles in Fig. 2). Finally, the standard error was obtained from the 95% C.I. and the number of data points.

#### Leaf stomatal conductance in relation to leaf water potential

Grazing's effect on  $g_s$  was not compared because the measurements of  $g_s$  for pastures of different grazing treatments were made on different days in both the 2002 and 2003 growing seasons. Instead, the overall trends of  $g_s$  as a function of leaf  $\psi$  were analyzed separately for *Pascopyrum* and *Poa*. To aid the interpretation of species-specific  $g_s - \psi$  relationship, we also computed the overall distributions of the turgor loss points for the two species separately. For *Poa*, for example, we assumed that the estimated four means of the turgor loss points in Table 1 (for different grazing treatments across different sampling periods) were drawn from a common normal distribution of *Poa*'s

turgor loss point:  $f(\psi) = \frac{1}{\sigma\sqrt{2\pi}} e^{-\frac{(\psi-\bar{\psi})^2}{2\sigma^2}}$ , where the average of  $\psi$ ,  $\bar{\psi}$ , was estimated

as  $\bar{\psi} = \sum_{i=1}^4 m_i / 4$ , and the standard deviation  $\sigma$  was estimated as  $\sigma = \sqrt{18 \sum_{i=1}^4 s_i^2 / 4}$ . In the

above,  $m_i$  and  $s_i$  are mean and standard error, respectively, for each treatment-sampling period combination for *Poa* in Table 1, and the factor 18 is the average data points used.

**Table 1.** A comparison of the leaf water potentials (MPa) at the turgor loss point for plants growing in an enclosure and in a grazed pasture, as determined from the pressure-volume curves. Leaf samples were collected three times in the growing season of 2003: Jun. 22 to Jul. 7 (Jun-Jul), Jul. 28 to Aug. 1 (Jul-Aug), and Sep. 6-8 (Sep). The data are means with standard errors and number of data points in parentheses. Within a row, different lower-case letters indicate the existence of statistically significant difference between grazing treatments ( $p=0.05$ )

Species	Sampling period	Enclosure	Grazed
<i>Poa</i>	Jun-Jul	-1.98 <sup>a</sup> (0.10,6)	-3.19 <sup>b</sup> (0.10,9)
	Jul-Aug	-2.21 <sup>a</sup> (0.05,38)	-2.31 <sup>a</sup> (0.17,16)
<i>Pascopyrum</i>	Jun-Jul	-2.73 <sup>b</sup> (0.06,8)	-2.27 <sup>a</sup> (0.11,21)
	Jul-Aug	-2.73 <sup>a</sup> (0.10,25)	-4.39 <sup>b</sup> (0.16,11)
	Sep	-4.77 <sup>a</sup> (0.21,15)	-4.13 <sup>a</sup> (0.17,16)

## Results

### Leaf water potentials and available soil water

In 2002, despite several heavy rains occurring in Jul. (total 143.7 mm) and late Aug., the driest condition in soils for both the 0-23 cm and 0-83 cm depths occurred in mid- to late Jun. and mid-Aug. (Fig. 3E,G). Despite the drought, the early morning leaf  $\psi$  of *Pascopyrum* maintained relatively stable, with values seldom dropping below -3 MPa (Fig. 3C). However, leaf  $\psi$  differed between *Poa* plants growing in the enclosure and in the grazed pasture (Fig. 3A): leaf  $\psi$  in the enclosure seldom dropped below -2 MPa, but the values for *Poa* from the grazed pasture tended to be much lower, with the lowest value reaching -5.42 MPa on Aug. 24, 2002.

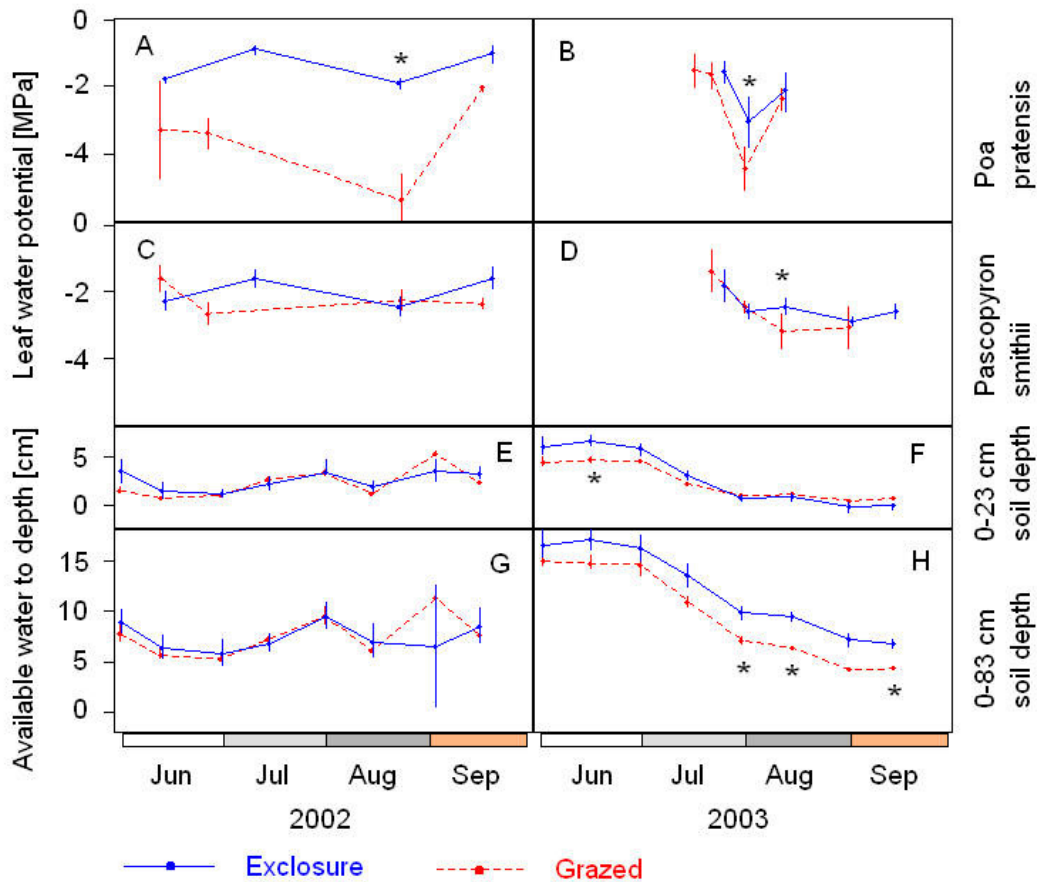


**Figure 3.** Leaf water potentials of *Poa pratensis* (A,B) and *Pascopyrum smithii* (C,D), as well as available soil water (E-H) in 2002 and 2003. The data of available soil water are for depths of 0-23 cm (E,F) and 0-83 cm (G,H). Vertical bars are 95% confidence intervals for leaf water potentials ( $n=5-6$ ) and standard errors for available soil water ( $n=3$ ). Cases of significant difference between grazing treatments ( $p<0.05$ ) are indicated with stars (for leaf water potentials, only the data in Aug. are compared)

As shown in Fig. 3F, H, the available soil water in Jun., 2003 started with high values for both the 0-23 cm and 0-83 cm depths, largely due to the above-average precipitation in May (data not shown) and Jun. However, with sharply reduced rainfall and increased potential evapotranspiration in Jul. (Fig. 1), soil water in both depths decreased rapidly. By early to mid-Aug., available soil water in the 0-23 cm depth had

decreased to minimum level for both the enclosure and the grazed pasture (Fig. 3F). Meanwhile, available soil water for the 0-83 cm depth dropped by 45% and 57% from the mid-Jun. values of 17.2 cm and 14.9 cm for the enclosure and grazed pasture, respectively. The larger percentage decline in available water in the grazed pasture resulted in lower available soil water in the grazed pasture than in the non-grazing enclosure in early to mid-Aug. (Fig. 3H). For *Poa*, the drought in early Aug. of 2003 resulted in a decreased leaf  $\psi$  for plants growing both in the enclosure and grazed pasture, with the average value in grazed pasture (-4.45 MPa) being significantly lower than that in the enclosure (-3.05 MPa), as measured on Aug. 1-2, 2003. For *Pascopyrum*, however, the overall decrease in leaf  $\psi$  was less in extent than in *Poa* on Aug. 1-2, and there was no significant difference associated with grazing. Following a 10.25 mm rainfall on Aug. 9, 2003, the *Pascopyrum*'s leaf  $\psi$  in the enclosure was slightly improved as measured on Aug. 12 (Fig. 3D), while the leaf  $\psi$  for *Pascopyrum* plants growing in the grazed pasture kept decreasing, resulting in a significantly lower  $\psi$  value (avg = -4.45 MPa) than the average value in the enclosure (-3.05 MPa). On the other hand, we can see that leaf  $\psi$  of *Poa* plants from both the enclosure and the grazed pasture improved following the Aug. 9 rain event (Fig. 3B).

#### ***Effects of grazing and season on specific leaf area and its two components***

For pooled data, there was no significant difference in leaf density between the two species (*t*-test Avg. = 0.31 g cm<sup>-3</sup>, df = 34, *p* = 0.98), while leaf thickness was significantly higher in *Pascopyrum* (avg. = 0.027 cm) than in *Poa* (avg. = 0.02 cm) (*p* < 0.001). As shown in Figs. 4 and 5, SLA was significantly lower in *Pascopyrum* (avg. = 128.4 cm<sup>2</sup>g<sup>-1</sup>) than in *Poa* (avg. = 173.5 cm<sup>2</sup>g<sup>-1</sup>) (*p* < 0.001).

#### ***Poa pratensis***

Both month and grazing had significant effects on SLA of *Poa* (*p* = 0.032 and *p* = 0.047, respectively). For the month factor, SLA did not change significantly from May to Jun-Jul (*p* = 0.41), but increased significantly from Jun-Jul to Aug. (*p* = 0.025). Overall, SLA was significantly higher under grazed than in enclosure (*p* = 0.048). However, this significance was mainly due to the marginally bigger contrasts in SLA between grazing treatments in Aug. (*p* = 0.094, see Fig. 4A). For leaf density of *Poa*, the factor of month had highly significant overall effect through the 2002 growing season (*p* < 0.0005), with a significant increase from May to Jun-Jul (*p* = 0.0007, Fig. 4B). The overall effect of grazing on leaf density was not significant (*p* = 0.128). For leaf thickness (Fig. 4C), the effect of month was again highly significant (*p* < 0.0005), with the average leaf thickness decreased from 0.023 cm in May to 0.019 cm in Jun-Jul (*p* = 0.002), and further decreased to 0.016 cm in Aug. (*p* = 0.018). Neither grazing (*p* = 0.43) nor the interaction of grazing and month (*p* = 0.61) had a significant effect.

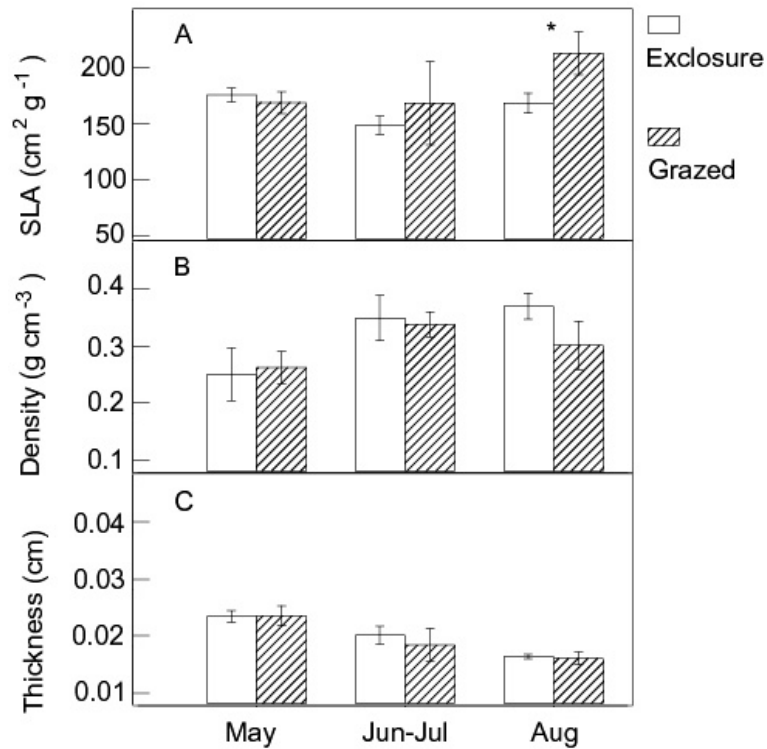


**Figure 4.** A comparison of three leaf properties (specific leaf area, leaf density and thickness) of *Poa pratensis* growing in ungrazed exclosures (white) and in grazed pastures (right slant) in different sampling periods from May to Aug., 2002. The data shown are the averaged values and standard deviations ( $n=3$ ). The symbol “\*” indicates marginal significant difference at  $p < 0.1$

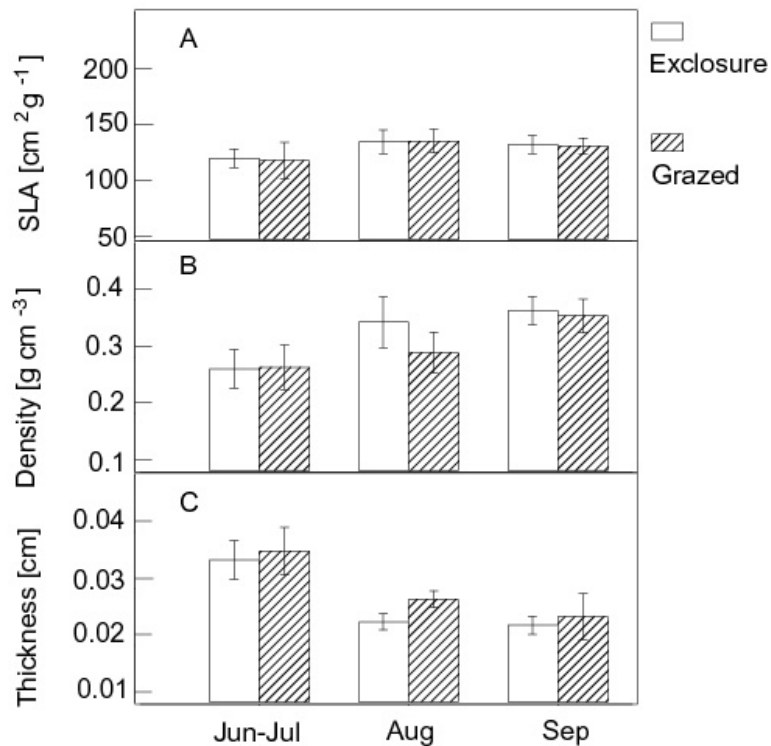


**Figure 5.** Same as in Figure 4, but with *Pascopyrum smithii*

*Pascopyrum smithii*

Month had a significant overall effect ( $p = 0.05$ ) on SLA of *Pascopyrum*, which resulted mainly from the significant increase in SLA from Jun-Jul to Aug. ( $p = 0.053$ , see Fig. 5A). However, neither grazing ( $p = 0.86$ ) nor the interaction of grazing and month ( $p=0.97$ ) had a significant effect, suggesting that in different sampling periods SLA had similar trends for different grazing treatments. Similar to SLA, leaf density of *Pascopyrum* was only significantly influenced by month ( $p = 0.002$ ), but not by grazing ( $p = 0.25$ ) or the interaction of grazing and month ( $p = 0.38$ , see Fig. 5B). Again similar to SLA, the significant overall month effect on leaf density resulted mainly from the significant increase in leaf density from Jun-Jul to Aug. ( $p = 0.05$ , see Fig. 5B). Leaf thickness of *Pascopyrum* was significantly influenced by month ( $p < 0.0005$ ).

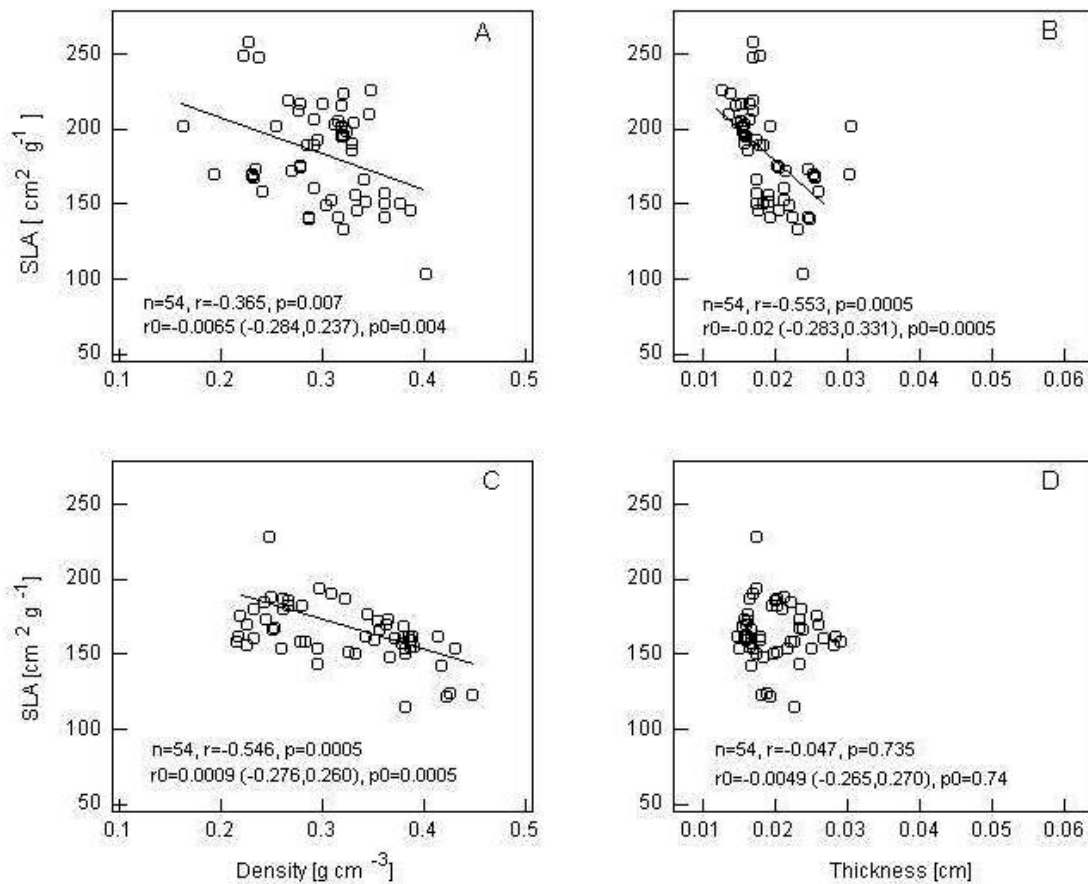


**Figure 6.** Correlations between specific leaf area (SLA) and leaf dry matter density and between SLA and leaf thickness for *Poa pratensis* plants growing in grazed pastures (A,B) and in ungrazed enclosures (C,D). Each data point represents the measurement made on a composite sample of 12-20 leaves. Shown in the figures are sample size ( $n$ ), the Pearson correlation coefficients ( $r$ ), and associated probabilities ( $p$ ). Also indicated are results from permutation resampling of the null model, including the medium values ( $r0$ ), the 95% confidence intervals of correlation coefficients of the null models, as well as the associated probabilities ( $p0$ )

### Correlations of specific leaf area with leaf density and leaf thickness

In *Poa*, the correlations of SLA with leaf density and leaf thickness show different patterns with different grazing treatments (Fig. 6). While under grazing both leaf density and leaf thickness were negatively correlated with SLA (Fig. 6A,B), in non-grazed enclosures the significant correlation existed between SLA and leaf density, but not between SLA and leaf thickness (Fig. 6C,D). In *Pascopyrum*, however, a similar pattern in the correlation between SLA and its two components was observed for different grazing treatments: SLA was significantly correlated with leaf thickness but not with leaf density for both grazing (Fig. 7A,B) and enclosures (Fig. 7C,D). In all cases, the results from standard Pearson correlation test were confirmed and reinforced by the results from permutation resampling.

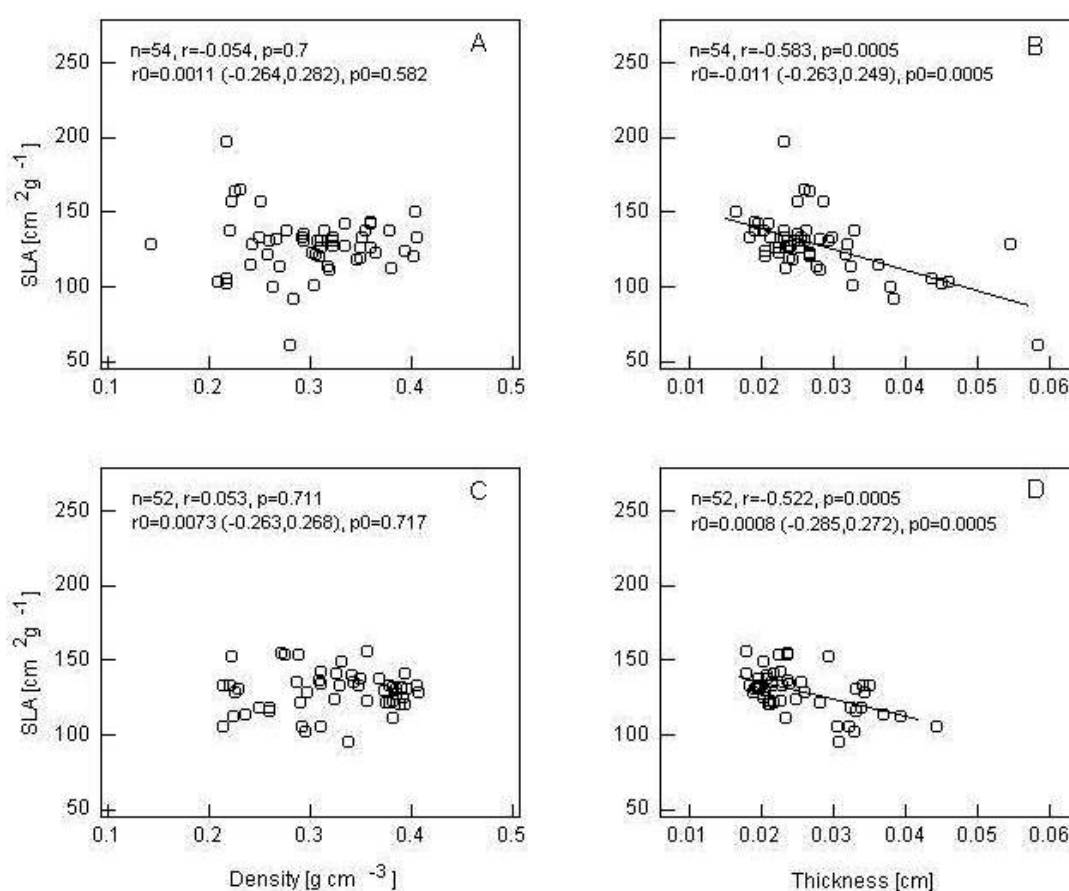


Figure 7. Same as in Figure 6 except that the data are for *Pascopyrum smithii*

### Leaf-water relations traits from pressure-volume analysis

In the Jun-Jul sampling period, the osmotic potential at full turgor ( $\psi_{\pi,s}$ ) for *Poa* plants growing in the grazed pasture was significantly lower than those in the enclosure. In Jul-Aug, however, there was no significant difference between grazing treatments, with an average  $\psi_{\pi,s}$  value of -1.56 MPa. For *Pascopyrum*, plants growing in the grazed pasture had significantly lower  $\psi_{\pi,s}$  values than in enclosure for both the Jun-Jul and Jul-Aug sampling periods, with the average value of  $\psi_{\pi,s}$  for grazed reaching as low as -3.07

MPa in Jul-Aug. Similar to *Poa*, the effect of grazing disappeared for the last sampling period (Sep. for *Pascopyrum*). Overall, the average value of  $\psi_{\pi,s}$  for *Pascopyrum* (-2.37 MPa) was marginally lower than that of *Poa* (-1.53 MPa) ( $p = 0.052$ ). The effect of grazing on leaf water potentials at turgor loss point ( $\psi_{tlp}$ ) was not as clear-cut as in  $\psi_{\pi,s}$ . As shown in *Table 1*,  $\psi_{tlp}$  was significantly lower under grazing than in enclosure for *Poa* in Jun-Jul and for *Pascopyrum* in Jul-Aug. However, for *Pascopyrum* in the Jun-Jul sampling period, the  $\psi_{tlp}$  value in enclosure was significantly lower than that in grazed. Similar to  $\psi_{\pi,s}$ , the effect of grazing on  $\psi_{tlp}$  was not observed in the last sampling periods of *Poa* (in Jul-Aug) and *Pascopyrum* (in Sep.).

### **Leaf stomatal conductance in relation to leaf water potential**

While the  $g_s$ - $\psi$  relationship for *Pascopyrum* was fitted using only one regression line, the relationship for *Poa* leaves was fitted using two regression lines with different slopes delineating a bimodal behavior of the  $g_s$ - $\psi$  relationship in less negative and more negative ranges of  $\psi$  in both years. As shown in *Fig. 9A*, in 2002, the  $g_s$ - $\psi$  relationship for *Poa* for less negative range of leaf  $\psi$  (with open, or unfolded leaves) was fitted using regression line  $g_s = 1.17 + 0.329\psi$  ( $R^2 = 0.55$ ,  $p = 0.014$ ), while the relationship for more negative range of leaf  $\psi$ , where the *Poa* leaves were folded, was described by the regression line  $g_s = 0.489 + 0.054\psi$  ( $R^2 = 0.79$ ,  $p = 0.303$ ). Although the only three data points for the folded *Poa* leaves (each was an average of data from 4-8 leaves) are not enough for establishing a statistically significant regression line, the trend of data suggests a bimodal behavior in the  $g_s$ - $\psi$  relationship in *Poa*. The intersection point of the two lines (for *Poa*) has a coordinate with  $\psi = -2.48$  MPa (solid arrow in *Fig. 9A*) and  $g_s = 0.356$  mol H<sub>2</sub>O m<sup>-2</sup> s<sup>-1</sup>. The  $g_s$ - $\psi$  relationship for *Pascopyrum* was fitted by a single regression line of  $g_s = 1.74 + 0.378\psi$  ( $R^2 = 0.62$ ,  $p = 0.001$ ), which intersects the line for folded *Poa* leaves at  $\psi = -3.86$  MPa (dashed arrow in *Fig. 9A*) and  $g_s = 0.281$  mol H<sub>2</sub>O m<sup>-2</sup> s<sup>-1</sup>. Interestingly, the solid arrow and dashed arrow fall within the 95% confidence intervals of the distribution of  $\psi_{tlp}$  for *Poa* and *Pascopyrum*, respectively. The means ( $\mu = -2.42$  MPa and  $\mu = -3.5$  MPa for *Poa* and *Pascopyrum*, respectively) and the standard deviations used for drawing the distribution (assumed normal) of  $\psi_{tlp}$  were obtained from data in *Table 1*. Although the “turning point” for *Pascopyrum* is only hypothetical, the above correspondence between the “turning points” of the  $g_s$ - $\psi$  relationship and the distribution of  $\psi_{tlp}$  provides evidence for a mutual support of the validity of both our measured stomatal behavior data and the PV-based parameter of leaf turgor maintenance.

The same pattern of the  $g_s$ - $\psi$  relationship and the “match” between stomatal behavior and  $\psi_{tlp}$  in *Poa* and *Pascopyrum* were also seen in the 2003 growing season (*Fig. 9B*), though the maximum  $g_s$  for both species tended lower in 2003 than in 2002. Also, the slopes of the regression lines of the  $g_s$ - $\psi$  relationship for both species were lower than the respective values in 2002, with unfolded and folded *Poa* leaves fitted to the regression lines of  $g_s = 0.356 + 0.065\psi$  ( $R^2 = 0.14$ ,  $p = 0.37$ ) and  $g_s = 0.241 + 0.025\psi$  (determined using two points), respectively, and *Pascopyrum* leaves fitted to the regression line of  $g_s = 0.774 + 0.166\psi$  ( $R^2 = 0.44$ ,  $p = 0.01$ ). The  $\psi$  values at the intersecting points for *Poa* and *Pascopyrum* are -2.76 MPa (solid arrow in *Fig. 9B*) and -3.77 MPa (dashed arrow in *Fig. 9B*), respectively. Note that, in *Pascopyrum*, the  $\psi$  values at the “turning points” of the  $g_s$ - $\psi$  relationship in 2002 and 2003 were quite similar, while in *Poa*, the  $\psi$  value for the “turning point” in 2003 was more negative than that in 2002.

## Discussion

Although the total precipitation received at our field site from Jun. to Sep. 2002 (280.3 mm) was higher than the 52-year long-term average (which was 264.6 mm), *Poa* plants growing in the grazed pasture experienced lower leaf  $\psi$  than the average of its turgor loss point starting early Jul. 2002 (Fig. 3A and Fig. 9). This occurred despite the observed similar available soil water in both the 0-23 cm and 0-83 cm soil depths in 2002. The severe drought of 2003 (with total precipitation from Jun. to Sep. of 170.3 mm) may have caused leaf  $\psi$  values to be close to or much below the  $\psi_{tlp}$  values of *Pascopyrum* and *Poa*, respectively, especially in mid-Aug. Our data (Fig. 3) suggest that growing season drought can exacerbate the soil and plant water status, with more detrimental impacts on shallow-rooted plants such as *Poa*. This is in agreement with a study from the same field site by Patton and Nyren (1998), but disagrees with several studies from other parts of the Great Plains of North America (Archer and Detling, 1986; Svejcar and Christiansen, 1987a, 1987b; Day and Detling, 1994; Bremer et al., 2001).

The results in Fig. 9 indicate that significant decrease in leaf  $g_s$  of *Poa* occurred near the turgor loss water potential ( $\psi_{tlp}$ ), which demarcates a higher  $\psi$  range, where leaf gas exchange responds sensitively to the change in  $\psi$ , and lower  $\psi$  range, where  $g_s$  stagnates at low or minimum values and leaf cells may experience partial to irreversible damage due to severe dehydration. Moreover, the average  $\psi_{tlp}$  of -2.42 MPa in *Poa* roughly corresponds to the leaf-folding  $\psi$  of -2.3 to -2.5 MPa in late Aug. 2002 at our study site (X. Dong, field observation). This is comparable with the leaf-rolling  $\psi$  of *Agropyron cristatum* of -2.6 MPa in early Jul. in the mixed-grass prairie as observed by Bittman and Simpson (1989), who also established that the narrow threshold of leaf-rolling  $\psi$  in *Agropyron cristatum* occurred roughly 0.1 MPa lower than the measured leaf  $\psi_{tlp}$ . In our study, no leaf-rolling or -folding was observed for *Pascopyrum*, and field measured leaf  $\psi$  of this grass was seldom lower than the 95% confidence interval of the distribution of  $\psi_{tlp}$  (Fig. 9). However, leaf-rolling in *Pascopyrum* was observed for the highly dehydrated leaves during the construction of the PV curves (X. Dong, personal observation). Thus, despite the drought in 2002 and 2003 growing seasons, *Pascopyrum* appeared to maintain its  $\psi$  from excessive decreasing, perhaps due to its deep-rooted habit in the mixed-prairie (Coupland and Johnson, 1965). Nevertheless, the fact that the intersection point between the single regression line of the  $g_s$ - $\psi$  relationship in *Pascopyrum* and that of *Poa* (Fig. 9) falls within the 95% confidence interval of *Pascopyrum*'s  $\psi_{tlp}$  distribution suggests that the  $g_s$ - $\psi$  relationship for whole range of leaf  $\psi$  in *Pascopyrum* might, though hypothetically, be described as shown in Fig. 9.



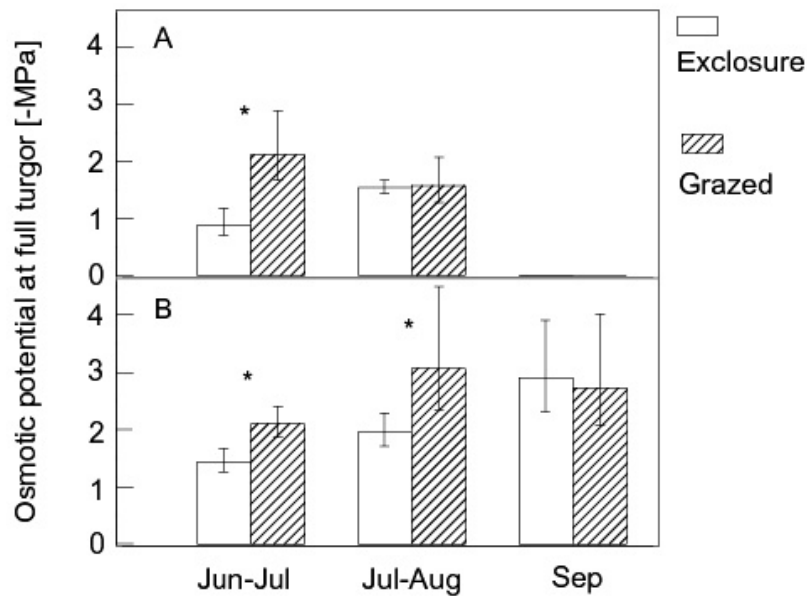


**Figure 8.** Osmotic potentials of leaves of *Poa pratensis* (A) and *Pascopyrum smithii* (B) as a function of grazing and season. The error bars represent the 95% confidence intervals for the means. The symbol \* indicates significant difference at  $p=0.05$

How does cattle grazing influence the leaf-water relations traits of *Poa* and *Pascopyrum*? Our data on both leaf structural (Figs. 4-5 and Figs. 6-7) and PV (Table 1 and Fig. 8) parameters suggest that, although both *Poa* and *Pascopyrum* responded to grazing with more negative osmotic potentials (and thus more concentrated cell solution) in months of peak growth, specific leaf area and its two components, i.e., leaf density and thickness, had minimum responses to grazing for *Pascopyrum*, while in *Poa*, a higher specific leaf area accompanied by a marginally lower leaf density was observed in grazed pastures compared with ungrazed exclosures, suggesting that long-term grazing encourages a higher potential growth rate but also a higher susceptibility to drought stress in *Poa* more than in *Pascopyrum*.

The consistent decrease in  $\psi_{\pi,s}$  of both grasses in Jun-Jul and Aug. in association with grazing may be considered primarily as a physiological response to the severe summer drought in 2003 (Fig. 3B,D,F,H), although it might to some extent be linked with increased  $g_s$  and photosynthetic rate due to grazing (Svejcar and Christiansen, 1987b), especially in the less drought affected *Pascopyrum* (see Fig. 3D). In *Pascopyrum*, the more negative values in both  $\psi_{\pi,s}$  (Fig. 8) and  $\psi_{tlp}$  (Table 1 and Fig. 9) than *Poa* suggests the greater osmotically effectiveness of the leaf solutes in *Pascopyrum*, which is in line with the conclusion of Frank (1994) that “stress response mechanisms that enhance proline and abscisic acid (accumulations) may be more operative in western (wheatgrass) (*Pascopyrum*) than crested (wheatgrass) (*Agropyron desertorum*)”.

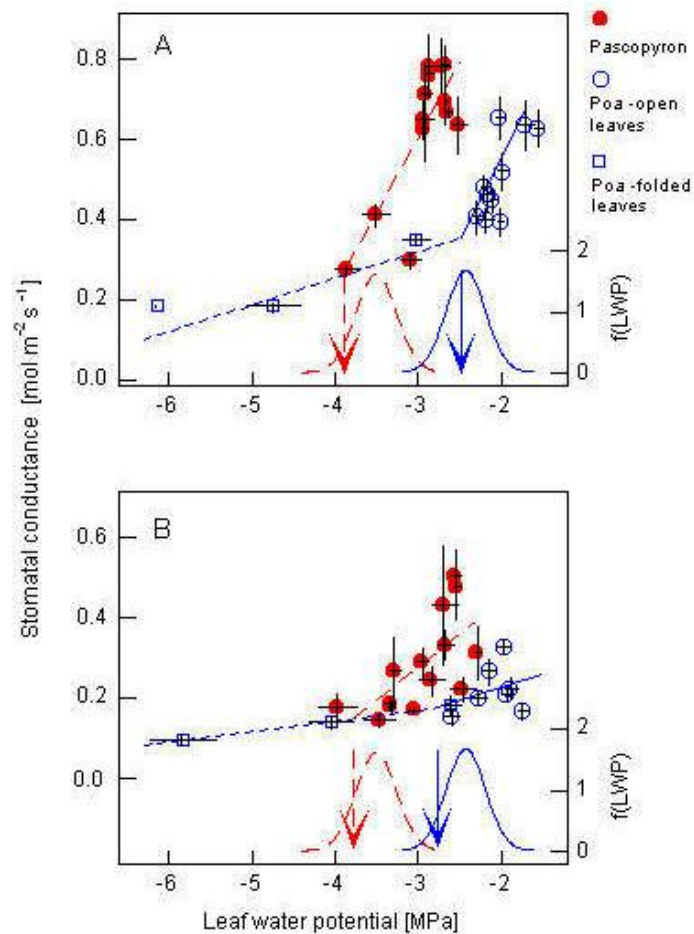


**Figure 9.** The observed bimodal relationship between stomatal conductance ( $g_s$ ) and leaf water potential ( $\psi$ ) of *Poa pratensis* leaves (open circles and squares) as measured under field conditions in 2002 (A) and 2003 (B). The mode of rapid change of  $g_s$  as a function of  $\psi$  is shown as open circles and fitted with a solid lines; the mode of slow change of  $g_s$  is shown as open squares and fitted with dotted lines. The  $\psi$  values for the junctions (solid arrows) fall within the 95% limits of the normal distribution ( $f(LWP)$ ) with mean and standard deviation derived from data of the initial turgor loss point for *Poa* in Table 1. Like data of *Pascopyrum smithii* (solid circles) was fitted with single linear regressions (dashed lines) and the  $\psi$  values for the hypothetical junction points (dashed arrows) also match the corresponding normal curve for data of the turgor loss point for *Pascopyrum* in Table 1. Each data point represents the averaged measurements on 3-12 leaves and the error bars are for standard errors

Regarding SLA and its components (leaf density and leaf thickness), although there is a general agreement between our results (Figs. 4-5) and literature data regarding effects of season (Mojzes et al., 2003) and animal grazing (Cingolani et al., 2007), our data suggest a contrast in leaf structural responses to grazing between *Poa* and *Pascopyrum*. In *Pascopyrum*, the responses of leaf density and leaf thickness to grazing largely canceled the effects of each other, resulting in an almost unchanged SLA, which departed from the predicted general responses according to Cingolani et al. (2007). This unresponsiveness in *Pascopyrum*'s leaf structure is further confirmed by the similarity

between grazing treatments in the pooled correlations of SLA and its two components (Fig. 7). Thus we conclude that leaf-water relations of *Pascopyrum* respond to grazing through significantly lowering osmotic potentials, instead of increasing leaf density or cell wall rigidity.

In *Poa*, the increased drought tolerance due to decreased  $\psi_{\pi,s}$  (Fig. 8) and  $\psi_{tlp}$  (Table 1) associated with grazing was countered by the tendency of increased SLA in the Jun-Jul and Aug. sampling periods (Fig. 4A), which were brought about by the tendency of concomitant decrease in leaf density (Fig. 4B) and leaf thickness (Fig. 4C), although only in Aug. there were marginally significant differences in SLA and leaf density between plants growing in the grazed pastures and those in the exclosures. Even though there were only three replicates ( $n = 3$ ) in our statistics, the information “content” of each measurement was high, because each measurement of SLA was the average of six composite samples each of which contained 50-60 leaves. Thus we consider the marginal significant results of Fig. 4 to be ecologically important. In addition, the responsiveness of *Poa*'s leaf structure to grazing is further confirmed by the contrast in correlations of SLA and its two components between the exclosures and grazed pastures (Fig. 6). The higher SLA for *Poa* plants in the grazed pastures, as compared with the exclosures, may be considered as a grazing mitigation strategy in that less leaf mass per unit of leaf area is removed in each defoliation event (Rotundo and Aguiar, 2008). However, a higher SLA and lower leaf density suggests a weakened capacity for water conservation through the reduction of leaf pressure potentials (Krasser and Kalapos, 2000; Niinemets, 2001), as about 80% of leaf water potential reduction of naturally transpiring leaves occurs between the full turgor and turgor loss point (Cheung et al., 1975; Maxwell and Redmann, 1978). On the other hand, a higher SLA associated with grazing also implies a higher relative growth rate (Rotundo and Aguiar, 2008) and a competitive advantage under good water supply (Martin and Chamber, 2001). This is in line with the conclusion that long-term overgrazing did not significantly weakened *Poa*'s vigor (in terms of above-ground plant biomass percentage) compared with moderate grazing, during the relatively wet spell of the past two decades from the same site as the current study (Patton et al., 2007). As a result, we conclude that, although leaf-water relations of *Poa* respond to grazing through significantly lowering osmotic potentials, increased SLA and leaf density associated with grazing render both an advantage of increased relative growth rate under good water availability and a disadvantage of susceptibility to water loss under drought stress.

One of the major goals of grassland management is to maintain and enhance the growth of native species, such as *Pascopyrum*, while keeping exotic species, such as *Poa*, in check (DeKeyser et al., 2010). Based on our analysis, we suggest that grazing in drought years may help to weaken *Poa*'s vigor and tip the relative competitiveness of the two species in favor of *Pascopyrum*. Thus, our data provide an enhanced understanding linking leaf-water relations traits of two dominant plant species with plant resource use and stress resistance on the mixed-grass prairie under cattle grazing.

**Acknowledgements.** This work was part of North Dakota Agricultural Experiment Station projects ND6146, ND6147 and ND6149. We appreciate the support of staff members of Central Grasslands Research Extension Center, North Dakota State University.

## REFERENCES

- [1] Abril, M., Hanano, R. (1998): Ecophysiological responses of three evergreen woody mediterranean species to water stress. – *ACTA Oecologia* 19: 377-387.
- [2] Archer, S., Detling, J.K. (1986): Evaluation of potential herbivore mediation of plant water status in a North American mixed-grass prairie. – *Oikos* 47: 287-291.
- [3] Biondini, M.E., Patton, B.D., Nyren, P.E. (1998): Grazing intensity and ecosystem processes in a northern mixed-grass prairie, U.S.A. – *Ecological Applications* 8: 469-479.
- [4] Bittman, S., Simpson, G.M. (1989): Drought effect on leaf conductance and leaf rolling in forage grasses. – *Crop Science* 29: 338-34.
- [5] Bremer, D.J., Auen, L.M., Ham, J.M., Owensby, C.E. (2001): Evapotranspiration in a prairie ecosystem: Effects of grazing by cattle. – *Agronomy Journal* 93: 338-348.
- [6] Chabot, B.F., Chabot, J.F. (1977): Effects of light and temperature on leaf anatomy and photosynthesis in *Fragaria vesca*. – *Oecologia* 26: 363-377.
- [7] Cheung, Y.N.S., Tyree, M.T., Dainty, J. (1975): Water relations parameters on single leaves obtained in a pressure bomb and some ecological interpretations. – *Canadian Journal of Botany* 53: 1342-1346.
- [8] Cingolani, A.M., Cabido, M., Gurvich, D.E., Renison, D., Díaz, S. (2007): Filtering processes in the assembly of plant communities: Are species presence and abundance driven by the same traits? – *Journal of Vegetation Science* 18: 911-920.
- [9] Coupland, R.T., Johnson, R.E. (1965): Rooting characteristics of native grassland species in Saskatchewan. – *Journal of Ecology* 53: 475-507.
- [10] Day, T.A., Detling, J.K. (1994): Water relations of *Agropyron smithii* and *Bouteloua gracilis* and community evapotranspiration following long-term grazing by prairie dogs. – *American Midland Naturalist* 132: 381-392.
- [11] DeKeyser, S., Meehan, M., Sedivec, K., Lura, C. (2010): Potential management alternatives for invaded rangelands in the Northern Great Plains. – *Rangelands* 32: 26-31.
- [12] Díaz, S., Noy-Meir, I., Cabido, M. (2001): Can grazing response of herbaceous plants be predicted from simple vegetative traits? – *Journal of Applied Ecology* 38: 497-508.
- [13] Dong, X., Zhang, X. (2001): Some observations of the adaptations of sandy shrubs to the arid environment in the Mu Us Sandland: Leaf water relations and anatomic features. – *Journal of Arid Environments* 48: 41-48.
- [14] Dong, X., Patton, B.D., Nyren, A.C., Nyren, P.E., Prunty, L.D. (2010): Quantifying root water extraction by rangeland plants through soil water modeling. – *Plant and Soil* 335: 181-198.
- [15] Fahnestock, J.T., Detling, J.K. (2000): Morphological and physiological responses of perennial grasses to long-term grazing in the Pryor Mountains, Montana. – *American Midland Naturalist* 143: 312-320.
- [16] Fahnestock, J.T., Knapp, A.K. (1993): Water relations and growth of tallgrass prairie forbs in response to selective grass herbivory by bison. – *International Journal of Plant Science* 154: 432-440.
- [17] Frank, A.B. (1994): Physiological comparisons of crested wheatgrass and western wheatgrass to water. – *Journal of Range Management* 47: 460-466.
- [18] Garnier, E., Shipley, B., Roumet, C., Laurent, G. (2001): A standardized protocol for the determination of specific leaf area and leaf dry matter content. – *Functional Ecology* 15: 68-695.
- [19] Gist, G.R., Smith, R.M. (1948): Root development of several common forage grasses to a depth of eighteen inches. – *Agronomy Journal* 40: 1036-1042.
- [20] Heitschmidt, R.K., Haferkamp, M.R., Karl, M.G., Hild, A.L. (1999): Interactive effects of drought and grazing on Northern Great Plains rangelands. – *Journal of Range Management* 52: 440-446.

- [21] Hesterberg, T., Moore, D.S., Monaghan, S., Clipson, A., Epstein, R. (2006): Bootstrap methods and permutation tests. – In: Moore, D.S., McCabe, G.P. (eds) Introduction to the Practice of Statistics, W. H. Freeman, New York, Chapter 14.
- [22] Jarvis, P.G. (1976): The interpretation of the variations in leaf water potential and stomatal conductance found in canopies in the field. – Philosophical Transactions of the Royal Society of London [Biology] 273: 593-610.
- [23] Jefferson, P.G., Cutforth, H.W. (2005): Comparative forage yield, water use, and water efficiency of alfalfa, crested wheatgrass and spring wheat in a semiarid climate in southern Saskatchewan. – Canadian Journal of Plant Science 85: 877-888.
- [24] Jiang, Y., Huang, B. (2001a): Effects of calcium on antioxidant activities and water relations associated with heat tolerance in two cool-season grasses. – Journal of Experimental Botany 52: 341-349.
- [25] Jiang, Y., Huang, B. (2001b). Osmotic adjustment and root growth associated with drought preconditioning-enhanced heat tolerance in Kentucky bluegrass. – Crop Science 41: 1168-1173.
- [26] Kim, J., Verma, S.B. (1991): Modeling canopy stomatal conductance in a temperate grassland ecosystem. – Agricultural and Forest Meteorology 55: 149-166.
- [27] Krasser, D., Kalapos, T. (2000): Leaf water relations for 23 angiosperm species from steppe grasslands and associated habitats in Hungary. – Community Ecology 1: 123-131.
- [28] Lenz, T.I., Wright, I.J., Westoby, M. (2006): Interrelations among pressure-volume curve traits across species and water availability gradients. – Physiologia Plantarum 127: 423-433.
- [29] Lura, C.L., Barker, W.T., Nyren, P.E. (1988): Range plant communities of the Central Grasslands Research Station in South Central North Dakota. – Prairie Naturalist 20: 177-192.
- [30] Martin, D.W., Chamber, J.C. (2001): Effects of water table, clipping, and species interactions on *Carex nebrascensis* and *Poa pratensis* in riparian meadows. – Wetlands 21: 422-430.
- [31] Maxwell, J.O., Redmann, R.E. (1978): Leaf water potential, component potentials and relative water content in a xeric grass, *Agropyron dasystachyum* (Hook.) Scribn. – Oecologia 35: 277-284.
- [32] Mohammad, N., Dwyer, D.D., Busby, F.E. (1982): Responses of crested wheatgrass and Russian wildrye to water stress and defoliation. – Journal of Range Management 35: 227-230.
- [33] Mojzes, A., Kalapos, T., Virágh, K. (2003): Plasticity of leaf and shoot morphology and leaf photochemistry for *Brachypodium pinnatum* (L.) Beauv. growing in contrasting microenvironments in a semiarid loess forest-steppe vegetation mosaic. – Flora 198: 304-320.
- [34] Monson, R.K., Smith, S.D. (1982): Seasonal water potential components of Sonoran Desert plants. – Ecology 63: 113-123.
- [35] Murphy, R.K., Grant, T.A. (2005): Land management history and floristics in mixed-grass prairie, North Dakota, USA. – Natural Areas Journal 25: 351-358.
- [36] Niinemets, U. (2001). Global-scale climatic controls of leaf dry mass per area, density, and thickness in trees and shrubs. – Ecology 82: 453-469.
- [37] Nobel, P.S. (1999): Physicochemical and Environmental Plant Physiology. – 2<sup>nd</sup> edn. Academic Press, San Diego, California, USA.
- [38] Nobel, P.S., Hartsock, T.L. (1981): Development of leaf thickness for *Plectranthus parviflorus*—influence of photosynthetically active radiation. – Physiologia Plantarum 51: 163-166.
- [39] Parker, W.C., Colombo, S.J. (1995): A critical re-examination of pressure-volume analysis of conifer shoots: Comparison of three procedures for generating PV curves on shoots of *Pinus resinosa* Ait. seedlings. – Journal of Experimental Botany 46: 1701-1709.
- [40] Patton, B.D., Nyren, P.E. (1998): The effect of grazing intensity on soil water and rangeland productivity in south-central North Dakota. – In: Potts, D.F. (ed) Proceedings

- of the American Water Resources Association Special Conference, Rangeland Management and Water Resources, American Water Resources Association, Herndon VA, TPS-98-1, pp 219-228
- [41] Patton, B.D., Dong, X., Nyren, P.E., Nyren, A. (2007): Effects of grazing intensity, precipitation, and temperature on forage production. – *Rangeland Ecology and Management* 60: 656-665.
- [42] Peterson, L.A., Newman, R.C., Smith, D. (1979): Rooting depth of Kentucky bluegrass sod as measured by N absorption. – *Agronomy Journal* 71: 490-492.
- [43] Rascio, A., Cedola, M.C., Topani, M., Flagella, Z., Wittmer, G. (1990): Leaf morphology and water status changes in *Triticum durum* under water stress. – *Physiologia Plantarum* 78: 462-467.
- [44] Roderick, M.L. (2001): On the use of thermodynamic methods to describe water relations in plants and soil. – *Australian Journal of Plant Physiology* 28: 729-742.
- [45] Roderick, M.L., Berry, S.L., Noble, I.R. (2000): A framework for understanding the relationship between environment and vegetation based on the surface area to volume ratio of leaves. – *Functional Ecology* 14: 423-437.
- [46] Rogers, W.M., Kirby, D.R., Nyren, P.E., Patton, B.D., Dekeyser, E.S. (2005): Grazing intensity effects on Northern Plains mixed-grass prairie. – *Prairie Naturalist* 37: 73-83.
- [47] Rotundo, J.L., Aguiar, M.R. (2008): Herbivory resistance traits in populations of *Poa ligularis* subjected to historically different sheep grazing pressure in Patagonia. – *Plant Ecology* 194: 121-133.
- [48] Schulte, P.J., Hinckley, T.M. (1985): A comparison of pressure-volume curve data analysis techniques. – *Journal of Experimental Botany* 36: 1590-1602.
- [49] Sinclair, R., Venables, W.N. (1983): An alternative method for analyzing pressure-volume curves produced with the pressure chamber. – *Plant, Cell and Environment* 6: 211-217.
- [50] Smith, M.D., Knapp, A.K. (2001): Physiological and morphological traits of exotic, invasive exotic, and native plant species in tallgrass prairie. – *International Journal of Plant Science* 162:785-792.
- [51] Stewart, J.R., Kjelgren, R., Johnson, P.G., Kuhns, M.R. (2004): Soil-water-use characteristics of precision-irrigated buffalograss and Kentucky bluegrass. – *Applied Turfgrass Science*. doi:10.1094/ATS-2004-1118-01-RS.
- [52] Svejcar, T., Christiansen, S. (1987a): Grazing effects on water relations of Caucasian bluestem. – *Journal of Range Management* 40: 15-18.
- [53] Svejcar, T., Christiansen, S. (1987b): The influence of grazing pressure on rooting dynamics of Caucasian bluestem. – *Journal of Range Management* 40: 224-227.
- [54] Turner, N.C. (1981): Techniques and experimental approaches for the measurement of plant water status. – *Plant and Soil* 58: 339-366.
- [55] Weaver, J.E. (1926): *Root Development of Field Crops*. – McGraw-Hill Book Company, Inc., New York
- [56] Weaver, J.E. (1958): Classification of root systems of forbs of grassland and a consideration of their significance. – *Ecology* 39: 394-401.
- [57] Witkowski, E.T.F., Lamont, B.B. (1991): Leaf specific mass confounds leaf density and thickness. – *Oecologia* 88: 486-493.
- [58] Wraith, J.M., Johnson, D.A., Hanks, R.J., Sisson, D.V. (1987): Soil and plant water relations in a crested wheatgrass pasture: Response to spring grazing by cattle. – *Oecologia* 73: 573-578.
- [59] Zar, J.H. (1984): *Biostatistical Analysis*. – 2<sup>nd</sup> edn. Prentice Hall, Englewood Cliffs, New Jersey.

## ENZYME ACTIVITY ANALYSES OF ANAEROBIC FERMENTED SEWAGE SLUDGES

KARDOS, L.<sup>1\*</sup> – JUHÁSZ, Á.<sup>1</sup> – PALKÓ, GY.<sup>2</sup> – OLÁH, J.<sup>2</sup> – BARKÁCS, K.<sup>3</sup> – ZÁRAY, GY.<sup>3</sup>

<sup>1</sup>*Department of Soil Science and Water Management, Corvinus University of Budapest  
H-1118 Budapest, Villányi út 29-43., Hungary  
(phone: +36-1-482-6466; fax: +36-1-428-6336)*

<sup>2</sup>*Budapest Sewage Works Ltd.  
H-1087 Budapest, Asztalos Sándor utca 4., Hungary  
(phone: +36-1-455-4100; fax: +36-1-459-1600)*

<sup>3</sup>*Cooperative Research Center for Environmental Sciences, Eötvös Loránd University  
H-1117 Budapest, Pázmány Péter sétány 1/a, Hungary  
(phone: +36-1-372-2607; fax: +36-1-372-2608)*

*\*Corresponding author  
e-mail: levente.kardos2@uni-corvinus.hu*

(Received 31<sup>st</sup> August 2011; accepted 17<sup>th</sup> October 2011)

**Abstract.** Biogas may be produced from communal sewage sludges by anaerobic decomposition. To follow up the decomposition processes enzyme activity tests have been applied. It is advantageous to use these activity tests if there are frequent substrate-, or specific organic matter load changes in the digesting towers. For describing the total activity of the cells, dehydrogenase-, while for following up the frequent substrate changes protease-, lipase- and cellulase enzyme activity analyses have been carried out. No internationally accepted standards are available for testing the enzyme activity of sewage sludges. Thus, in our experimental work we modified the enzyme activity analyses described earlier in the special literature for the tests of other than sewage sludge samples. Our enzyme activity tests can be completed quickly and at a relative low cost, thus it is possible to use them in generally equipped wastewater treatment laboratories also.

**Keywords:** *sludge, dehydrogenase, lipase, protease, cellulase*

### Introduction

In a communal wastewater treatment plant large volumes of sewage sludge occur from which it is possible to produce biogas by anaerobic fermentation. The energetical use of the produced biogas takes a part in the increasing power independence of the plant as burning the produced biogas the total electric power demand of the plant can be met. Treated or untreated sewage sludge can be made extensive use like agricultural soil improving material too (Yudhistra Kumar and Vikram Reddy, 2010). Biogas is a very important renewable energy source in the world. For example in India the government sponsors the building of further 3 million family scale biogas reactors by 2012 (Raghuvanshi et al., 2008). For this reason an increase both in biogas volume and in heating power is an important goal, and may be answered if the anaerobic fermentation process is understood more thoroughly. In the course of our research the enzyme activities of sludge samples originating from anaerobic sewage sludge fermentation plants were studied under different operating conditions – which were described in our former article (Kardos et al., 2009). In the present article enzyme activity

measurements used for following up the anaerobic decomposition are described in more details.

With the enzyme activity measurements the initial hydrolysis processes of the anaerobic decomposition can be described – being also the rate determining step of the complete process (Thiel et al., 1968).

## Material and methods

The sludge samples originated from the South-Pest Wastewater Treatment Plant (Budapest, Hungary) where communal wastewater is treated. The Plant has a capacity of 80000 m<sup>3</sup>/day. One thermophilic, three mesophilic anaerobic full scale fermenters and three pilot plant scale fermenters can be found in the Plant. The thermophilic plant tower is of 2000 m<sup>3</sup> while each mesophilic tower has a capacity of 2600 m<sup>3</sup>. The average operating temperature of the thermophilic tower is 55°C and it is 35°C in the case of the mesophilic towers. The useful capacity of the pilot plant scale fermenters is 1.5, 2.0 and 2.5 m<sup>3</sup> respectively, and their temperature can be varied. For our experiments the anaerobic sludge was taken from all these fermenters, however here only some measured data are shown – as examples – related to sludge samples derived from the pilot plant scale fermenters.

Our enzyme activity analyses covered dehydrogenase enzyme activity typical of the total activity of the cells, and three substrate specific enzyme activities; i.e. protease-, lipase- and cellulase enzyme activities. The analysis of the substrate specific enzyme activities was reasoned by the frequent changes in the protein- and fat content of the sludge. The cellulase enzyme activity was analysed only in those cases when the sewage sludge and the horticultural wastes had been fermented together (studying co-substrate effect).

There are no internationally accepted standards for the enzyme activity tests of the anaerobic sewage sludge samples, thus our used formulas were based on earlier prescriptions. Each enzyme activity measurement was thus optimised in our adopted recipes related to the applied temperature, incubation period and also the sludge mass (latter expressed as dry material /reagent unit ratio). The blank samples composition and role were also investigated, and the proper one was selected for each enzyme activity test type.

The basis for the measurement of the *dehydrogenase* enzyme activity typical of the total activity of the cells was provided by the Hungarian Standard MSZ-08-1721/3:1986. As this standard described the determination of the actual dehydrogenase enzyme activity of soil samples, we adapted the method of this measurement to anaerobic sludge samples. In the course of our work the testing results of Skujins (1976), García et al. (1993) and Griebe et al. (1997) were also used. The principle of the measurement is – as a result of the process catalyzed by the enzyme – that 2,3,5-triphenyltetrazolium chloride (TTC) transforms to a red colour triphenyl-phormazane (TP), the quantity of which could be spectrophotometrically measured. Knowing the measured sludge quantity, the produced triphenyl-phormazane concentration is converted to specific units of mg TP/g organic matter/hour.

To follow up the enzyme activity, 1 cm<sup>3</sup> TTC-solution of 1 m/m% was added to the sludge samples in addition to the saturated NaHCO<sub>3</sub> puffer solution. Sludge samples of 0.5, 1.0, 2.0 and 4.0 cm<sup>3</sup> were used in our series of experiments. Each case the blank sample was further treated in the same way but of course no substrate had been added



yet. Also the effect of a change in the incubation temperature was analysed. The original recipe suggested a temperature of 37°C. For studying the dependence on temperature, four temperatures were selected; i.e. room temperature (20°C), 37°C (temperature of the mesophilic sludge treatment), 45°C and 55°C (temperature of the thermophilic sludge treatment).

We analysed the incubation period too. The incubation period was varied between half an hour to four hours, after which the enzyme activity of each sample was stopped by absolute ethanol. Immediately before ethanol addition, 1 cm<sup>3</sup> substrate was added to the blank samples. After 10 minutes of sedimentation, the samples were filtered and the red solutions were photometered at 485 nm against ethanol.

The principle of the *protease* enzyme activity measurement is the follow up of the protein (casein) transition to amino acid (tyrosine). The protease activity measurement of sewage sludges was described by Thiel and Hattingh (1967). In our series of experiments each sample contained 1/3 volume part of sludge sample, 1/3 volume part substrate (0.25 m/m% casein-solution), and 1/3 volume part distilled water. After incubation at room temperature for 1 hour (according to the original recipe) the reaction was stopped by trichloroacetic acid. After alkalization following filtering – due to the separating iron precipitate – it was filtered again and after adding Folin-reagent to the sample the appearing blue colour was measured at 660 nm in comparison to the blank sample. The anaerobic sludge treated in the above ratios without incubation served as a blank sample following the immediate trichloroacetic acid treatment. The measured data are expressed in mg tyrosine/g organic matter/hour units.

Also in the case of the protease enzyme activity tests, the volume of the sludge sample was changed (0.5, 1.0, 2.0 and 4.0 cm<sup>3</sup>). In another test series the incubation temperature was altered; in this case also the applied temperatures were the followings: room temperature (20°C on an average); 37°C; 45°C, and 55°C. The incubation period was selected between half hour and four hour. In addition the appropriate concentration of the trichloroacetic acid and the rate of the alkalization following the precipitation with trichloroacetic acid were also analysed. We adjusted the optimum pH of the samples. The blue colour appears immediately after the addition of the Folin-reagent and can be measured at 660 nm. Also the time dependence of the blue colour stability was tested when the intensity variation of the blue colour was being studied for 40 minutes.

For measuring *lipase* enzyme activity, the work of Vorderwülbecke et al. (1992) and Li and Chróst (2006) were used as a basis. For the measurement, the emulsion of two reagent (containing 4-nitrophenyl palmitate -NPP- as substrate) solutions had to be prepared that was added to a predetermined portion of the supernatant layer of the centrifuged sludge. After one hour incubation at 45°C (according to the original recipe), the absorption of the sample was measured at 410 nm in comparison with the blank sample. In the course of the enzyme processes, the 4-nitrophenyl palmitate – being present as a substrate – was transforming to 4-nitrophenol (NP) that could be measured spectrophotometrically. The activity was expressed in 4-nitrophenol mass produced hourly by 1 g organic sludge. Improving the recipe in this case also the incubation temperatures and the change of incubation period as described above were studied.

In measuring the *cellulase* enzyme activity, the work by Lee et al. (2002) and Rivard et al. (1994) served as a starting point. In the course of the measurement, the cellulose decomposition of the fermented sludge was examined at 37°C for an incubation period of 24 hours according to the original recipe. Each case an easily decomposing cellulose

by-product (carboxymethyl cellulose, CMC) and ground grass dried to a mass steadiness – that can be decomposed with more difficulty – were added to a portion of the sludge sample. After incubation the suspension was centrifuged. In the centrifuged product the glucose - liberated from the cellulose products - was determined with the addition of a dinitro-salicylic acid (DNS) reagent. The sample got brown to an extent which depended on its reducing sugar content and was photometered at 550 nm. Glucose originating from the decomposition of the sludge was corrected with a blank sample containing no substrate. The evaluation was made with the aid of glucose calibration. The activity was stated in glucose quantity liberated daily by a unit of organic sludge.

For improving the recipe, in this case also the incubation temperatures and the change of the incubating period were studied.

## Results

Among the results presented in the followings, data of minimum 25 samples referring to each test series are described. The examined sludge had an average pH = 7.1 ± 0.5, average dry material content 56.8 ± 9.6 g/kg, average organic material content 26.7 ± 7.6 g/kg.

During the analysis of the *dehydrogenase* enzyme activity rising the volume of the sludge samples – that is sludge mass ratio related to the applied reagent quantity – a nonlinear increase in the measured absorbances was observed. We stated that in the case of 1 cm<sup>3</sup> substrate solution (1 mm% TTC) the reliable sludge volume was 1cm<sup>3</sup> testing sludge samples having the earlier mentioned organic mass concentration. In line with raising the incubating temperature an increasing enzyme activity was indicated by the higher absorbance values. From our results it was concluded that this enzyme tests can be made at any temperature between 30 and 55°C. In mesophilic anaerobic fermentation the incubation at about 37°C, while in thermophilic fermentation incubation at about 55°C is suggested, as these temperatures are near to the optimal life conditions of the mesophilic and thermophilic bacteria. The optimal incubation time determined at each temperature turned to be 1 hour.

On the basis of our *protease* activity measurement, in the case of the used substrate concentration, the 2 cm<sup>3</sup> sludge sample volume having the given mass concentration the most suitable. On the basis of our experiences – independently of the mesophilic or thermophilic origin of the sludge – considering both the activity and the reproducibility - the most advantageous temperature turned to be 37°C. The 3 cm<sup>3</sup> 10 m/m% trichloroacetic acid concentration included in the original recipe was not adequate, thus a concentration of 15 m/m% was used. Due to application of both acid and Folin-reagent (diluted to 1:1), the samples had to be alkalized, thus 3 cm<sup>3</sup> 2 mol/dm<sup>3</sup> NaOH solution was used before adding the Folin-reagent. The ratio of Folin-reagent and sample was in volume: 0.1: 1. On the basis of the time dependence analysis for the occurring blue colour it can be stated that the blue colour had been stabilized after a period of approximately 15 minutes.

As a result of the *lipase* enzyme activity tests it can be stated that - due to the activity and the reproducibility data - the suitable incubation temperature is 45°C, and it does not depend on the preliminary fermentation temperature. The optimum incubation time was between 60 and 80 minutes.

Our *cellulase* analyses proved that the suitable incubation temperature is 37°C. We suggest an incubation period of 24 hour which can be appropriately applied also by an average laboratory of a wastewater treatment plant. The incubation period of 24 hours is reasoned by the fact that during this period the hydrolysis of cellulase molecules – which can be decomposed with difficulty - will be suitably completed.

Here we show some results of vegetable waste and sludge cofermentation (cosubstrate effect) from our pilot plant scale experiments. It can be seen, that during the experiment the cellulase- and protease enzyme activities showed a close correlation with the alteration of the daily gas volume (*Figure 1*). The changes in substrate load were properly indicated by our enzyme activity measurements (organic matter load varied:  $5.24 \pm 1.4 \text{ kg/m}^3 \cdot \text{d}$ ). The supply of the grass waste was preceded by a control period of 36 days during which only sludge was added. The control period was followed by a grass supplying period of 76 days meanwhile each working day 1.5 kg dried ground grass together with  $200 \text{ dm}^3$  sludge was added. On the basis of our tests it can be stated that the simultaneous sludge and grass feeding presented suitable nutriment for the anaerobic microbe population.

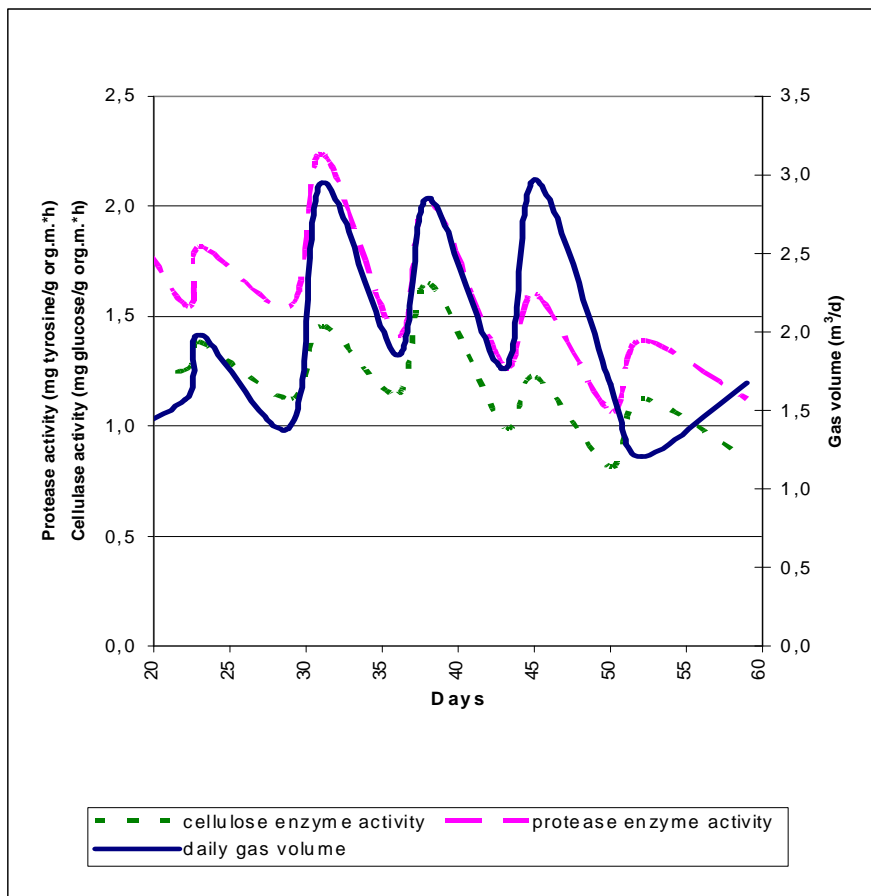


**Figure 1.** Variation of cellulase and protease enzyme activities in a selected experimental period in pilot plant scale reactor (org.m.= organic material)

Our observations supported that the decomposability of a substrate can be described by the hydrolytic enzyme activity as the speed of the substrate decomposition is the function of enzyme activity, and this is an important condition for biogas

transformation. More results of full scale and pilot plant fermentation are published elsewhere (Kardos et al, 2009).

## Summary

As a summary our experiences on the recipe modifications are described in *Table 1*.

**Table 1.** Summary of the enzyme activity tests (tested sludge:  $pH = 7.1 \pm 0.5$ , average dry material content  $56.8 \pm 9.6$  g/kg, average organic material content  $26.7 \pm 7.6$  g/kg)

Enzyme	Substrate	Product of metabolism	Sludge volume (cm <sup>3</sup> )	Incubation temperature	Others
Dehydrogenase	2,3,5-triphenyl-tetrazolium chloride (TTC)	triphenyl-phormazane (TP)	1	In case of a mesophilic sludge: 37°C, in case of a thermophilic sludge: 55°C	Incubation for 1 hour
Protease	casein	tyrosine	2	37°C, independently of the preliminary sludge fermentation temperature	Treatment with 15 m/m% trichloroacetic acid and 2 mol/dm <sup>3</sup> NaOH Incubation for 1 hour
Lipase	4-nitrophenyl palmitate (NPP)	4-nitrophenol (NP)	1 (liquid extract of sludge)	45°C	Incubation between 60 and 80 minutes
Cellulase	Carboxymethyl cellulose (CMC) or grass	glucose	2 (liquid extract of sludge)	37°C	Incubation for 24 hours

In case of the substrate specific enzyme activity analyses, the stated incubation temperatures have not shown any relationship with the preliminary fermentation temperature of the sludge; it is explained by the fact that in these cases the fat-, protein- and cellulose contents of the sludge are more determinative.

**Acknowledgement.** We express our thanks to the staff of the Wastewater Treatment Plant of South Pest, for the operation of the plant- and pilot plant scale reactors and the Research and Development Group for their assistance. This research was supported by the TÁMOP 4.2.1/B-09/01/KMR/2010-0005 project.

## REFERENCES

- [1] Analysis of soil biological activity by method of dehydrogenase enzyme activity (1986): Soil analysis of agricultural land treated with sewage and sewage sludge. MSZ-08-1721/3-86 (Hungarian Standard), Budapest, Hungary.
- [2] Griebe, T., Schaule, G., Wuertz, S. (1997): Determination of microbial respiratory and redox activity in activated sludge. – Journal of Industrial Microbiology and Biotechnology 19(2): 118-122.

- [3] García, C., Hernandez, T., Albaladejo, J., Castilla, V., Roldan, A. (1998): Revegetation in senierid zone: influence of terracinn gand organic refuse on microbial activity. – Soil Science Society of America Journal 62: 670-676.
- [4] Kardos, L., Palkó, Gy., Oláh, J., Barkács, K., Záray, Gy. (2009): Operation control of anaerobic digesters on the basis of enzyme activity tests. – Water Science and Technology 64(4): 957-964.
- [5] Lee, S.-M., Lin, J., Koo, Y.-M. (2002): Hydrolysis of paper sludge using mixed cellulase system: Enzymtic Hydrolysis of paper sludge. – Biological Systems Engineering, ACS Symposium Series 830: 121-138.
- [6] Li, Y., Chróst, J. R. (2006): Microbial enzyme activities in anaerobic activated sludge model – Enzyme Microbiological Technology 39(4): 568-572.
- [7] Raghuvanshi, S., P., Raghav, A. K., Chandra, A. (2008): Renewable energy resources for climate change mitigation. – Applied Ecology and Environmental Research 6(4): 15-27.
- [8] Rivard, C. J., Nieves, R. A., Nagle, N. J., Himmel, M. E. (1994): Evaluation of discrete cellulase enzyme activities from anaerobic digester sludge fed a municipal solid waste feedstock. – Applied Biochemistry and Biotechnology 45-46(1): 453-462.
- [9] Skujins, J. (1976): Enzymes in soil. – In: Mc Laren A.D., Peterson, G.H. (eds.). Soil Biochemistry, Marcel Dekker, Inc. New York, USA: 371-414.
- [10] Thiel, P. G., Hattingh, W., H. J. (1967): Determination of hydrolytic enzyme activites in anaerobic digestion. – Water Research 1: 191-196.
- [11] Thiel, P., G., Toerien, D. F., Hattingh, W., H., J., Kotzé, J. P., Siebert, M., L. (1968): Interrelations between biological and chemical characteristics in anaerobic digestion. – Water Research 2: 393-408.
- [12] Vorderwülbecke, T., Kieslich, K., Erdmann, H. (1992): Comparison of lipases by different assays. – Enzyme Microbiological Technology 14: 631-639.
- [13] Yudhistra Kumar, A., Vikram Reddy, M. (2010): Effects of municipal sewage on the growth performance of *Casuarina equisetifolia* (Forst. & Forst.) on sandy soli of east coast at Kalpakkam (Tamil Nadu, India) – Applied Ecology and Environmental Research 8(1): 77-85.

# NUMERICAL SIMULATION OF ADVECTION-DISPERSION FOR MONITORING THERMAL PLUME RE-CIRCULATION IN A SHALLOW COASTAL ENVIRONMENT

PANIGRAHI, J.K.<sup>1\*</sup> – TRIPATHY, J.K.<sup>2</sup>

<sup>1</sup>*L&T-RAMBOLL, India*

<sup>2</sup>*Department of Remote Sensing & GIS, North Orissa University, India*

*\*Corresponding author  
e-mail: Jeetendra@scientist.com*

(Received 24<sup>th</sup> April 2008; accepted 26<sup>th</sup> August 2011)

**Abstract.** A numerical simulation study is carried out to assess the possible reject water circulation pattern around the Lekki coast, Nigeria. Critical decision like selection of suitable location for intake and outfall systems are decided based on the simulation results. The tide and wave induced flow pattern and the advection-dispersion of disposed thermal plume in the vicinity of the Lekki coast are established using hydrodynamic model (HD) and advection-dispersion (AD) model of Mike-21 suite of programs respectively. The modeling and simulation experiment is performed using the field measurements and the end results for critical scenarios are presented in this paper. The performance of the model is encouraging and it is a reliable tool for marine environmental monitoring.

**Keywords:** *advection-dispersion, wastewater disposal, thermal plume*

## Introduction

The ocean has for all time been the ultimate sink for water-borne waste products coming from the industries. Marine disposal of wastewater is nothing more than a cosmetic name for the relocation of industrial effluent and the other associated wastes, whether it be treated or not and dumped into the sea by an outfall. The disposal is carried out by constructing a pipeline on the bed of the ocean with tunnel or risers and appropriate diffusers. The fundamental intent of wastewater disposal is to mix the effluent thoroughly with large volumes of ambient water. If the ocean is stratified then the diluted pollutant may reach an equilibrium level below the surface of the ocean and the ocean currents transport the effluent, it is further diluted by the surrounding turbulence (Rodi, 1980). However, in the shallow seas the diluted pollutant usually fail to find an intermediate equilibrium level and reaches the surface of the ocean with a density less than the salt water. In addition to the diffusion caused by ambient turbulence the effluent will spread because of its density difference. When wastewater enters the marine environment from the diffuser it is buoyant and tends to rise. This effluent, initially travelling horizontally after leaving the holes, or ports, gradually ascends on a more vertical path. Throughout its path, whether largely horizontal or vertical, the effluent mixes with ambient seawater. Generally marine outfall need to be located in minimum environmentally sensitive zone; therefore an open sea always preferred over estuary or bay. Depending on the natural topography of ocean permits, discharges usually made at a depth of 7 to 20 m or more (Wood et al., 1993). The depth is the important parameter because of two basic reasons, firstly where depth is more, significant density stratification exists in seawater column especially during summer months. In such cases mixed effluent plume won't rise to the ocean surface and will

remain submerged at an intermediate location. Secondly, under unstratified ocean conditions, assuming density of discharged effluent to be less than the usual density of seawater, effluent would tend to rise to surface to form surfacing field. It is well known that the sea area microbiologically polluted by a given effluent discharge does not depend only on the effluent volume, but also, to a considerable extent, on the velocity and the direction of the sea currents affecting the discharge point; hence the point of discharge is of great importance for defining the area concerned. The coastal ecology is likely to get disturbed due to accumulation of waste in the estuarine region if the effluent is disposed near to the shore as sufficient dilution and dispersion is not available in such areas. Some times these discharged effluents may float on the surface, in case heavy or no circulation of waves and current the disposed effluent gets accumulated at the bottom of the seabed. Most reject waters has essentially the same density as fresh water and heated seawater used as cooling water is of less dense then seawater at normal temperature. So, it is buoyant and rises to the surface as turbulent jet. Here, a simulation study to assess heated water spreading is demonstrated as a real world problem.

The paper describes results of the numerical simulation for reject water re-circulation and advection-dispersion of thermal plumes coming from a polymer complex at Lekki free trade zone at Lagos state Nigeria. The total volume of seawater at the intake location and reject water at the outfall location is catered for 400,000 m<sup>3</sup>/hr. The reject water is planned to be discharged through an open channel located in 2m water depth on the seaward side of the western breakwater (*Fig.1b*), while the intake is located within the dredged harbor basin, along the eastern breakwater. Further selecting a correct location of intake structure with respect to discharge point carries great importance for efficiency of the system and for reduction of operational costs. In order to minimize environmental sensitivity and take appropriate engineering decision for confirming set of intake and outfall location, advection-dispersion modeling are performed coupling HD (hydrodynamic) and AD (Advection-Dispersion) model of Mike-21 (Abbott, 1985) suites of program. These models were developed by Danish Hydraulic Institute (DHI), Denmark and are being widely used worldwide for many coastal engineering applications.

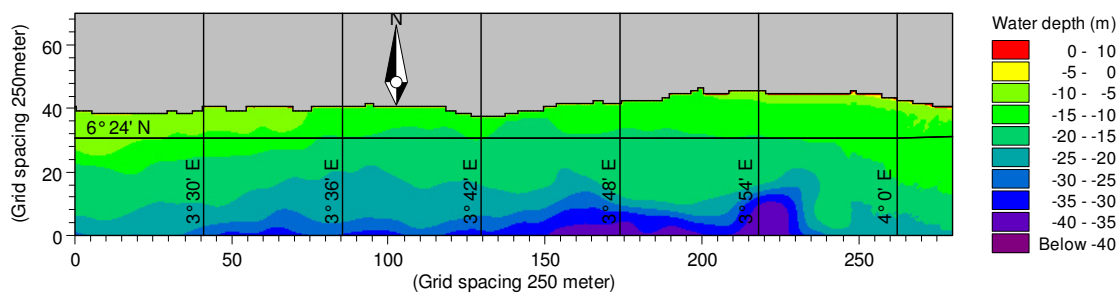


**Figure 1a** Coarse grid bathymetry

## Materials and methods

In order to assess the circulation pattern of reject water hydrodynamic modeling and to determine movement of thermal plume, Advection-Dispersion modeling is implemented. The flow pattern and the associated current velocities in the surrounding

waters primarily govern the movement of reject water from the outfall location. The currents in the coastal waters are generally governed by forcing due to tides and waves. Hence tide, wave and bathymetry data for the coast is collected by field measurements.

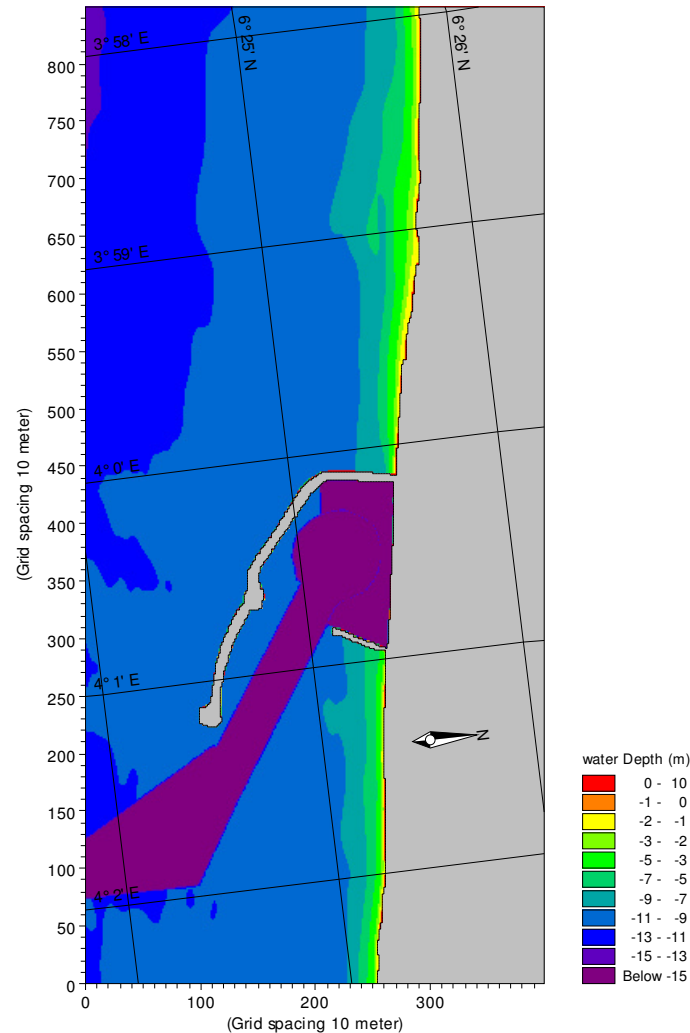


**Figure 1b** Fine grid bathymetry

A regional bathymetry on a coarse grid covering an area of 70 km × 17.5km with a 250m × 250m grid spacing is prepared using the water depth information available in the British Admiralty Chart 1863 (*Fig.1a*). The model area extends from Lagos in the west to the study location at Lekki in the east. Again a local bathymetry covering a 9 km × 11 km area with a finer grid spacing of 10m x 10m, is prepared using the water depth data obtained from field surveys (*Fig.1b*). The harbour facilities like the harbour breakwaters, navigational channel and seawater intake inside the port and outfall adjacent to eastern breakwater are digitally laid on the bathymetry. The tidal forcing at the eastern and western boundaries of the coarse grid model is used to drive the circulation within the fine grid model. The surface elevations at the eastern boundary (Lekki) and the western boundary (Lagos), are taken from tidal measurements observed for a period of 18 days. The same has formed as the boundary conditions for the HD



simulations in the coarse grid. The observed tides at Lekki and Lagos are presented in *Fig. 2a & 2b*, which shows that the tidal range at Lekki during spring tide is close to 2.5m while that during neap tide is 1.2.

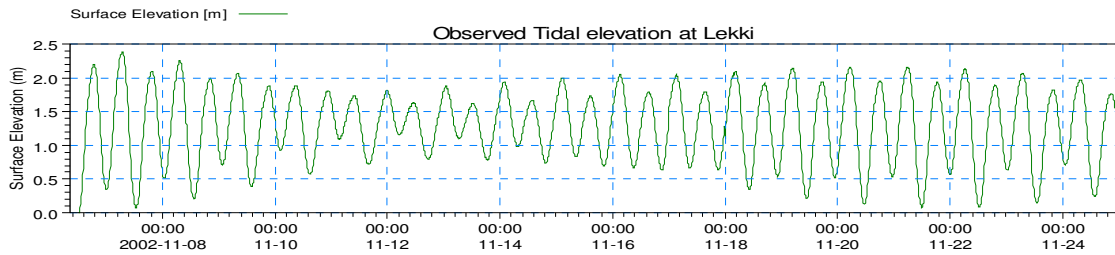


*Figure 2a* Observed tide at Lekki

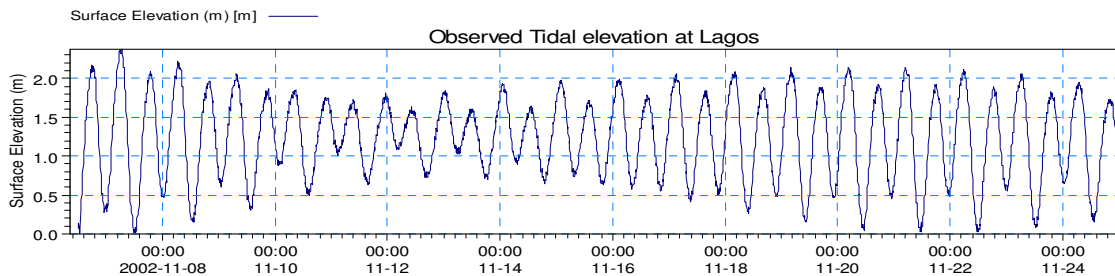


*Figure 2b* Observed tide at Lagos

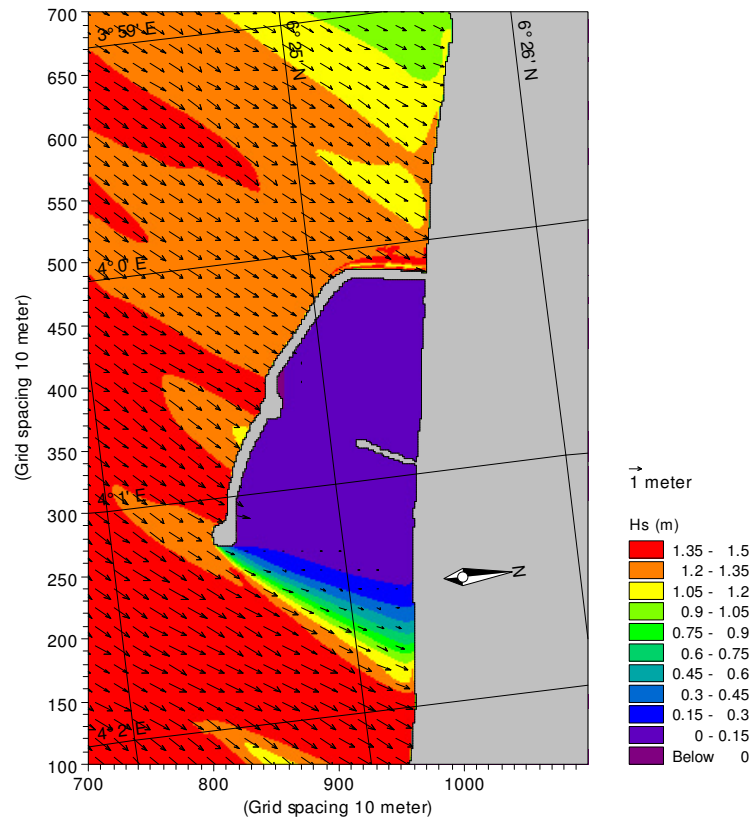


*Figure 2c* Simulated waves for the coastal stretch of study area

Apart, wave plays a major role in shallow water hydrodynamics since wave induced radiation stress in the bulk of water contributes significantly to currents. The wave climate experienced at the study area is predominantly governed by the deep-water waves from south. Waves at shallow water generate radiation stress, which is responsible for mass transport. Hence wave induced radiation stress is modeled for creating input to combined wave-tide induced flow simulation. The near shore waves for the coast is simulated using parabolic mild slope wave model (boundary  $H_s = 1.5\text{m}$ ,  $T_m = 5.2\text{s}$ ) and the wave field is shown in the *Fig. 2c*. Two sets of model executions are performed spring and neap tide with waves.

### Model formulation

The MIKE 21 Flow model (HD) simulates two-dimensional free-surface flows (Abbott et al., 1981). It calculates non-steady flow and transport phenomena that result from tidal and meteorological forcing on a spherical, or rectilinear or curvilinear boundary fitted grid. This model is applicable for the simulation of flow fields in natural water bodies, such as lakes, estuaries, bays, coastal areas and seas wherever stratification can be neglected. It can be used to model the processes like: tide and wind-driven flows, stratified and density driven flows, thermal stratification in lakes, seas and reservoirs, cooling water re-circulation, transport of dissolved material and pollutants and wave-driven currents etc.

It is a multi-dimensional 2D, hydrodynamic flow simulation model, which solves shallow-water equations for given boundary conditions to compute non-steady flow fields in response to a variety of environmental forcing and processes in natural water bodies. The environmental forcing and processes include: bottom shear stress, wind shear stress, barometric pressure gradients, Coriolis force, momentum dispersion, sources and sinks, evaporation, flooding and drying and wave radiation stresses.

This model uses an Alternate Direction Implicit (ADI) Finite Difference Method on staggered orthogonal grids and also has the option to use Finite Element Method (Abbott, 1979). The basic shallow-water equations in the Cartesian co-ordinate system used in the HD flow modules are:

Continuity equation (1):

$$\frac{\partial \zeta}{\partial t} + \frac{\partial p}{\partial X} + \frac{\partial q}{\partial Y} = S - e \quad (\text{Eq.1})$$

Momentum equations in x- and y- directions (2 & 3):

$$\frac{\partial p}{\partial t} + \frac{\partial}{\partial X} \left[ \frac{p^2}{h} \right] + \frac{\partial}{\partial Y} \left[ \frac{p \cdot q}{h} \right] + gh \frac{\partial \zeta}{\partial X} + F_{bx} - K_a WW_x - \frac{h}{\rho_w} \cdot \frac{\partial p_a}{\partial X} - \Omega q - F_{EX} = S_{ix} \quad (\text{Eq.2})$$

$$\frac{\partial q}{\partial t} + \frac{\partial}{\partial X} \left[ \frac{p \cdot q}{h} \right] + \frac{\partial}{\partial Y} \left[ \frac{q^2}{h} \right] + gh \frac{\partial \zeta}{\partial Y} + F_{by} - K_a WW_y - \frac{h}{\rho_w} \cdot \frac{\partial p_a}{\partial Y} + \Omega p - F_{EY} = S_{iy} \quad (\text{Eq.3})$$

Where:

$$F_{EX} = \left[ \frac{\partial}{\partial X} \left[ \epsilon_x \cdot h \cdot \frac{\partial u}{\partial X} \right] + \frac{\partial}{\partial Y} \left[ \epsilon_y \cdot h \cdot \frac{\partial u}{\partial Y} \right] \right]$$

$$F_{EY} = \left[ \frac{\partial}{\partial X} \left[ \epsilon_x \cdot h \cdot \frac{\partial u}{\partial X} \right] + \frac{\partial}{\partial Y} \left[ \epsilon_y \cdot h \cdot \frac{\partial u}{\partial Y} \right] \right]$$

$$F_{bx} = \frac{g}{C^2} \sqrt{\frac{p^2}{h^2} + \frac{q^2}{h^2}} \cdot \frac{p}{h}$$

$$F_{by} = \frac{g}{C^2} \sqrt{\frac{p^2}{h^2} + \frac{q^2}{h^2}} \cdot \frac{q}{h}$$

Where the following symbols are as:

$\zeta(x, y, t)$	Water surface level above datum (m)
$p(x, y, t)$	flux density in the x-direction ( $m^3/s/m$ )
$q(x, y, t)$	flux density in the y-direction ( $m^3/s/m$ )
$h(x, y, t)$	water depth (m)
$S$	source magnitude per unit horizontal area ( $m^3/s/m^2$ )
$S_{ix}, S_{iy}$	source impulse in x and y-directions ( $m^3/s/m^2 \cdot m/s$ )
$e$	evaporation rate (m/s)
$g$	gravitational acceleration ( $m/s^2$ )
$C$	Chezy resistance No. ( $m^{1/2}/s$ )
$K_a$	$C_w \frac{\rho_{air}}{\rho_{Water}}$
$C_w$	wind friction factor
$W, W_x, W_y(x, y, t)$	wind speed and components in x - and y - directions (m/s)
$p_a(x, y, t)$	barometric pressure ( $Kg/m/s^2$ )
$\rho_w$	density of water ( $kg/m^3$ )
$\Omega$	Coriolis coefficient (latitude dependent) ( $s^{-1}$ )
$\epsilon(x, y)$	eddy or momentum dispersion coefficient ( $m^2/s$ )
$x, y$	space coordinates (m)
$t$	time (s)

In this study the intake volume of 400,000  $m^3/hr$  is included in the model as several isolated sinks, while the reject water at the outfall location is included in the model as isolated sources. These sources / sinks discharge / remove the above volume of seawater

throughout the simulation period. A heat dissipating component with a temperature difference of +10 °C above the ambient seawater temperature is specified at the individual sources in the outfall location, to study the movement of the reject water plume in space and time. The simulations are carried out for duration of 60 hrs in each case, out of which the model is allowed to warm up (stabilize) for the initial 12 hours and the results for the subsequent 48 hours only are used for further analysis. The result of these simulations is formed the hydrodynamic basis for the subsequent advection-dispersion modeling to study the movement of the reject water.

The advection-dispersion model (AD) of the MIKE 21 system simulates the spreading of effluent in an aquatic environment under the influence of the fluid transport and associated natural dispersion process (Gross et al., 2002). The substance may be a pollutant of any kind, conservative or non-conservative, inorganic or organic: e.g. salt, heat, dissolved oxygen, inorganic phosphorus, nitrogen and other such water quality parameters.

The temperature/concentration of the substance is calculated at each point of a rectangular grid covering the area of interest, in a way similar to the hydrodynamic computations. This module determines the concentration of the substance by solving the equation of conservation of heat/mass for a dissolved or suspended substance using a two-dimensional form of the finite difference scheme (Ekebjærg and Justesen, 1991). The MIKE 21 HD model provides information on the transport, i.e. currents and water depths at each point of the grid. Other data required includes substance temperature/concentration and discharge quantities at outfalls, together with temperature/concentrations at boundaries.

The AD module solves the advection-dispersion equation for dissolved or suspended substances in two dimensions (Gross et al., 1998). This is in reality the mass/heat conservation equation to which quantities of substances discharged and their concentrations/temperature at source and sink points are included together with their decay rate (Vieira, 1992). The layer integrated advective transport equation for a substance  $c$  was stated in Eq.1, and including source/sink terms it reads:

$$\frac{\partial hc}{\partial t} + \nabla \cdot (\bar{u}fc) + (wc)^+ - (wc)^- = S_{AD} \quad (\text{Eq.4})$$

$$S_{AD} = Pc_P - Ec_E + \frac{Q_H}{\rho C_{HW}} + \sum_{i_s=1}^{N_s} \delta(\bar{X} - \bar{X}_{S,i_s}) c_{S,i_s} Q_{S,i_s} + \sum_{i_D=1}^{N_D} \delta(\bar{X} - \bar{X}_{D,i_D}) D_{i_D} \quad (\text{Eq.5})$$

Where the following symbols are as:

$c$	Temperature
$\delta$	delta function of horizontal coordinates, $m^{-2}$
$\bar{X}_{S,i_s}$	horizontal coordinate of point source/sink No. $i_s$
$c_{S,i_s}$	Temperature of point source/sink No. $i_s$ , [c]
$Q_{S,i_s}$	discharge at point source/sink No. $i_s$
$P$	precipitation rate at surface

$c_p$	air temperature
$E$	evaporation rate at surface
$c_E$	temperature of the ambient water
$Q_H$	heat flux from heat exchange module (if $c$ is temperature), $W/m^2$
$\rho$	density of water, $kg/m^3$
$C_{HW}$	specific heat of water, $4186 J/(kg \cdot ^\circ K)$
$D_{i_D}$	dry deposition rate, [c]
$\bar{X}_{D,i_D}$	horizontal coordinate of dry contributor No. $i_D$

## Results

The combined wave-tide induced flow hydrodynamics for the study area is simulated and results are presented in this section. The flow pattern during spring tide, with waves resulted the strongest currents along the western breakwater, during flood (inflow) and ebb (outflow) phases of the tide shown in *Fig. 3a* and *4a* respectively.

The flow pattern during ebb is slightly altered at outfall location and the reject water flows eastwards close to the western breakwater, while the general flow is directed westwards. The speed of the eastward flowing current along the western breakwater are higher during flood phase, due to the combined action of waves, tidal flow and reject water outfall. Current speeds approaching  $0.5 m/s$  are simulated along the western breakwater during flood phase, while the regions of the entrance channel behind the western breakwater and the harbour basin are generally calm. The currents are altered at the tip of western breakwater resulting in different flow patterns, depending on the direction of flow during the tidal cycle.

The corresponding reject water plume movement during flood and ebb are shown in *Fig. 3b* and *4b* respectively. The combined effects of the waves and tides tend to dilute the temperature of the reject water plume, thus resulting a temperature differences at intake location during flood and ebb phases is less than  $0.5 ^\circ C$ . The maximum temperature difference is observed at the harbour entrance  $0.8 ^\circ C$ . It shows that the maximum increase in temperature over the ambient seawater, is close to  $2.0 ^\circ C$  at the harbour, though this decreases to a maximum of  $0.5 ^\circ C$  at the intake location.

Similarly, current vectors depicting the flow pattern during neap tide along with waves are presented in *Fig. 5a* and *6a*. The eastward flowing currents along the western breakwater is present in both phases, the current speeds being higher during flood than the ebb phase. This shows that the weak tidal currents do not seem to influence the direction of movement of the reject water, irrespective of the flood or the ebb phase of the tide. The reject water plumes for neap tides with waves are presented in *Fig. 5b* and *6b*. It is seen that the plume movement is similar to that during spring tide. There are exception with the increase in temperature over the ambient waters and slightly higher during neap tide, due to the weaker tidal currents.

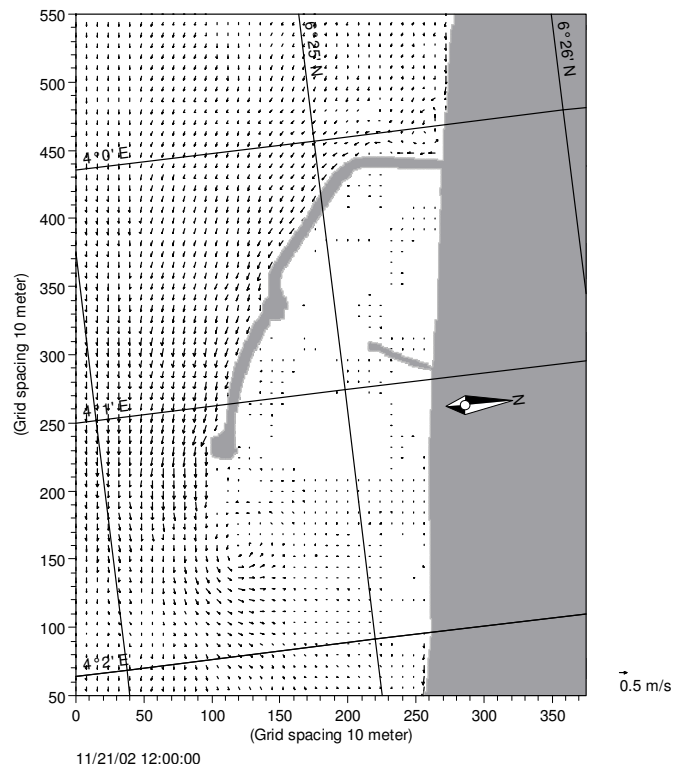


**Figure 3a** Hydrodynamic flow pattern for spring tide (flood) with waves

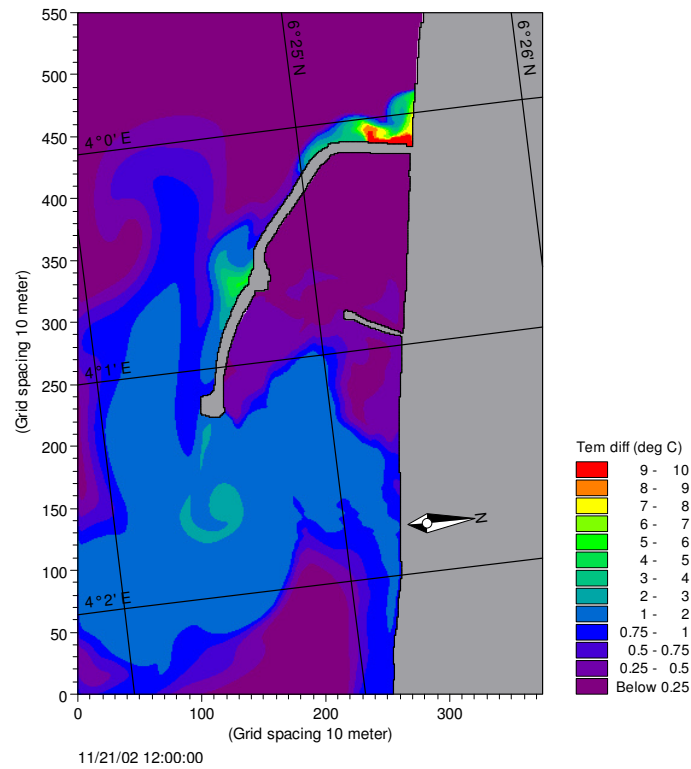


**Figure 3b** Advection dispersion corresponding to 3(a)

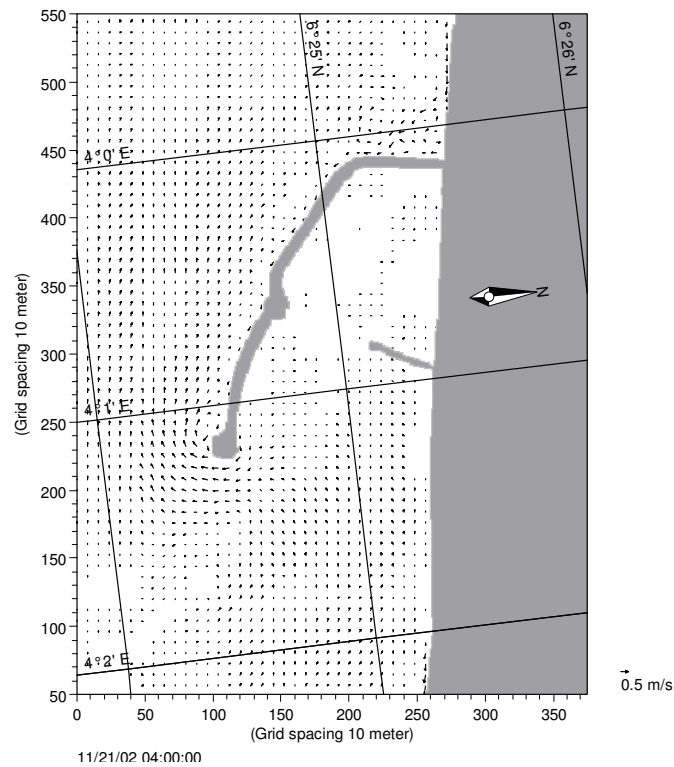


**Figure 4a** Hydrodynamic flow pattern for spring tide (ebb) with waves

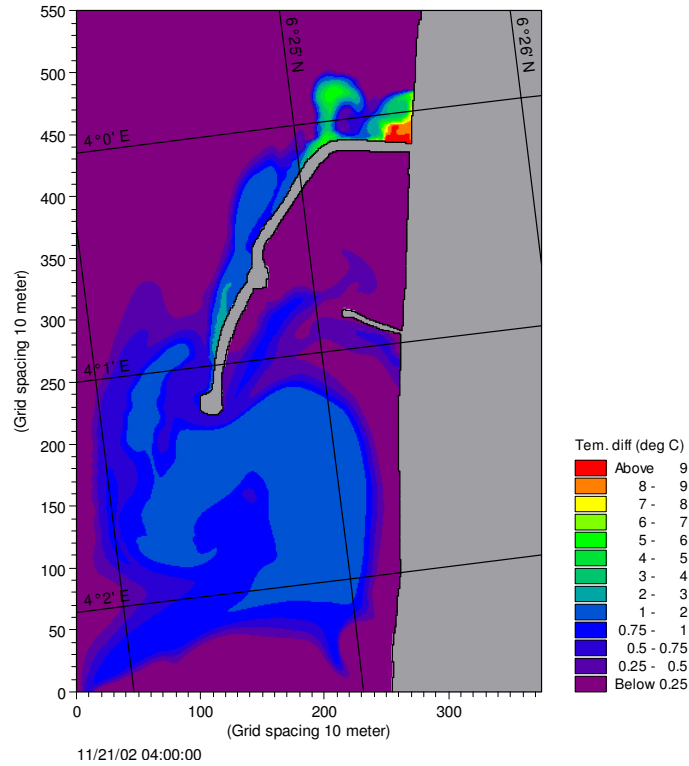


**Figure 4b** Advection dispersion corresponding to 4(a)

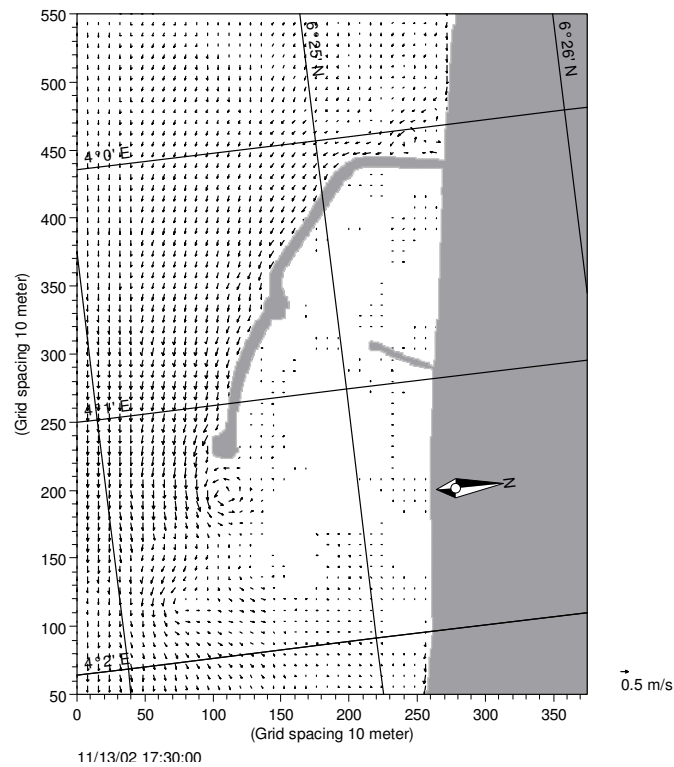


**Figure 5a** Hydrodynamic flow pattern for neap tide (flood) with waves

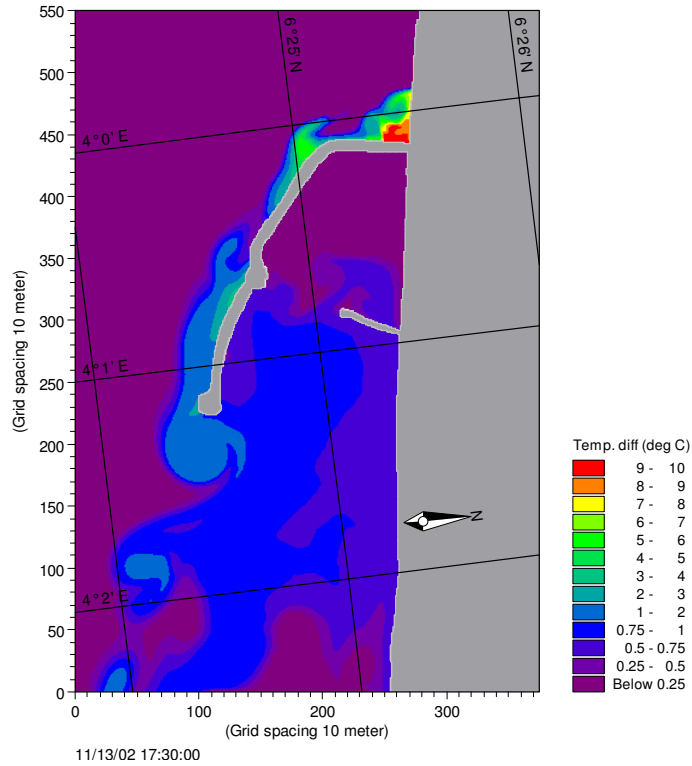


**Figure 5b** Advection dispersion corresponding to 5(a)



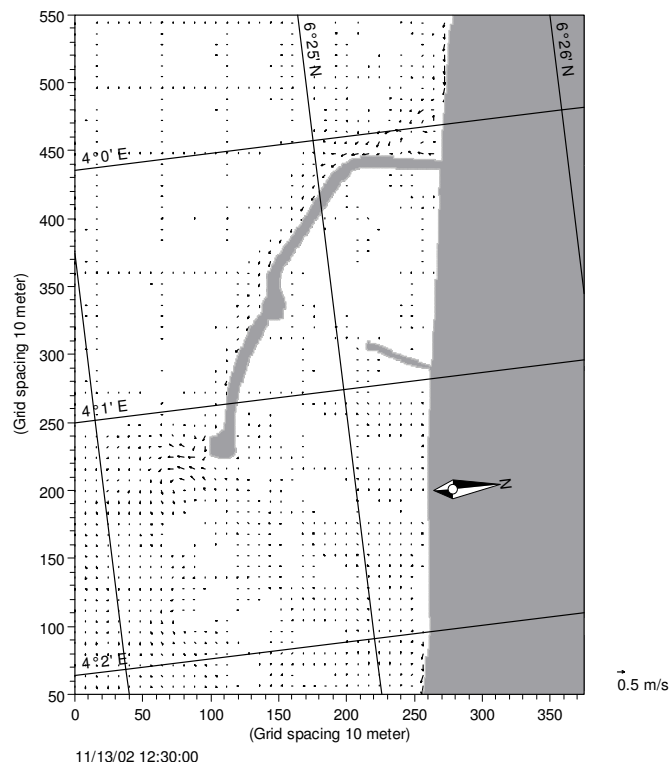


**Figure 6a** Hydrodynamic flow pattern for neap tide (ebb) with waves

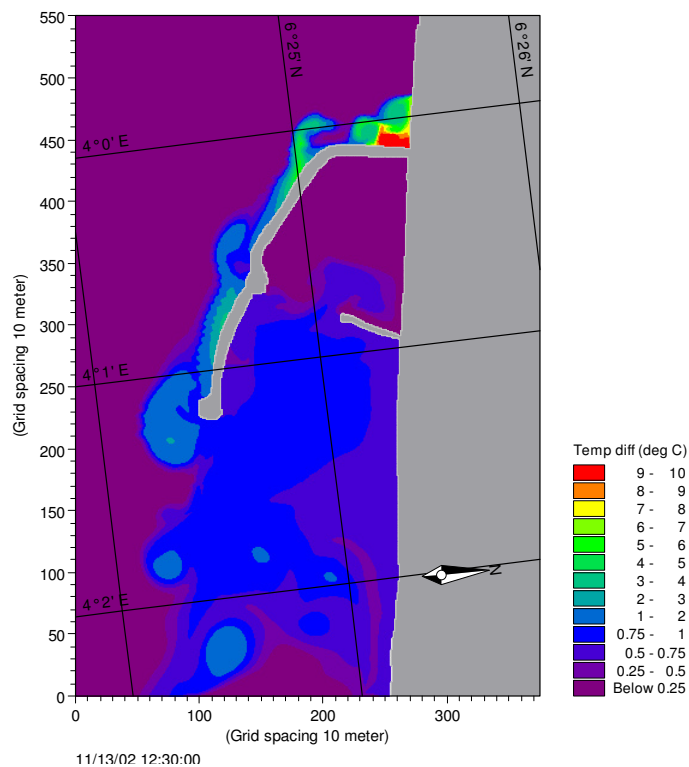


**Figure 6b** Advection dispersion corresponding to 6(a)

## Discussions and conclusion

The results of the Advection- Dispersion simulations show that the reject water moves eastwards along the western breakwater during spring tide for both the flood phase and ebb phase of the tide. The extent of the plume movement and temperature increase over the ambient waters is higher during the flood phase than that during ebb. The combined effect of the waves and tidal currents during spring tide increases the plume dilution, thus resulting in smaller temperature differences. The reject water plumes for neap tides with waves show that the temperature increase over the ambient waters is higher due to the weaker tidal currents. The Advection Dispersion simulations for combined tide and waves show that there is no effect of the reject water on the temperature of the seawater at the intake location. Also the dilution is increasing with distance from the discharge point. The flow pattern in the coastal waters ensures sufficient dilution of the reject and the maximum temperature increase of the ambient seawater is close to 2 °C at the entrance to the harbour, while this value decreases to 0.5 °C at the intake location. The plume dispersion doesn't significantly influence the environment as the maximum rise in temperature is < 2 °C, which is well within the environmental guidelines. The immediate coastal environment at disposal location has a temperature difference in the order of 5-10 °C for an area of 200 × 300 m. This study shows that numerical models play an important role in this regard, as steady state analytical calculations fail to address the temporal and spatial change in these parameters. The model is an useful tool to select disposal location but it needs calibration to make more meaningful. It fairly monitors the heated water spreading and a good decision support system for environmental impact assessment.

**Acknowledgements.** The authors are thankful to L&T-Ramboll for the encouragement and support during this work.

## REFERENCES

- [1] Abbott, M.B. (1985): Modeling circulation's in depth-integrated flows. Part-1: The accumulation of the evidence. – *Journal of Hydraulic Research* 23(4).
- [2] Abbott, M.B. (1979): *Computational Hydraulics – Elements of the Theory of Free Surface Flows.* – Pitman, London.
- [3] Abbott, M.B., Mc Cowan, Warren, I.R. (1981): Numerical Modeling of Free-Surface Flows that are two-dimensional in Plan. – *Proceedings of a symposium on predictive ability of transport models for Inland and Coastal waters*, Academic Press.
- [4] Ekebjærge, L., Justesen, P. (1991): An explicit Scheme for Advection Diffusion Modeling in two dimensions. – *Compute Methods in Applied Mechanics and Engineering* 88(3): 287-297.
- [5] Gross, E.S., Bonaventura, L., Rosatti, G. (2002): Consistency with Continuity in Conservative Advective Schemes for Free Surface Models. – *International Journal for Numerical Methods in Fluids* 38: 307-327.
- [6] Gross, E.S., Casulli, V., Bonaventura, L., Koseff, J.R. (1998): A semi-Implicit Method for Vertical Transport in Multidimensional Models. – *International Journal for Numerical Methods in Fluids* 28: 157-186.
- [7] Rodi, W. (1980): Turbulence Models and their applications in Hydraulics. A State of the Art Review. – SFB 80/T/127.

- [8] Vieira, J.R. (1992): On the general dispersive coefficients used in mathematical models of flow circulation and transport. – Coastal, Estuarial and Harbour Engineer's Reference Book.
- [9] Wood, I.R., Bell, R.G., Wilkinson, D.L. (1993): Ocean disposal of wastewater. – Advanced series on Ocean Engineering, vol. 8, World Scientific, Singapore.

## ORIBATID MITES (ACARI: ORIBATIDA) IN MICROCOSMS - A REVIEW

GERGÓCS, V.<sup>1\*</sup> – HUFNAGEL, L.<sup>2</sup>

<sup>1</sup>*Eötvös Loránd University, Department of Plant Taxonomy and Ecology  
H-1117 Budapest, Pázmány Péter sétány 1/C, Hungary*

<sup>2</sup>*Corvinus University of Budapest, Department of Mathematics and Informatics  
H-1118 Budapest, Villányi út 29-43, Hungary  
(phone: +36-1-294-9875)*

*\*Corresponding author  
e-mail: veragergocs@gmail.com*

(Received 13<sup>th</sup> November 2011; accepted 2<sup>nd</sup> December 2011)

**Abstract.** Oribatid mites are one of the most abundant and species rich group in soil mesofauna. In spite of this, we have limited knowledge on the role they play in ecological processes. Since they are small like other mesofauna members and live a hidden life, their observation is difficult. Their life style, interactions with other organisms and role in soil decomposition processes can be investigated with laboratory experiments more exactly and effectively. While the literature of microcosm studies is very extensive, relatively few review papers have been written about the methodology of microcosm studies. The present review summarizes details of techniques that have been applied laboratory microcosms involving oribatid mites. It is shown what one should keep in mind in planning, composing and setting up a microcosm. Our comparative evaluation reveals how the laboratory experiments were maintained and manipulated and what kind of information was extracted. This methodological review can be useful in preparing microcosm experiments applied to other animal groups as well.

**Keywords:** *ecosystem, community ecology, microcosms, mesofauna, soil ecology, methodology*

### Introduction

Oribatid mites are one of the most abundant and species rich mesofauna group particularly in temperate deciduous forests and boreal coniferous forests (Wallwork, 1983). They occur almost in every type of terrestrial (and in some freshwater) habitat of the world, in all kinds of microhabitats, and for this reason they can have great significance in the area of indication researches (Balogh et al, 2008; Gergócs and Hufnagel 2009; Gergócs et al, 2010, 2011).

Most of the species are generalists regarding feeding mode and habitat preference (Maraun et al., 2007), a large part of the species feed on saprotrophic fungi but there are also bacteria feeders, detritivorous species and some of them feed on carrion (Behan-Pelletier, 1999). However, many questions have remained unanswered in oribatid ecology. Despite their large density and species richness, we still do not know the answers to the following questions: why are they so diverse, what kind of interactions they have with other soil dweller animals and microorganisms, what kind of role they play in decomposition, do they facilitate or obstruct mineralization, etc.. Since oribatid mites are small animals (the largest species are about 1 mm long) they are difficult to observe directly. Even Wallwork (1983) suggested that they should be studied in microcosms.

Accordingly, many studies related to oribatid mites have been performed in laboratory microcosms. By definition, microcosms are „miniature constructed

ecosystems in which physical and biological constraints are imposed to enable the controlled study of ecological processes” (Drake and Kramer, 2011), or formulating briefly: „small ecosystems in containers” (Fraser and Keddy, 1997), or „enclosed model ecosystems” (Kampichler et al., 2001). The latter study emphasized that all the microcosm experiments are performed in laboratory under artificial circumstances and they should not be confused with mesocosms, which are „bounded and partially enclosed outdoor experimental set-ups, that is, field enclosures with reduced or controlled input and output from and to its surrounding environment”. The scientific relevance of microcosm experiments is controversial, both camps (pro and contra microcosms) present several arguments in favor of their opinions. The critical comments against microcosms were divided into three groups by Drake and Kramer (2011): 1. Microcosms are ecologically too simple and the results coming from simplified processes cannot be extrapolated to nature. 2. Microcosms are too small and the experiments are too short in time so they cannot reflect realistic spatial and temporal changes. 3. The results of this kind of experiments are only valid under artificial circumstances. Nevertheless, microcosm experiments have many advantages because they are relative cheap, easy to carry out, they can be done close to the researchers’ workplace, they can be controlled easily and the constraints can be set exactly. The above mentioned problems are not necessarily drawbacks because complex natural processes often cannot be studied in intact state, microcosms can separate mechanisms and therefore we can test our theories after simplification more effectively (Drake and Kramer, 2011).

Most of the organisms living in soil and taking part in decomposition processes are small and cannot be investigated with naked eye. This explains why microcosm experiments have been conducted since the 1960s (Huhta, 2007). It is advantageous to use mini ecosystem experiments to examine processes taking place in soil because they can be studied easily under laboratory circumstances thanks to their small size and short generation time of the soil biota. In addition, microcosms are good models for recognizing interactions among organisms living in soil (Moore et al., 1996).

The compilation of microcosms is a difficult procedure. We must pay attention to many factors if we want to imitate nature under artificial circumstances. We have to decide on the kinds of organisms to be included, and the environment to be ensured. Life conditions of microorganisms, animals and at times plants must be created in such a way that the processes we want to examine will not be bothered by anything. Microcosm experiments last comparatively long therefore the adequate circumstances (e.g. humidity) must be monitored and maintained for long time as well. Finally, data collection is also an important aspect, because it must reflect the changes taking place during the experiment.

Microcosm studies have been reviewed by many articles analysing the results in many aspects (e.g. Fraser and Keddy, 1996) except for methodological ones. The aim of this study is to compensate this gap. Microcosm experiments are very extensive and are applied in many fields of science, so their set-up is also different. Therefore, we have narrowed down the issue of our review to the part of soil ecology related to oribatid mites kept in microcosms. Since these mites are in connection with many other soil-dwelling organisms, the methods we discuss in this paper can be useful not only for studying oribatid mites but for examining other faunal groups as well.

The experiments are very diverse even in this narrower field. At first, we demonstrate what kinds of problems have been approached with laboratory microcosms.

Then, we discuss to what we pay attention during composing and keeping a microcosm. In this part of the paper, we summarize the methods that were used in 46 publications we have included in this review. We suggest that any microcosm experiment can be divided into three phases. The first one is setting up the microcosm itself, planning the experiment and setting the starting conditions. The second one is incubation when the system runs according to the initial settings. The third phase is the extraction of information. The construction of this paper follows the above sections.

### ***Objectives of microcosm studies***

There are many research issues related to microcosms including oribatid mites. One of them concerns the effect of temperature on oribatid species or communities. Uvarov (2003) showed that *Nothrus silvestris* Nicolet, 1855 living in temperate deciduous forests survives large temperature changes (5-25 °C). Temperature tolerance of five other species was studied by Deere et al. (2006) in microcosms. Søvic and Leinaas (2003) monitored the changes of artificially composed populations of *Ameronothrus lineatus* Thorell, for several years in laboratory. This microcosm experiment made possible that the density changes of the specimens in different life history stages could be examined according to the seasonal fluctuations of temperature. In other studies, the effects of changing temperature on soil dwelling mesofauna and on decomposition processes were analysed. In these papers (e.g. Sulkava and Huhta, 2003) it was revealed that little temperature fluctuations around freezing point (-2 °C and +2 °C) had minor effects on oribatid communities in boreal and subarctic habitats (Sulkava and Huhta 2003; Sjørnsen et al. 2005). Only extreme freeze caused greater loss of abundance of certain species (Sulkava and Huhta, 2003).

The behaviour of specimens can be investigated more effectively under controlled conditions. Such behaviour is, for example, the running and migration speed of small animals, which was measured either for each specimen on a paper sheet with a frame of 1-mm<sup>2</sup> or with a whole animal community in their natural microhabitat. As measured on a paper sheet, speed was very different over oribatida species because the specimens covered 1 cm distance in 10-100 s (Smrž, 2006). When migration of species was analysed in their natural substrates, it was revealed that species living in litter layer migrated faster than those living in soil but there were also great differences between speed values (Ojala and Huhta, 2001). Domes et al. (2007) carried out a similar experiment by comparing migration speed of sexual and parthenogenetic oribatid mites but they could not reveal any difference between the migration ability of the two groups.

Studying the feeding of oribatid mites has already been approached from many aspects. Some of the laboratory experiments involve food preference examinations when the animals are generally kept on artificial substrates (e.g. wet plaster of Paris and charcoal) and they are offered various kinds of food. Quality of consumed food is determined from the decrease of food and from gut content examinations (e.g. Smrž, 2006). In other cases, animals are offered special food in a microcosm filled with natural substrates. Remén et al. (2010) and Crowther et al. (2005, 2010) carried out soil microcosms with only one oribatid species and with a single micorrhiza or saprotrophic fungi species and the decrease of fungus biomass consumed by mites was monitored. Crotty et al. (2010) introduced bacteria enriched to 99 atom% in <sup>13</sup>C and <sup>15</sup>N to soil cores in laboratory and traced the flow of isotopes through the food web. They found that some of the oribatid mite species were enriched both in <sup>13</sup>C and <sup>15</sup>N, reflecting that

these species are bacterial feeders. Besides feeding habits, competition between oribatid species can also be examined under laboratory conditions. Anderson (1978) demonstrated in a microcosm experiment that *Nothrus silvestris* and *Hermannietta granulata* Nicolet, 1855 compete with each other because the presence of both species in mini ecosystems affected their feeding and distribution over microcosm layers.

Until recently, the role of oribatid mites in soil decomposition processes has not been clarified completely. There are some microcosm studies examining the role of oribatid mites in decomposition of given plant materials. Wickings and Grandy (2011) traced the role of *Scheloribates moestus*, Banks 1895 in litter decomposition of red oak (*Quercus rubra*, L. 1753) and corn (*Zea mays*, L. 1753). They found that the presence of mite specimens influenced corn litter chemistry: mineralization of C and N and extracellular enzyme activities increased. Siepel and Maaskamp (1994) investigated several species belonging to different feeding guilds. They found that fungivorous grazer species (e.g. *Nothrus silvestris*) indirectly stimulated decomposition: saprotrophic fungi could grow faster because of the great amount of N released from fungal cell-walls by grazing.

The most extensive microcosm examinations including oribatid mites are related to the interactions among soil microorganisms, soil fauna and plants. There are many experiments where oribatid mites are categorised only as microarthropoda so this larger group is examined only as a whole. Accordingly, oribatid mites are not always discussed separately. In most experiments, the density of microarthropoda or their richness divided to greater groups (e.g. Cole et al., 2004), or the effect of their absence (e.g. Setälä and Huhta, 1991), or their interactions with earthworms (e.g. Adeyujigbe et al., 2006), with microorganisms (e.g. Liiri et al, 2002b), or with the primary production of plants and the mineralization processes (e.g. Cole et al., 2004) are studied. From these studies, we can get information only indirectly about the role of oribatid mites in given processes. If they are mentioned separately in such examinations, oribatid mites are reported not to have much effect on the studied functions (e.g. Setälä, 2000).

However, there are many other studies that discuss actual interactions between oribatid mites and other soil organisms. These studies examine, for example, the relationship between oribatid and predator mites. The results of these examinations generally show that most oribatid species are protected by their hard shell and are therefore not threatened by predators (e.g. Schneider and Maraun, 2009). Lopez et al. (2003, 2007) revealed that earthworms have negative effect on many oribatid mite species. Besides this, the oribatid mites and other microarthropoda can decrease the abundance of enchytraeids (Huhta et al., 1998). If oribatid mites' feeding on different fungus species is not studied directly, then their ability is investigated in facilitating reproduction and activities of soil fungi. Results showed that they can promote respiration and biomass production of soil fungi (Maraun et al., 1998).

Finally, there are studies on the effects of human impact on the environment (e.g. fragmentation, application of herbicides, pesticides, ash etc.) of soil mesofauna including oribatid mites. Rantalainen et al. (2004) and Staddon et al. (2010) established (micro)habitat islands or patches connected with corridors under laboratory conditions. The size of isolated (i.e. having no corridors) patches or islands was large enough for oribatid populations to increase during the incubation. Mixing natural substrates with ash is a more serious intervention. Liiri et al. (2002a) showed that application of wood ash in an acidophilous deciduous forest soil caused decrease in species number and density of oribatida communities. Heneghan and Bolger (1996) studied the effects of components of acid rain on soil fauna and found that application of potential pollutants

of acid rain had impact on soil nutrient flow and decomposition processes, but different oribatid species responded in different ways, e.g. the populations of *Oppiella nova* Oudemans, 1902 did not change under nitric acid treatment.

The effects of sewage sludge on soil living organisms can also be examined in microcosms. Andres and Domene (2005) tested how sewage sludge treatment influenced soil communities. They found that different members of mesofauna responded to the various treatments of sewage sludge in different ways. Most of the groups of organisms suffered from the sludge only when it had been dried before adding to microcosms except for oribatid mites, whose density did not change considerably during the treatments. Pernin et al. (2005) tested the effects of sewage sludge with copper enrichment and found that the number of oribatid mites was decreased by the most serious treatment. Salminen et al. (1997) studied the effects of pentachlorophenol (PCP) on the structure of soil communities and on decomposition processes. This herbicide had direct or indirect negative effects on most of the organisms.

### ***Establishing a microcosm***

Many things must be considered while composing a microcosm since we want to imitate nature but a microcosm can only approximate its complexity. Laboratory microcosms can be stored in many kinds of containers. There are simple glass jars, plastic and glass cylinders, tailor-made boxes etc. Their size depends on the amount of substrates placed in them. In some studies, larger systems were created (e.g. Huhta and Setälä, 1990; Salminen and Sulkava, 1996) in which many other smaller microcosms were located. In these experiments not only the smaller microcosms were examined separately but the whole system and the interactions between the patches were also studied.

In case of containers, one must be careful that the microcosm dwelling organisms should not escape from the system and other animals should not come into the microcosm so all the mini ecosystems must be closed. Aeration is generally allowed by picking a hole or holes on the lid of containers which are closed with a cotton plug or with a gauze of a mesh size of ~0,05-0,1 mm. Other boxes are totally closed and there are some holes on them through which constant air flow is maintained by a compressor (e.g. Huhta and Setälä, 1990). With the former method, air humidity can be kept constant and CO<sub>2</sub>-concentrations can be measured. In most of the cases, redundant water added to the system during the incubation must be left to flow out of the container. There are some studies in which the containers have a hole on their bottom for leaching water or a mesh is adjusted on the base of the container with open bottom (e.g. Andrés and Domene, 2005).

In most cases, humus and litter-layers of coniferous forest floor are placed into a microcosm of oribatid mites and other soil organisms. Out of the 46 reviewed publications 22 examined the soil fauna of coniferous forests, 8 papers were concerned with temperate deciduous forests and in the rest of the publications samples were taken from grasslands (e.g. Lopez et al., 2003), from agricultural fields (e.g. Adeyujigbe et al., 2006), and from subarctic fields (pl. Sjørusen et al., 2005). Occasionally, animals were kept on artificial substrates (e.g. Fujikawa, 1999). We found coniferous forest floor substrate preference among the studies that examined plant seedlings and their interactions with soil animals and soil ecological processes because in ten out of 14 publications plant seedlings were planted into humus and litter substrate originated from coniferous forest floor. The amount of substrate applied in microcosms is very variable.



In reference to studies applying coniferous forest floor, the microcosms mainly include humus and /or leaf litter but in half of these studies mineral soil is also layered under the above mentioned materials. This choice does not correlate with study objectives. The average dry mass of leaf litter (L and/or F-layer) placed in microcosms is 5.7g (SD=4.3), the average dry mass of humus (in some cases called as organic horizon) is 44.0g (SD=30.6). The applied amount of substrates did not depend on research objectives.

The substrates placed in microcosms are treated in many ways depending on the soil layer they originate from and on the purpose of the study. Treatments are usually made for homogenization and defaunation, i.e. killing almost all the living organisms in microhabitats collected from natural habitats. Mineral soil is generally sieved with 2-4 mm mesh and is washed with (warm) tap water to remove debris. In most of the cases, after mixing humus is sieved through a 1 cm mesh for homogenization, but after heating or drying it can be sieved even through 2-6 mm mesh. Leaf litter is often cut into pieces of 0.5-2 cm<sup>2</sup> and there are some cases when litter material is washed with distilled water. Bigger twigs, roots and stone pieces are always removed from the substrates.

Before or after these treatments follows a more serious and more effective way of defaunation, which kills the whole biota or one part of the biota in a given sample. About three quarters of the investigated studies used some sort of defaunation. These methods are also very variable and cannot be linked exclusively to any study objective. The simplest defaunation method is drying but a more intensive method is heating. A wide range of temperatures (from 35 °C to 105 °C) is applied for heating with a duration from 2.5 hours to 8 weeks. There are some methods for killing the animals with freeze: from -18 °C to -40 °C; from 24 hours to 3 days. In other methods, temperature is changed between very low and very high values. Soil animals can be killed from the substrate also in a microwave oven.

The effectiveness and justification of applying a particular defaunation method have been rarely mentioned. Huhta et al. (1989) studied various defaunation methods and compared their effectiveness and side effects on soil fauna and soil characteristics. Repeated microwaving (380 W, 3 minutes) and repeated freezing-thawing and drying (-80 °C, 0 °C, +60 °C and drying) proved to be a really effective technique for killing microarthropods together with oribatid mites. Domes et al. (2007) executed a control experiment in which heating the samples at 60 °C for 8 weeks destroyed all the microarthropods. Heating treatment for 2,5 hours at 65°C is not enough for killing all the Protozoa, fungi and bacteria (Laakso and Setälä, 1999). Freezing at -20 °C does not destroy the whole microfauna and all the eggs of microarthropods (Lenoir et al., 2007). Defaunation techniques have some side-effects on soil characteristics e.g. autoclaving increases soil acidity (Liiri et al., 2002), whereas microwaving reduces water holding capacity (Huhta et al., 1989). All the techniques are used in many fields of experiments; there is no standard method for defaunation.

The aim of defaunation is generally to know the refaunated system exactly or to create a new community in accordance with the goals of the study. The composition of communities of microcosm experiments involving intact samples is determined with immediate parallel sampling and extracting (e.g. Lopez et al., 2003). Alternatively, there is no identification because only the control and the treated samples will be compared. These latter examinations are general in studies of human environmental disturbance (e.g. Rantalainen et al., 2004; Heneghan and Bolger, 1996). In further cases knowledge

of the composition of organismal communities is not important because only biomass is measured after different treatments (Laakso and Setälä, 1999; Taylor et al., 2010).

Defaunation is followed by refaunation by reinoculation of microcosms with organisms. Oribatid mites can be reinoculated into the system in many ways. In arctic and subarctic habitats, some oribatid species can be collected with a single brush because the specimens run on the surface of rocks or cyanobacteria-layer (Sovik and Leinaas, 2003). In most of the cases, specimens are extracted from different soil layers either with Tullgren (Berlese-) funnel or with high-gradient extractor. These methods are used almost in all studies of oribatid mites or microarthropods but for refaunation the animals must be extracted alive. There are several techniques to extract mites alive. The simplest technique is direct extracting when animals are extracted directly from the donor sample into the target sample, i.e. into a (defaunated) microcosm. Intact, original substrates are heated at the top of a funnel or an extractor, while the target substrates are cooled and wetted at the bottom (e.g. Taylor et al., 2010). In this case, we do not know the exact composition of the extracted community but we can evaluate it with parallel communities from the same habitat with retrieving them into alcohol. Microarthropods can be extracted into jars with moist filter papers or water. In this case, animals are placed into microcosms with a brush or the whole filter paper is placed onto the surface of the substrate. Filter papers are left in microcosms for 1-21 days. Large (about 80cm×80cm) Tullgren funnels are often applied for such extractions and under the funnels there is a rotating disc with some collecting jars with moist tissue papers. This can assure homogeneous content of jars. If animals are extracted directly into water, they must be transported more often into the microcosms (minimum once a day). Transporting can be made with a brush, a small spoon or with pipette. These extracting techniques are suitable to compose a community with known components at species level (e.g. Laakso and Setälä, 1999). In some experiments, animals are extracted onto moist plaster of Paris and they are stored for some days before reinoculation (e.g. Salminen et al., 1997). Kuperman et al. (2007) used another method for refaunation. They mixed the sulphur mustard polluted, defaunated soil samples with intact homogenized samples.

During extraction larger predator insects and spiders also run into collecting jars. These animals can be dangerous to microarthropods so they are often removed from filter papers or from the water except when the aim of the study is to examine the effects of predators on other organisms (e.g. Schneider and Maraun, 2009). There are some cases when animals should not transport alien microorganisms into the new system so they must be sterilized. A simple technique is to wash mite or worm specimens under tap water (Setälä, 2000) but using streptomycin sulphate is a more effective method (Moore et al., 1985).

The simplest refaunated microcosms contain only the specimens of one or several oribatid mite species in addition to microbiota. In such experiments their tolerance (e.g. Uvarov, 2003), their role in decomposition (e.g. Wickings et al) and their feeding habits (e.g. Crowther et al., 2011a,b) are studied. To get more complex systems, specimens from more taxonomic groups are reinoculated. Microorganisms are reinoculated with soil and water suspension when the knowledge about their exact taxonomic identity is not important in the study. In cases when preparing the suspension is described at all, humus from the collecting place is usually mixed with distilled or tap water ( $\sim 15\text{-}300 \text{ g humus} \times 1^{-1} \text{ water}$ ) then it is sieved with a 5-10  $\mu\text{m}$  mesh and equal portions are added

to microcosms. Anderson (1978) stored defaunated samples for 10 weeks on forest floor in a mesh which was not permeable for microarthropods.

After microorganisms, nematodes and enchytraeids, finally microarthropods are added to microcosms. In some cases collembola and mites are reinoculated separately. The order and the timing of inoculation vary. In case of direct inoculations, all organisms get the target sample at the same time. In other cases, incubation time is left between inoculations of different animal groups. In the examined studies, the incubation time between the addition of the microorganisms and then microarthropods changed between 7-119 days. If there is a planting treatment in the experiment, plants are added to the system either 7-36 days before the microarthropods (e.g. Laakso and Setälä, 1999) or e.g. 13 weeks after them (Liiri et al., 2002b). In some studies, nematodes and enchytraeids are inoculated 4-8 days after the microorganisms and 1-2 weeks later microarthropods come to the system (e.g. Sulkava and Huhta, 2003).

Animal abundances applied in these experiments are very variable. In most cases, no explanation is given for values used but there are some studies in which densities are set to the values found under field conditions (e.g. Lenoir et al., 2007). Taylor et al. (2010) applied direct extraction and inoculation because they thought it was important that the rates of animal densities in a microcosm were close to natural.

### **Incubation**

The second phase of experiments with microcosms is letting the system to work. Durations of examinations are very variable. The shortest ones last only for 7-14 days. Crotty et al. (2011) tracked the flow of  $^{13}\text{C}$  and  $^{15}\text{N}$  through soil faunal food web for 11 days, Kuperman et al. (2006) investigated the reaction of soil fauna on mustard gas for 7 days and Anderson (1978) measured the competition between two oribatid mite species for 14 days. Among the longest examinations, there is the complex “macrocosm” study of Huhta and Setälä (1990), in which there were several smaller microcosms in a larger container and densities of different animal groups living in the macrocosms were monitored for 125 days. The second longest experiment was made by Søvik and Leinaas (2003), who investigated the life history of *Ameronothrus lineatus* Thorell for 21 months. Between the two extreme durations, there are many other applied values. Seven laboratory experiments lasted 7-42 days, twelve examinations lasted 56-98 days, 9 ones lasted 105-180 days and 14 ones lasted 276-875 days.

In a laboratory system, the climate must be set by researchers carefully, usually in a climate chamber. Microcosms without plants are generally kept in darkness but there are some examples when light and darkness change daily even though there is no plant seedling in the microcosm (e.g. Wickings et al., 2011). Temperature is always constant in darkness and it is set commonly between 12-25 °C but the most often used constant temperature is 15 °C. When plants are also used in microcosms (e.g. Setälä and Huhta, 1991) or intact samples are collected with plants on their surface (e.g. Sjørnsen et al., 2005), controlling climate in chambers becomes more complex depending on duration. If an examination lasts longer (about  $308 \pm 96$  days), seasons also are differentiated even with more than one growing periods (e.g. Liiri et al., 2002b). If complex temperature and lighting periods are not set in microcosm experiments but there are plants in them and diurnal temperatures are constant, the studies last for only short time (e.g. Remén et al., 2010). Unique settings are applied when reactions of soil fauna are investigated under special or extreme temperature circumstances (e.g. Sulkava and Huhta, 2003).

In most cases, only temperature and light can be controlled automatically in a climate chamber. Suitable water content of microcosms is generally maintained with gravimetric water supplement. That is, the whole microcosm with suitable water content is weighed at the beginning of the experiment and hereafter this weight is maintained. Tap or distilled water is generally added to the system with spraying or just watering and there is a study in which simulated rainwater is applied (Staddon et al., 2010). Watering frequency depends on evaporation. Mini ecosystems kept in constant darkness and temperature are watered commonly once a week but there are water supplements applied more rarely or twice and three times a week. There are some unique solutions: for example, Wickings et al. (2011) elevated the substrates about 5 mm above water on polypropylene stands in closed jars. Staddon et al. (2010) decreased evaporation by compressing humidified air into the chambers.

During incubation, an essential arrangement is climate control. If the only aim of an experiment is to study the changes of microcosm under given circumstances adjusted at the beginning of the experiment, data will be extracted after the end of the incubation, i.e. microarthropods and other animals will be made run out, abiotic factors will be measured, plant materials will be weighed etc. This method was noted in about 50% of the examined papers. In the other half of the publications examined by us sampling and even other treatments are applied during incubation. Frequency of sampling was very variable: it was 2-6 times during the incubation and the time between sampling ranged from 6 days to 1 year. In half of the cases, the aim of intermediate sampling was tracking the temporal changes in microcosms. In the other half of the papers, the aim of sampling during incubation was monitoring changes after intermediate treatments. Such treatments can be changing the temperature (e.g. Liiri et al., 2002b), or adding predators and /or herbicide to microcosms (e.g. Salminen et al., 1997).

Sampling design depends on the size of the micro ecosystem. If microcosm size is relatively large, subsamples can be collected (e.g. Domes et al., 2007). In other cases, the experiment includes many smaller parallel microcosms and intermediate sampling means the examination of a whole microcosm (e.g. Andres and Domene, 2005). We reckon measuring abiotic factors during intermediate sampling, i.e. measuring CO<sub>2</sub>- and nutrient concentration and, if there are plants in the experiments, also plant biomass can be sampled.

### ***Data extraction from microcosms***

The third phase of experiments is extracting information from microcosms. Depending on starting conditions and logistics, there are many opportunities for data extraction. Information related to oribatid mites can be principally acquired with making them run out from the microcosm. In about half of the relevant studies (13 out of 32), Tullgren funnel is applied for extracting microarthropods. The other 19 experiments used high-gradient extractor. In some experiments, samples are divided into subsamples, from which different animal groups are extracted, because the above mentioned techniques are optimal only for mites, since nematodes, enchytraeids and earthworms have different running characteristics.

Taxonomic examination follows extraction. Part of the studies identified oribatid mites at species level but in others mites were classified into microarthropods used as a single variable. The larger part of microcosm experiments (24 out of 42) with oribatid mites examined the characters of communities or specimens at species level. The other studies relied on family or suborder level. Oribatid mites were examined at species level

when their tolerance, behaviour, feeding habits, role in decomposition, interactions with other organisms and the effects of pollutants or other human disturbance on them were monitored. At family or suborder level, interest was usually focused on either interactions among microorganisms, soil fauna and plants, or the effects of microhabitat complexity on microarthropods or the role of soil fauna in decomposition processes.

In addition to the taxonomic composition of soil fauna, other factors can be measured in a microcosm experiment. In many cases pH, water content, organic matter content, inorganic N-, C- and P-content of organic soil, humus and litter substrates can be measured. The most often examined ions are  $\text{NH}_4^+$  and  $\text{NO}_3^-$ . These soil characteristics were measured in 56% of the studies examined. These values can be compared with changes in community composition and in many cases concentrations of ions and chemicals are monitored during the whole experiment. Maraun et al. (1998) revealed that in presence of oribatid mites leaching of nutrients was greater than in their absence. Nutrients are measured either by mixing water with soil and/or humus samples separately (e.g. Sulkava and Huhta, 2003) or distilled water is made flow over the system and the dissolved ions and other materials can flow through a hole at the bottom of the container into a collecting vessel (e.g. Cole et al., 2004).

Production of  $\text{CO}_2$  and its changes are often measured in microcosms because these serve important information about the degree of microbial activity through respiration intensity. The most general method for measuring  $\text{CO}_2$ -concentration in microcosms is to sample the atmosphere of the mini ecosystem. Then, the microcosm is sealed hermetically for some hours and sampling is carried out (e.g. with a syringe) before sealing and after sealing and finally the difference is calculated. Besides respiration, there are many methods for measuring biomass of bacteria and fungi. This is important in studies examining oribatid mites since most of them feed on fungi and there are also bacteria feeders (Schneider et al., 2004) and many experiments examine the interactions between microorganisms and oribatid mites (e.g. Kaneko et al., 1998).

If there are plants and/or leaf litter in microcosm experiments, characteristics and changes of animal and microbial communities can be compared with those of plant leaves, roots or shoots: i.e. biomass, water content, C-, N-, K- Ca-, Mg contents and lignin, tannin, cellulose content (e.g. Katajisto et al., 1999; Wickings et al., 2011).

## Summary

Microcosm experiments extend our knowledge about oribatid mites living in soil by circumventing difficulties arising from their small size and hidden way of life. Most of these studies were performed under laboratory circumstances. It has to be noted, however, that microcosms are artificial systems and the information extracted from them depends on the conditions we made. Therefore, field experiments should be applied parallel to laboratory studies in all cases because without field data we cannot adopt our results to natural conditions (Kampich et al., 2001).

We could see that there are many aspects we have to consider in planning, composing and maintaining a microcosm. If a researcher has decided to find answers to theoretical questions, like in case of other experiments many setting combinations can be chosen. We could also see that in a laboratory microcosm experiments there is no universal rule for selecting a method, the usefulness, validity and limitations of a given technique do not correlate with research objectives. There are many unique solutions and neither of them can always be declared to be the best for our aims. The size of a

microcosm, the amount of substrate placed in it, abundance and composition of applied animal communities are very variable. We could find many kinds of extraction and incubation methods, experiment duration types and climate chamber settings. Besides this, research issues are very variable so we cannot talk about standardisation with the exception of narrow research fields where the researchers are usually the same (e.g. Sulkava and Huhta, 1998; Sulkava et al., 2001).

Apart from the above difficulties, many useful ideas can be found in other studies. We could see what microcosm experiments can be used for, when only some specimens of a species are studied or when the whole soil community is experimented with. We also saw what kinds of habitats of microarthropods are examined with different manipulations. We could see how a microcosm should be set up; and overviewed the conditions under which the mini ecosystems are kept. We examined how animals can be used for inoculation into defaunated microcosms. If mini ecosystems are ready, then it is important to ensure the natural conditions unless we are interested to see how human impacts modifies microcosm life, this can bring new approaches in the resolution of complex ecological problems (Szlávik and Csete, 2010). In addition, we saw various types of information that can be extracted about the state of microcosms at the end of the experiment.

**Acknowledgements.** The authors gratefully acknowledges the contribution of Prof. János Podani for his kind linguistic help. This work was supported by the Bolyai János Research Scholarship of MTA Doctoral Council, „ALÖKI” Applied Ecological Research and Forensic Institute Ltd., and the TÁMOP 4.2.1/B-09/1/KMR-2010-0005 project.

## REFERENCES

- [1] Adejuyigbe, C.O., Tian, G., Adeoye, G.O. (2006): Microcosmic study of soil microarthropod and earthworm interaction in litter decomposition and nutrient turnover. – *Nutrient Cycling in Agroecosystems* 75(1-3): 47-55.
- [2] Anderson, J.M. (1978): Competition between two unrelated species of soil Cryptostigmata (acari) in experimental microcosms. – *Journal of Animal Ecology* 47(3): 787-803.
- [3] Andres, P., Domene, X. (2005): Ecotoxicological and fertilizing effects of dewatered, composted and dry sewage sludge on soil mesofauna: A TME Experiment. – *Ecotoxicology* 14(5): 545-557.
- [4] Balogh, P., Gergócs, V., Hufnagel, L., Farkas, E., Farkas, P., Kocsis, M. (2008): Oribatid assemblies of tropical high mountains on some points of the “Gondwana-Bridge” – a case study – *Applied Ecology and Environmental Research* 6(3): 127-159.
- [5] Cole, L. Dromph, K.M., Boaglio, V., Bardgett, R.D. (2004): Effect of density and species richness of soil mesofauna on nutrient mineralisation and plant growth. – *Biology and Fertility of Soil* 39(5): 337-343.
- [6] Crotty, F.V., Blackshaw, R.P., Murray, P.J. (2010): Tracking the flow of bacterially derived <sup>13</sup>C and <sup>15</sup>N through soil faunal feeding channels. – *Rapid Communications in Mass Spectrometry* 25(11): 1503-1513.
- [7] Crowther, T.W., Boddy, L., Jones, T.H. (2011a): Species-specific effects of soil fauna on fungal foraging and decomposition. – *Oecologia* 167(2): 535-545.
- [8] Crowther, T.W., Jones, T.H., Boddy, L. (2011b): Species-specific effects of grazing invertebrates on mycelial emergence and growth from woody resources into soil. – *Fungal Ecology* 4(5): 33-341.

- [9] Deere, J.A., Sinclair, B.J., Marshall, D.J., Chown, S.L. (2006): Phenotypic plasticity of thermal tolerances in five oribatid mite species from sub-Antarctic Marion Island. – *Journal of Insect Physiology* 52(7): 693-700.
- [10] Drake, J.M., Kramer, A. (2011): Mechanistic analogy: how microcosms explain nature. – *Theoretical Ecology*, DOI: 10.1007/s12080-011-0134-0.
- [11] Domes, K., Scheu, S., Maraun, M. (2007): Resources and sex: Soil re-colonization by sexual and parthenogenetic oribatid mites. – *Pedobiologia* 51(1): 1-11.
- [12] Fraser, L.H., Keddy, P. (1997): The role of experimental microcosms in ecological research. – *Trends in Ecology and Evolution* 12(12): 478-481.
- [13] Fujikawa, T. (1999): Individual variations of two reared oribatid species, *Tectocephus velatus* (Michael, 1880) and *Oppiella nova* (Oudemans, 1902). – *Edaphologia* 62: 11-46.
- [14] Gergócs, V., Hufnagel, L. (2009): Application of Oribatid Mites as indicators (Review) – *Applied Ecology and Environmental Research* 7(1): 79-98.
- [15] Gergócs, V., Garamvölgyi, Á., Hufnagel, L. (2010): Indication strength of coenological similarity patterns based on genus-level taxon lists. – *Applied Ecology and Environmental Research* 8(1): 63-76.
- [16] Gergócs, V., Garamvölgyi, Á., Homoródi, R., Hufnagel, L. (2011): Seasonal change of oribatid mite communities (Acari, Oribatida) in three different types of microhabitats in an oak forest. – *Applied Ecology and Environmental Research* 9(2): 181-195.
- [17] Heneghan, L., Bolger, T. (1996): Effects of components of 'acid rain' on the contribution of soil microarthropods to ecosystem function. – *Journal of Appl. Ecol.* 33(6): 1329-1344.
- [18] Huhta, V., Wright, D.H., Coleman, D.C. (1989): Characteristics of soil fauna. I: A comparison of three techniques applied to two different forest soils. – *Pedobiologia* 33: 417-426.
- [19] Huhta, V., Sulkava, P., Viberg, K. (1998): Interactions between enchytraeid (*Cognettia sphagnetorum*), microarthropod and nematode populations in forest soil at different moistures. – *Applied Soil Ecology* 9(1-3): 53-58.
- [20] Huhta, V. (2007): The role of soil fauna in ecosystems: A historical review. – *Pedobiologia* 50(6): 489-495.
- [21] Jonsson, L.M., Dighton, J., Lussenhop, J., Koide, R.T. (2006): The effect of mixing ground leaf litters to soil on the development of pitch pine ectomycorrhizal and soil arthropod communities in natural soil microcosm systems. – *Soil Biology & Biochemistry* 38(1): 134-144.
- [22] Kaneko, N., McLean, M.A., Parkinson, D. (1998): Do mites and Collembola affect pine litter fungal biomass and microbial respiration? – *Applied Soil Ecology* 9(1-3): 209-213.
- [23] Kampichler, C., Bruckner, A., Kandeler, A. (2001): Use of enclosed model ecosystems in soil ecology: a bias towards laboratory research. – *Soil Biology and Biochemistry* 33(3): 269-275.
- [24] Katajisto, J., Huhta, V., Laakso, J. (1999): Plant effects on the soil community: A microcosm experiment. – *European Journal of Soil Biology* 35(1): 17-21.
- [25] Kuperman, R.G., Phillips, C.T., Checkai, R.T. (2007): Toxicity of chemical warfare agent HD (mustard) to the soil microinvertebrate community in natural soils with contrasting properties. – *Pedobiologia* 60(6): 535-542.
- [26] Laakso, J., Setälä, H. (1999): Sensitivity of primary production to changes in the architecture of belowground food webs. – *Oikos* 87(1): 57-64.
- [27] Lenoir, L., Persson, T., Bengtsson, J., Wallander, H., Wirén, A. (2007): Bottom-up or top-down control in forest soil microcosms? Effects of soil fauna on fungal biomass and C/N mineralisation. – *Biology and Fertility of Soils* 43(3): 281-294.
- [28] Liiri, M., Haimi, J., Setälä, H. (2002a): Community composition of soil microarthropods of acid forest soils as affected by wood ash application. – *Pedobiologia* 46(2): 108-124.
- [29] Liiri, M., Setälä, H., Haimi, J., Pennanen, T., Fritze, H. (2002b): Relationship between soil microarthropod species diversity and plant growth does not change when the system is disturbed. – *Oikos* 96(1): 137-149.

- [30] Lopez, M.G., Matesanz, M.R., Lidón, J.B.J., Cosín, D.J.D. (2003): The effect of *Hormogaster elisae* (Hormogastridae) on the abundance of soil Collembola and Acari in laboratory cultures. – *Biology and Fertility of Soil* 37(4): 231-236.
- [31] Lopez, M.G., Lidón, J.B.J., Aza, D.T., Rodriguez, M.N., Cosín, D.J.D. (2008): Is there food competition between *Hormogaster elisae* (Oligochaeta, Hormogastridae) and soil microarthropods at El Molar (Madrid)? – *European Journal of Soil Ecol.* 44(2): 207-212.
- [32] Maraun, M., Visser, S., Scheu, S. (1998): Oribatid mites enhance the recovery of the microbial community after a strong disturbance. – *Applied Soil Ecology* 9(1-3): 175-181.
- [33] Maraun, M., Schatz, H., Scheu, S. (2007) Awesome or ordinary? Global diversity patterns of oribatid mites. – *Ecography* 30(2): 209-216.
- [34] Moore, J.C., Trofymow, J.A., Morley, C.R. (1985): A technique to decontaminate soil microarthropods for introduction to gnotobiotic systems. – *Pedobiologia* 28(3): 185-190.
- [35] Moore, de Ruiter, P.C., Hunt, H.W., Coleman, D.C., Freckman, D.W. (1996): Microcosms and soil ecology: critical linkages between field studies and modelling food webs. – *Ecology* 77(3): 694-705.
- [36] Ojala, R., Huhta, V. (2001): Dispersal of microarthropods in forest soil. – *Pedobiologia* 45(5): 443-450.
- [37] Pernin, C., Ambrosi, J.P., Cortet, J., Joffre, R., Petit, J.L., Tabone, E., Torre, F., Krogh, P.H. (2005): Effects of sewage sludge and copper enrichment on both soil mesofauna community and decomposition of oak leaves (*Quercus suber*) in a mesocosm. – *Biology and Fertility of Soils* 43(1): 39-50.
- [38] Rantalainen, M.L., Haimi, J., Setälä, H. (2004): Testing the usefulness of habitat corridors in mitigating the negative effects of fragmentation: the soil faunal community as a model system. – *Applied Soil Ecology* 25(3): 267-274.
- [39] Remen, C., Fransson, P., Persson, T. (2010): Population responses of oribatids and enchytraeids to ectomycorrhizal and saprotrophic fungi in plant – soil microcosms. – *Soil Biology and Biochemistry* 42(6): 978-985.
- [40] Salminen, J., Setälä, H., Haimi, J. (1997): Regulation of decomposer community structure and decomposition processes in herbicide stressed humus soil. – *Applied Soil Ecology* 6(3): 265-274.
- [41] Schneider, K., Maraun, M. (2009): Top-down control of soil microarthropods – Evidence from a laboratory experiment. – *Soil Biology & Biochemistry* 41(1): 170-175.
- [42] Schneider, K., Migge, S., Norton, R.A., Scheu, S., Langel, R., Reineking, A., Maraun, M. (2004): Trophic niche differentiation in soil microarthropods (Oribatida, Acari): evidence from stable isotope ratios ( $^{15}\text{N}/^{14}\text{N}$ ). – *Soil Biology and Biochemistry* 36(1): 1769-1774.
- [43] Setälä, H., Huhta, V. (1991): Soil fauna increase *Betula pendula* growth: laboratory experiments with coniferous forest floor. – *Ecology* 72(2): 665-671.
- [44] Setälä, H. (2000): Reciprocal interactions between Scots pine and soil food web structure in the presence and absence of ectomycorrhiza. – *Oecologia* 125(1): 109-118.
- [45] Sipel, H., Maaskamp, F. (1994): Mites of different feeding guilds affect decomposition of organic matter. – *Soil Biology and Biochemistry* 26(10): 1389-1394.
- [46] Sjørnsen, H., Michelsen, A., Holmstrup, M. (2005): Effects of freeze-thaw cycles on microarthropods and nutrient availability in a sub-Arctic soil. – *Applied Soil Ecology* 28(1): 79-93.
- [47] Smrz, J. (2006): Microhabitat selection in the simple oribatid community dwelling in epilithic moss cover (Acari: Oribatida). – *Naturwissenschaften* 93(11): 570-576.
- [48] Søvik, G., Leinaas, H.P. (2003): Long life cycle and high adult survival in an arctic population of the mite *Ameronothrus lineatus* (Acari, Oribatida) from Svalbard. – *Polar Biology* 26(8): 500-508.
- [49] Staddon, P., Lindo, Z., Crittenden, P.D., Gilbert, F., Gonzalez, A. (2010): Connectivity, non-random extinction and ecosystem function in experimental metacommunities. – *Ecology Letters* 13(5): 543-552.



- [50] Sulkava, P., Huhta, V. (1998): Habitat patchiness affects decomposition and faunal diversity: a microcosm experiment on forest floor. – *Oecologia* 116(3): 390-396.
- [51] Sulkava, P., Huhta, V., Laakso, J., Gylén, E.R. (2001): Influence of soil fauna and habitat patchiness on plant (*Betula pendula*) growth and carbon dynamics in a microcosm experiment. – *Oecologia* 129(1): 133-138.
- [52] Sulkava, P., Huhta, V. (2003): Effects of hard frost and freeze-thaw cycles on decomposer communities and N mineralisation in boreal forest soil. – *Applied Soil Ecology* 22(3): 225-239.
- [53] Szlavik, J., Csete, M. (2010): Climate change and economics of rehabilitation and reconstruction. Chapter 20. – In: *Climate Change and Hungary: Mitigating the Hazard and Preparing for the Impacts (The „VAHAVA” Report)*. (Farago, T., Lang, I., Csete, L. eds.) Budapest, 2010. ISBN 978-963-508-605-4 (pp.109-114)
- [54] Taylor, A.R., Pflug, A., Schröter, D., Wolters, V. (2010): Impact of microarthropod biomass on the composition of the soil fauna community and ecosystem processes. – *European Journal of Soil Biology* 46(2): 80-86.
- [55] Wickings, K., Grandy, A.S. (2011): The oribatid mite *Scheloribates moestus* (Acari: Oribatida) alters litter chemistry and nutrient cycling during decomposition. – *Soil Biology and Biochemistry* 43(2): 351-358.
- [56] Uvarov, A.V. (2003): Effects of diurnal temperature fluctuations on population responses of forest floor mites. – *Pedobiologia* 47(4): 331-339.
- [57] Wallwork, J.A. (1983): Oribatids in Forest Ecosystems. – *Annual Review of Entomology* 28: 109-130.

# CARBON SEQUESTRATION IN EIGHT WOODY NON-TIMBER FOREST SPECIES AND THEIR ECONOMIC POTENTIALS IN SOUTHWESTERN CAMEROON

EGBE, E.A.\* – TABOT, P.T.

*Department of Plant and Animal Science, University of Buea  
P.O. Box 63 Buea, Cameroon  
(phone: + 237 77671037)*

*Corresponding author  
e-mail: [egbe1@yahoo.com](mailto:egbe1@yahoo.com)*

(Received 22<sup>nd</sup> March 2010; accepted 26<sup>th</sup> August 2011)

**Abstract.** Carbon sequestration potentials of 8 woody species were assessed on an ecosystem level, using the CO<sub>2</sub>FIXV.2 model, for two scenarios. Net carbon sequestration potentials ranged from 246.23 to 306.22 Mg C ha<sup>-1</sup> with complete rotation every 40 years, and 292 to 359.3 Mg C ha<sup>-1</sup> with partial cut. *Ricinodendron heudelotii* had the highest net carbon sequestration potential (306.22 and 359.3 Mg C ha<sup>-1</sup> for the complete and partial cuts respectively), while *Cola lepidota* had the least under both scenarios. There were higher carbon stocks in plant biomass than soil for all agroforests under both management regimes. Fine litter had the highest soil carbon fraction and soluble compounds had the least in all the agroforests. Under complete rotation, the agroforests had potential carbon credit values ranging from US\$2756 to \$3264/ha/rotation, and \$ 3114 to \$3678/ha/rotation with partial cut. Partial cuts allowed for higher rates of carbon accumulation, and the farmer always has a standing crop. Economic prioritization showed that *Irvingia wombulu* was the best (US\$6.67/Kg), followed by *Ricinodendron heudelotii* and *Afrostryax lepidophyllus* (\$5.55/Kg) and the least was *Trycocypha abut* (\$0.33/Kg). These results would aid policy makers in mitigating climate change, improving rural livelihoods, and contributing to sustainable development.

**Keywords:** *carbon stocks, CO<sub>2</sub>FIXV.2 model, sustainability, climate change and carbon trade*

## Introduction

Forests are long-lived dynamic systems that are involved in climate regulation. Cameroon's forest (22 million hectares) is of economic, cultural and socio-political importance to the countries of the Congo basin, and of ecological and scientific interest to the rest of the world (Djeumo, 2001). According to Fomete (2001) logging of timber represents approximately 25% of the country's exports. However, agriculture is the main economic activity of more than 80% of the 16 million inhabitants, with both subsistence and extensive plantation schemes. Large expanses of tropical forests are cut yearly to make way for these plantations. This coupled with the agricultural method of slash and burn, poses a threat to the biodiversity of the region, degrades the soil, and emits enormous amounts of greenhouse gases (GHGs). The Global Canopy Program estimates that deforestation accounts for 80% of greenhouse gases. Greenhouse gas emissions and the potential for climate change are the focus of increasing international concern (Cacho et al., 2003; Mutuo et al., 2005; Stern, 2006). However, enhanced greenhouse effect can be mitigated by reducing carbon sources or increasing carbon sinks. Karjalainen et al. (2002) have reported that terrestrial carbon sinks can be strengthened either by increasing the density of vegetation cover in currently vegetated areas or increasing the area covered by vegetation. The former can be achieved by in-

situ conservation and enrichment of woody non-timber forest products (NTFPs) in their natural habitats, and the latter by establishment of agroforestry/plantation schemes in deforested areas.

Agroforestry is eligible under the clean development mechanism of the Kyoto Protocol if carried out on land deforested prior to 1990. Sales of carbon credits will consequently represent both an incentive for conservation and an added value to agroforest systems. But there is lack of empirical data on the carbon sequestration potential of different species, which limits the feasibility of initiating carbon-offset projects (Glenday, 2006; Shin et al., 2007).

This paper evaluates the carbon stocks in eight important woody NTFPs in Southwestern Cameroon under two management regimes (complete and partial cut), it also compares the impacts of farm management on the carbon stocks of different pools, and uses the income-generating potentials of the different NTFPs to determine species with best ecological and economic value.

## Materials and methods

### Study site

The study was carried out in Manyu Division of Southwestern Cameroon. Manyu Division lies at the northwestern end of the region, bordered by UTM coordinates 48234, 629115m to the West, 597372, 615667 m to the East, 572470, 722248 m to the North and 522168, 586781 m to the South (all UTM values based on the N32,WGS 24 base datum). It covers a surface area of about 945720.6 ha. It is a low plateau with undulating topography and an altitude of 135 to 1000 m (Nkwatcho, 2000).

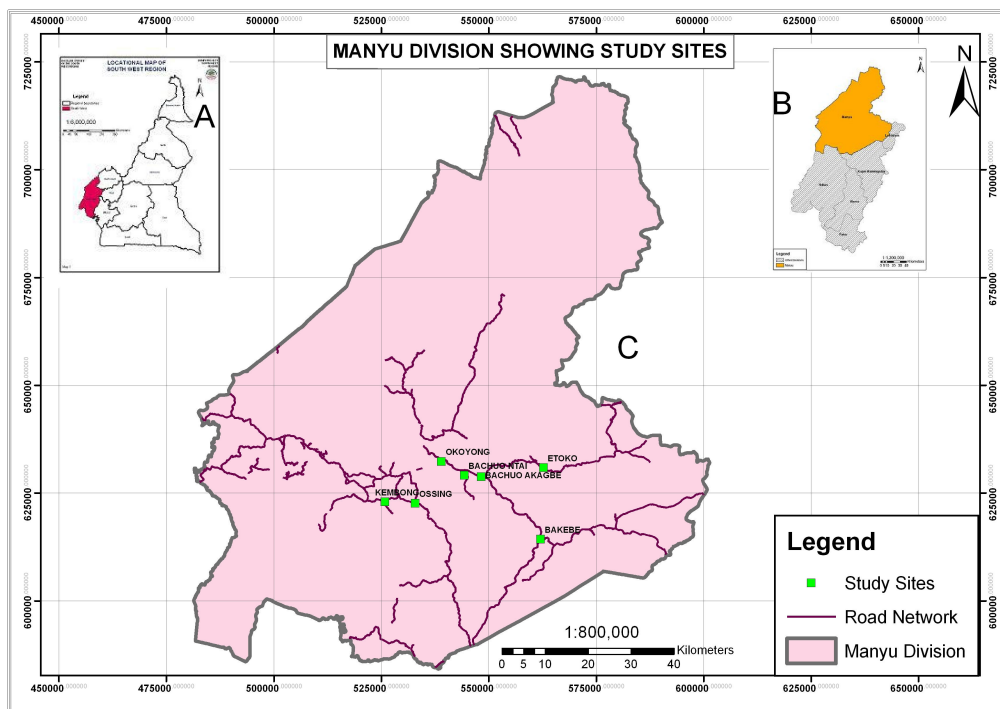


**Figure 1.** A: Map of Cameroon; B: Map of Southwest region and C: Map of Manyu division showing the study sites

There are two seasons, a dry season from November to March, and a wet season from April to October. Mean annual rainfall of 2000-2500 mm is recorded, with a mean annual temperature range of 26 to 35 °C. The natural vegetation is the lowland equatorial rainforest, interspersed with secondary regrowth as a result of agricultural practices and logging of timber in some areas. Its forests have a higher diverse flora, richer in species than any other African rainforest for which comparable data are available (Nkwatoh, 2000). The soils are acidic and predominantly sandy-loam which are heavily leached as a result of low water retention capacity and frequent heavy rainfall. Agriculture is the main economic activity, with previously large expanses of vegetation replaced by agroforestry schemes ranging from subsistence farms and smallholder schemes to private plantations.

### **Methods**

A reconnaissance survey was carried out to select possible study locations. Eight locations were selected namely, Bakebe, Bachuo-Akagbe and Etoko, all in Upper Banyang subdivision; Okoyong, Bachuo-Ntai and Besongabang in Mamfe Central subdivision as well as Kembong and Ossing in Eyumojock subdivision (*Fig. 1*). The selection of study locations was based on the population, farming practices and accessibility. Leaders of farmers' groups and guides were identified in the various locations.

The study species were Bitter cola (*Garcinia cola*), Dry season bush mango (*Irvingia wombulu*), Rainy season bush mango (*Irvingia gabonensis*), Monkey cola (*Cola lepidota*), Plum (*Dacryodes edulis*), Okoyong fruit (*Trichocypa abut*), Njangsa (*Ricinodendron heudelotii*) and contry onion (*Afrostryax lepidophyllus*).

Plant parameters determined included stem diameter, height and wood density. An average of 50 plants per species and a total of 400 plants were measured, in the field. Stem diameters were measured at breast height (Masera et al., 2003), using a diameter tape. Plant heights were measured using a 2 m range pole and estimated by the ruler method. This method was preferred to the altimeter-based measurement because of the closed canopy in most of the study sites. Standing volumes were calculated (at  $R^2 > 90\%$  and standard error = 1.283) from the dbh using the power 2 equation in Eba'a Atyi (2000) below:

$$V = 8.872(DBH)^{2.270}$$

Where:

V = standing volume, and

DBH = Diameter at breast height.

The diameters were graded into five classes based on the life stage of the plants (biomass/maximum biomass), for each species, and the current annual increments calculated as the difference in volume between successive stages. Turnover rates were used for roots (0.05), branches (0.05) and leaves (0.6-0.8) based on field observations.

Leaf litter was collected from three 50 × 50 cm quadrats set randomly at the base of the plants, within one metre from the tree. In each quadrat, all litter was collected and the leaf litter of the species sorted out and bulked in labelled polybags. The litter was weighed, and sub samples of 200g put in aluminium foil and oven-dried at 60 °C for 72

hours, then reweighed. These samples were then milled in a plant mill and sieved in a 1mm sieve. Organic carbon was determined by ashing 10 g of the milled sample in a Kendro furnace at 550 °C for 2 hours (Gallardo et al., 1987; Delaney et al., 1997; Matthiessen et al., 2005). The carbon content of the litter was calculated as the difference between the oven-dried mass and the resultant ash.

Soil samples were collected systematically from one metre from the stands of each species and from newly cleared adjacent forest, and used to determine the initial situation of soil carbon at the time of establishment of these agro-ecosystems. Soil samples were collected from three depths viz 0-10, 10-20 and 20-30 cm using a soil auger. Soil samples of the same depth were bulked into labelled polybags. These samples were air-dried for three weeks, sieved in a 2mm sieve, and further dried in an oven at 105 °C for 72 hours. The carbon content was determined by ashing 10 g of the soil in a Kendro furnace at 550 °C for 2 hours. The carbon content of the soil was calculated as the difference between the oven-dried mass and the resultant ash. All carbon values were expressed as a percentage of the soil mass for the plough layer per hectare ( $2 \times 10^6$  Kg/ha). The soil module of CO2FIXV.2 was adjusted for the specific study location by adjusting the potential evapotranspiration based on mean monthly temperature and mean monthly rainfall for the year 2006.

Wood densities of the different species were determined according to the methodology established by Delaney et al. (1997). For plants whose stems could not be got, average wood density values were gotten from Gisel et al. (1992). The resulting data were used as inputs into the CO2FIXV.2 model for carbon stocks simulations.

Carbon stocks were simulated as a function of tree size, using the CO2FIXV.2 approach. This is an ecosystem-based method in which complete carbon accounting is applied (Masera et al. 2003). Two management regimes were simulated, that is, complete rotation in which all the plants are cut and simultaneously replanted every 40 years, and partial cut in which half of the plantation is cut and simultaneously replanted every 40 years, while the other half continues production for another 10 years before being cut. We term this intervening 10 years between the first half-cut and the second a 'shunt gap'. The simulation length, which is the entire duration of cultivation at the same site, was 200 years, while the rotation length/period which is the economic lifespan of the plantation, is 40 years. The rate of carbon accumulation was calculated by dividing the stock at any time interval, by the time elapsed (Eq.1):

$$Rc = \frac{Ct}{t} \quad (\text{Eq.1})$$

where Rc is the rate of carbon accumulation, Ct is the carbon stock at time t, and t is the time elapsed.

The value of sequestered carbon in the international market was determined by multiplying the mean carbon stock for the rotation by \$10 (mean price per Mg C) (Eq.2 and Eq.3):

$$X = Cm \times \$10 \quad (\text{Eq.2})$$

and

$$Cm = \frac{C1+C2+C3+C4+C5}{5} \quad (\text{Eq.3})$$

where X is the cash value of sequestered carbon,  $C_m$  is the mean carbon stock (Mg/ha) for a rotation, and C1, C2, C3, C4 and C5 are the carbon stocks at the end of the different cycles, \$=US dollars.

Net carbon stocks were calculated by subtracting the carbon stock at the end of the simulation period from the initial carbon stock in the system, and used in the determination of 'best ecology and best economy model'.

The economic value of the different species was evaluated using semi-structured questionnaires. Participatory rural appraisal (PRA) was used to administer an average of 30 questionnaires in each of the study locations, making a total of 240 questionnaires. For the purpose of this paper, only the farm gate prices of produce were used, for the economic potentials of these plants. Farm gate prices were determined from the selling price of produce per kilogram at the various sites. Multivariate analysis was used to determine species with best income-generating and carbon sequestration potentials.

## Results

At the end of the simulation period, total carbon stocks ranged from 277.38 to 337.37 Mg ha<sup>-1</sup> with complete rotation and 323.15 to 390.45 Mg ha<sup>-1</sup> with partial cut. *Ricinodendron heudelotii* was found to have the highest carbon sequestration potential of all species studied, while *Cola lepidota* had the least under both regimes. Under complete rotation, *R. heudelotii* would sequester 300.36 Mg C ha<sup>-1</sup> in biomass while *Cola lepidota* had the least potential and sequesters 247.42 Mg C ha<sup>-1</sup> (Fig. 2). In partial cut, biomass carbon stocks in the first rotation ranged from 125.97 to 152.69 Mg C ha<sup>-1</sup>, with *R. heudelotii* having the highest and *Cola lepidota* the least stock. Carbon stocks in plant at the fifth rotation ranged from 147.84 to 173.43 Mg C ha<sup>-1</sup> with the highest stock in *R. heudelotii* and the least in *Cola lepidota* agroforests (Fig. 3).

Under complete rotation total soil carbon stocks in the first rotation ranged from 53.38 to 75.36 Mg C ha<sup>-1</sup> and in the fifth rotation it had a range of 56.87 to 81.25 Mg C ha<sup>-1</sup> with *R. heudelotii* having the highest, and *D. edulis* the least stock in both situations (Fig. 4). The first rotation under the partial cut regime had a range of 35.62 to 63.5 Mg C ha<sup>-1</sup>, while the fifth rotation had a range of 43.84 to 72.29 Mg C ha<sup>-1</sup> and *G. cola* had the highest, and *A. lepidophyllus* the least stock in both situations (Fig. 5). Tables 1a and 1b show soil carbon stocks in the various fractions under the different management regimes. Fine litter had the highest carbon stock, followed by humus and coarse litter, non-woody litter, holocellulose, lignin and soluble compounds, for most of the species; except for *R. heudelotii*. In complete rotation, the carbon stocks in the different soil carbon fractions in *R. heudelotii* had the following trend; coarse litter (170.11 Mg C ha<sup>-1</sup>) > fine litter (34.49 Mg C ha<sup>-1</sup>) > humus (28.67 Mg C ha<sup>-1</sup>) > non-woody litter (11.42 Mg C ha<sup>-1</sup>) > holocellulose (2.63 Mg C ha<sup>-1</sup>) > lignin (2.16 Mg C ha<sup>-1</sup>) > soluble compounds (1.33 Mg C ha<sup>-1</sup>). In *Cola lepidota* with the least stocks, the trend was fine litter (20.66 Mg C ha<sup>-1</sup>) > humus (17.3 Mg C ha<sup>-1</sup>) > coarse litter (7.82 Mg C ha<sup>-1</sup>) > non woody litter (7.76 Mg C ha<sup>-1</sup>) > holocellulose (1.82 Mg C ha<sup>-1</sup>) > lignin (1.51 Mg C ha<sup>-1</sup>) > soluble compounds (0.94 Mg C ha<sup>-1</sup>). Under the partial cut regime, *R. heudelotii* had soil carbon fractions with the range of 1.36 to 98.94 Mg C ha<sup>-1</sup> with coarse litter > humus > fine litter > non woody litter > holocellulose > lignin > soluble compounds. The pattern of carbon fractions in *Cola lepidota* showed that humus had the highest stock (19.52 Mg C ha<sup>-1</sup>) and soluble compounds the least (0.94 Mg C ha<sup>-1</sup>).

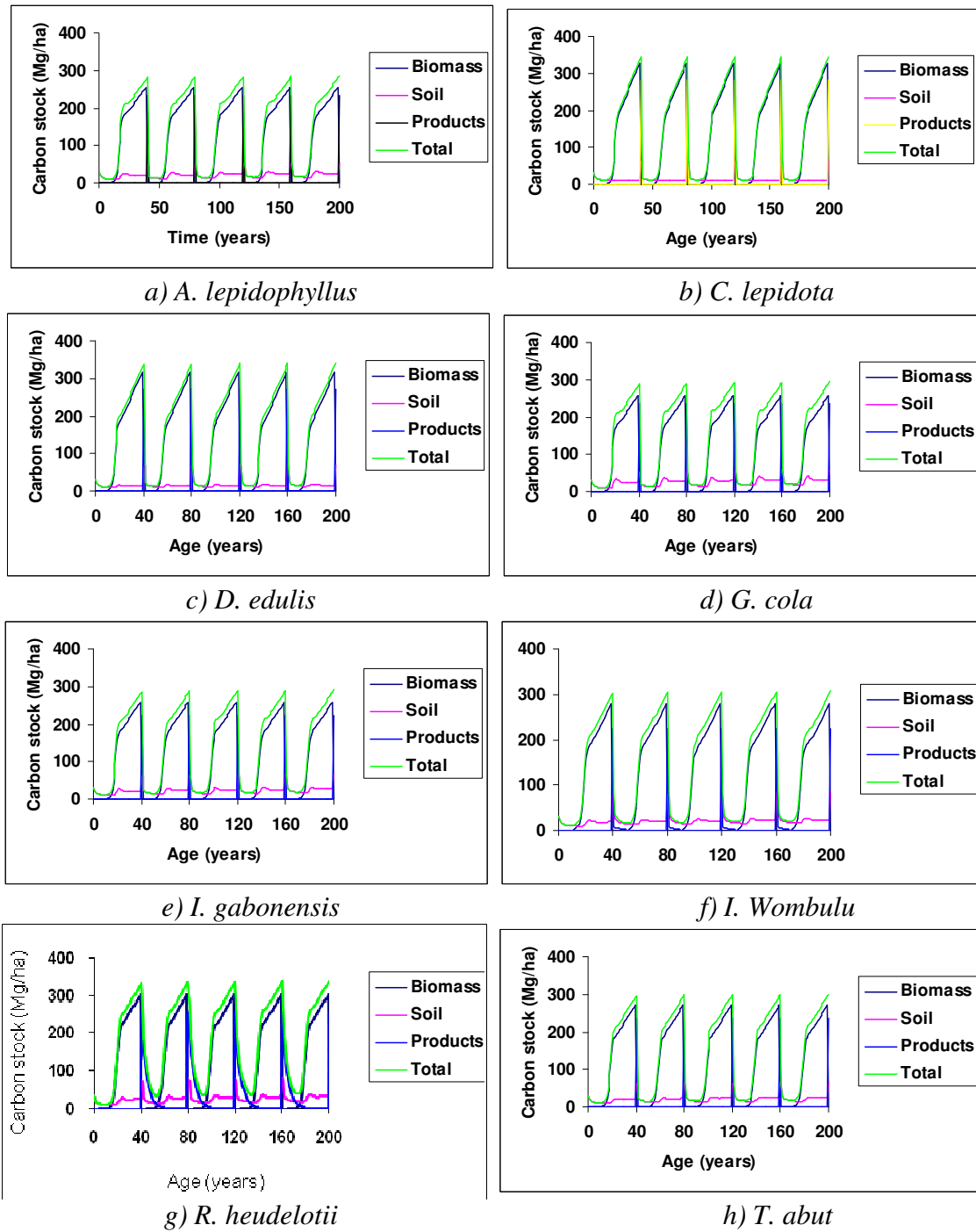


**Figure 2.** Carbon sequestration in the different agroforests with complete rotation every 40 years, for five cycles

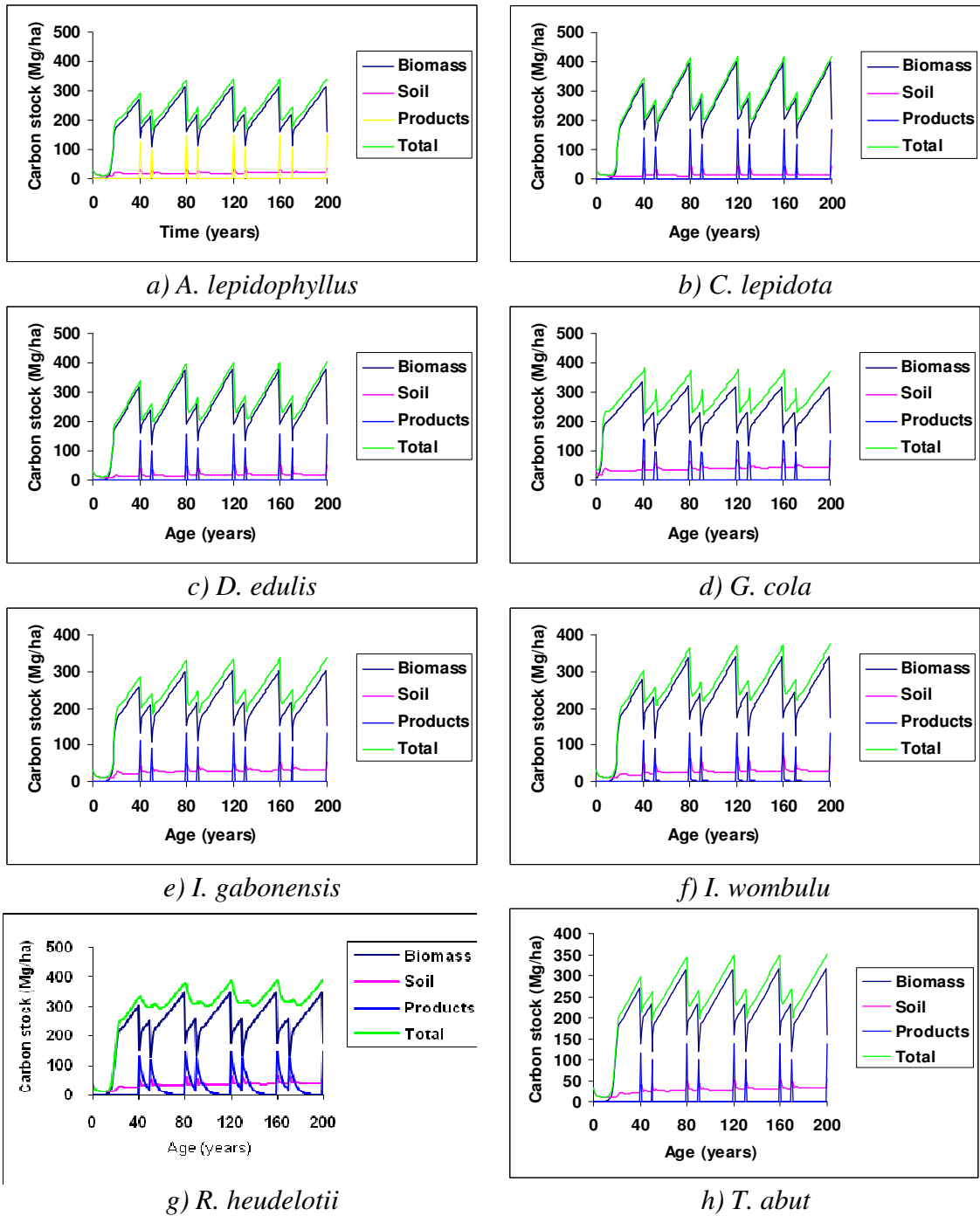


**Figure 3.** Carbon sequestration in the different agroforests with partial cut every 40 years, and a shut gap of 10 years, for five cycles



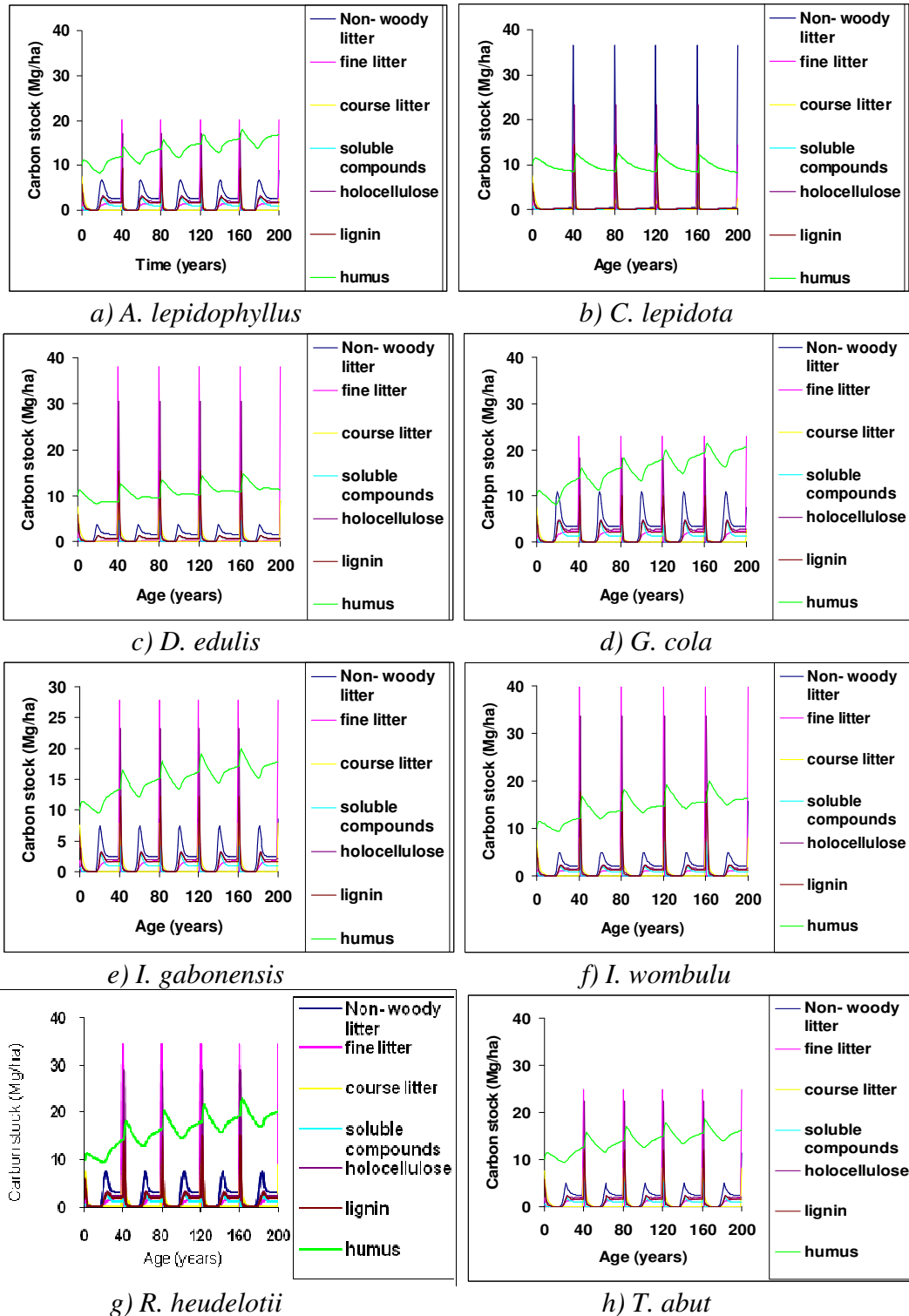


**Figure 4.** Soil carbon dynamics in the different agroforests with complete rotation every 40 years, for five cycles

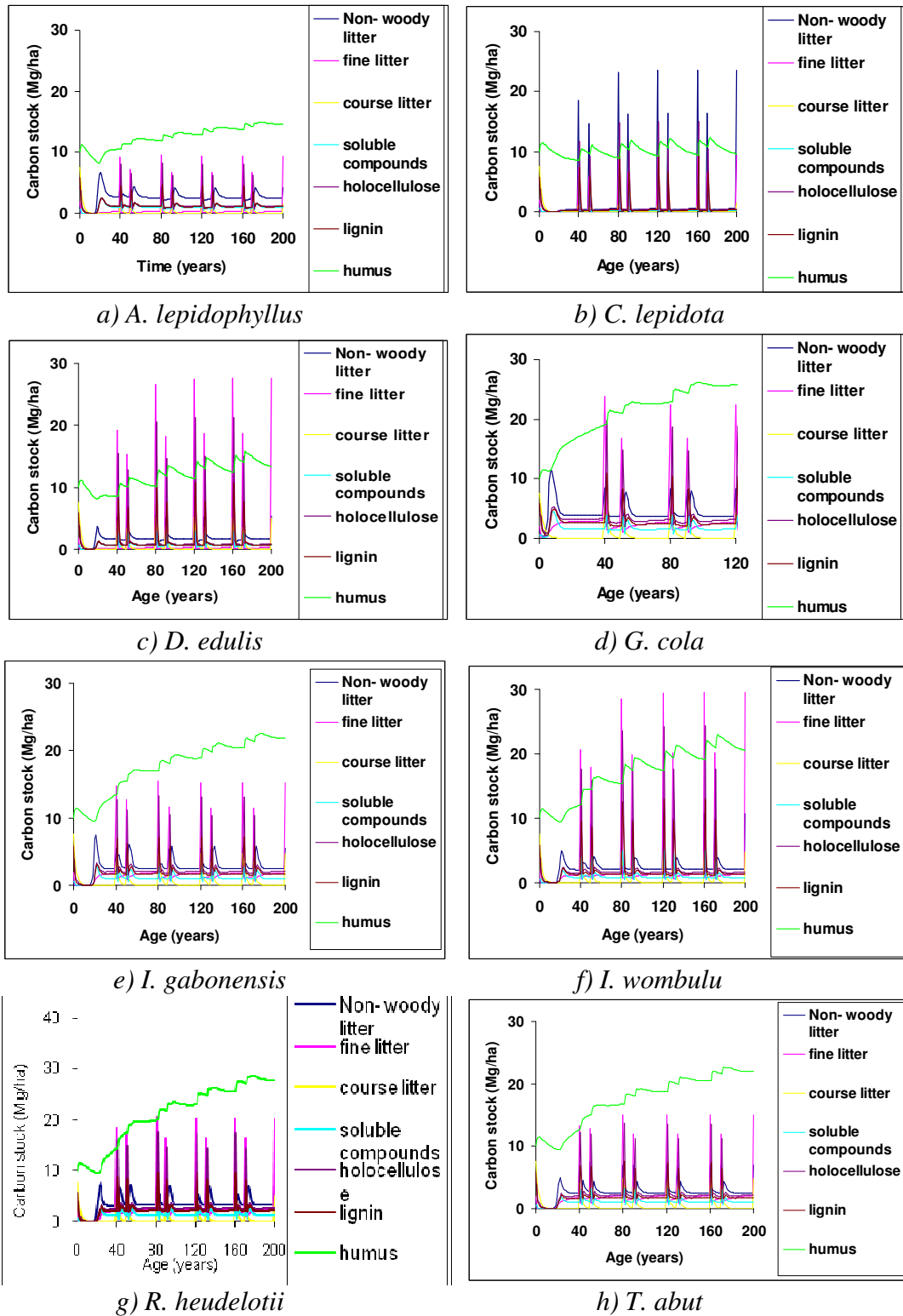


**Figure 5.** Soil carbon dynamics in the different agroforests with partial cut every 40 years and a shunt gap of 10 years, for five cycles

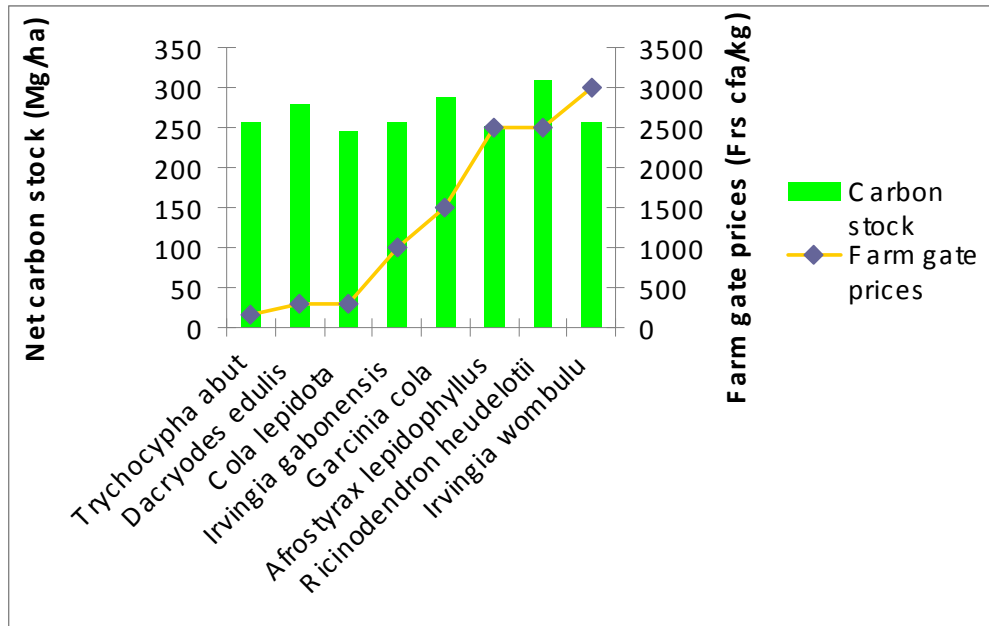


Figure 6. a. Net carbon stock and income generating potential with complete rotation cut of eight NTFPs

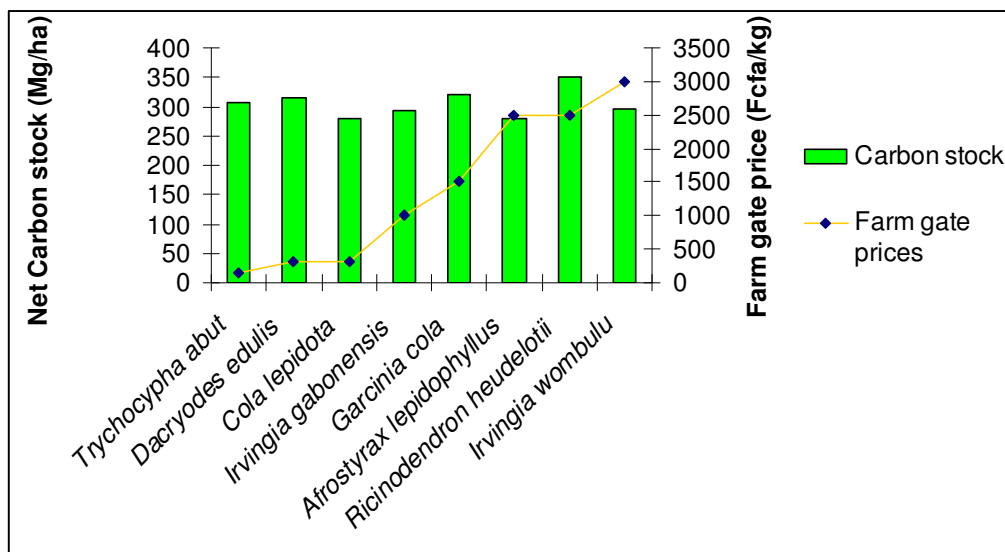


Figure 6. b. Net carbon stock and income generating potential in partial cut of eight NTFPs

Table 2 shows the mean carbon stocks and accumulation rates of the different agroforests after five rotations. Mean carbon stocks for complete rotation had a range of 275.65 to 399.59 Mg C ha<sup>-1</sup>, and mean carbon accumulation rates in this case had a range of 6.89 to 8.48 Mg C ha<sup>-1</sup>yr<sup>-1</sup>. Under the partial cut regime, mean carbon stocks ranged from 311.40 to 380.51 Mg C ha<sup>-1</sup> and the mean rate of carbon accumulation in the different ecosystems ranged from 7.78 to 9.51 Mg C ha<sup>-1</sup>yr<sup>-1</sup>. *Ricinodendron heudelotii* had the highest mean sequestration rate and *Cola lepidota* the least, under both management regimes.

Figures 6a and 6b shows species prioritization, and the carbon credits value of the different species under the two management regimes. *Irvingia wombulu* had the highest farm-gate price of 3000 frs cfa (\$6.67) per kilogram while *Trichocypha abut* had the least, 150 frs cfa (\$0.33) per Kg. Carbon credits potentials of the agro-ecosystems studied ranged from US\$ 2756 to \$3264 ha<sup>-1</sup> (1,102,400 to 1,305,600 frs cfa ha<sup>-1</sup>) for each complete rotation while with partial cut, the range was US\$3114 to 3678 ha<sup>-1</sup> (1,245,600 to 1,471,200 frs cfa ha<sup>-1</sup>) per rotation (1USD = 400frs cfa).

**Table 1. a.** Soil carbon fractions of species with complete rotation every 40 years

Species	Soil carbon fraction (Mg C/ha)						Humus
	Non-woody litter	Fine litter	Coarse litter	Soluble compounds	Holo-cellulose	Lignin	
<i>Afrostryrax lepidophyllus</i>	12.11	22.93	7.86	1.00	1.94	1.60	17.40
<i>Cola lepidota</i>	7.76	20.66	7.82	0.94	1.82	1.51	17.30
<i>Dacryodes edulis</i>	8.88	20.98	9.20	0.78	1.72	1.38	13.93
<i>Garcinia cola</i>	12.97	43.69	7.54	1.53	3.22	2.61	25.62
<i>Irvingia gabonensis</i>	8.61	27.81	7.90	1.01	2.08	1.69	17.85
<i>Irvingia wombulu</i>	12.21	25.11	7.89	1.01	2.03	1.66	17.11
<i>Ricinodendron heudelotii</i>	11.42	34.49	170.11	1.33	2.63	2.16	28.67
<i>Trichocypha abut</i>	11.50	24.76	8.26	0.99	2.06	1.67	16.23

**Table 1. b.** Soil carbon fractions of species with partial cut every 40 years and a shunt gap of 10 year

Species	Soil carbon fraction (Mg C/ha)						Humus
	Non-woody litter	Fine litter	Coarse litter	Soluble compounds	Holo-cellulose	Lignin	
<i>Afrostryrax lepidophyllus</i>	6.64	9.88	4.73	0.94	1.76	1.47	18.36
<i>Cola lepidota</i>	5.05	10.58	4.76	0.94	1.77	1.47	19.62
<i>Dacryodes edulis</i>	5.42	12.01	5.31	0.78	1.80	1.43	17.08
<i>Garcinia cola</i>	8.36	22.40	4.58	1.52	3.14	2.55	29.75
<i>Irvingia gabonensis</i>	5.58	15.21	4.72	1.02	2.12	1.72	21.79
<i>Irvingia wombulu</i>	7.39	14.27	4.71	1.02	2.11	1.72	21.56
<i>Ricinodendron heudelotii</i>	7.45	20.36	98.94	1.36	2.38	2.30	36.48
<i>Trichocypha abut</i>	7.04	14.97	4.87	1.00	2.23	1.79	21.94

**Table 2.** Mean carbon stocks and carbon accumulation rates after five rotations of the different agroforest ecosystems

Species	Mean carbon stocks per rotation			
	Complete rotation		Partial cut	
	Carbon stock (Mg C/ha)	Carbon accumulation rate (Mg C/ha/yr)	Carbon stock (Mg C/ha)	Carbon accumulation rate (Mg C/ha/yr)
<i>Cola lepidota</i>	275.65	6.89	311.48	7.78
<i>Afrostryax lepidophyllus</i>	283.60	7.09	311.40	7.78
<i>Irvingia wombulu</i>	288.78	7.21	325.78	8.14
<i>Irvingia gabonensis</i>	288.83	7.22	324.75	8.11
<i>Trichocypha abut</i>	298.77	7.46	337.93	8.44
<i>Dacryodes edulis</i>	311.28	7.78	344.91	8.62
<i>Garcinia cola</i>	318.94	7.97	352.53	8.81
<i>Ricinodendron heudelotii</i>	339.59	8.48	380.51	9.51

## Discussion

The range of total carbon stocks of both complete and partial cut obtained in this study falls within the range obtained by other authors such as Delaney et al. (1997) and Shin et al. (2005) and could be explained by intrinsic differences in the plants, as well as the management system simulated. Plant age, wood density and tree volume are some determinants of carbon stocks in plants. In the different agroforests studied, all these factors have contributed to give the observed trend. Since all agroforests were modeled based on the same time scale, the contribution of time to the observed differences is bound to be minimal. Thus the final observed stocks are as a result of synergistic effects of volume increment and wood density as the main determinants. Volume increment gives a measure of the biomass growth while wood density determines the actual proportion of carbon represented in plant biomass, and both were found to be inversely proportional. The highest stocks in *R. heudelotii* can be explained by the very high rate of diameter increment in this species. It had the highest current annual increment of all species studied, and consequently the highest carbon stocks, in spite of its relatively low wood density. This is consistent with the findings of Vieira et al. (2005) who reported higher carbon stocks in plants with a higher rate of diameter increment. Wood density also influenced the observed pattern, probably by influencing the current annual increment of the species. Apart from *R. heudelotii*, carbon sequestration potentials in the other NTFPs reflect an interplay between wood density and diameter increment. Thus *Garcinia cola* with the highest wood density (0.78g/cm<sup>3</sup>), has the second sequestration potential after *R. heudelotii*, with complete rotation. These findings are consistent with those of Rahayu et al. (2005) who reported higher carbon stocks in land use systems consisting of trees with high wood densities compared to those with low wood densities and similar diameters, implying a direct role for diameter increment in carbon sequestration.

Net carbon stocks in biomass were higher for most of these species than average biomass of moist tropical forests (241Mg ha<sup>-1</sup>). Pure stands of high-density trees are bound to have higher carbon stocks than those in mixed stands of tropical forests, with most having low wood density and diameters. Moreover, logging of timber reduces

carbon stocks of the tropical forests (Masera et al., 2003). Carbon stocks in biomass were constant at the end of each complete rotation, but increased progressively under the partial cut regime. This might be principally due to the management system. For the complete rotation there is complete clear-felling every 40 years, whereas in partial cut, during each cycle, half of the plantation is cut and later regenerate while the other half continues to accumulate carbon, and the rotation cycle will only be complete ten years later when the newly established half of the plantation is already a net carbon sink. The carbon stocks at the end of the shunt gap thus include carbon stocks of the un-cut section, and carbon accumulated in the replanted section. This system is economically more productive than complete rotation where the whole plantation is clear-felled. Carbon sequestration potentials in the current study are closely related to findings by Kotto-Same et al. (1997), Niles et al. (2002), Vieira et al. (2005).

Soil carbon stocks of most species were within the range obtained by Lasco et al. (2005) who reported a range of 30.7 to 106.2 Mg C ha<sup>-1</sup> for soil carbon in a selectively logged Dipterocarp forest while Delaney et al. (1997) found a range of 73 to 319 Mg C ha<sup>-1</sup> in a study carried out in Venezuela. Generally, organic matter is added to the soil during each rotation, accounting for the increase in soil carbon of the species studied, across the different rotation cycles. During the first 3 years in both management regimes, there is a drop in soil carbon. This could be attributed to the increased decomposition and leaching as well as low inputs primarily from litter and roots turnover, following site disturbances that accompany establishment of the agroforests. At the end of the first complete rotation, there is a sharp increase in soil carbon, higher than the case for partial cut. This may be due to the higher organic inputs following complete clear-felling resulting in peaks of coarse litter, soluble compounds, and fine litter and other component at the end of each rotation. These components are however short-lived due to rapid decomposition, increase in microbial respiration, biological oxidation and consequently, most of the carbon is emitted to the atmosphere while soluble compounds are rapidly leached. Humus is therefore the most permanent component of soil carbon. The lower soil carbon stocks in the current study with partial cut by the fifth cycle as compared to complete rotation may equally be as a result of the management system, which influence organic matter inputs, decomposition and retention of carbon in soils. In *Afrostryax lepidophyllus* agroforest for instance, with complete rotation, soil carbon increases from 31.15 Mg C ha<sup>-1</sup> to 59.41 Mg C ha<sup>-1</sup> in 40 years (end of rotation), with the addition of 28.26 Mg C ha<sup>-1</sup> from the cut plants and litter turnover. 10 years later, there is actually a loss of 59% (18.41Mg C ha<sup>-1</sup>) of original soil carbon but by the next rotation, net carbon added to the soil increases to 61.24 Mg C ha<sup>-1</sup>, a rate of 0.75 Mg C ha<sup>-1</sup>yr<sup>-1</sup> between rotations. With partial cut, the corresponding sequestration rate over the same period is 0.07 Mg C ha<sup>-1</sup>yr<sup>-1</sup> between rotations.

Partial cuts allow for slower accumulation of organic matter in the soil since organic inputs at each half cut are less, coupled with higher rates of decomposition and leaching than with complete rotation, and resulting to lower carbon retention in soils. The trend of soil carbon sequestration in the two management regimes is thus in conformity with the findings of Pretty et al. (2002). They reported net carbon sequestration increases with management practices that increase plant material returned to, and retained in the soil. But the rates of carbon sequestration in soils (1.40 to 6.11 Mg ha<sup>-1</sup> with complete rotation and 1.03 to 3.92 Mg ha<sup>-1</sup> under the partial cut regime) are contrary to the

findings of Palm et al. (2000) who reported insignificant variation in soil carbon stocks due to the low sequestration potential in tropical soils (0.3 to 0.6 Mg ha<sup>-1</sup>yr<sup>-1</sup>).

Consistently, total soil carbon stocks are less than carbon stored in plant biomass. Furthermore, the ratio of soil to biomass carbon is highly dependent on the end uses of the cut wood. While 95% of the cut wood is exported from the site and used as energy for the other species, further reducing organic inputs to soil and resulting in lower soil sequestration. In *R. heudelotii*, the wood quality is very poor for fuel wood and when cut, is often left onsite to decay, resulting in an approximately equal ratio between biomass and soil carbon under both management regimes. These results for soil carbon in *R. heudelotii* corroborate studies carried out by Delaney et al. (1997) who reported higher carbon stock in soils as opposed to plant biomass, in three out of five life zones in Venezuela, in which felled wood was allocated to soil carbon. Tschakert et al. (2007) also reported that soils in an evergreen Tropical rainforest in Panama accounted for 45 to 73% of total carbon.

The rate of carbon accumulation varied between species and the management system. The rates of sequestration are dependent on the combined effect of the wood densities and volume increments of the species, and are higher with partial cut since this system favours carbon accumulation in biomass, and the higher soil sequestration rates with complete rotation are not enough to compensate. These findings are consistent with those of Niles et al. (2002) who reported carbon accumulation rates of 2.5 to 5.0 Mg C ha<sup>-1</sup>yr<sup>-1</sup> for humid tropical regions, but are contrary to those of Kotto-Same et al. (1997) for an 8 year old fallow in Cameroon (28.12 Mg C ha<sup>-1</sup>yr<sup>-1</sup>), in spite of similar climatic and site characteristics, similar land use trends as well as similarity in the flora of the different sites.

*Irvingia wombulu* was the most prioritized species due to its high farm-gate price, while *T. abut* was the least prioritized. Farm gate prices were the preferred index of prioritization because they are the most authentic measure of the income farmers realize from sales of their produce. For a 'best ecology and economy' scenario, *I. wombulu* was the species of choice, followed by *R. heudelotii*, while *T. abut* was the least. This is because although *T. abut* had a high carbon sequestration potential, its income generating potential was very low. These findings are similar to those of Niles et al. (2002) who reported that for CDM reforestation projects, NTFPs are vital as opposed to established timber species, for both technical and rural livelihoods purposes.

The higher potential carbon credit values of the different agroforests with partial cut as opposed to complete rotation is due to the higher rates of carbon accumulation under the partial cut regime. Moreover, this potential value of carbon in the international market will serve as added value to agroforest systems, in addition to social, economic and environmental benefits, if implemented appropriately (IPCC, 2001). Coupled with prioritization, species with best ecological and economic potentials can be chosen for climate change mitigation schemes.

## Conclusion

NTFPs have significant potentials in climate change mitigation through carbon sequestration. Generally, carbon sequestration potentials depended on both wood density and volume increments. Management regimes are relevant to any agroforest carbon project. Partial cut could be tailored to ensure net sequestration and used in preference to complete rotation to mitigate climate change and improve rural

livelihoods. These results would aid policy makers, researchers and investors in Clean Development Mechanism projects.

**Acknowledgements.** We thank Masera, O.R., Garza-Caligaris, J.F., Kanninen, M., Karjalainen, T., Liski, J., Nabuurs, G.J., Passinen, A., De Jong, B.H.J. and Mohren, G.M.J. for providing us with a copy of the CO2FIXV.2 software, and the farmers/communities in Manyu Division where this study was carried out.

## REFERENCES

- [1] Bele, M.Y. (2003): Inventory, distribution and uses of the Annonaceae of Mount Cameroon. – M.Sc. thesis, University of Buea, 147 pp.
- [2] Boateng, S.A. (2005): How much carbon do Ghana's Teak Plantations sequester? – ITTO Tropical Forest Update 15(4): 22-23.
- [3] Brennan, S., Wittgott, J. (2005): Environment, the science behind the stories. – Macgraw Hills.
- [4] Cacho, O.J., Hean, R.L., Wise, R.M. (2003): Carbon accounting methods and reforestation incentives. – Australian Journal of Agriculture and Resource Economics 47(2): 153-179.
- [5] Climate Network Africa (2004): Contraction and Convergence. – Workshop Report, Nairobi. 33 pp.
- [6] Delaney, M., Brown, S., Lugo, A.E., Torres-Lezama, A., Quintero, N.B. (1997): The distribution of organic carbon in major components of forests located in five life zones of Venezuela. – Journal of Tropical Ecology 13: 697-708.
- [7] Djeumo, A. (2001): Development of community forests in Cameroon: Origins, Current situation and Constraints. – Rural Development Forestry Network Paper 25(b): 1-17.
- [8] Eba'a Atyi, R. (2000): TROPFOMS: A Decision Support Model for Sustainable Management of South-Cameroon's Rain forests. – TROPEBOS International Publication; Cameroon Series 2. 202 pp.
- [9] ECCM (2002): Carbon sinks in the Amazon. – The Edinburg Centre for Carbon Management. Technical Note. 5 pp.
- [10] Elbakkidze, L., Mccarl, B.H. (2007): Sequestration offsets versus direct emission reductions: consideration of environmental co-effects. – Ecological Economics 60(3): 564-571.
- [11] Fomete, T. (2001): The forestry taxation system and the involvement of local communities in Forest Management in Cameroon. – Rural Development Forestry Network Paper 25(b): 17-27.
- [12] Gallardo, J.F., Saavedra, J., Martin-Patino, T., Millan, A. (1987): Soil Organic matter determination. – Communications in Soil Science and Plant analysis 18(6): 699-707.
- [13] Gisel, R., Sandra, B., Jonathan, C., Ariel, L.E. (1992): Wood densities of tropical species. – US department of agriculture, Forest Service, South West Experimental Station. New Orleans. 15 pp.
- [14] Glenday, J. (2006): Carbon storage and emission offset potential in an east African Tropical Rain forest. – Forest Ecology and Management 235(1-3): 72-83.
- [15] Gronkvist, S., Mollerstern, K., Pingoud, K. (2006): Equal opportunity for Biomass in greenhouse gas accounting of CO2 capture and storage: a step towards more cost effective climate change mitigation regimes. – Mitigation and Adaptation Strategies for Global Change 11(5-6): 1083-1096.
- [16] Houghton, R.A. (2005): Above ground forest biomass and the global carbon balance. – Global Change Biology 11: 945-958.
- [17] Karjalainen, T., Pussinem, A., Liski, J., Nabuurs, G., Erhard, M., Eggers, T., Sonnteg, M., Mohren, G.M.J. (2002): An approach towards an estimate of the impact of forest



- management and climate change on the European Forest Sector carbon budget: Germany as a case study. – *Forest Ecology and Management* 162: 87-103.
- [18] Kotto-Same, J., Woomer, P.L., Appolinaire, M., Louis, Z. (1997): Forest dynamics in slash and burn agriculture and landuse alternatives of the humid forest zone in Cameroon. – *Agriculture, Ecosystem & Environment* 65(3): 245-256.
- [19] Lasco, R.D., MacDicken, K.A., Pulhin, F.B., Guillermo, I.Q., Sales, R.F., Cruz, R.V.O. (2005): Carbon stocks in a selectively logged Dipterocarp forest. – *Journal of Tropical Forest Science* 18(14): 166-172.
- [20] Maser, O.R., Garza-Caligaris, J.F., Kanninen, M., Karjalainen, T., Liski, J., Nabuurs, G.J., Passinen, A., De Jong, B.H.J., Mohren, G.M.J. (2003): Modelling carbon sequestration in Afforestation, agroforestry and forest management projects: the CO2FIXV.2 Approach. – *Ecological Modelling* 164: 177-199.
- [21] Matthiesen, M.K., Lamey, F.J., Selinger, L.B., Olson, A.F. (2005): Influence of loss-on-ignition temperature and heating time on ash content of compost and manure. – *Communications in Soil Science and Plant Analysis* 36(17-18): 2561-2573.
- [22] Mccarl, B.A., Metting, F.B., Rice, C. (2007): Soil carbon sequestration. – *Climatic Change* 80(1-2): 1-3.
- [23] Mccarl, B.A., Sands, R.D. (2007): Competitiveness of terrestrial Greenhouse Gas offsets: Are they a bridge to the future. – *Climatic Change* 80(1-2): 109-126.
- [24] Mutuo, P.K., Cadisch, U., Albrecht, A., Palm, C.A., Verchot, L. (2005): Potential of Agroforestry for carbon sequestration and mitigation of greenhouse gas emissions from soils in the tropics. – *Nutrient Cycling in Agroecosystems* 71(1): 43-54.
- [25] Nabuurs, G.J., Garza-Caligaris, J.F., Kanninen, M., Karjalainen, T., Lapvetalainen, T., Liski, J., Maser, O.R., Mohren, G.M.J., Pussinen, A., Schelhaas, M.J. (2001): CO2FIXV2.0 – Manual of a model for quantifying carbon sequestration in forest ecosystems and wood products. – *ALTERRA Report xx*. Wageningen, 2001. 48pp.
- [26] Niles, J.O., Btown, S., Pretty, J.N., Ball, A., Fay, J. (2000): Potential carbon mitigation and income in developing countries from changes in use and management of Agricultural and forest lands. – *Royal Society Transactions A: Carbon, Biodiversity, Conservation and Income*. 24pp.
- [27] Nkwatoh, A.F. (2000): Evaluation of trade in non-timber Forest Products in the Ejagham forest reserve of Southwest Cameroon. – Ph.D. Thesis, university of Ibadan.
- [28] Palm, C.A., Van Noordwijk, M., Woomer, P.L., Alegre, J., Castilla, C., Cordeiro, D.G., Hairiah, K., Kotto-Same, J., Moukam, A., Njomgang, R., Ricse, A., Rodrigues, V. (2000): Carbon losses and sequestration potentials of alternatives to slash and burn agriculture. – In: *The biology and fertility of tropical soils*. TSBF, Nairobi.
- [29] Pretty, J.N., Ball, A.S., Xiaoyun, L., Ravindranath, N.H. (2002): The role of sustainable agriculture and renewable resource management in reducing greenhouse gas emissions and increasing sinks in India and China. – *Philosophical Transactions of the Royal Society Series A* 360: 1741-1761.
- [30] Pretty, J.N., Noble, A.D., Bossio, S., Dixon, J., Hine, F.W.T., Penning De Vries, Morison, J.I.L. (2006): Resource conserving agriculture increases yields in developing countries. – *Environmental Science and Technology* 40: 1114-1119.
- [31] Rahayu, S., Lusiana, B., Van Noordwijk, M. (2005): Above ground carbon stock assessment for various land use systems in Nunukan, East Kalimantan. – In: Lusiana, B., Van Noordwijk, M. and Rahayu, S. eds. (2005): *Carbon in Nunukan: A spatial Monitoring approach and modeling*. – Report from carbon monitoring team of forest resource Management and Carbon sequestration (FORMACS) project. Bogor, Indonesia, World Agroforestry Centre, SEA Regional Office. 21-33.
- [32] Shin, M.Y., Miah, M.D., Lee, K.H. (2007): Potential contribution of the forest sector in Bangladesh to carbon sequestration. – *Journal of Environmental Management* 82(2): 260-276.

- [33] Stern, N. (2006): Stern Review report on the economics of climate change. – HM Treasury, London. 575pp.
- [34] Tschakert, P., Coomes, O.T., Potvin, C. (2007): Indigenous livelihoods, slash and burn agriculture and carbon stocks in Eastern Panama. – *Ecological Economics* 60: 807-820.
- [35] Vieira, S., Trumbone, S., Carnargo, P.B., Sethorst, D., Chambers, J.Q., Higuchi, N., Martinelli, L.A. (2005): Slow growth rates of Amazonian trees: Implications for carbon sequestration. – *PNAS* 102(51): 18502-18507.

## ANALYSIS OF PROJECTED CLIMATE CHANGE FOR HUNGARY USING ENSEMBLES SIMULATIONS

PONGRÁCZ, R.\* – BARTHOLY, J. – MIKLÓS, E.

*Eötvös Loránd University, Department of Meteorology  
1117 Budapest, Pázmány Péter sétány 1/A, Hungary  
(phone: +36-1-372-2945; fax: +36-1-372-2904)*

*\*Corresponding author  
e-mail: prita@elte.hu*

(Received 27<sup>th</sup> October 2011; accepted 10<sup>th</sup> November 2011)

**Abstract.** In order to estimate the future regional climate change for the Carpathian Basin located in Central/Eastern Europe, outputs from several RCMs (from the completed European project ENSEMBLES) are summarized and analyzed using the SRES A1B scenario. Composite maps of the projected annual and seasonal temperature and precipitation changes are generated using RCM simulations (with 25 km spatial resolution) for the reference period 1961-1990, and the target periods 2021-2050, 2071-2100. Overall, the results suggest significant warming in Hungary. Projected seasonal warming is 1-3 °C, and 2-6 °C for 2021-2050, and 2071-2100, respectively. The largest temperature increase is likely to occur in summer. In case of precipitation, the annual sum is not likely to change significantly in the region. However, the summer precipitation is projected to decrease significantly during the 21st century, autumn and winter precipitation amounts are projected to increase.

**Keywords:** *regional climate modeling, climate change, ENSEMBLES project, temperature, precipitation*

### Introduction

Several recently increased regional environmental problems are related to climate change. The Intergovernmental Panel on Climate Change (IPCC) Assessment Reports summarize the global warming issues, detected changes, possible causes, global model projections, as well, as regional adaptation and mitigation strategies. Since the last IPCC report published in 2007, new model experiments with fine resolution have been completed and new results became available (e.g., van der Linden and Mitchell, 2009). For our region, previously 50 km horizontal resolution climate change analysis was summarized in Bartholy et al. (2007) using PRUDENCE outputs (Christensen et al., 2007) for the end of the 21st century. In the recent years regional climate models (RCMs) were run with finer resolution and for longer time periods than previously. For a region with the size of the Carpathian Basin, RCMs are essential to provide appropriate details of climate variables. They are limited area models (Giorgi, 1990) nested in global climate models (GCMs), i.e., the initial and the boundary conditions of RCMs are provided by the GCM outputs. GCM outputs alone may be misleading to compose regional climate change scenarios due to their coarse spatial resolution, which is typically 100-200 km. Evidently, this spatial resolution is not capable to describe regional climate processes (especially, the precipitation-related meteorological interactions and events), therefore, downscaling of GCM outputs is necessary in order to estimate future regional climatic trends. In this paper, new simulation results for Hungary and its vicinity are summarized and analyzed using the RCM experiments of the completed ENSEMBLES project (van der Linden and Mitchell, 2009). For the selected target region covering the latitude 44°-50°N, and longitude 14°-26°E,

composite maps of projected temperature and precipitation changes are generated using the RCM simulations for the periods of 1961-1990 (as the reference period), 2021-2050, and 2071-2100.

First, the project ENSEMBLES is briefly introduced. Then, in order to estimate the bias of the different RCMs, ERA-40 driven runs are compared to the so-called E-OBS datasets (Haylock et al., 2009) containing gridded daily temperature and precipitation values. For the evaluation of annual, seasonal, and monthly projected climatic changes, GCM-driven runs of the reference and the future periods are compared.

**Table 1.** List of the participating institutes, their applied RCMs with the driving GCMs, and the completed simulation for A1B (\* on the right indicates the experiments used in this paper)

Institute/Contact	Driving GCM	Regional model	Simulating period	
CNRM M. Déqué	ARPEGE ARPEGE_RM5.1	ALADIN ALADIN	1950-2100 1950-2100	*
KNMI E. van Meijgaard	ECHAM5-r3	RACMO	1950-2100	*
OURANOS D. Paquin	CGCM3	CRCM	1951-2050	
SMHI E. Kjellström	BCM ECHAM5-r3 HadCM3Q3	RCA RCA RCA	1961-2100 1961-2100 1961-2100	* * *
MPI D. Jacob	ECHAM5-r3	REMO	1951-2100	*
OMETNO J. E. Haugen	BCM HadCM3Q0	HIRHAM HIRHAM	1951-2100 1951-2100	
C4I R. McGrath	HadCM3Q16	RCA3	1951-2100	*
UCLM M. de Castro	HadCM3Q0	PROMES	1951-2050	
ETHZ C. Schär	HadCM3Q0	CLM	1951-2100	*
HC E. Buonomo	HadCM3Q0 HadCM3Q3 HadCM3Q16	HadRM3Q0 HadRM3Q3 HadRM3Q16	1951-2100 1951-2100 1951-2100	*  
DMI O. B. Christensen	ARPEGE ECHAM5-r3 BCM	HIRHAM HIRHAM5 HIRHAM5	1951-2100 1951-2100 1957-2096	* * 
ICTP F. Giorgi	ECHAM5-r3	RegCM	1951-2100	*
VMGO I. Shkolnik	HadCM3Q0	RRCM	1951-2050	
GKSS B. Rockel	IPSL	CLM	1963-2050	

## The ENSEMBLES project

The ENSEMBLES project (van der Linden and Mitchell, 2009) has been funded by the European Union 6th framework programme. The project was accomplished between 2004 and 2009 with the lead of the UK MetOffice, and 66 other institutes from 20 countries (mostly from Europe) participated. The main aims of the research program

were as follows: (i) to develop an ensemble climate prediction system on seasonal to centennial time-scales; (ii) to quantify and reduce the uncertainty in modelling climate change; (iii) to link the outputs of the ensemble prediction system to a range of applications. For all these purposes an intermediate emission scenario has been selected, namely, SRES A1B (Nakicenovic and Swart, 2000). According to this scenario fast economical and technological development is projected, the world population is estimated to increase by the mid-century up to 9 billion, then slightly decrease by the end of the 21st century to 7 billion. The energy demand is estimated to be fulfilled both from fossil fuels and renewable and/or nuclear sources. As a consequence, CO<sub>2</sub> content of the atmosphere continues to increase in the coming decades. The estimated CO<sub>2</sub> concentration levels by 2050 and by 2100 are 532 ppm, and 717 ppm, respectively.

*Table 1* summarizes the completed RCM experiments with 25 km horizontal resolution. In the present analysis 11 RCM experiments are used, they all were run for the entire 1951-2100 period. The driving lateral and boundary conditions are provided by three different GCMs, namely, (i) ECHAM developed by the Max Planck Institute in Hamburg (Roeckner et al., 2006), (ii) HadCM developed by the UK MetOffice Hadley Centre (Gordon et al., 2000; Rowell, 2005), and (iii) ARPEGE developed by Météo-France (Déqué et al., 1998).

### Validation of RCM results

In order to estimate the bias of the different RCMs, ERA-40 (European Centre for Medium-range Weather Forecast, ECMWF, re-analysis dataset described in Uppala et al., 2005) driven runs are compared to the E-OBS datasets (Haylock et al., 2008) containing observation-based daily temperature and precipitation values for Europe. In case of each RCM experiment, monthly mean bias values have been calculated for each grid point located in Hungary, and then, the spatial averages for the country have been determined for all months. Figs. 1 and 2 compare the total numbers of months, in which the RCM results over/underestimate significantly (at 0.05 level using t-test) the average temperature or precipitation values calculated from E-OBS data. Although 11 RCM experiments are analyzed for the future, two of them (i.e., RCA, HIRHAM) were run using different GCMs. Therefore, only 9 ERA-40 driven RCM validation runs are necessary to evaluate.

In case of temperature (*Fig. 1*), three models (HadRM3Q, RCA3, RCA) can be considered bias-free, i.e., the monthly differences between the RCM outputs and the E-OBS data are not significant at 0.05 level and do not exceed 1 °C in any month. The most overestimations (in 7 months) can be identified in REMO simulations (from May to November). Moreover, RegCM outputs significantly underestimate the monthly mean temperature calculated from E-OBS data in 4 months (February, March, April, and October).

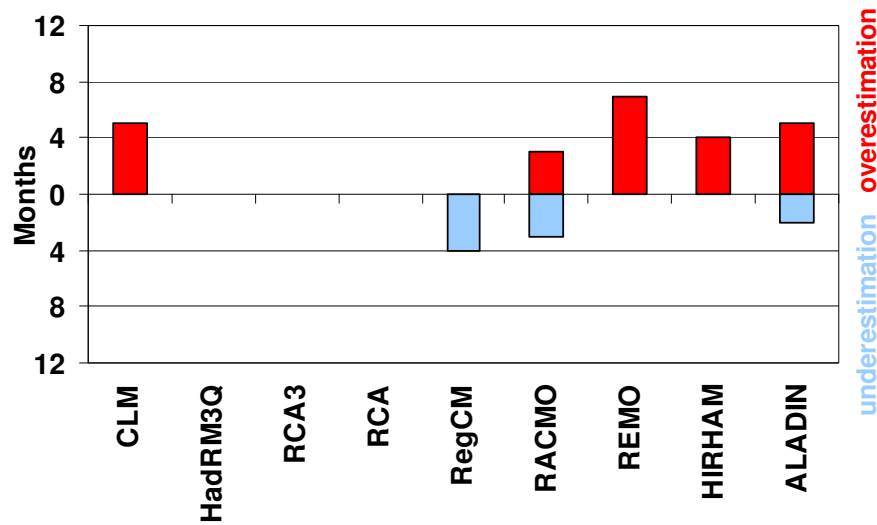


**Figure 1.** Validation of temperature in case of the ERA40-driven RCM experiments (1961-1990)

In case of monthly precipitation (Fig. 2), RCMs are less successful in reconstructing current climatic conditions than in case of monthly temperature. The HadRM3Q is the only model that can be considered bias-free, i.e., the monthly differences between the RCM outputs and the E-OBS data are not significant at 0.05 level, and do not exceed 10 mm. In general, RCM simulations significantly overestimate monthly precipitation. In case of models RegCM, RCA3, RCA, CLM, and HIRHAM, simulated precipitation is significantly larger than the E-OBS data in most part of the year (especially, in winter and early spring). However, most RCMs underestimate the monthly precipitation in a month or two (typically in August). The most underestimation appears in case of ALADIN simulations (in 6 months: from August to December).

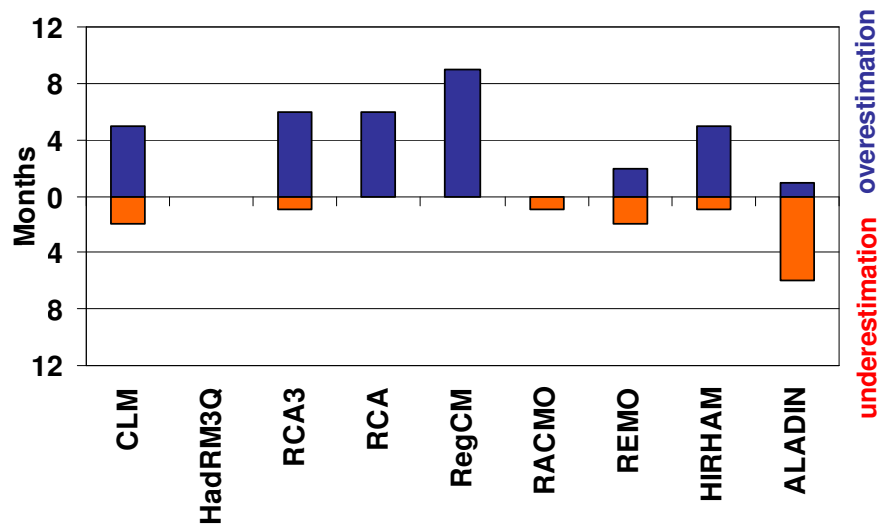


**Figure 2.** Validation of precipitation in case of the ERA40-driven RCM experiments (1961-1990)

Overall, the validation results suggest that the RCMs are generally able to reconstruct the temperature sufficiently. In case of precipitation, simulated values often significantly overestimate the observations.

### Analysis of future regional temperature trends

For the evaluation of annual, seasonal, and monthly projected climatic changes, GCM-driven runs of the reference and the future periods are compared. *Figs. 3-5* show the annual and seasonal mean projected warming for Hungary for each RCMs. All projected temperature changes are significant at 0.05 level using t-test.

All the ECHAM driven RCMs (*Fig. 3*) project 0.7-1.7 °C and 1.9-4.0 °C seasonal and annual warming by 2021-2050 and 2071-2100, respectively. The largest annual increase is projected by REMO for both period. In case of seasonal warming, the largest rate is likely to occur in summer and autumn by the middle of the 21st century, while in summer and winter by the end of the 21st century.

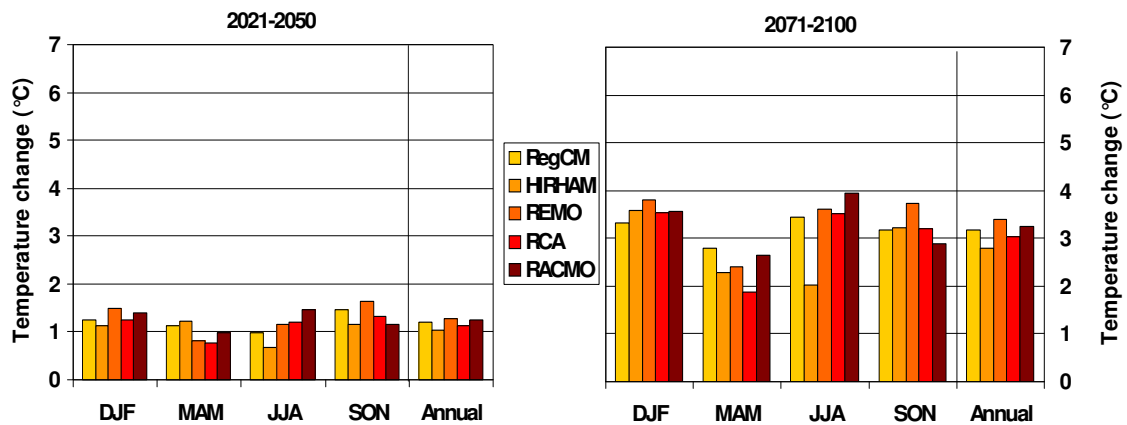


**Figure 3.** Projected temperature changes for Hungary by 2021-2050 and 2071-2100 using ECHAM as driving GCM (reference period: 1961-1990). All seasonal and annual changes are significant at 0.05 level

The HadCM-driven RCMs (*Fig. 4*) project larger increase in temperature than the ECHAM-driven RCMs. By the mid-century the simulations suggest 1.1-3.4 °C seasonal warming, which are likely to double by the late-century (up to 2.2-6.4 °C). The largest seasonal warming is clearly projected by HadRM3Q experiment for summer. Moreover, the largest annual warming is also simulated by HadRM3Q (2.5 °C and 5.0 °C by 2021-2050 and 2071-2100, respectively). HadCM-driven RCMs project the largest temperature increase for summer and winter by the near future, and mostly for summer by the end of the 21st century (except RCA).

In case of ARPEGE-driven RCMs (*Fig. 5*), the projected seasonal changes by 2021-2050 and 2071-2100 are 0.8-2.1 °C, and 1.7-5.0 °C, respectively. In general, the ALADIN experiment results greater warming than the HIRHAM experiment. The largest seasonal increase is projected for summer in both future period, and by both RCMs.

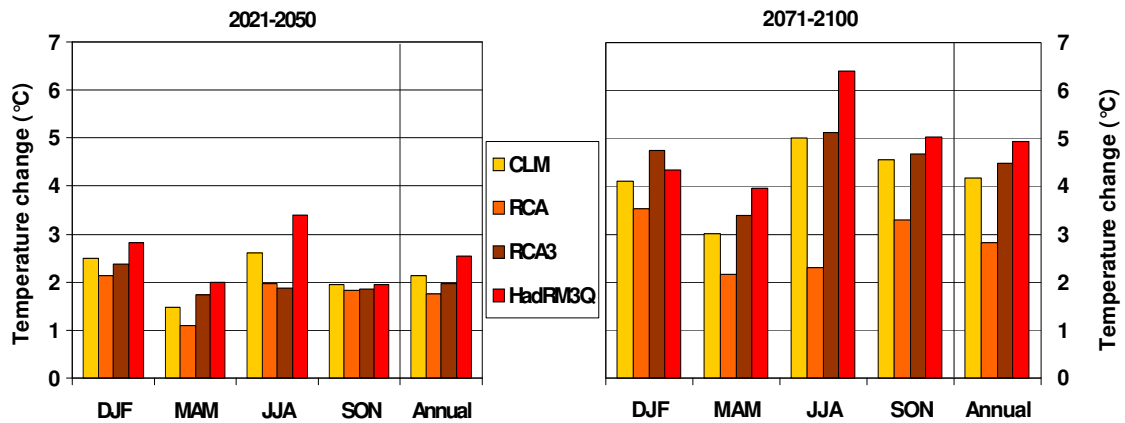


**Figure 4.** Projected temperature changes for Hungary by 2021-2050 and 2071-2100 using HadCM as driving GCM (reference period: 1961-1990). All seasonal and annual changes are significant at 0.05 level

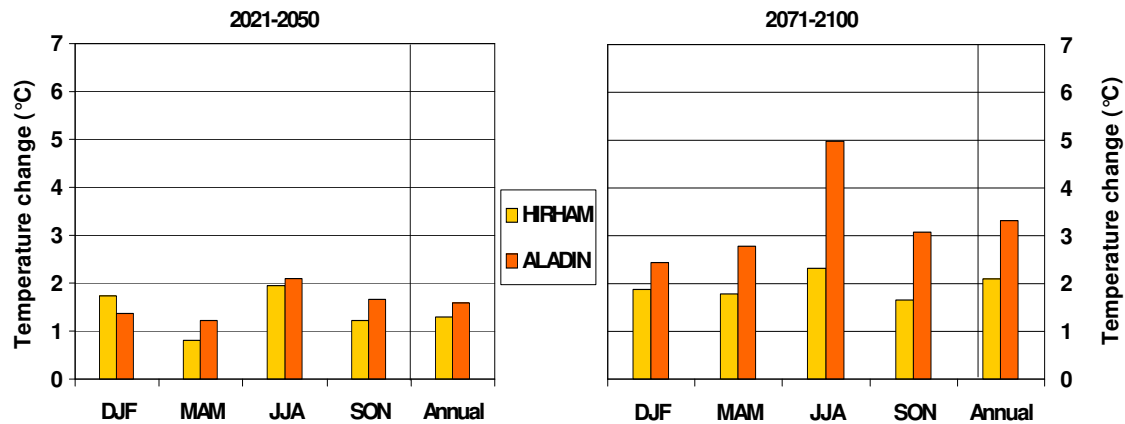


**Figure 5.** Projected temperature changes for Hungary by 2021-2050 and 2071-2100 using ARPEGE as driving GCM (reference period: 1961-1990). All seasonal and annual changes are significant at 0.05 level

Fig. 6 presents the seasonal spatial structure of composite maps calculated from projected seasonal temperature changes by the mid- and late-century for all the 11 RCM experiments considered in this analysis. In summer and autumn zonal structures can be recognized, the simulated changes are likely to increase from north to south. The projected changes by 2021-2050 are 1.2-1.8 °C. The largest warming is likely to occur in autumn in the southern/southeastern part of the country. The smallest increase is projected for spring. By 2071-2100 the projected seasonal changes are 2.6-4.0 °C. The largest warming is projected in summer and autumn, and the smallest in spring.



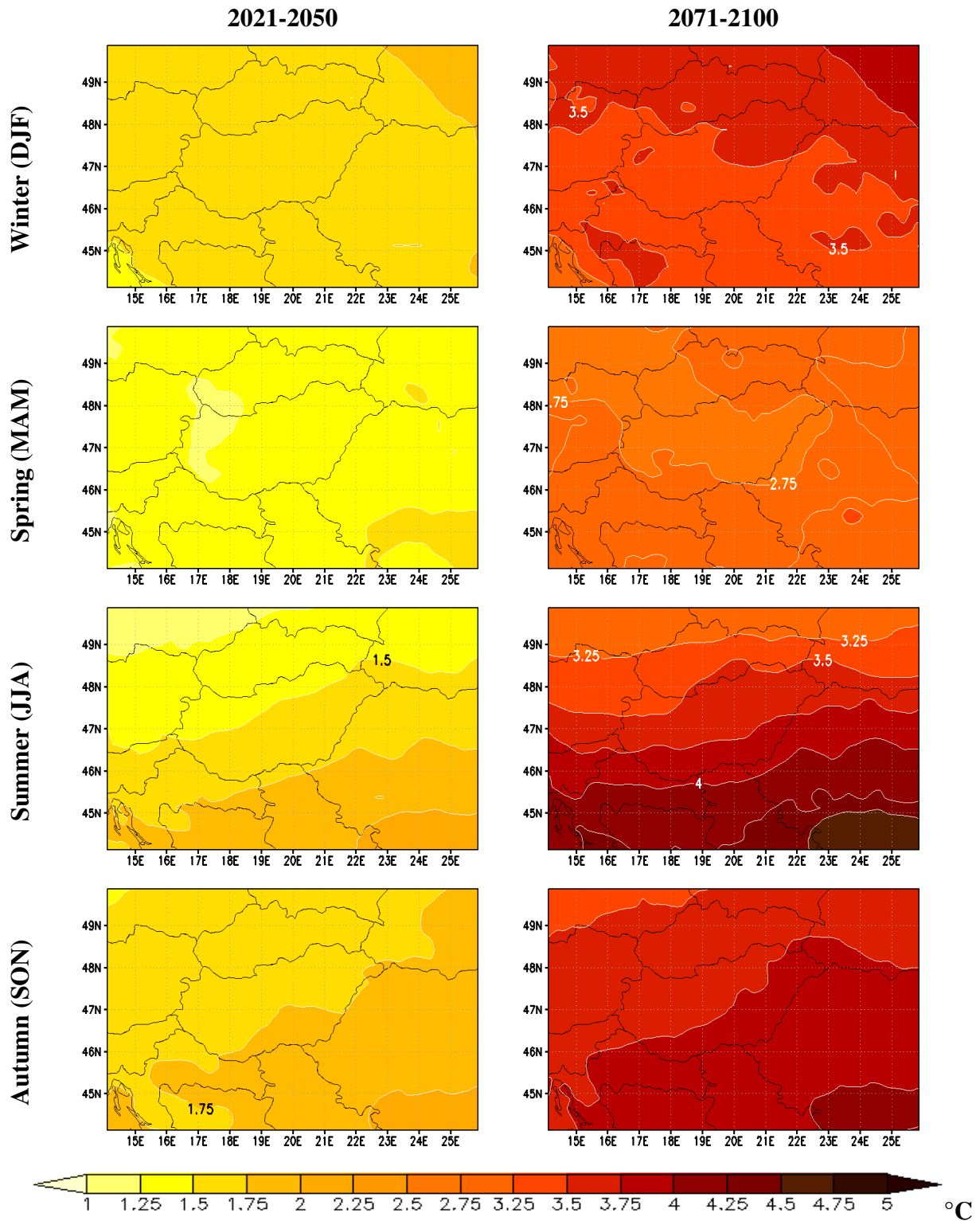


**Figure 6.** Composite map of the projected seasonal mean temperature changes (°C) by 2021-2050 and 2071-2100 (reference period: 1961-1990)

## Analysis of future regional precipitation trends

Annual and seasonal mean projected precipitation changes for Hungary are shown in Figs. 7-9, separated according to the driving GCMs. All the changes being significant at 0.05 level using t-test are marked on the graphs (using an asterisk). More estimated changes are significant by 2071-2100 than by 2021-2050 due to the more clear climate change signal.

All the ECHAM-driven RCMs project precipitation increase in winter (by 20-30%) and autumn (by 15-25%), and decrease in summer (by 5-25%) for both periods (Fig. 7). Most of these projections are significant by 2071-2100, unlike by 2021-2050. According to these experiments, overall, the Hungarian climate is projected slightly wetter by the late 21st century, the estimated annual precipitation increase do not exceed 10%, and it is significant only in the case of RegCM and HIRHAM simulations.

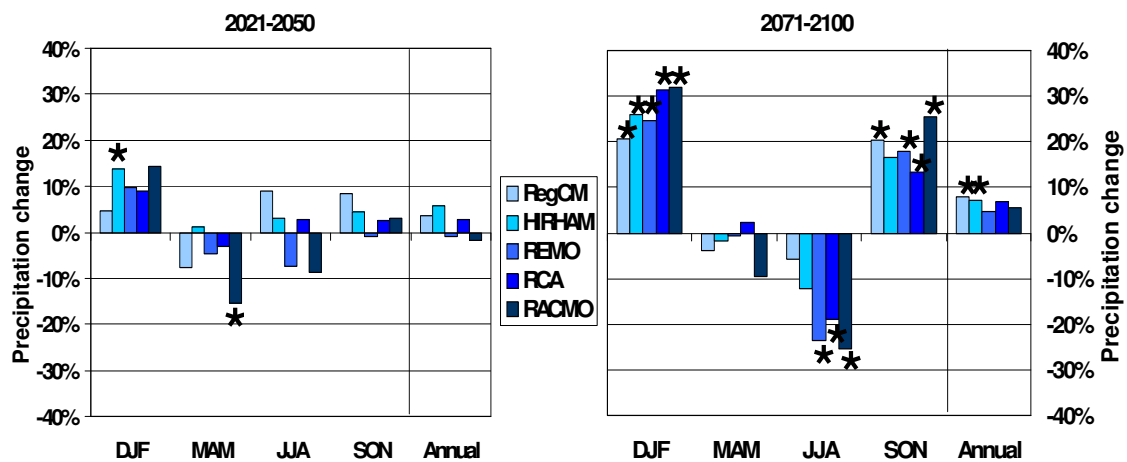


**Figure 7.** Projected precipitation changes for Hungary by 2021-2050 and 2071-2100 using ECHAM as driving GCM (reference period: 1961-1990). Significant seasonal and annual changes are indicated by '\*'

Similarly to the ECHAM-driven experiments, HadCM-driven RCM simulations project wetter winters and drier summers (Fig. 8) for the future than the present conditions. The estimated winter increase and summer decrease by 2071-2100 is 7-27% and 3-41%, respectively. However, less of these projected changes are significant than those by the RCMs shown in Fig. 7. On the other hand, among all the 11 RCM experiments discussed in the present paper, CLM and HadRM3Q simulations project the largest precipitation decrease (~40%).

Only two RCM experiments are driven by ARPEGE, namely, HIRHAM and ALADIN. Most of their seasonal precipitation projections for Hungary are not significant at 0.05 level. However, the significant summer drying estimated by the other GCM-driven RCM simulations is also projected by both ARPEGE-driven RCMs (Fig. 9). The estimated average precipitation decrease for the entire country is 4% (HIRHAM) and 28% (ALADIN). Overall, a slight annual precipitation decrease (by about 10%) is also projected for the country by 2071-2100, which is significant in case of ALADIN simulations. Unlike the other GCM-driven RCM experiments, these two RCM simulations do not project significant changes in winter neither by the middle, nor the end of the 21st century.

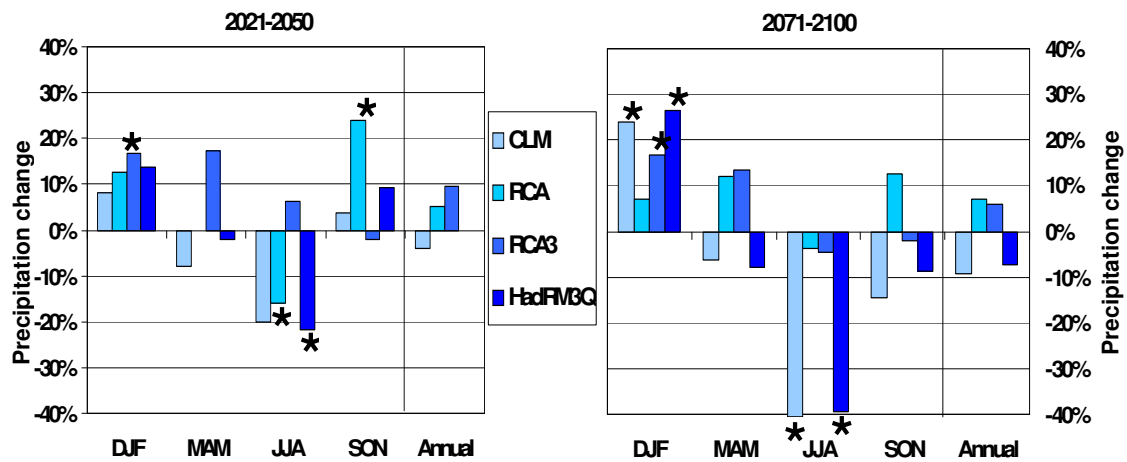


**Figure 8.** Projected precipitation changes for Hungary by 2071-2100 using HadCM as driving GCM (reference period: 1961-1990). Significant seasonal and annual changes are indicated by '\*'

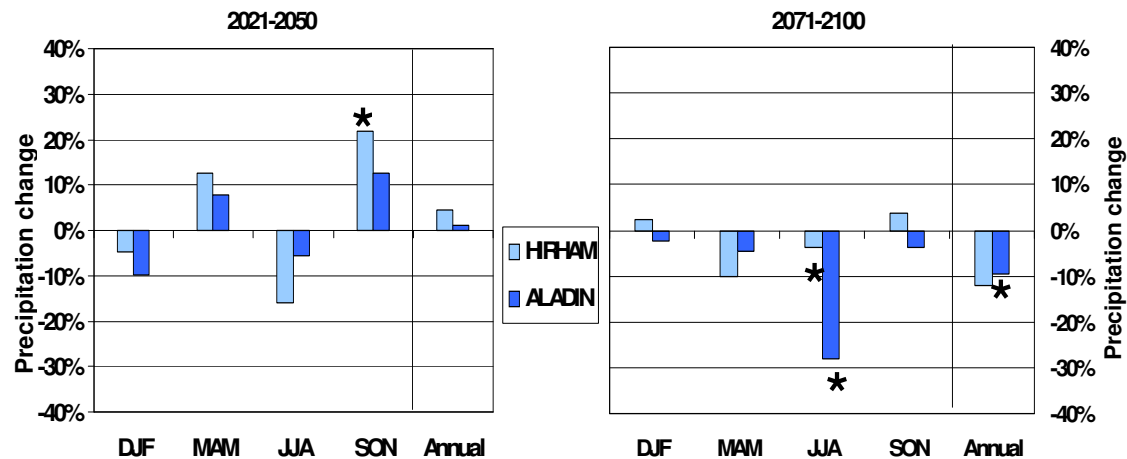


**Figure 9.** Projected precipitation changes for Hungary by 2071-2100 using ARPEGE as driving GCM (reference period: 1961-1990). Significant seasonal and annual changes are indicated by '\*'

Fig. 10 presents the seasonal spatial structure of composite precipitation changes for the mid- and the late-century using all the 11 RCMs considered in this paper. The composite maps clearly suggest drier summers and wetter climatic conditions for the other three seasons for both future periods compared to the 1961-1990 reference period. The estimated changes are larger (by about a factor of 2) for 2071-2100 than for 2021-2050. The largest precipitation increase by the middle and the end of this century is projected for autumn (7-12%) and for winter (14-19%), respectively. The rate of precipitation change in autumn increase from southwest to northwest for both periods. As the spatial average changes already suggested, summers are very likely to become drier in the coming decades. Nevertheless, spatial differences within Hungary can be identified in the composite maps. Future summers are projected much drier in the southeastern part of the country than in the northwestern region. By the late century the

estimated seasonal precipitation decrease exceeds 20% in the southeastern part of the Great Hungarian Plain.

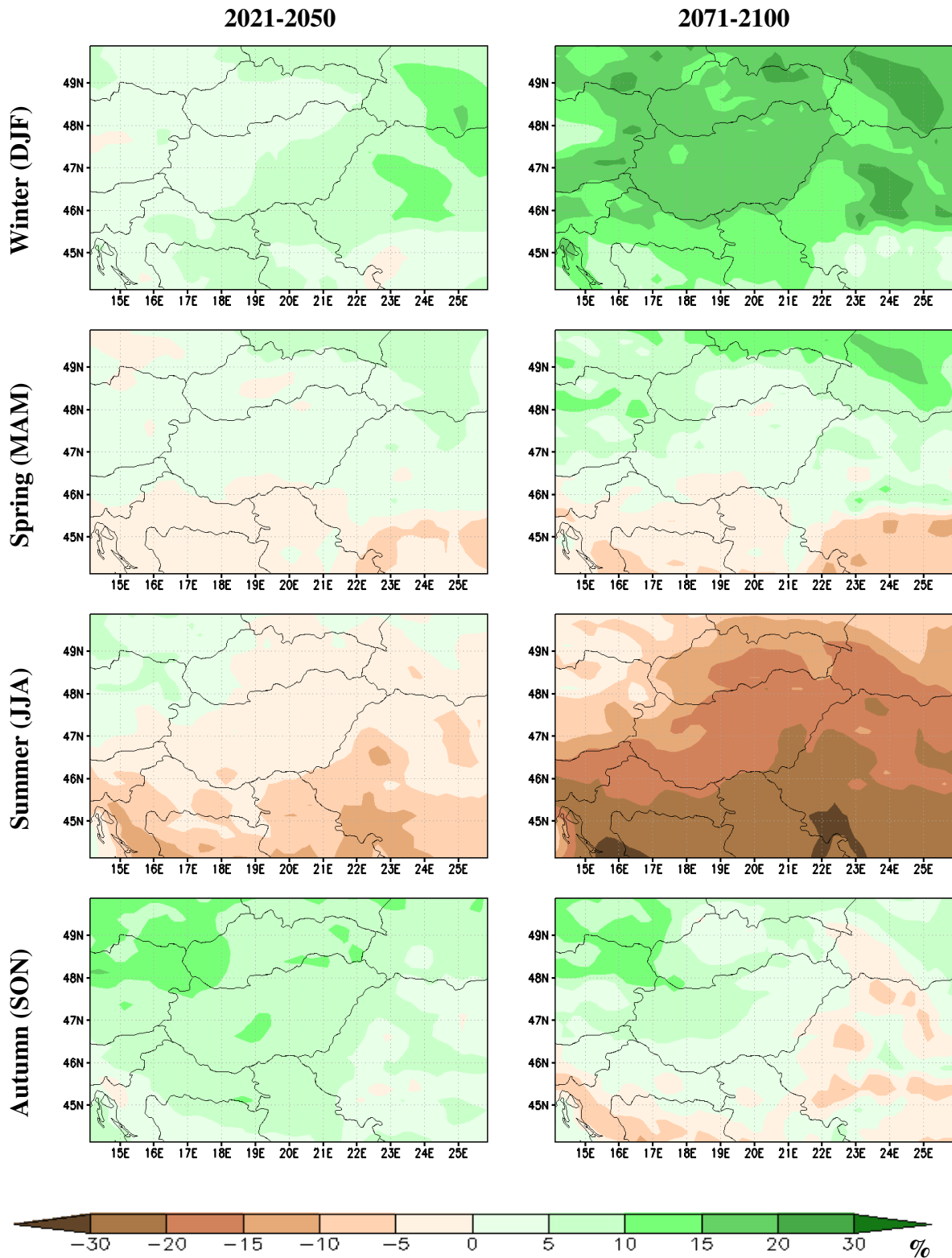


**Figure 10.** Composite map of the projected seasonal mean precipitation changes (%) by 2021-2050 and 2071-2100 (reference period: 1961-1990)

Finally, in spring the composite maps indicate wetter conditions in the northern part of the selected domain and drier climate in the southern regions compared to the 1961-1990 reference period. In the gridpoints located within the borders of Hungary the estimated seasonal changes are small and not significant.

## Conclusions

Based on the regional climate change analysis discussed for Hungary in this paper, the following conclusions can be drawn.

(i) All of the evaluated RCM simulations from the project ENSEMBLES suggest that the temperature is very likely to increase significantly in the future in all months and seasons. The projected annual warming is about 1-2.5 °C, and 2-5 °C for 2021-2050, and 2071-2100, respectively. Annual and seasonal mean projected changes for Hungary are summarized in Fig. 11, the different driving GCMs are also indicated.

(ii) Most of the RCMs suggest that the winter and autumn precipitation is likely to increase (Fig. 12), while summer precipitation is projected to decrease during the 21st century. The mean change by 2021-2050 is not likely to exceed 20% in any season. By 2071-2100 remarkable winter precipitation increase (10-30%) and significant summer precipitation decrease (15-40%) are projected for Hungary.

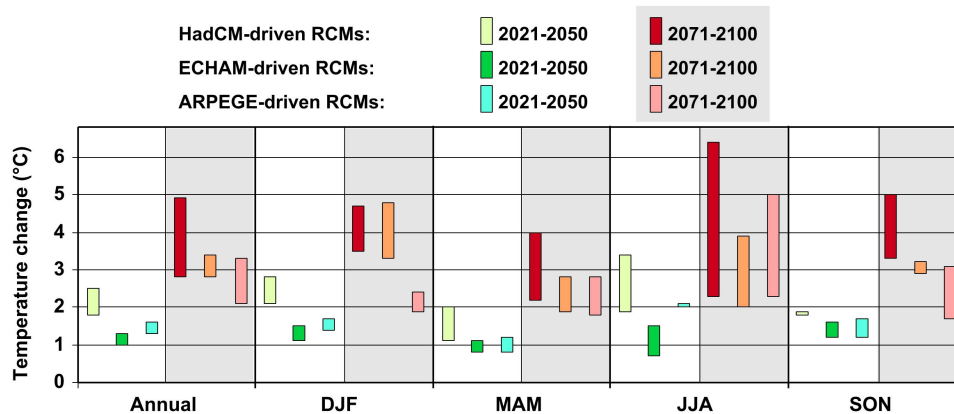


**Figure 11.** Summary of projected temperature changes for Hungary by 2021-2050 and 2071-2100 separated according to the driving GCM (reference period: 1961-1990)

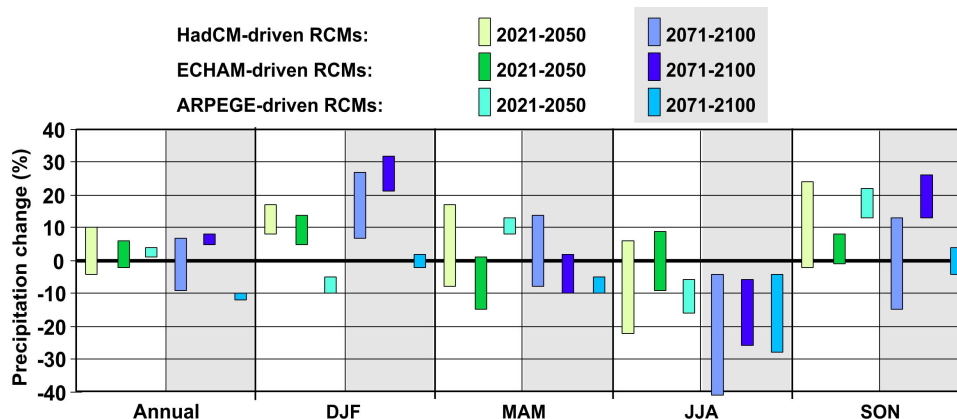


**Figure 12.** Summary of projected precipitation changes for Hungary by 2021-2050 and 2071-2100 separated according to the driving GCM (reference period: 1961-1990)

**Acknowledgements.** Research leading to this paper has been supported by the following sources: the Hungarian Academy of Sciences under the program 2006/TKI/246 titled Adaptation to climate change, the Hungarian National Science Research Foundation under grants T-049824, K-69164, K-78125, and K-67626, the Hungarian Ministry of Environment and Water under the National Climate Strategy Development project, the CC-WATERS project of the European Regional Development Fund (SEE/A/022/2.1/X), the European Union and the European Social Fund (TÁMOP-4.2.1/B-09/1/KMR-2010-0003).

## REFERENCES

- [1] Bartholy, J., Pongrácz, R., Gelybó, Gy. (2007): Regional climate change expected in Hungary for 2071-2100. – *Applied Ecology and Environmental Research* 5: 1-17.
- [2] Déqué, M., Marquet, P., Jones, R.G. (1998): Simulation of climate change over Europe using a global variable resolution general circulation mode. – *Climate Dyn.* 14: 173-189.
- [3] Giorgi, F. (1990): Simulation of regional climate using a limited area model nested in a general circulation model. – *J. Climate* 3: 941-963.
- [4] Gordon, C., Cooper, C., Senior, C.A., Banks, H., Gregory, J.M., Johns, T.C., Mitchell, J.F.B., Wood, R.A. (2000): The simulation of SST, sea ice extents and ocean heat transports in a version of the Hadley Centre coupled model without flux adjustments. – *Climate Dynamics* 16: 147-168.
- [5] Haylock, M.R., Hofstra, N., Klein Tank, A.M.G., Klok, E.J., Jones, P.D., New, M. (2008): A European daily high-resolution gridded dataset of surface temperature and precipitation. – *J. Geophys. Res (Atmospheres)* 113, D20119, doi:10.1029/2008JD10201.
- [6] Nakicenovic, N., Swart, R. (2000): Emissions Scenarios. A special reports of IPCC Working Group III. – Cambridge University Press, UK. 570p.
- [7] Roeckner, E., Brokopf, R., Esch, M., Giorgetta, M., Hagemann, S., Kornbluh, L., Manzini, E., Schlese, U., Schulzweida, U. (2006): Sensitivity of simulated climate to horizontal and vertical resolution in the ECHAM5 atmosphere model. – *J. Climate* 19: 3771-3791.
- [8] Rowell, D.P.(2005): A scenario of European climate change for the late 21st century: seasonal means and interannual variability. – *Climate Dynamics* 25: 837-849.
- [9] Uppala, S.M., Kallberg, P.W., Simmons, A.J., Andrae, U., da Costa Bechtold, V., Fiorino, M., Gibson, J.K., Haseler, J., Hernandez, A., Kelly, G.A., Li, X., Onogi, K., Saarinen, S., Sokka, N., Allan, R.P., Andersson, E., Arpe, K., Balmaseda, M.A., Beljaars, A.C.M., van de Berg, L., Bidlot, J., Bormann, N., Caires, S., Chevallier, F., Dethof, A., Dragosavac, M., Fisher, M., Fuentes, M., Hagemann, S., Holm, E., Hoskins, B.J., Isaksen, L., Janssen, P.A.E.M., Jenne, R., McNally, A.P., Mahfouf, J.-F., Morcrette, J.-J., Rayner, N.A., Saunders, R.W., Simon, P., Sterl, A., Trenberth, K.E., Untch, A., Vasiljevic, D., Viterbo, P., Woollen, J. (2005): The ERA-40 re-analysis. – *Quart. J. R. Meteorol. Soc.* 131: 2961-3012. doi:10.1256/qj.04.176.
- [10] van der Linden, P., Mitchell, J.F.B. (eds.) (2009): ENSEMBLES: Climate Change and Its Impacts: Summary of research and results from the ENSEMBLES project. – UK Met Office Hadley Centre, Exeter, UK, 160p.

## A GAME THEORY APPROACH TO SALINIZATION PROBLEM OF THE ARAL SEA BASIN

AKHMEDJONOV, A.<sup>1\*</sup> – SUYUNDIKOV, A.<sup>2</sup>

<sup>1</sup>*Assistant Professor of Economics, Zirve University  
Gaziantep 27260 Turkey  
(phone: +90-342-211-6666 ext. 6846)*

<sup>2</sup>*Department of Statistics, Utah State University  
1400 Old Main Hill, Logan 84322 Utah, USA  
(phone: +1-435-797-0017)*

*\*Corresponding author  
e-mail: alisherakhmedjonov@zirve.edu.tr*

(Received 1<sup>st</sup> April 2011; accepted 2<sup>nd</sup> December 2011)

**Abstract.** This paper studies a transboundary economy with two countries located in a lake basin. Each country withdraws water from the lake for irrigation purposes, which in turn causes the lake to desiccate. The receding lake leaves surfaces covered with salt dust, which is transported by wind to the surrounding area, increasing the salinity of the two countries' lands. This paper examines whether a partially cooperative water – allocation scheme, where a central authority chooses the two countries' respective abatement levels (of salt dust) *after* the countries individually choose per-unit taxes on water withdrawal, induces the countries to withdraw water at the socially efficient level. We find that the partial scheme works, i.e. it induces both countries to optimally choose to withdraw at the socially efficient level.

**Keywords:** *interbasin water resources allocation, water quality, benefit reallocation, optimization, game theory*

### Introduction

The problem of optimal water use in international river basins has become a major concern. There are more than 200 river basins in the world that are shared by two or more countries (WRI, 2000). Rapid population and economic growth, increasing prices for food and other commodities, and the scarcity of water resources make water consumption a key issue in international river basins. According to the World Resource Institute (2000), roughly 3.5 billion people world wide are expected to live in water-stressed river basins by 2025.

Inefficient water use by riparian countries not only causes hydropolitical conflicts, but also compromises the socio-economic and environmental sustainability of the countries' water basins. For example, the Aral Sea (formerly one of the four largest lakes of the world, with an area of 68,000 square kilometres (26,000 sq mi)), has been steadily shrinking since the 1960s, after the rivers feeding it were diverted by Soviet Union irrigation projects (Micklin and Aladin, 2008). The Soviet Union pursued cotton production on a massive scale in the Aral Sea basin. As a result, Uzbekistan is now the world's sixth-largest producer and second-largest exporter of cotton (Cotton This Week, 2005). However, the drying sea has destroyed marine, coastal and delta ecosystems, altered the local climate, increased salination of crop lands, and compromised the livelihoods of hundreds of thousands of people. A lack of fresh water and extremely polluted air has turned the Aral Sea basin into an ecologic disaster zone, with an

accelerated rate of health problems (Godwin, 2003). The receding sea has left huge plains covered with salt and toxic chemicals – the results of weapons testing, industrial projects, pesticides and fertilizer runoff – which are picked up and carried away by the wind as toxic dust and spread throughout the surrounding area (Mangold and Goldberg, 2001). For example, wind-blown sand and salt production in the dried Aral seabed area on average reaches 40-45 million tons per year. The main dust and salt transport processes occur within 300 km of the coastal lands. Annual volumes of dust emission into the atmosphere from the dried Aral seabed area amount to 15-75 million tons, which has an adverse effect on irrigated farming (Mangold and Goldberg, 2001).

Several studies have estimated the environmental impact of cotton irrigation on the Aral Sea basin's water resources. Gillham (1995) asserts that cotton production requires heavy application of agricultural chemicals, which pollute freshwater ecosystems with nutrients, salts and pesticides. Gillham also classifies water withdrawal for extensive irrigation as one of the mechanisms by which cotton production impacts rivers, lakes and wetlands. He examines surface salination of the depleted Aral Sea in particular, which is the most severe consequence of extensive water withdrawal. In Uzbekistan, for example, 50% of the irrigated area is affected by salinity.

A number of economic studies show that a cooperative water – resource allocation would lead to reduction in total water withdrawal for irrigation purposes in international river and lake basins. For example, Rogers (1969) formulates a cooperative game of water allocation for the Ganges and Nile rivers and shows how cooperation leads to a Pareto efficient allocation. Hardin (1968) provides an explanation of the “tragedy of the commons”, which explains why water resources are sometimes heavily overexploited because of noncooperation among competing users. In a noncooperative setting, the resulting Nash equilibrium leads the riparian countries to exploit water resources in a noncontrolled and unregulated fashion. Moulin (1995) demonstrates that aggregate water use under full cooperation is generally smaller than under noncooperation when general conditions are met.

In this paper, we examine whether a partially cooperative water allocation scheme can reduce the level of salination in a river basin such as the Aral Sea basin. By “partially cooperative” we mean that the national governments and a separate central authority share policy instruments in such a way that the national governments choose on their own the socially-efficient salination levels. In this regard, the acid rain model developed by Caplan and Silva (1999) is particularly relevant. Following their work, we consider a model where two countries withdraw water from a lake for irrigation purposes. Water withdrawal causes the lake to desiccate; desiccation that extends to adjacent areas by increasing the salination of irrigated lands in both countries. In contrast with Caplan and Silva (1999), we assume both countries are “downwinders” in the sense that a country's water withdrawal not only affects its own national environment, but that of its neighbor (in Caplan and Silva, 1999), one of the countries' emissions affected solely itself (downwind country), while the other's emissions affected both itself and the other country (upwind country)). In particular, we investigate “decentralized leadership” regime, where a central authority chooses the two countries' respective abatement levels (of spit dust) after the countries individually choose per – unit taxes on water withdrawal. As in Caplan and Silva (1999), we find that this regime leads to a socially efficient water allocation.



## Model

Following Caplan and Silva (1999), we consider an economy in which two countries exist in a lake basin. The countries, indexed by  $i$ ,  $i = 1, 2$ , withdraw water from the lake for irrigation purposes. There are two private goods,  $x$  and  $y$ : good  $x$  is a numeraire and  $y$  is “cotton”. We further assume that each country has an identical cotton production technology. Each country withdraws water from the lake to maximize their own economic benefit from cotton production, which causes the lake to desiccate. The desiccating lake leaves surfaces covered with salt, which in turn is transported by the wind as dust that spreads to surrounding areas.

We assume that country  $i$  produces  $Y_i$  units of cotton and consequently  $Y_i$  units of salt. However, the country can adopt a more efficient irrigation system and drip watering in cotton cultivation that reduces the dessication of the lake, and thus decreases its contribution to salination. If country  $i$  produces  $Y_i$  units of cotton and reduces salt emission by  $a_i$  units, through adoption of a new thechnology, the level of salt dust ultimately emitted is  $E_i = Y_i - a_i$ ,  $i = 1, 2$ . Capacity levels for cotton production and salt abatement are denoted as  $Y_c$  and  $a_c$ , respectively. These levels are sufficiently high enough to never be reached.

We denote the level of damage in country  $i$  from salination as  $D_i$ , defined as:

$$D_i \equiv \alpha_i E_i + (1 - \alpha_j) E_j \equiv \alpha_i (Y_i - a_i) + (1 - \alpha_j) (Y_j - a_j), \quad i, j = 1, 2 \quad (\text{Eq.1})$$

where  $\alpha_i$  and  $\alpha_j$  are the fractions of salt dust that damage countries  $i$  and  $j$ , respectively. The remaining fractions,  $(1 - \alpha_i)$  and  $(1 - \alpha_j)$  are the fractions of salt dust emitted in countries  $i$  and  $j$  that affect countries  $j$  and  $i$ , respectively. As a result,  $(1 - \alpha_1) E_1$  and  $(1 - \alpha_2) E_2$  are the tranboundary damages affecting countries 2 and 1, respectively.

As in Caplan and Silva (1999), we assume  $n$  residents reside in each country, which for simplicity we normalize to 1. An individual who resides in country  $i$  derives the following welfare from consumption of  $x_i$ ,  $y_i$ , and  $D_i$ :

$$W_i = x_i + u(y_i) - v(D_i), \quad i = 1, 2 \quad (\text{Eq.2})$$

where  $u$  is increasing and strictly concave and  $v$  is increasing and strictly convex. Assume numeraire good  $x_i$  is used for consumption and as an input in the production of cotton and dust abatement in each country. The total cost of cotton and abatement production in country  $i$  can therefore be written as:

$$K + pY_i + sa_i, \quad i = 1, 2$$

where  $K > 0$  is a fixed cost,  $p > 0$  is the cost per unit of cotton produced, and  $s > 0$  is the cost per unit of salt dust abatement produced. In equilibrium country  $i$ 's cotton supply is its demand; namely,  $Y_i = y_i$ . Country  $i$  provides its consumers with cotton at

per – unit price  $p + t_i$ , where the excess of the price over marginal cost,  $t_i$ , represents a per – unit pollution tax. Each resident of country  $i$  is imposed a head tax in the amount of  $K + sa_i$  that compensates both the fixed and abatement components of total production cost. The revenue collected from the per-unit pollution tax in country  $i$  is returned to this country's residents as a lump-sum payment  $r_i = t_i y_i$ ,  $i = 1, 2$ .

Thus, the budget constraint for the representative resident of country  $i$  can be written as:

$$x_i + (p + t_i)y_i + K + sa_i = I + r_i, \quad i = 1, 2 \quad (\text{Eq.3})$$

where, for each  $i$ , the left-hand side of (3) shows the representative resident's total expenditure and the right-hand side of (3) gives his total income (income  $I$  plus the lump-sum tax revenue  $r_i$ ).

### Consumers' maximization problems

In this section we examine the maximization problems of consumers (residents) in order to calculate how residents respond to the policy choices introduced by the governments of both countries, as well as the choices of a central authority. Thus, a resident in country  $i$  chooses  $\{x_i, y_i\}$  to maximize utility (2) subject to his/ her budget constraint (3), taking as given governmental policy variables and the overall level of salination. The solutions to the individuals' optimization problems are:

$$x_i = I - py_i - K - sa_i, \quad i = 1, 2 \quad (\text{Eq.4})$$

$$u'(y_i) = p + t_i, \quad i = 1, 2 \quad (\text{Eq.5})$$

where equation (4) is derived from equation (3) using the equality  $r_i \equiv t_i y_i$ , for all  $t_i \geq 0$ ,  $i = 1, 2$ . Equation (5) is the typical first – order condition where the marginal rate of substitution,  $u'(y_i)$ , equals relative prices,  $p + t_i$  (recall that  $x_i$  is a numeraire good, with price equal to 1). For each  $i$ , equations (4) and (5) define  $x_i$  and  $y_i$  as implicit functions of  $t_i, a_i, p, s, I$  and  $K$ , denoted  $x_i^0$  and  $y_i^0$ . Note that  $y_i^0$  does not depend on  $a_i$  from equation (5). We can therefore define the individual's demand functions as  $x_i^0 \equiv x_i^0(t_i, a_i)$  and  $y_i^0 \equiv y_i^0(t_i)$ .

The individuals' responses to changes in the governmental policy variables are the same as in Caplan and Silva (1999):

$$\frac{\partial x_i^0}{\partial t_i} = -p \frac{\partial y_i^0}{\partial t_i} = -\frac{p}{u''(y_i^0)} > 0, \quad i = 1, 2 \quad (\text{Eq.6})$$

$$\frac{\partial x_i^0}{\partial a_i} = -s < 0, \quad i = 1, 2 \quad (\text{Eq.7})$$

Here we can see that equations (6) and (7) are a straightforward implication of the implicit function theorem. We assume that in a subgame perfect Stackelberg Equilibrium the governments and the central authority know the consumers' response functions (6) and (7) when choosing their environmental policies.

### Noncooperative benchmark equilibrium

In the case of noncooperative water allocations, each country concerns itself with maximizing its own utility. Therefore, country 1 chooses  $\{t_1, a_1\}$  to maximize

$$W_1(t_1, t_2, a_1, a_2) = x_1^0(t_1, a_1) + u(y_1^0(t_1)) - v(\alpha_1(y_1^0(t_1) - a_1) + (1 - \alpha_2)(y_2^0(t_2) - a_2)), \quad (\text{Eq.8a})$$

taking  $\{t_2, a_2\}$  as given. Similarly, country 2 chooses  $\{t_2, a_2\}$  to maximize

$$W_2(t_1, t_2, a_1, a_2) = x_2^0(t_2, a_2) + u(y_2^0(t_2)) - v((1 - \alpha_1)(y_1^0(t_1) - a_1) + \alpha_2(y_2^0(t_2) - a_2)), \quad (\text{Eq.8b})$$

taking as given  $\{t_1, a_1\}$ . In equations (8a) and (8b),  $(1 - \alpha_2)(y_2^0(t_2) - a_2)$  and  $(1 - \alpha_1)(y_1^0(t_1) - a_1)$  are the transboundary externality components.

The first order interior conditions for the problem faced by country 1 are:

$$\begin{aligned} \frac{\partial x_1^0}{\partial t_1} + (u'(y_1^0) - \alpha_1 v'(D_1)) \left( \frac{\partial y_1^0}{\partial t_1} \right) &= 0, \\ \frac{\partial x_1^0}{\partial a_1} + \alpha_1 v'(D_1) &= 0. \end{aligned}$$

By substituting equations (5) – (7) into the above equations, we can express them as:

$$\begin{aligned} -p \frac{\partial y_1^0}{\partial t_1} + (p + t_1 - \alpha_1 v'(D_1)) \left( \frac{\partial y_1^0}{\partial t_1} \right) &= 0, \\ -s + \alpha_1 v'(D_1) &= 0 \end{aligned}$$

which leads to:

$$t_1 = \alpha_1 v'(D_1), \quad (\text{Eq.9})$$

$$\alpha_1 v'(D_1) = s. \quad (\text{Eq.10})$$

The first order interior conditions for the problem faced by country 2 similarly result in:

$$t_2 = \alpha_2 v'(D_2), \quad (\text{Eq.11})$$

$$\alpha_2 v'(D_2) = s. \quad (\text{Eq.12})$$

From equation (9) we see that country 1 sets its pollution tax equal to the marginal damage incurred solely from the salination level within its own boundary. Equation (10) demonstrates that country 1 produces abatement up to the level that equates marginal benefit and cost from abatement. The marginal benefit from abatement corresponds to the marginal salination damage avoided due to the country's production of an extra unit of abatement. Equations (11) and (12) are the analogues of equations (9) and (10), respectively, for country 2.

Since the noncooperative water allocation is a Nash equilibrium, we use the superscript "N" to denote our key noncooperative results. From equations (9) – (12) we obtain  $t_1 = \alpha_1 v'(D_1) = s$  and  $t_2 = \alpha_2 v'(D_2) = s$ , which lead to:

$$t_1^N = t_2^N = s. \quad (\text{Eq.13})$$

Combining equations (13) with (5), and recalling our curvature assumptions on  $u(\cdot)$  yields

$$y_1^N = y_2^N = y^N. \quad (\text{Eq.14})$$

In addition, equations (10) and (12), result in  $\alpha_1 v'(D_1) = \alpha_2 v'(D_2)$ , which, given our curvature assumptions on  $v(\cdot)$ , lead to:

$$\alpha_1 \neq \alpha_2 \Rightarrow \begin{cases} D_1^N > D_2^N \\ D_1^N = D_2^N \\ D_1^N < D_2^N \end{cases} \quad (\text{Eq.15})$$

To see this result, note that  $\alpha_1 v'(D_1) = \alpha_2 v'(D_2)$  can be written as  $\frac{v'(D_1)}{v'(D_2)} = \frac{\alpha_2}{\alpha_1}$ .

From this equality and the assumption that  $v'' > 0$ , the following result is immediate:

$$\alpha_1 > \alpha_2 \Rightarrow v'(D_2^N) > v'(D_1^N) \Rightarrow D_1^N < D_2^N$$

$$\alpha_1 = \alpha_2 \Rightarrow v'(D_2^N) = v'(D_1^N) \Rightarrow D_1^N = D_2^N$$

$$\alpha_1 < \alpha_2 \Rightarrow v'(D_2^N) < v'(D_1^N) \Rightarrow D_1^N > D_2^N$$

Above result tells us that a country's water withdrawal affects more the level of salination of a neighbor country than that of itself in the Nash equilibrium. We can see for example in the first inequality that country 2 will incur greater level of damage from salination than country 1 when the fraction of emitted salt dust in country 1 is higher than that in country 2.

### Fully cooperative salination benchmark

Next we consider a fully cooperative water allocation. To obtain this allocation, we assume a central government, or benevolent social planner, takes into consideration the aggregate economic benefits of the lake basin countries. In this regard, the central government chooses  $\{a_i, t_i\}_{i=1,2}$  to maximize the aggregate sum of the two counties' welfares:

$$W_1(t_1, t_2, a_1, a_2) + W_2(t_1, t_2, a_1, a_2)$$

$$x_1^0(t_1, a_1) + u(y_1^0(t_1)) - v(\alpha_1(y_1^0(t_1) - a_1) + (1 - \alpha_2)(y_2^0(t_2) - a_2)) +$$

$$x_2^0(t_2, a_2) + u(y_2^0(t_2)) - v((1 - \alpha_1)(y_1^0(t_1) - a_1) + \alpha_2(y_2^0(t_2) - a_2)). \quad (\text{Eq.16})$$

First-order conditions are:

$$\frac{\partial x_1^0}{\partial t_1} + (u'(y_1^0) - \alpha_1 v'(D_1) - (1 - \alpha_1)v'(D_2)) \left( \frac{\partial y_1^0}{\partial t_1} \right) = 0,$$

$$\frac{\partial x_2^0}{\partial t_2} + (u'(y_2^0) - (1 - \alpha_2)v'(D_1) - \alpha_2 v'(D_2)) \left( \frac{\partial y_2^0}{\partial t_2} \right) = 0,$$

$$\frac{\partial x_1^0}{\partial a_1} + \alpha_1 v'(D_1) + (1 - \alpha_1)v'(D_2) = 0,$$

$$\frac{\partial x_2^0}{\partial a_2} + (1 - \alpha_2)v'(D_1) + \alpha_2 v'(D_2) = 0.$$

Similar to the derivation of equations (9) – (15), using equations (5) – (7), we obtain  $t_1 = \alpha_1 v'(D_1) + (1 - \alpha_1)v'(D_2) = s$  and  $t_2 = (1 - \alpha_2)v'(D_1) + \alpha_2 v'(D_2) = s$ . We denote the cooperative allocation conditions by the superscript “\*” that result in:

$$t_1^* = t_2^* = s, \quad (\text{Eq.17})$$

$$\alpha_1 v'(D_1^*) + (1 - \alpha_1)v'(D_2^*) = (1 - \alpha_2)v'(D_1^*) + \alpha_2 v'(D_2^*) = s. \quad (\text{Eq.18})$$

Equation (17) parallels equation (13) from the noncooperative equilibrium. Similarly (18) parallels to (10) and (12). As in the noncooperative equilibrium, (5) can again be used to show:

$$y_1^* = y_2^* = y^*. \quad (\text{Eq.19})$$

As a consequence of the equalization of marginal social damages in (18), total damages equate as well. To see this, note from the first equality in (18) that  $(1 - \alpha_1 - \alpha_2)v'(D_1^*) = (1 - \alpha_1 - \alpha_2)v'(D_2^*)$ , which implies

$$D_1^* = D_2^* = D^*. \quad (\text{Eq.20})$$

In other words, unlike in the Nash equilibrium, where the relative signs of  $D_1$  and  $D_2$  depend on the sizes of  $\alpha_1$  and  $\alpha_2$ , the socially efficient damages equate irrespective of the values of  $\alpha_1$  and  $\alpha_2$ .

The following proposition compares the Nash Equilibrium with the cooperative solution.

*Proposition 1.* The comparison between noncooperative and cooperative allocations reveals that

$$D_1^N > D_1^*, \quad D_2^N > D_2^*, \quad E_1^N + E_2^N = E^N > E^* = E_1^* + E_2^*, \quad y^N = y^*, \\ a_1^N + a_2^N = a^N < a^* = a_1^* + a_2^*.$$

*Proof:* Comparing equations (13) and (17), we see that  $t_i^N = t_i^*$ ,  $i = 1, 2$ . Thus, equations (14) and (19) imply that  $y^N = y^*$  for given  $p$ . Given (20) and  $\alpha_2 < 1$ , comparing the second equality in (18) with (12) yields  $v'(D_2^*) = s = \alpha_2 v'(D_2^N) \Rightarrow D_2^N > D_2^*$ . Similarly, comparing the first equality in (18) with (10) yields  $v'(D_1^*) = s = \alpha_1 v'(D_1^N) \Rightarrow D_1^N > D_1^*$ . The inequalities  $D_i^N > D_i^*$ ,  $i = 1, 2$ , in turn imply the following two inequalities:

$$\alpha_1 (y_1^N - a_1^N) + (1 - \alpha_2)(y_2^N - a_2^N) > \alpha_1 (y_1^* - a_1^*) + (1 - \alpha_2)(y_2^* - a_2^*) \quad \text{and} \\ (1 - \alpha_1)(y_1^N - a_1^N) + \alpha_2 (y_2^N - a_2^N) > (1 - \alpha_1)(y_1^* - a_1^*) + \alpha_2 (y_2^* - a_2^*).$$

Adding these two inequalities results in  $(y_1^N - a_1^N) + (y_2^N - a_2^N) > (y_1^* - a_1^*) + (y_2^* - a_2^*)$ , i.e.  $E_1^N + E_2^N = E^N > E^* = E_1^* + E_2^*$ . The result  $y^N = y^*$  then implies that  $a_1^N + a_2^N = a^N < a^* = a_1^* + a_2^*$ .

As expected, *Proposition 1* shows that lake basin countries produce too little pollution abatement in the Nash Equilibrium and consequently generate too much salination relative to the respective socially efficient levels. Interestingly, in the Nash Equilibrium the two countries set efficient tax rates, which in turn yield socially efficient withdrawal levels. These results indicate that in a partially cooperative regime, where the national governments share authority with a central government, it is necessary to give abatement authority to the central government, while allowing the national governments to retain authority over pollution taxes. We explore this sharing arrangement in the next section, with the added condition that the national governments set their tax rates *prior to* the central government's choice of abatement levels. This scheme is called "Decentralized Leadership".

### Decentralized leadership game

Following Caplan and Silva (1999), we examine a Stackelberg Equilibrium, whereby the national governments choose their respective tax rates before a central government chooses their abatement levels. Their arrangement presumes that countries 1 and 2 have integrated into a union with the central government. The central and national governments have agreed beforehand to form the union. Under the decentralized – leadership framework, the national governments act as Stackelberg leaders and the central government as a Stackelberg follower. *Fig. 1* depicts their arrangement.

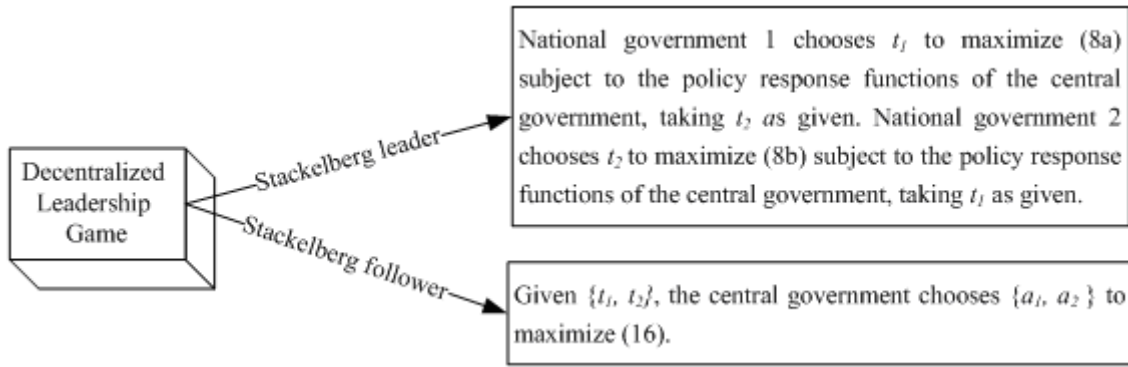


**Figure 1** The Decentralized Leadership Game

We solve for this game’s subgame perfect equilibrium by backward induction, therefore starting with the central government’s choice of  $\{a_1, a_2\}$  to maximize (16), taking  $\{t_1, t_2\}$  as given.

Noting equations (1) and (7), this problem yields the following first order conditions:

$$\alpha_1 v'(D_1) + (1 - \alpha_1) v'(D_2) = s, \quad (\text{Eq.21})$$

$$(1 - \alpha_2) v'(D_1) + \alpha_2 v'(D_2) = s. \quad (\text{Eq.22})$$

Via comparison with equation (18), equations (21) and (22) show that the equilibrium salination damages in this game,  $D_1^1$  and  $D_2^1$ , are both equal to  $D^*$ . In other words, when endowed with the authority to set abatement levels in the final stage of a two-stage game with the national governments, the central government has no other incentive than to follow its optimal abatement rule. Defining the abatement levels as implicit functions of  $t_1$  and  $t_2$ , i.e.  $a_i^1(t_1, t_2)^1$ ,  $i = 1, 2$ , we can now specify the central government’s abatement responses by first differentiating equations (21) and (22) with respect to  $t_1$ , which yields

$$\alpha_1 v''(D_1) \left( \alpha_1 \left( \frac{\partial y_1^0}{\partial t_1} - \frac{\partial a_1^1}{\partial t_1} \right) - (1 - \alpha_2) \frac{\partial a_2^1}{\partial t_1} \right) + (1 - \alpha_1) v''(D_2) \left( (1 - \alpha_1) \left( \frac{\partial y_1^0}{\partial t_1} - \frac{\partial a_1^1}{\partial t_1} \right) - \alpha_2 \frac{\partial a_2^1}{\partial t_1} \right) = 0, \quad (\text{Eq.23a})$$

$$(1 - \alpha_2) v''(D_1) \left( \alpha_1 \left( \frac{\partial y_1^0}{\partial t_1} - \frac{\partial a_1^1}{\partial t_1} \right) - (1 - \alpha_2) \frac{\partial a_2^1}{\partial t_1} \right) + \alpha_2 v''(D_2) \left( (1 - \alpha_1) \left( \frac{\partial y_1^0}{\partial t_1} - \frac{\partial a_1^1}{\partial t_1} \right) - \alpha_2 \frac{\partial a_2^1}{\partial t_1} \right) = 0, \quad (\text{Eq.23b})$$

Since  $D_1^1 = D_2^1 = D^*$  and  $v'' > 0$ , we can rewrite equations (23a) and (23b) as follows:

$$\alpha_1 \left( \alpha_1 \left( \frac{\partial y_1^0}{\partial t_1} - \frac{\partial a_1^1}{\partial t_1} \right) - (1 - \alpha_2) \frac{\partial a_2^1}{\partial t_1} \right) + (1 - \alpha_1) \left( (1 - \alpha_1) \left( \frac{\partial y_1^0}{\partial t_1} - \frac{\partial a_1^1}{\partial t_1} \right) - \alpha_2 \frac{\partial a_2^1}{\partial t_1} \right) = 0,$$

<sup>1</sup> We use superscript “1” to denote equilibrium quantities in this game.

$$(1 - \alpha_2) \left( \alpha_1 \left( \frac{\partial y_1^0}{\partial t_1} - \frac{\partial a_1^1}{\partial t_1} \right) - (1 - \alpha_2) \frac{\partial a_2^1}{\partial t_1} \right) + \alpha_2 \left( (1 - \alpha_1) \left( \frac{\partial y_1^0}{\partial t_1} - \frac{\partial a_1^1}{\partial t_1} \right) - \alpha_2 \frac{\partial a_2^1}{\partial t_1} \right) = 0,$$

Solving the above equations simultaneously, yields

$$\frac{\partial y_1^0}{\partial t_1} - \frac{\partial a_1^1}{\partial t_1} = \frac{\partial a_2^1}{\partial t_1} = 0 \quad (\text{Eq.24})$$

for  $\alpha_1 + \alpha_2 \neq 1^2$ .

Similarly, differentiation of equations (21) and (22) with respect to  $t_2$  and simultaneous solution yields

$$\frac{\partial y_2^0}{\partial t_2} - \frac{\partial a_2^1}{\partial t_2} = \frac{\partial a_1^1}{\partial t_2} = 0 \quad (\text{Eq.25})$$

for  $\alpha_1 + \alpha_2 \neq 1$ .

From (Eq.24) and (Eq.25), we can write  $a_i^1 = a_i^1(t_i)$ ,  $i = 1, 2$ . We also see that the central government responds to changes in each country's pollution tax by choosing abatement such that salination remains at its socially efficient level in each country.

As a Stackelberg leader, national government 1 chooses  $t_1$  to maximize (Eq.8a) subject to  $a_1^1 = a_1^1(t_1)$  derived in (Eq.24). Similarly, national government 2 chooses  $t_2$  to maximize (Eq.8b) subject to  $a_2^1 = a_2^1(t_2)$  derived in (Eq.25). Using (Eq.6), (Eq.7), and (Eq.24) and (Eq.25) respectively, we find that the first – order conditions characterizing the Nash equilibrium in the second – stage of the game reduces to:

$$u'(y_i) = p + s, \quad i = 1, 2 \quad (\text{Eq.26})$$

Combining equations (26) with (5), and recalling (21) and (22), we see that the subgame perfect equilibrium for Game 1 satisfies the fully cooperative allocation conditions (17) and (18). These cooperative allocation conditions describe the Nash equilibrium tax rates in stage 1 of the decentralized – leadership game:

$$t_1^1 = t_1^* = \alpha_1 v'(D_1^*) + (1 - \alpha_1) v'(D_2^*) \quad (\text{Eq.27a})$$

$$t_2^1 = t_2^* = (1 - \alpha_2) v'(D_1^*) + \alpha_2 v'(D_2^*) \quad (\text{Eq.27b})$$

Equations (27a) and (27b) demonstrate that the national governments choose to set their respective pollution tax rates equal to the marginal social damage caused by their country's water withdrawal level. Their result is driven by the national governments' anticipation of the central government's pollution abatement policy response to their respective pollution tax policies. If a national government sets the pollution tax too low (relative to the socially efficient rate), thereby encouraging excessive water use for

<sup>2</sup> This stage of the game does not admit a definite solution for the case of  $\alpha_1 + \alpha_2 = 1$



irrigation, the central government responds with an abatement level that offsets the expansionary effect of the low tax on the irrigation level generated in the basin. Correspondingly, if the national government sets the pollution tax too high, the central government will offset with reduced abatement for this country in order to maintain that country's salination at the socially efficient level. This leads to our second and final proposition.

*Proposition 2. The subgame perfect equilibrium for Game 1 is a socially optimal.*

*Proof:* Equations (21) and (22) are identical to (18). Equations (17) are implied by equations (5) and (26).

## Conclusion

Our analysis suggests that a partially cooperative water withdrawal agreement between countries that share a lake basin used for cotton irrigation can reduce the level of salination to its socially efficient level. Our findings show that under an agreement where a central government sets a salination abatement levels *after* the national governments impose taxes an irrigation, the socially efficient level of salination can be attained. Both policy instruments – abatement and the tax – do not need to be controlled by a central authority.

In this paper we do not investigate the other three Stackelberg Equilibrium games that Caplan and Silva (1999) examine. If we analyzed them, we would expect results similar to Caplan and Silva (1999) for acid rain in an upstream – downstream setting. Particularly, we would see that the central government is unable to respond completely to the national governments' abatement policies by their pollution taxes in the second subgame of the decentralized leadership. The pollution tax rates would be higher in the second subgame equilibrium than tax rates in the first subgame equilibrium that we have studied.

In the centralized leadership subgames, where the central government acts as a Stackelberg leader and the national governments act as Stackelberg followers, we could see that the national governments are ignoring to follow the central government's policies. The results would demonstrate that country did not recognize the salination damage that its water withdrawal caused in the neighbor country. Consequently, basin's countries would not obtain the social efficient salination levels.

Finally, we hope that our findings should enable local and central policymakers to better assess the implication of cooperative water withdrawing practices in international river and lake basins. As we have shown in this paper, a Pareto optimal allocation can be attained through partial cooperation.

## REFERENCES

- [1] Cotton This Week, International Cotton Advisory Committee, February 2005.
- [2] Gillham, F. et al. (1995): Cotton Production Prospects for the Next Decade, World Bank Technical Paper Number 287. – The World Bank, Washington D.C.
- [3] Godwin, O., Obasi, P. (2003): Challenges and Opportunities in Water Resource Management. – World Meteorological Organization (Lecture at the 93rd Annual Meeting of the American Meteorological Society, February 11, 2003).

- [4] Hardin, G. (1968): The Tragedy of the Commons. – Science 162: 1243-1248.
- [5] ICG (2002): Central Asia: Water and Conflict. – ICG Asia Report N34, Brussels.
- [6] Mangold, T., Goldberg, J. (2001): Plague Wars: The Terrifying Reality of Biological Warfare. – Macmillan, pp.46-47, ISBN 9780312263799.
- [7] Micklin, P., Aladin, N.V. (2008): Reclaiming the Aral Sea. – Scientific American 3.
- [8] Moulin, H. (1995): Cooperative Microeconomics: a Game – Theoretic Introduction. – Princeton University Press, Princeton.
- [9] Rogers, P. (1969): A Game Theory Approach to the Problems of International River Basins. – Water Resources Res 5(4): 749-760.
- [10] Silva, E.C.D., Caplan, A. (1999): Federal Acid Rain Games. – Journal of Urban Economics 46: 25-52.
- [11] UNESCO (2000): Water Related Vision for the Aral Sea Basin for the Year 2025. – Paris.
- [12] Willis, T.M., Black, A.S. (1996): Irrigation Increases Groundwater Recharge in the Macquairie Valley. – Australian Journal of Soil Research 34(6): 837-847.
- [13] WRI (2000): World Resources 2000-2001: People and Ecosystems: the Fraying Web of Life. – World Resources Institute, Washington, D.C.
- [14] Zilberman, D. (1998): The Impact of Agriculture on Water Quality. – In: OECD: Sustainable Management of Water in Agriculture: Issues and Policies, Paris, p.133-149.

## TREE APPRAISAL METHODS AND THEIR APPLICATION – FIRST RESULTS IN ONE OF BUDAPEST'S DISTRICTS

HEGEDÜS, A.<sup>1\*</sup> – GAÁL, M.<sup>1</sup> – BÉRCES, R.<sup>2</sup>

<sup>1</sup>*Corvinus University of Budapest, Department of Mathematics and Informatics  
1118 Budapest Villányi út 29-43., Hungary  
(phone: +36-1-482-6261; fax: +36-1-466-9273)*

<sup>2</sup>*Budapest University of Technology and Economics, Department of Management and  
Corporate Economics  
1117 Budapest, Magyar tudósok körútja 2., Hungary  
(phone: +36-1-463- 2782; fax: +36-1-463-1606)*

*\*Corresponding author  
e-mail: andras.hegedus@uni-corvinus.hu*

(Received 21<sup>st</sup> November 2011; accepted 2<sup>nd</sup> December 2011)

**Abstract.** Street trees provide a number of environmental and social benefits, including contributing to climate change adaptation and mitigation and providing urban green space. In all settlements is important to know the quantity and quality of the trees and develop up-to-date tree cadastres. Frequently there is a need to place a monetary value on amenity trees, therefore several methods with different approaches have been developed. In our paper we discuss and compare some widely applied international and Hungarian methods taken into consideration their benefits and disadvantages. A tree survey was done in the year 2010, in one of the greenest districts of Budapest. Based on the survey species composition, distribution by age of the trees, condition of the trees, proportion of the fruit and ornamental trees were analysed and calculations were done regarding the tree values. Results show that good judgement through experience is important in selecting the method to use, for no one method can be used under every condition.

**Keywords:** *tree appraisal, Budapest, tree value calculation, Radó method, Párkányi method*

### Introduction

Street trees should be considered as a part of a settlement's infrastructure, namely the "green infrastructure". Therefore tree cadastral assessments should be among the important and regularly performed activities in all settlements and cities. These surveys can give an adequate picture of the species, age, condition and the exact location of the trees in the public areas. All people expect to have a healthy living environment therefore a reasonable demand is for the professional maintenance of the green areas. The planning of the maintenance works (e.g., need of manpower to clean up of the falling crops, pruning to prevent accidents, determine the trees that may be removed) requires also the accurate knowledge of the trees. Tree cadastre has an important role in defining the commons (aesthetic value as well), on the other hand in determining the value of the – with or without permission – removed trees, calculating the extent of the caused damages.

During the surveys the precise mapping should be emphasised. The cadastral maps should be kept continuously up to date, i.e. all planting and cutting must be marked immediately, the state of the storm damaged trees should be updated to keep up to date information available. Besides respecting these basic updates a full survey should be needed every 5 years recording the changes during that time and controlling the

intermediate updates. Experience, however, that most of the settlements do not carry out tree cadastral surveys, due too the lack of financial resources. When they do, the survey often does not extend beyond the data recording and some basic statistics.

Many times there is a need for using such methods that allows defining the values (whether expressed in monetary value) of the trees by standard criteria, so the trees become comparable. Amenity tree evaluation systems are widely used all around the world. They place a monetary value on trees, usually for the purposes of insurance, compensation and litigation. However, the major significance of placing such a value on trees is that they are then recognised as assets.

## Review of literature

### *Factors in the tree evaluation methods*

The terms valuation (or evaluation) and appraisal are frequently used interchangeably (Kielbaso, 1979; Watson, 2002; Cullen, 2007; Sarajevs, 2011), and that is the intent here. However, they may be distinguished in particular practice settings, as the term appraisal may describe non-monetary values (Litchfield, 2010).

Several tree evaluation methods were developed in the world, in Hungary some domestic methods are in use. Their particular uses vary with the size of tree, species, purpose, nature of loss, etc. Plant appraisal may involve more than just trees; it often includes shrubs, vines, ground plants and landscape structures (Dreesen, 2005).

All calculations have some kind of **base value**. In most cases this is the producer price of the given nursery. This can raise now some problems in itself, because no matter how old, how many times replaced and what size has the sapling considered for the basic value. Revised Burnley method uses a specific approach, as the base value is the cost per cubic meter of retail nursery stock (Moor, 1991).

Determining the base value it is advised using the average prices of several nurseries, because even within the country may be 200-300% price difference among the ornamental trees with the same size and other properties. Bulř (2009) made calculations for the base tree prices in the Czech Republic. His calculations indicate that prices of individual taxa may differ considerably. The differences are caused by the following factors: tree species (cultivar) itself, chosen young plant size, genetic qualities of the evaluated taxon – and above all, speed of maturation growth and crown size.

The calculation of the planted price is also common, which means the cost of planting and follow-up care (from planting to the beginning of the growing) of a given variety with a defined size at a certain place.

Choosing the sapling for planting must be considered that the tree can fulfil its function and reaches the value of the formerly removed tree as soon as possible. Therefore the replacement cost method is also commonly used. However, replace the same number and size of plants is usually used on small trees and shrubs. According to King (1977) for trees over 18 inches (45 cm) in diameter, this may be impractical. The other possibility is replacing a large tree with several small trees which may equal the total diameter of the large tree. Calculating the replacement cost, the tree size is a limiting factor. It is not possible to plant a tree of any size, not all of tree species have available elderly specimen and large plants are often unrealistically expensive. This is partly due to the additional costs and manning requirement, on the other hand a much smaller supply compared to the young plants results in a higher than realistic price.

The base value should be corrected with different factors. Size, species, condition and location are the generally used appraisal factors.

There are different opinions about the consideration of the **tree size** and its quantification. Several methods use values of trunk circumferences, height or crown volume. In case of a given species these can be important factors, but in a tree survey, where several different species can be found, these can lead astray, since the species have very different growth types and vigour.

It is advised using the age (as well), because this can be a basis for comparison independently from the species. Age, as a characteristic of the size, is independent from the place of the planting and specific ecological conditions, is acceptable as an appreciation factor, and a frequently used argument is that the maintenance costs during the years can be included in the value of the tree. In this case the higher age means more cost and also a higher tree value.

Based on studies most of the environmental impacts of the trees are related to the canopy. Therefore, some methods are based on the size of canopy (Jószainé Párkányi, 2004). However, the canopy size is proportional to the age and during the surveys the determination of the age is easier.

Tree size can also be determined by the cross-sectional area of the trunk. According to Dreesen (2005) for trees with a diameter of 4 inches or smaller, the diameter should be determined at a height of 6 inches above the ground. For trees with a diameter of 5 to 8 inches, the diameter is determined 12 inches above the ground. For trees with diameters larger than 8 inches, the diameter is determined at a height of 4.5 feet. For multi-trunked trees, full diameter of the largest trunk plus half the diameter of the other trunks determines the diameter for computing the cross section area. Application of the trunk size is also desirable if trees are cut for timber use.

Tree **species** and cultivars vary widely in aesthetic, functional and maintenance characteristics and/or requirements. Species ratings are affected by adaptability to soil and climatic differences; growth characteristics; maintenance requirements; susceptibility to insects, diseases and air pollution; allergenic properties and aesthetic values (Kissinger and Van Ells, 1998). Species rating is usually expressed as a percentage relative to a „high quality” specimen, and often varies geographically. The influence of species quality on appraised value varies with method (Watson, 2002). Grouping tree species into value classes is subjective and may vary also from one part of the state and one tree specialist to another.

**Location** can have different aspects in the appraisal. The design and quality of the surroundings is an important factor. For example, a tree in a well-maintained suburban residential area will rate very differently than that same tree in front of a factory. The aesthetic aspect usually means „the right tree in the right place”, but with the location factor we might even consider „a wrong tree in the right place” (Kielbaso, 1979). A plant's placement may determine its functional attributes, like providing summer shade, windbreak, erosion control, etc.

The **condition** of a tree depends on overall vigour, size, form, decay, insect and disease problems and expected life (Kielbaso, 1979). As trees become old they often become defective through decay, broken limbs, damage by humans or uneven growth. Only an experienced evaluator can make accurate condition determinations, as knowledge of tree pathology, entomology and physiology is important to do it. The specialist appraising the tree usually must judge the condition on a percentage basis. A tree that has a hazardous condition (cracks, weak branches) could even have a negative

value if it is unsafe and should be removed. In this case there will be a cost for removal and cleanup (Kissinger and Van Ells, 1998). To the air quality improvement only trees with a healthy assimilation surface can contribute.

Some methods use other special factors, too. For example the Standard Tree Evaluation Method for trees over 50 years old takes into account historic, relict, scientific features (Watson, 2002).

### ***International methods***

There are several ways to place a value on plant material. Armstrong (1947) reviewed various formulas and concluded that they were all arbitrary. Calculations based on different methods can lead to very different results. Therefore good judgment through experience is important in selecting the method to use, for no one method can be used under every condition (King, 1977).

The commonly used appraisal methods are presented in *Table 1*. One of the simplest formulas (Kielbaso, 1979), based on which other methods were elaborated is:

$$\text{Value} = \text{basic value or replacement cost} \times \text{species} \times \text{condition} \times \text{location.}$$

**Table 1.** *International tree appraisal methods*

<b>Method</b>	<b>Formula</b>
CTLA – Guide for Plant Appraisal (USA)	trunk area at 1.4m (4.5 ft) × basic price × species × condition × location
Revised Burnley Method (Australia)	tree volume × base value × life expectancy × form and vigour × location
Helliwell – Amenity Valuation of Trees and Woodlands (Great Britain)	tree size (cross-sectional area of the crown) × life expectancy × importance in the landscape × presence of other trees × relation to setting × form × special factors × monetary conversion value (£25 in 2008)
STEM – Standard Tree Evaluation Method (New Zealand)	[total points of 20 tree attributes (540 possible) × wholesale cost + planting cost + maintenance cost] × retail conversion factor (2 suggested)
Norma Granada (Spain)	(value factor based on species and size × wholesale cost × condition) × [1 + life expectancy + (aesthetic value + species rarity + site suitability + extraordinary)]
CAVAT – Capital Asset Value for Amenity Trees (Great Britain)	basic value based on the trunk area × location-accessibility factor × functional factor × amenity and appropriateness factor × safe life expectancy factor
Koch (Germany)	planting cost + follow-up care (first 3 years) + maintenance costs of the further period

Some methods are based on the measurement of the cross-sectional area of the trunk at 1.4 m (4.5 ft) multiplied by a monetary value per square inch (Watson, 2002; Grey and Deneke, 1986). According to Dreesen (2005) the trunk formula method usually underestimates the value of small trees, but is frequently used in estimating values of trees larger than 8 inches in diameter measured at 4.5 feet above the ground. According to the Guide for Plant Appraisal (USA), this value should be modified by species, condition and location. Dreesen (2005) presents the tables for species grouping, condition classification and location values used in Texas. This method is outstanding in the determination of the condition. There are six condition factors, each rating from one to five. The sum of the rating for each of the six factors is the tree's condition rating.

The Helliwell method (Helliwell, 2000) is very easy to use. It is based on six standard factors and any special factors such as historical association or exceptional rarity can also be applied where required. Each factor is scored from 1 to 4 points and the scores for all factors are multiplied to give an assessment for a given tree. At the end an assigned monetary value per point can be used.

There are two versions of the CAVAT method. The Full Method is recommended for use in decisions concerning individual trees or groups, when precision is required and sufficient time is available for a full assessment. The Quick Method is intended specifically as a strategic tool for management of the stock as a whole, as if it were a financial asset of the community (Neilan, 2010). The Quick Method involves three steps and key variables:

- Basic value / size
- CTI (Community Tree Index) value
- Functional value.

The basic value is determined by the trunk diameter, according to given categories. For the purposes of CAVAT the exact size is not needed. The basic value of the tree population will be adjusted according to the population density of the urban areas. The functional value can be retained at 100%, but may be reduced according to the crown size or the condition (e.g., need for any immediate works).

Watson (2002) compared five tree appraisal methods (CTLA, Standard Tree Evaluation Method, Helliwell, Norma Granada and Burnley) used in different countries. In his study nine individuals with professional interest in the value of urban trees appraised the same six trees using all five methods. He found that there is not only an essential difference among the resulting values of the methods, but a strong relationship between variation among appraisers and the mathematical operations used in the formulas. Formulas, which multiply all of the rated factors together, consistently produced highest variation among appraisers, while methods which add all the factors together, consistently produced the lowest variation among appraisers.

Sarajevs (2011) compared the CAVAT, Helliwell and i-Tree methods. He also stated that the valuation systems differ significantly in methodology, data requirements and outputs. While the Helliwell method is based on expert judgements, the i-Tree requires data collected from a sample or a complete inventory of the street tree population as well as community-specific information (e.g., programme management costs, city population size, and price of residential electricity), and CAVAT is somewhere in between. CAVAT and i-Tree take substantial account of the social/cultural value component of trees. But Sarajevs (2011) calls the attention that none of the three systems is able to comprehensively quantify the biodiversity or social/cultural benefits of the trees despite these value components often being considered the most important to society.

### ***Hungarian methods***

In Hungary the most commonly used method was developed by Dezső Radó (Radó, 1981), based on multiplication of factor values. The base value in this method is the cost of a standard four-year sapling at a given location in the assessment period. The base value should be modified according to the age, location and condition of the tree. The life-time factor is given by leaf counting up to 70 years of age, above this there is no differentiation. The base value of the location and condition factors is 1. In case of worse condition of a tree, the value of this factor can be 0.7 or 0.4. Regarding the

location, the value of 1 refers to crowded urban areas, in case of smaller towns 0.7, in villages and rural areas 0.4 should be used.

Less common is the Párkányi method (Jószainé Párkányi, 2007). This calculation is based on the canopy size, taking into account the growth phases of the trees, including species specific growth functions. Therefore, the method is more complicated, but a table, which holds average growth values, simplifies its use. The values of the crown condition factor are the same as in case of Radó method, but the age and location factors are different, the multiplication values are slightly lower in this method.

The advantage of the Radó method is its reputation, most of the professionals can use it. However, a serious problem is the application of the standard four-year sapling as a base value. Over the years, buyers and landscape architectures are becoming more demanding regarding the size of the trees, so the nursery production shifted to the older and larger plants. Thus, the standard four-year sapling (about 8/10 circumference) is not included in most of the nursery offers. The Párkányi method attempts to improve the Radó method. On the one hand the age factor is given up to 190 years, on the other hand two-times replaced sapling with a size of 10/12 circumference is used as base value. Both methods have the obvious advantage that the initial value is determined by the price of a sapling (Table 2), which can be in any currency.

**Table 2.** Hungarian tree appraisal methods

Method	Formula
Radó	basic price × age × location × condition
Párkányi	basic price × age × crown condition × location

## Materials and methods

The tree survey held place in one the greenest districts of Budapest in the summer of 2010, financed by a tender. The last similar district-wide survey was in 1996, in the intermediate time only the major changes were recorded.

The area of the district is 36.34 km<sup>2</sup>, but the survey was carried out only in the inner city areas of 22.64 km<sup>2</sup> size. The survey covered all of the trees in public areas managed by the local government. However, the district has some parts belonging to the management of the capital, where no survey was done (about 5% of the trees in the district). The survey was based on a parcel-level map of the district, divided in 102 sectors and carried out by measuring pairs by sectors. The exact location of the trees was determined relative to the locations of the properties using measuring tapes and laser distance meters and marked on the map. The attributes of the trees were recorded in previously prepared form sheets. The location, species (in Hungarian and Latin name), age and some properties (height, crown diameter, height and circumference of the trunk) were recorded. Beside the condition of the crown, trunk and roots, the state of protection or endangered and also the lack of management operations were examined. The potential negative effects of the tree (risks for transport, public utilities or accidents) were also assessed.

Each tree got a unique identifier formed from the letter of the measurement group, the sector number and the number of the tree within the sector. A digital photo was taken too, documenting the condition and the surroundings of each tree. At the end of the day the measuring groups uploaded all data and photo through an Internet-based



system. After completing a sector, the trees marked on the paper maps were digitised by landscape architects using AutoCAD. From there it was possible to calculate the EOV coordinates of the trees.

## Results

### *Composition of the trees*

During the survey 27450 records were admitted, but there were not so many trees. In 414 cases the name was “stock”, when in a small space like in a splay several trees/shrubs live together, but have a dominant species. In 483 cases lack of tree was recorded, that appears to have ever a tree there as a remaining trunk or furrow could be observed, but no living tree can be found. The local government had particular interest in the lack of trees, which may be important for the future re-plantings. There were 4 records called “root”, in these cases only some root pieces were left in the place of the trees, it can be considered same as lack of tree. In 57 cases the tree was unrecognisable, the measuring groups could not identify because they were completely dry or had severe disease. Therefore, a total of 26492 separate accurately identified trees were found in the area examined, which form the basic of the further analyses.

According to the database 220 species can be found in the district. In case of 90 species there are less than 10 specimens, in case of 22 species only 1-1 sample can be found in the area, so these species are negligible in maintenance and work-organisational aspects. The most significant species (*Table 3*) have more than 300 specimens.

*Table 3. The most significant species of the district*

<b>Botanical name</b>	<b>Count</b>
<i>Acer platanoides</i>	2377
<i>Robinia pseudoacacia</i>	2127
<i>Juglans regia</i>	1702
<i>Fraxinus excelsior</i>	1334
<i>Prunus cerasifera</i>	1218
<i>Prunus domestica</i>	979
<i>Prunus cerasus</i>	823
<i>Tilia cordata</i>	819
<i>Sophora japonica</i>	794
<i>Betula pendula</i>	706
<i>Aesculus hippocastanum</i>	633
<i>Celtis occidentalis</i>	622
<i>Acer campestre</i>	603
<i>Fraxinus ornus</i>	599
<i>Ailanthus altissima</i>	536
<i>Tilia tomentosa</i>	443
<i>Acer negundo</i>	434
<i>Thuja occidentalis</i>	426
<i>Tilia platyphyllos</i>	393
<i>Koelreuteria paniculata</i>	389
<i>Platanus x hybrida</i>	321
<i>Acer pseudoplatanus</i>	321

It is worth examining the ratio of the deciduous and evergreen species as well. There are 177 deciduous species with a total of 24523 specimens, while 43 evergreen species

with 1980 specimens in the district. Evergreens are often of higher demand for environmental factors and are less tolerant to polluted air that can be an explanation for this somewhat distorted ratio. It should be noted, however, that the nursery price of the evergreens is higher than that of deciduous trees, so deciduous trees are more favoured to reduce the planting cost.

According to Simson (2010), trees that have the greatest capacity to improve urban air quality are:

- *Acer campestre* (603)
- *Acer platanoides* (2377)
- *Alnus glutinosa* (8)
- *Betula pendula* (706)
- *Fraxinus excelsior* (1334)
- *Larix* sps. (12)
- some *Pinus* species.

The numbers in parentheses indicate the numbers of the specimens found in the district examined. As it can be seen, the great number of *Acer platanoides* and *Fraxinus excelsior* is favourable. *Larix* and *Alnus* species are rarely found in public places in Hungary, there are only few individuals in the study area. *Pinus* species can be found mainly in mountainous settlements, in Budapest they are rare. In the study area *Pinus nigra* (141) and *P. sylverstris* (37) can be found in considerable amount. These species are only about 20% of the total plants, the optimal ratio would be 30-40%.

### ***The age of the trees***

The overall average age of the trees in the district is 19.29 years. Considering the average values (Table 4), even the youngest important species are over ten years.

**Table 4.** Age of the most significant species

<b>Botanical name</b>	<b>Average of the age</b>	<b>St. deviation of the age</b>
<i>Sophora japonica</i>	38.58	15.74
<i>Aesculus hippocastanum</i>	31.57	15.39
<i>Koelreuteria paniculata</i>	28.42	16.48
<i>Tilia platyphyllos</i>	27.65	14.02
<i>Juglans regia</i>	26.71	11.94
<i>Platanus x hybrida</i>	26.23	22.15
<i>Tilia tomentosa</i>	25.44	13.60
<i>Celtis occidentalis</i>	23.93	14.77
<i>Acer negundo</i>	22.48	14.97
<i>Tilia cordata</i>	22.04	14.09
<i>Robinia pseudoacacia</i>	22.00	13.41
<i>Acer campestre</i>	19.96	13.29
<i>Betula pendula</i>	19.05	8.90
<i>Acer pseudoplatanus</i>	19.03	12.42
<i>Ailanthus altissima</i>	18.48	12.10
<i>Prunus cerasus</i>	18.47	8.56
<i>Prunus domestica</i>	16.66	8.08
<i>Fraxinus excelsior</i>	16.40	11.51
<i>Acer platanoides</i>	15.85	9.40
<i>Prunus cerasifera</i>	15.61	8.73
<i>Fraxinus ornus</i>	15.38	8.36
<i>Thuja occidentalis</i>	10.36	5.18

The oldest species are *Sophora japonica*, *Aesculus hippocastanum*, *Populus x Canadensis* and *Tilia europea*. This is not surprising, since these were the most popular ornamental trees in the past, and were planted almost entirely in certain eras.

### Condition

The crown condition is a critical parameter in the tree evaluation. *Table 5* indicate the proportion of the trees with entire crown in case of the most important species.

The bad value of the *Robinia pseudoacacia* should be highlighted. This is the second most common species in the district, but 40% of the trees do not have entire, healthy crown. This is problematic both aesthetic reasons and due to the possible risk of accidents. In another survey conducted also in Budapest (VIII. District, Orczy Garden) in the year 2007, *Robinia pseudoacacia* showed similarly poor results (Hegedüs, 2008). Based on the experiences this species has a high susceptibility for drying, especially in case of older trees there are more dried ones compared to other species.

In case of the species composition it was mentioned now that because of the absence or severe damages 544 trees should be replaced by all means in the area examined.

**Table 5.** Proportion of the trees with entire crown

Botanical name	Entire crown
<i>Thuja occidentalis</i>	88%
<i>Betula pendula</i>	83%
<i>Acer pseudoplatanus</i>	79%
<i>Prunus cerasifera</i>	79%
<i>Fraxinus excelsior</i>	78%
<i>Fraxinus ornus</i>	76%
<i>Aesculus hippocastanum</i>	75%
<i>Ailanthus altissima</i>	75%
<i>Juglans regia</i>	74%
<i>Platanus x hybrida</i>	74%
<i>Acer platanoides</i>	73%
<i>Acer campestre</i>	72%
<i>Tilia cordata</i>	72%
<i>Tilia tomentosa</i>	72%
<i>Celtis occidentalis</i>	67%
<i>Tilia platyphyllos</i>	67%
<i>Prunus domestica</i>	66%
<i>Acer negundo</i>	62%
<i>Robinia pseudoacacia</i>	60%
<i>Koelreuteria paniculata</i>	58%
<i>Prunus cerasus</i>	53%
<i>Sophora japonica</i>	53%

### Proportion of the fruit trees and ornamental trees

In case of street trees the number of the fruit trees needs a special attention. The formulas for tree evaluation usually cannot determine the value of fruit or nut bearing trees, which can be appropriately determined by crop yield.

In the previous decades it was usual in Hungary planting fruit trees along the streets, but due to the resulting problems nowadays they are not planted. The most important problem of the fruit trees is caused by the falling fruits, requiring continuous cleaning in the ripening season to avoid slipping and accidents. The falling fruits are attractive for

various insects and especially wasps are problematic because of their dangerous sting. Interesting question could be also the proliferation of the pests, as in public areas the plant protection is unusual. These pests can easily infect the trees in home gardens, and despite the treatments carried out in the gardens, that trees can get an infection again from the public places.

A total of 4366 fruit trees have been recorded in the district. 315 belong to the nuts (e.g., *Castanea sativa*, *Coryllus colurna*, *Jugland regia*), which cause less pollution, so the fruit trees should be evaluated without this specimens. However, the remaining 4051 fruit trees require special attention. The district has a garden suburb region, fruit trees are dominant there.

It is worth to examine the ownership status of these trees. Trees in public areas belong to the local government, therefore planting, cutting or trimming requires permission. However, many people planted fruit trees in front of their houses, which they consider their own property. Since the life cycle of the fruit trees is usually shorter than that of the ornamental trees, cutting and replacement is more frequent. Few people applies for the required permission, therefore penalty occurs often.

### **Monetary value of the trees**

In the review of literature it was mentioned now, that calculations based on different methods can lead to very different results. In this study only some calculations were done as an example. In *Table 6* monetary values of three different species can be seen. The condition of the trees was considered good in all cases and the location was also assumed to be the same (appropriate to the value 1 in the Radó method), while the age of the trees was different to present its effect.

**Table 6.** Tree values calculated with different methods (in HUF)

<b>Method</b>	<b><i>Acer platanoides</i> 20 years</b>	<b><i>Celtis occidentalis</i> 40 years</b>	<b><i>Fraxinus excelsior</i> 20 years</b>
Radó method	180 000	800 000	120 000
Párkányi method	360 750	2 047 500	277 500
Revised Burnley Method	558 795	5 747 607	347 695
CAVAT quick method	716 380	4 815 080	1 203 940
CTLA (Texas)	274 873	2 681 042	1 932 700
Helliwell	380 800	1 713 600	380 800

The very different results of the methods can be observed, but we can find some explanations for them.

The age of *Celtis occidentalis* was considered more than that of the other two trees. It is reflected in the results, as its monetary value is much higher in every calculation.

Comparing the Hungarian methods, Párkányi method is based on greater sapling size (10/12 circumference, while 8/10 is in case of Radó), so the basic prices are higher with about 2000 HUF. The multiplication values regarding the condition are the same, however there are differences concerning the location and the age. These values are higher in the Párkányi method.

The Helliwell method does not take into account the species, therefore the resulting values of two very different species can be the same.

The CTLA method has a grouping system for species. Based on the table used in Texas, *Fraxinus excelsior* has higher species value than *Acer platanoides*, this is the reason of the different values in case of two trees with similar parameters and location.

Revised Burnley method uses a specific approach, as the base value is the cost per cubic meter of retail nursery stock. This is a problematic part in the calculation, as Hungarian nurseries have other price formation system, therefore the suggested 77 USD was used. In this method tree size is measured as volume of the tree approximated by an inverted cone. In this respect *Celtis occidentalis* is much greater than the other two species, so the price should be multiple.

Calculation of the replacement cost is also among the used methods, which can be problematic in case of old trees. Let it compare the value of a 15 years old tree, planted as a four-year sapling and the price of a 15 years old tree, which can be bought in a nursery. An *Aesculus carnea* 'Briotii' in that age and with 35 cm circumference is 450 Euro in an Italian nursery price list – Hungarian nurseries does not offer such specimens – and the costs of shipping and planting must be added, too. However, the value of a 15 years old tree would be 167 Euro based on Radó method, and 236 Euro according to Párkányi.

## Discussion

There are a number of factors that need to be considered in case of determination of urban tree values. Most of the methods use as a base value the producer price of the nurseries. However, in many cases this could be a wrong solution, as the nursery price depends first of all on the production cost of the given sapling and in small part on the market demand. Therefore, it can occur that a tree with higher production cost but not so valuable in the given conditions would have higher calculated value than another, most suitable one. It can also happen that some varieties of a given species can be propagated only with grafting, others without it. As grafting needs more manpower, these saplings are more expensive. For example, a variety with a globe crown will have higher price than a variety with conventional crown form of the same species, even if the conventional one shows better result in growing vigour and canopy size. Of course the nursery price cannot be avoided during the calculations, but could have less importance.

The value of the trees in crowded and polluted urban areas is higher than in a small settlement. The Hungarian methods do not take it into account with proper extent. Instead of the currently used three categories five location types are suggested:

- inner districts of the capital
- green areas of the capital
- main great cities of the country
- suburban regions
- villages and small settlements.

The species are tolerant to the urban environment in different extent. This value should be determined based on several factors, like tolerance to the dry and warm periods, salinity, pests and diseases. The climate tolerance becomes important in the last years. It is especially important in case of trees, where the change of varieties is slow and they are planted for long time. As the climate scenarios based on different models give different results, exact values cannot be given for this. However, species could be grouped in three categories based on the experiences of the last decades.

The maintenance cost is also important factor. All the trees have some basic maintenance needs, but species are very different in this aspect. Some species require much more maintenance work, for example continuous cleaning because of the falling crops (*Aesculus hippocastanum*) or falling flowers (*Tilia sp.*), or because of the high risk of broken branches (*Gleditsia triacanthos*). The extra costs slightly decrease the value of these trees.

The re-evaluation of the trees after the maintenance works is an interesting question. There are cases, when the professional maintenance works (e.g., removal of dry branches, plant protection) increase the tree value. It calls the attention again to the continuous update of the tree cadastral databases. All manipulations must be recorded immediately and tree values must be re-calculated.

**Acknowledgements.** The authors would like to express their gratitude for the “Green Budapest” scholarship of the Viva Natura Foundation providing support for the study.

## REFERENCES

- [1] Armstrong, N. (1947): Shade tree evaluation formulas and their use. – Proceedings of the 23rd International Shade Tree Conference, p. 38-48.
- [2] Bulř, P. (2009): Testing of Koch method applied for evaluation of ornamental trees in the Czech Republic. – Hort. Sci. (Prague), 36(4): 154–161.
- [3] Cullen, S. (2007): Putting a value on trees – CTLA guidance and methods. – Arboricultural Journal 30: 21-43.
- [4] Dreesen, A.D. (2005): Evaluation of Texas shade trees. – Texas Cooperative Extension, <http://www.plantanswers.com/EvaluationOfTexasShadeTrees.pdf>
- [5] Grey, G.W., Deneke, F.J. (1986): Urban Forestry. – John Wiley and Sons, New York.
- [6] Hegedüs, A. (2008): Az Orczy-kert dendrológiai felmérése. – Kertgazdaság 40(2): 58-62.
- [7] Helliwell, D.R. (2000): Amenity valuation of trees and woodlands (rev. ed.). – Arboricultural Association, Romsey, Hants, United Kingdom.
- [8] Józsaíné Párkányi, I. (2004): Értékbecslési módszerek. – In: Schmidt G., Varga G. (szerk.): Famutató. Fásítási útmutató tervezéshez, kivitelezéshez és fenntartáshoz. – Hillebrand Nyomda, Sopron
- [9] Józsaíné Párkányi, I. (2007): Zöldfelület-gazdálkodás, parkfenntartás. – Mezőgazdasági Kiadó, Budapest
- [10] Kielbaso, J. (1979): Evaluation of trees in urban areas. – Journal of Arboriculture 5(3): 70-72.
- [11] King, G.S. (1977): Plant material evaluation. – Journal of Arboriculture 3(4): 61-64.
- [12] Kissinger, D., Van Ells, J. (1998): Tree Evaluation and appraisal. – Wisconsin Urban & Community Forests 6(3): 1 and 9-11.
- [13] Litchfield, G. (2010): A simple tree evaluation system. – Latvijas Kokkopju-Arboristu Biedriba Seminar, 27<sup>th</sup> May 2010, Riga  
[http://www.kokiem.lv/seminars-koks-ka-patiesa-vertiba/6\\_De\\_G\\_Litchfield\\_tree\\_valuation.pdf](http://www.kokiem.lv/seminars-koks-ka-patiesa-vertiba/6_De_G_Litchfield_tree_valuation.pdf)
- [14] Moor, G.M. (1991): Amenity tree evaluation: A revised method. – In: The Scientific Management of Plants in the Urban Environment. Proceedings of the Burnley Centenary Conference, Centre for Urban Horticulture, Melbourne, Australia., p. 166-171.  
<http://www.arborcad.com/wp-content/uploads/2011/08/Arborcad-Revised-Burnley-Method-of-Tree-Valuation.pdf>

- [15] Neilan, C. (2010): CAVAT, Quick Method: User's Guide. – London Tree Officers Association,  
[http://www.ltoa.org.uk/documents/resource-home/doc\\_download/140-cavat-quick-method-user-guide-updated-september-2010](http://www.ltoa.org.uk/documents/resource-home/doc_download/140-cavat-quick-method-user-guide-updated-september-2010)
- [16] Radó, D. (1981): Fák a betonrengetegben. – Mezőgazdasági Kiadó, Budapest
- [17] Sarajevs, V. (2011): Street tree valuation systems. – Forest Research, April 2011, p. 1-6.  
[http://www.forestry.gov.uk/pdf/FCRN008.pdf/\\$FILE/FCRN008.pdf](http://www.forestry.gov.uk/pdf/FCRN008.pdf/$FILE/FCRN008.pdf)
- [18] Simson, A. (2010): The value of trees –  
[http://www.historictownsforum.org/files/documents/presentations/Oxford\\_10/Alan\\_Simson.pdf](http://www.historictownsforum.org/files/documents/presentations/Oxford_10/Alan_Simson.pdf)
- [19] Watson, G. (2002): Comparing formula methods of tree appraisal. – Journal of Arboriculture 28(1): 11-18.

## EVALUATION OF THE PLOTLESS SAMPLING METHOD TO ESTIMATE ABOVEGROUND BIOMASS AND OTHER STAND PARAMETERS IN TROPICAL RAIN FORESTS

KUMARATHUNGE, D.P.<sup>1,2\*</sup> – THATTIL, R.O.<sup>2</sup> – NISSANKA, S.P.<sup>2</sup>

<sup>1</sup>*Institute of Fundamental Studies, Hantana Road, Kandy, Sri Lanka  
(phone: 0094 81 2232002; fax: 0094 81 2232131)*

<sup>2</sup>*Department of Crop Science, Faculty of Agriculture, University of Peradeniya, Sri Lanka*

*\*Corresponding author  
e-mail: dkumarathunge@gmail.com*

(Received 22<sup>nd</sup> March 2010; accepted 26<sup>th</sup> August 2011)

**Abstract.** Use of sampling techniques is of paramount importance since the precision of estimates greatly depend on it. Different methods of sampling have to be investigated to find out the best sampling technique for a given situation. This study was conducted to determine the best sampling technique to estimate tree diversity and aboveground biomass in Sinharaja forest. Three sampling techniques, namely; Quadrat method, Transect method, and Point centered quarter method (PCQ) were evaluated in this study. Sampling techniques were compared for tree density, basal area, aboveground biomass and diversity indices estimated by each technique. According to the results, PCQ method gave the highest precision for most of the parameters estimated. The non-linear functions fitted for the species – area (Quadrat method) and species – point (PCQ method) relationships estimated that the minimum total sampling area required to assess the number of tree species (in an area of 50 ha) of Sinharaja forest as 6000 m<sup>2</sup> for Quadrat method and 160 sampling points for PCQ method. It was difficult to estimate the minimum sampling area required to estimate the above ground biomass in Sinharaja since there was no clear cut relationship between biomass and number of sampling units. The results of the study emphasized that the PCQ method is a precise sampling technique that can be used to estimate the tree density, tree diversity and above ground biomass in natural forests. The random distribution of individuals is not necessary for tree diversity and biomass estimation by PCQ method if site stratification and random placement of sampling points in the study area are performed. Considering the higher precision of estimates and the saving of time and cost, the PCQ method can be recommended as an effective sampling technique for tree diversity and biomass studies.

**Keywords:** *sampling techniques, point centered quarter method, rain forests, aboveground biomass, bio diversity*

### Introduction

Aboveground biomass is one of the “master variables” in determining especially the present status of, specially, the natural forests. Over the last few decades, estimation of aboveground biomass in natural forests as well as in plantations is made in the context of mitigating climate change. Carbon management in forests will be the single most important agenda of the first half of the 21<sup>st</sup> century in most of the developed countries and some developing countries (Ramachandra et al., 2007). Under the United Nations Framework on Climate Change, countries have to report regularly the state of their forest resources and emerging mechanisms such as reducing emission from deforestation in developing countries (REDD) and they are likely to require temporally and specially fine-grained assessments of carbon stocks (UNFCCC, 2008). Therefore, estimation of aboveground biomass frequently in natural forests is of paramount importance. Studies have been carried out, following many sampling techniques such as



random plots of various dimensions and sizes, viz. 100×100 m (Mani and Parthasarathy, 2007), 100 ha (Keller et al., 2001), 20×20 m (Ramachandra et al., 2007). Although these studies contributed to the knowledge of aboveground biomass in tropics, it is uncertain whether the sampling technique adapted in these studies truly represents the aboveground biomass or not. Secondly, in the discussion part of many of the above studies, the results are compared with those of similar studies conducted elsewhere, to rank the aboveground biomass as equal, higher or lower. We presume that these kinds of comparisons may not be rational and may give a false impression about the aboveground biomass of a forest or a region. Estimation of aboveground measures will depend on the sampling methods used. Permanent sampling plots (Alder and Synot, 1992) have been used for biomass inventories but establishment and maintenance of these plots is costly and time consuming. Due to high natural variability in tropical forests especially in terms of topography, species diversity etc. a few permanent or temporary sampling plots do not give a clear picture of the aboveground biomass. There is no clear-cut method available to determine the optimum plot size (which is a key variable that affects the accuracy of the estimates) required for biomass studies. Many scientists have been working on area independent sampling techniques as a solution to the disadvantages of area dependent methods i.e. plot based methods, but no information is found on the applicability of those techniques in the area of biomass studies. In this paper the applicability of an area independent sampling technique i.e. point centered quarter (pcq) method (Krebs, 1989) in biomass studies will be evaluated with comparison to the other conventional techniques.

## **Materials and methods**

### ***Research site***

This study was carried out in the Singharaja forest located in the low country wet zone of Sri Lanka. (6°25'00"N, 80°30'00"E). The entire area receives more than 2500 mm of rainfall annually with no long dry spells. Up to 900 m from the mean sea level, the vegetation is classified as tropical wet evergreen forest and above 900 m as sub montane evergreen forest (Gunatilleke et al., 2004).

### ***Site stratification***

The Landsat ETM+ image of the Sinharaja forest acquired in year 2005 was used for site stratification. The image was subjected to unsupervised classification using the Erdas Imagine 8.6 software. After classification, five different classes were identified based on the reflectance from different vegetation types. An area about 50ha that represents all the five classes was selected as the study area. Latitude and longitude was noted for each stratum for identification of these different vegetations inside the forest.

### ***Evaluation of sampling techniques***

In this study, the PCQ method was compared with two other conventional sampling techniques namely; Quadrat method and Transect method. Here, the quadrat method is considered as the standard sampling method and other two were compared as substitute techniques for the quadrat method. Initially, the stratified image of the study area was divided in to 50 m grids and a random value of latitude and longitude was selected for each grid. This random point was considered as the sampling points for the PCQ

method. The pre determined sampling points were located in the field with the hand held Global Positioning System (GPS) which has an accuracy of less than 5 m. at each sampling point. The area around was divided in to four quadrants (*Fig. 1*). The nearest tree to the sampling point which had more than 5 cm diameter at 1.3 above the tree base (DBH) in each quadrant was selected for sampling and, therefore, four trees were included in the sample at each selected sampling point. The distance from the point to each selected tree was measured and in each selected tree, the DBH and tree height were measured using DBH tape and Clinometer. Species name of the trees was also recorded. This method was continued for a total of 120 sampling points.

For the quadrat method, 25, 15×15 m temporary sampling plots were used to sample vegetation. The plots were demarcated using a rope and a hand held compass. Plots were distributed in each stratum in such a way that each stratum contained at least five plots. The slope of the plots was recorded for slope correction. All trees having DBH greater than 5 cm within each quadrat were sampled for their DBH, height and species level. For the transect method, eleven, 5×100 transects were used for sampling. The sampling procedure was the same as for the quadrat method.

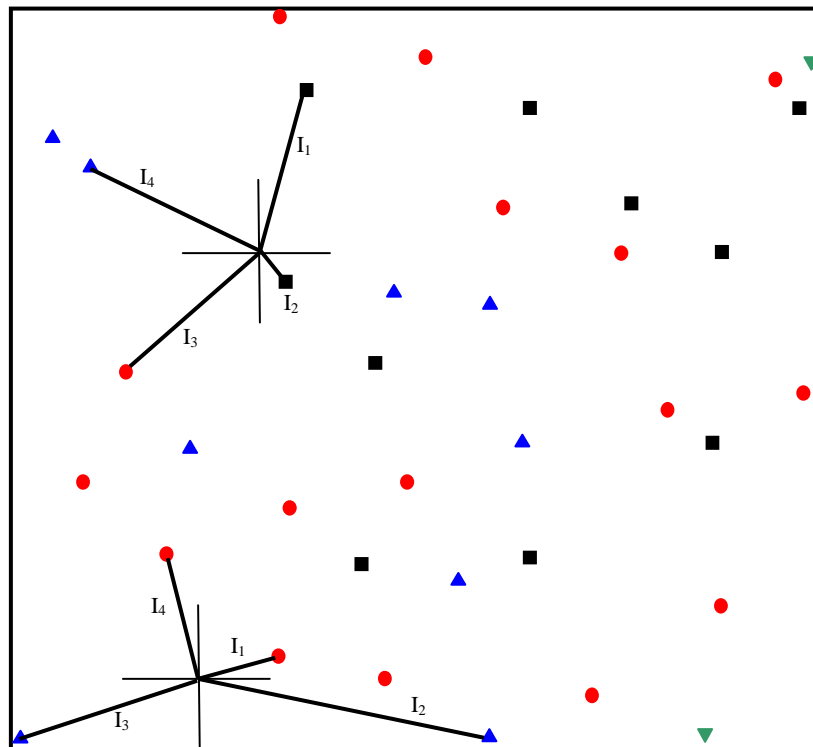


**Figure 1.** The point centered quarter method. The + represents the random point, around which four quadrants are established, and the distance to the nearest tree,  $I_i$  is measured in each quadrant. The symbols ● ▼ ■ ▲ represent four different tree species.

Since three sampling techniques are different from each other, it is impossible to allocate equal conditions (i.e. size of a single sampling unit) for each method. To overcome this, pre determined, total sampling area was selected as 50 ha and the interesting parameters of this area were evaluated using three different sampling techniques. Therefore, for comparison, size of a single sampling unit in each technique might not necessarily be the same since all techniques estimates the interesting

parameters in a same area. But, the total sampling area of quadrat and transect methods were kept equal as much as possible.

### ***Estimation of aboveground biomass***

Here we used a general model to calculate the aboveground biomass. This model assumes a universal form factor for all tree species, which is considered as 0.7 (Browns, 1989). Biomass is calculated using the following formula.

$$Biomass = h \times \left( \frac{\pi (DBH^2)}{4} \right) \times f \times \rho \quad (\text{Eq.1})$$

Where  $h$  = stem height (m),  $f$  = form factor and  $\rho$  = wood specific gravity ( $\text{kg/m}^3$ ). Since the general way of estimating the biomass density (biomass per ha) cannot be applied to the PCQ method, a formula was derived considering the maximum area belonging to a particular sampling point. The formula is

$$\text{Biomass density (kg/ha)} = \frac{B_i}{\pi r_{\max}} \times 10^4 \quad (\text{Eq.2})$$

Where  $B_i$  = total aboveground biomass of  $i^{\text{th}}$  sampling point,  $r_{\max}$  = maximum length measured in  $i^{\text{th}}$  sampling point and  $\pi = 3.14159$ .

Apart from the aboveground biomass, the tree sampling techniques were compared for other forest stand parameters such as absolute tree density, basal area and diversity indices. The widely used Shannon-Wiener diversity index was calculated according to Magurran (1988).

$$H = -\sum p_i \ln p_i \quad (\text{Eq.3})$$

Where  $H$  = species abundance,  $p_i$  = proportion of individuals

The nonlinear regression procedure in Statistical Analysis System (SAS, 2000) was used to model the aboveground biomass and other interesting parameters with the size of the sampling units (for both PCQ and quadrat methods). Several non-linear models were fitted for the above relationships to find out the best-fitted model. Parameter estimation for each model was done using the PROC MODEL and PROC NLIN procedures in SAS.

### **Results and discussion**

The total number of tree species recorded by the quadrat, Transect and PCQ methods was 107, 103 and 87 respectively. The highest number of species per 100 individuals (18.12%) was recorded by the PCQ method. The mean tree density estimated by quadrat and Transect methods was not significantly different (*Table 1*). But the PCQ method was the most precise technique to estimate the tree density since the standard error of estimate was very small compared to the other methods.

**Table 1.** Estimated forest parameters by three different sampling techniques (values in parentheses are standard errors of estimates)

Sampling technique	Species percentage	Tree density (trees ha <sup>-1</sup> )	Basal area (m <sup>2</sup> ha <sup>-1</sup> )	Diversity index (Shannon-Wiener index)
Quadrat	10.84%	1712 (81.5)	42.5 (2.62)	3.86 (0.008)
Transect	18.12%	1710 (74.8)	39.5 (4.32)	3.91 (0.016)
PCQ	17.19%	1632 (3.40)	42.5 (4.72)	3.72 (0.0036)

Based on the standard error (SE) of estimate quadrat method is the most precise technique to estimate basal area. But the SE of PCQ method is not very different. So both these estimates can be considered as precise estimates.

### **Aboveground biomass**

The average aboveground biomass density of the study area in terms of the different sampling techniques is given in *Table 2*. The results emphasizes that, the PCQ technique is the most precise sampling technique to estimate aboveground biomass in the study area. Considering the basic principles, sampling units of the PCQ technique can be distributed throughout the study area with low cost and time compared to the quadrat method. One of the limitations of quadrat sampling is that when the size of the quadrat increases, the cost associated with including one additional plot is much higher. So in most of the situations, the number of sampling units that can be accommodated in the study may not be enough to represent the spatial variability of the aboveground biomass in the study area. The PCQ method can easily overcome this, since there is no limiting to increase the number of sampling units. And this technique is an important technique to determine the spatial variability of aboveground biomass since it allows more sampling units that can cover a large area. Quadrat method is not a good technique in such a situation because it is impossible to have large number of plots to represent the spatial variability accurately. Other than that, when taking measurements from large number of trees, the error associated with measurements increase. In PCQ method, only four trees are sampled per sampling point thus the total number of trees to be sampled is lower than other conventional techniques.

**Table 2.** Estimated aboveground biomass and their standard errors

Sampling technique	Biomass (Mt ha-1)	Standard error
Quadrat	358.9	46.9
Transect	394.5	56.1
PCQ	339.4	38.8

The PCQ method can be precisely used to model the relationship between number of sampling units and number of tree species in the study area (*Fig. 2a*). The best-fitted model was

$Y = 106.06 - 96.63e^{0.015P}$  ( $R^2 = 0.98$ ) where Y is the expected number of species and P is no of points required. According to this model the minimum number of sampling points required to assess the number of tree species in an area of 50 ha is 160. The same procedure was followed to model the species-area relationship (for quadrat method) and the best-fitted model was

$Y = 124.608 - 131.2678 e^{-0.0052A}$  ( $R^2=0.99$ ) where Y is the expected number of species and A is the area. According to the derived curve, it is clear that the number of species do not show a significant increment after 6000 m<sup>2</sup>. After this point, the increment of number of species is declining and it is around 0.1 species per 100 m<sup>2</sup>. Therefore 6000 m<sup>2</sup> will be the minimum and economical sampling area required to assess the number of tree species in the study area, using the quadrat method. These estimates can be recommended for biomass studies as well because the inclusion of practically all the tree species in 50 ha of the study area is assured. When the total study area is larger than 50 ha, the number of sampling units should increase proportionately.

It was difficult to estimate the minimum sampling area required to estimate aboveground biomass in Sinharaja by all three methods. However with the PCQ method there was an indication that around 70 sampling points was adequate to estimate the aboveground biomass.

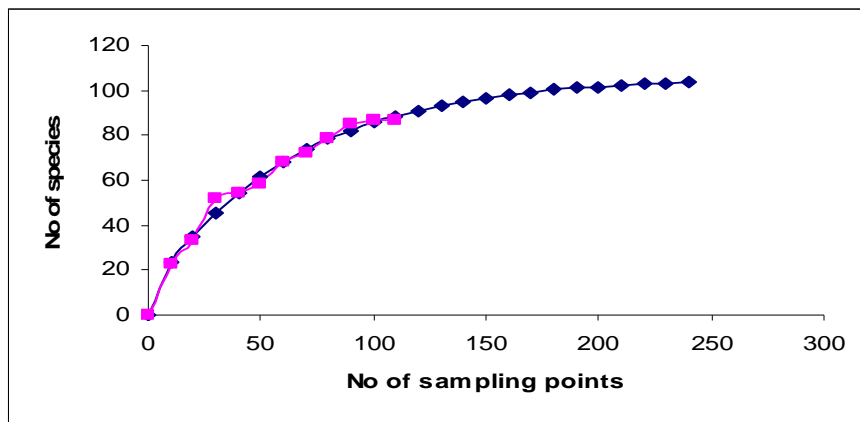


**Figure 2. a** Derived species - point curve for the study area. The fitted curve reaches a plateau at about 160 sampling points which is the minimum number of sampling points required for the PCQ method to estimate the tree diversity of the study area

■ = Expected no of species, ■ = Observed no of species

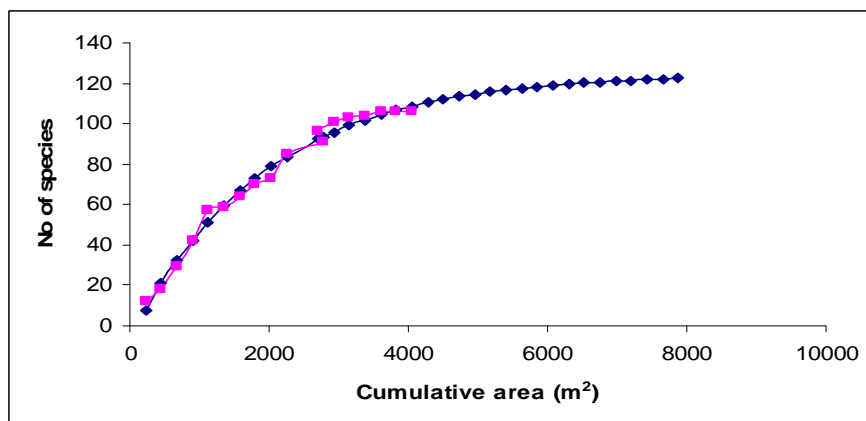


**Figure 2. b** Derived species - area curve for the study area. The fitted curve reaches a plateau at about 6000 m<sup>2</sup> which is the minimum sampling area required for the quadrat method to estimate the tree diversity of the study area.

■ = Expected no of species, ■ = Observed no of species

### **Sampling efficiency**

In this study, the average number of sampling points (in PCQ method) per man day is inbetween 15-20, under clear weather. For quadrat method and transect method the average number of plots per man-day is 3 and 2 respectively. So it is clear that, PCQ method is both a cost and time saving sampling method, compared to other conventional sampling techniques. Spatial variability can be easily handled by this method because the researcher can allocate more and more sampling units if necessary without much increase in cost and time.

### **Conclusion**

Considering the higher precision of estimates and the saving of time and cost, the PCQ method can be recommended as an effective sampling technique for aboveground biomass studies in tropical wet evergreen forests. The present study stimulates certain issues worth considering in future studies: (a) experimental designs to estimate the minimum sampling area required to estimate the aboveground biomass and (b) validation of these results for other forest types in the tropics.

**Acknowledgements.** Authors wish to thank Conservator General of forests, Department of forestry, Battaramulla for giving the permission to carry out this study in Sinharaja forest. Mr. R.H.G Ranil and Mr.P.S.Pathinayake, Department of Crop Science, Faculty of Agriculture, University of Peradeniya are also acknowledged for the valuable support given throughout the study.

### **REFERENCES**

- [1] Alder, D., Synnott, T.J. (1992): Permanent sample plot techniques for mixed tropical forests. Tropical forestry papers (25) – Oxford forestry institute, University of Oxford.
- [2] Browns, S. Gillespie, A.J.R. Lugo, A.E. (1989): Biomass estimation methods for tropical forests with application to the forest inventory data. – Forest Science. 35(4): 881-902.
- [3] Gunatilleke, C.V.S., Gunatilleke, I.A.U.N., Ethugala, A.U.K., Esufali, S. (2004): Ecology of Sinharaja forest and the Forest Dynamics Plot. – WHT publication Ltd, Colombo, Sri Lanka.
- [4] Keller, M., Palace, M., Hurtt, G. (2001): Biomass estimation in the Topajos national forest, Brazil. Estimation of sampling and allometric uncertainties. – Forest Ecology and Management 154: 371-382.
- [5] Krebs, C.J. (1999): Ecological Methodology. – Second edition. Addison-Welsey, Canada.
- [6] Magurran, A.E. (1987): Ecological Diversity and its Measurement. – Champan and Hall Limited, London.
- [7] Mani, S., Parthasarathy, N. (2007): Above-ground biomass estimation in ten tropical dry evergreen forest sites of peninsular India. – Biomass and Bioenergy 31: 284-290.
- [8] Ramachandran, A., Jayakumar, S., Haroon, R.M., Bhaskaran, A., Arockiasami, D.I. (2007): Carbon sequestration: estimation of carbon stocks in natural forests using geospatial technology in the Eastern Ghats of Tamil Nadu, India. – Current Science 92(3).
- [9] SAS Version 8(2000): SAS Institute Inc. Cary, NC, USA.
- [10] UNFCCC (United Nations Framework Convention on Climate Change) (2008): Report of the conference of the parties on its thirteen session. – Bali, 3-15 December 2007. Addendum, part 2. Document FCCC/CP/2007/6 Add.1. UNFCCC. Bonn, Germany.

## A POPULATION DYNAMICAL MODEL OF *OPEROPHTERA BRUMATA*, L. EXTENDED BY CLIMATIC FACTORS

KÚTI, ZS.<sup>1\*</sup> – HIRKA, A.<sup>2</sup> – HUFNAGEL, L.<sup>1</sup> – LADÁNYI, M.<sup>1\*</sup>

<sup>1</sup>*Corvinus University of Budapest, Dept. of Mathematics and Informatics  
H-1118 Budapest, Villányi út 29-43.  
(phone: +36-1-482-6261; fax: +36-1-466-9273)*

<sup>2</sup>*Hungarian Forest Research Institute, Dept. of Forest Protection  
H-3232 Mátrafüred, Hegyalja út 18.  
(phone: +36-37-320-129; fax: +36-37-520-047)*

*\*Corresponding authors*

*e-mail: marta.ladanyi@uni-corvinus.hu, kutizsuzsi@gmail.com*

(Received 13<sup>th</sup> November 2011; accepted 2<sup>nd</sup> December 2011)

**Abstract.** Setting out from the database of *Operophtera brumata*, L. in between 1973 and 2000 due to the Light Trap Network in Hungary, we introduce a simple theta-logistic population dynamical model based on endogenous and exogenous factors, only. We create an indicator set from which we can choose some elements with which we can improve the fitting results the most effectively. Then we extend the basic simple model with additive climatic factors. The parameter optimization is based on the minimized root mean square error. The best model is chosen according to the Akaike Information Criterion. Finally we run the calibrated extended model with daily outputs of the regional climate model RegCM3.1, regarding 1961-1990 as reference period and 2021-2050 with 2071-2100 as future predictions. The results of the three time intervals are fitted with Beta distributions and compared statistically. The expected changes are discussed.

**Keywords:** *Operophtera brumata*, L., population dynamical model, climatic indicators, climate change, RegCM

### Introduction

Climate change is a global environmental problem, which has now become a central issue. According to the 2007 Fourth Assessment Report by the Intergovernmental Panel on Climate Change (IPCC), global surface temperature increased about 1 °C in the 20<sup>th</sup> century and further 3-4 °C increment in mean temperature is predicted towards the end of the 21<sup>st</sup> century. The rise of the number and intensity of the extreme meteorological events are the most serious consequence of global warming, which can result in the change of both the global and the regional climate.

The question about the way and rate the climatic factors and their changes affect the agricultural and forest pests was investigated by several researchers. The past and the expected effects of the climatic parameters to invertebrate populations have been measured in the previous years by a number of researchers (Drégelyi-Kiss et al., 2008, 2009; Sipkay et al., 2008, 2009; Diós et al., 2009; Bale et al., 2002). The impact on population dynamics of insect pests was studied earlier by Porter et al. (1991), Cammel and Knight (1992), Woiwod (1997) and recently by Estay et al. (2009). Parmesan (2007) focuses on phenological responses of insects while Merril et al. (2008), Musolin (2007) and Olfert and Weiss (2006) investigate complex effects.

In this paper the population dynamics of a multitudinous forest- and horticultural Lepidoptera pest species, the *Operophtera brumata* (Linnaeus, 1758) will be examined

according to their most important endogenous and exogenous factors described by a first order density dependent reproductive function and meteorological parameters.

*Operophtera brumata*, L. is one of the earliest known forest- and fruit tree invasive pest species of Geometridae family occurring periodically in multitudinous colonies. During cool springs, if weather hinders leaf expansion, the winter moth caterpillar can cause high levels of injury to the leaves, thus examining its population dynamics is extremely important.

## Materials and methods

Data of the National Plant Protection and Forestry Light Trap Network (1973-2000) with 252 traps were analysed. Traps are situated in nine regions (Felsőtárkány, Gerla-Gyula, Mátraháza, Répáshuta, Sopron, Szentpéterföldre, Tolna, Tompa, Várgesztes (Fig. 1)

The light trap network was developed in Hungary in the early 1960's by the Ministry of Agriculture and Food Plant Protection Service. More than 150 light traps are now more than 40 years old, providing data on swarming phenology for entomological research of great scientific value.

Light trap data of 28 years (1973-2000) with the same monitoring standard method were used for model evaluation. *Operophtera brumata*, L. was detected in each year and in each trap.

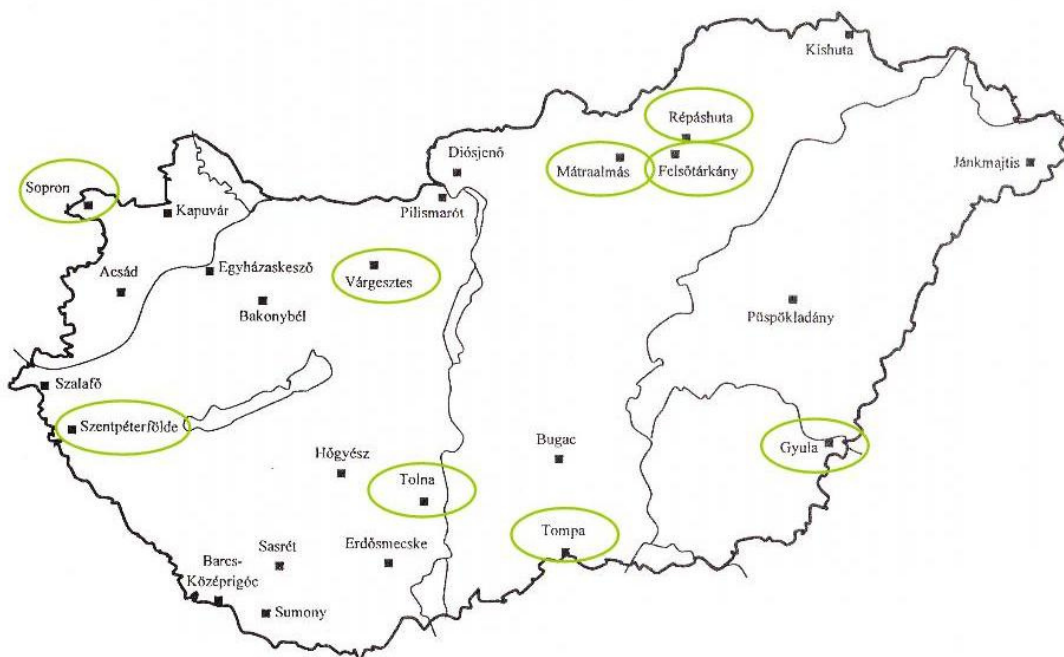


**Figure 1.** Light trap network in Hungary. The regions involved in the analysis are circled

The daily meteorological data (precipitation [mm], mean temperature [°C], maximal temperature [°C] and minimal temperature [°C]) were taken from the Hungarian Meteorological Service. For climate change impact study we applied RegCM 3.1 which was downscaled at Eötvös Loránd University, Budapest, Department of Meteorology



for A1B scenario (Giorgi et al., 1993; Bartholy et. al., 2009; Torma et. al., 2008). We considered three different time scales: 1961-1990 as reference period, 2021-2050 and 2071-2100 as prediction time intervals.

### ***Characterization of Operophtera brumata*, L.**

The Winter Moth (*Operophtera brumata*, L.) is a polyphagous moth of the family Geometridae. It is an abundant species of Europe and has been already introduced to North America and United Kingdom (England and Scotland) from Europe. The diversity of its food plants is very wide: oak, maple, chestnut, hazel, pear, basswood, ash, apple, cherry, blueberry, raspberry etc.

After mating in late fall or winter, the female lay 200-300 or in some years even 450-500 eggs in clusters of 2-3 eggs, usually on tree trunks and branches. The adult moths then die and the eggs over-winter. Eggs hatch when the mean daily temperature is appropriate (over 12-13 °C), usually in early-middle March. This means that egg-hatch can occur before bud break of some of its host plants. Young larvae (caterpillars) are tiny black headed dark colour inchworms and have just 2 pairs of prolegs.

They tunnel into buds where they feed, usually at night. These caterpillars move from bud to bud as they feed. They often crawl up tree trunks and produce a long silken strand of silk with the help of which they can “balloon”. Delayed bud opening due to cool weather conditions can lead to bud death as the caterpillars have longer time to feed. Older larvae feed flowers and leaf clusters. A single species demands 40-50 m<sup>2</sup> leaf area.

Larvae need, depending on weather, 25-40 days to maturity passing 5 phenophases mm. At maturity, the caterpillars are 25-30 mm long. They feed voraciously until mid-May, and then they start to migrate to the soil (up to 3-8 mm depth) under the tree for pupation. They will stay in the soil in a hard-covered pupal stage until, usually after some rainy days and not before the first fall frost, they emerge as adult moths on a late October day with no frost. Males are emerging usually some days earlier than females and occurrence is earlier in forests at 5-7 days than in orchards. The female is wingless and cannot fly, but the male is fully winged and flies strongly. The wingspan of a mature male is 28-33 mm. The adults are active from sunset up to midnight, throughout the winter from October to January, even when there is lightly snowing. Males are attracted to light and females, activity of males increases significantly in case of low air pressure. Swarming lasts 6-8 weeks with eventually some pauses on heavy frosty days or great amount of snow. Optimal daily mean temperature for flying is 5-10 °C, wet evenings are beneficial.

Moths (the adult stage) of the winter moth emerge from the soil usually in late November and can be active into January. The male moths are small, light brown to tan in colour and have four wings that are fringed with small elongate scales that give the hind margins a hairy or fringed appearance. The female is gray, wingless and, therefore, cannot fly. She emits a sex pheromone or scent that often attracts clouds of male moths. Females are usually found at the base of trees but can be found almost anywhere.

After copulation hours males live 2-3, females 8-9 days long. Long, warm and rainy falls are beneficial for the defoliation in high populations while it is impeded by cold and rainy springs. Late spring frosts can cause high mortality of caterpillars. Gradations develop very quickly, intensively, and persist for only a relatively short period of 3-5 years (Schwerdtfeger, 1969; Szontagh, 1980; Childs et al. 2009; Chinery, 1991) with a

cycle of 10-11 years. Gradation peaks of *Operophtera brumata*, L. in Hungary were in years 1961, 1971, 1982, 1992.

For the sake of decreasing the modification effects of different abiotic factors and the different number of collections in different collection sites, we used the data merging, reducing, filtering and smoothing moving average methods (Moon and Kim, 2007; Heuvelink and Webster, 2001; Gimesi and Hufnagel, 2010). As a result, we got a dimensionless aggregated data set with a time series of yearly steps referring to the population size of *Operophtera brumata*, L species of a given year.

### The basic model

We set out from a simple discrete population dynamical model (sometimes called the theta-logistic model):

$$N_{t+1} = N_t * \exp\left(R_{\max} * \left(1 - \frac{N_t}{K}\right)^\theta\right) \quad (\text{Eq.1})$$

which is a nonlinear version of the classic logistic model (Ricker, 1954; Verhulst 1838; Richards 1959; Nelder 1961; Gilpin and Ayala 1973; Berryman 1999). In the model we denote by  $N_{t+1}$  the number of individuals in year  $t+1$ , which, through an exponential function, depends on the number of individuals in the previous year  $N_t$ , on the maximal growth rate  $R_{\max}$ , on the carrying capacity  $K$  and on the power parameter  $\theta$ .

We introduce the notation  $R_t$  as:

$$R_t = \ln\left(\frac{N_{t+1}}{N_t}\right) = R_{\max} * \left(1 - \frac{N_t}{K}\right)^\theta = R_{\max} - R_{\max} \left(\frac{1}{K}\right)^\theta N_t^\theta \quad (\text{Eq.2})$$

Note that in case of a population without source restriction ( $K$  is huge) and with small  $\theta$  we have  $\left(\frac{1}{K}\right)^\theta \approx 1$ . We can rewrite the above formula as:

$$R_t = R_{\max} - R_{\max} \left(\frac{1}{K}\right)^\theta N_t^\theta = R_{\max} - aN_t^\theta \quad (\text{Eq.3})$$

with  $a = R_{\max} \left(\frac{1}{K}\right)^\theta$ .

### Fitting and validation procedure

The root mean square error (RMSE) was defined as the root of the average sum of the squares of the differences between the observed ( $R_t$ ) and model predicted ( $R_{t, \text{pred}}$ ) values:

$$\text{RMSE} = \sqrt{\frac{1}{n} \sum_j (R_t - R_{t, \text{pred}})^2} \quad (\text{Eq.4})$$

where  $n$  denotes the number of years. RMSE was minimized while three parameters, namely the maximal growth rate  $R_{\max}$ , the carrying capacity  $K$  and the power parameter  $\theta$  were varied. For optimization we used Palisade's Risk Evolver that is based on

innovative genetic algorithm (GA technology), a stochastic directed searching technique with several thousands of iteration. This method does not get stuck at local solutions, but instead looks at the entire range of possible solutions which enables us to find the global optimal solution instead of a local extreme value (Weise, 2009).

### ***Climatic Indicator Data Set***

From the meteorological daily data we calculated climatic indicators. We cut the 365 or 366 days of the years into decades (of ten days) and for a year  $t$  we calculated

- the average of the daily mean temperatures of the  $i^{\text{th}}$  decade ( $TMt\_i$ )
- the average of the daily minimum temperatures of the  $i^{\text{th}}$  decade ( $TNt\_i$ )
- the average of the daily maximum temperatures of the  $i^{\text{th}}$  decade ( $TXt\_i$ )
- the average of the daily precipitation of the  $i^{\text{th}}$  decade ( $Pt\_i$ )
- the minimum of the daily minimum temperatures of the  $i^{\text{th}}$  decade ( $TNNt\_i$ )
- the maximum of the daily maximum temperatures of the  $i^{\text{th}}$  decade ( $TXXt\_i$ ).

We also calculated the monthly climatic indicators as well:

- the average of the daily mean temperatures of the  $j^{\text{th}}$  month ( $TMmt\_j$ )
- the average of the daily minimum temperatures of the  $j^{\text{th}}$  month ( $TNmt\_j$ )
- the average of the daily maximum temperatures of the  $j^{\text{th}}$  month ( $TXmt\_j$ )
- the average of the daily precipitation of the  $j^{\text{th}}$  month ( $Pmt\_j$ )
- the minimum of the daily minimum temperatures of the  $j^{\text{th}}$  month ( $TNNmt\_j$ )
- the maximum of the daily maximum temperatures of the  $j^{\text{th}}$  month ( $TXXmt\_j$ ).

For  $t=1973, \dots, 1999$  the vector  $(R_t) = \left( \ln \left( \frac{N_{t+1}}{N_t} \right) \right)$  was correlated with all the climatic indicator vectors  $(I_t)$  and  $(I_{t+1})$  to find the connection between the population change from the year  $t$  to the year  $t+1$  denoted by  $(R_t) = \left( \ln \left( \frac{N_{t+1}}{N_t} \right) \right)$  and the indicators of the year  $t+1$  and the ones of the previous year  $t$ . The indicators with significantly high correlation values  $R^2$  were selected. We have found some highly correlated indicators referring consecutive decades, thus we completed the indicator set with some extra indicators called summer (calculated from 20<sup>th</sup> of July to 15<sup>th</sup> of August) and fall (calculated from 15<sup>th</sup> of October to 15<sup>th</sup> of November) indicators as follows.

Between 20<sup>th</sup> of July and 15<sup>th</sup> of August:

- the average of the daily mean temperatures ( $STMt\_i$ )
- the average of the daily minimum temperatures ( $STNt\_i$ )
- the average of the daily maximum temperatures ( $STXt\_i$ )
- the average of the daily precipitation ( $SPt\_i$ )
- the minimum of the daily minimum temperatures of ( $STNNt\_i$ )
- the maximum of the daily maximum temperatures ( $STXXt\_i$ ) and

between 15<sup>th</sup> of October to 15<sup>th</sup> of November:

- the average of the daily mean temperatures ( $FTMt\_i$ )
- the average of the daily minimum temperatures ( $FTNt\_i$ )

- the average of the daily maximum temperatures (FTXt<sub>i</sub>)
- the average of the daily precipitation (FPt<sub>i</sub>)
- the minimum of the daily minimum temperatures (FTNNt<sub>i</sub>)
- the maximum of the daily maximum temperatures (FTXXt<sub>i</sub>).

We created an indicator data base with the years in the first column, the  $N_t$  values in the second one, and then we have 612 further columns:

6\*37\*2 columns for the decade indicators of 6 types, 37 decades, 2 years;

6\*12\*2 columns for the month indicators of 6 types, 12 months, 2 years;

6\*2\*2 columns for the extra indicators of 6 types, 2 seasons, 2 years.

### Model development

Besides describing the basic structure of the effect of endogenous and exogenous forces, with a more sophisticated model, we can express the impact of the climatic indicators as well. With this step we aim to refine the model for a better fitting solution. The form of the model is:

$$R_t = R_{\max} - R_{\max} \left( \frac{1}{K} \right)^\theta N_t^\theta + \sum_k C_k I_k \quad (\text{Eq.5})$$

where  $I_k$  are climatic indicators,  $C_k \in \mathbf{R}$  are parameters to optimize.

First we took an only climatic indicator  $I_1$ , the one which has the highest correlation with the vector  $(R_t)$ . The root mean square error was minimized with innovative genetic algorithm while three plus one parameters, namely the maximal growth rate  $R_{\max}$ , the carrying capacity  $K$  and the power parameter  $\theta$  together with  $C_1$  were varied in the parameter space. Then we took a second climatic indicator  $I_2$  from the indicator data set, the one which has the (second) highest correlation with the vector  $(R_t)$ . Again, the root mean square error was minimized while one more parameter together with the formerly optimized four ones were varied. In each step we calculated the Akaike Information Criterion with a Bayesian bias-adjustment in case the number of parameters  $k$  is large relative to the number of cases  $n$  ( $n/k < 40$ ), which is the case we face (Turkheimer et al., 2003; Schwarz, 1978):

$$AIC_B = n \ln \left( \frac{RMSE}{n} \right) + 2k + \frac{2k(k+1)}{n-k-1} \quad (\text{Eq.6})$$

where  $k$  denotes the number of parameters,  $n$  is the number of fitted values (years).

We went on with more and more climatic indicators involved in the model step by step and calculated the Akaike Information Criterion. The model was selected as the best one which had its lowest  $AIC_B$  value.

Moreover, in each step we calculated the explained variance ratio as well:

$$R^2 = \frac{\sum (R_{t,pred} - \overline{R_t})^2}{\sum (R_t - \overline{R_t})^2} \quad (\text{Eq.7})$$

where  $\overline{R_t}$  denotes the average of the observed  $R_t$  values.

### Regional climate model prediction survey

The calibrated best model was run with input coming from the regional climate model RegCM 3.1 for three time intervals: 1961-1990 as reference period, 2021-2050 and 2071-2100 for prediction. We calculated the  $(R_t)$  predictions for these three time intervals. The results of the three time intervals were compared with one-way ANOVA after a logarithmic data transformation to make the data more suitable for ANOVA demands. We tested them with the so-called difference contrast expressed by the matrix

$$\begin{pmatrix} 1 & -1 & 0 \\ 1 & 0 & -1 \\ 0 & 1 & -1 \end{pmatrix}. \text{ Variance homogeneity was checked with Levene test. Normality of}$$

residuals was checked with Kolmogorov-Smirnov test.

The results of the three time intervals were then fitted by Beta distribution which has the general formula

$$f(x) = \frac{(x-a)^{p-1}(b-x)^{q-1}}{B(p; q)(b-a)^{p+q-1}} \quad (\text{Eq.8})$$

where the values of the variable are in between  $a$  and  $b$ ;  $p$  and  $q$  are positive parameters of the distribution and the Beta function is as follows:

$$B(p; q) = \int_0^1 t^{p-1}(1-t)^{q-1} dt \quad (\text{Eq.9})$$

The distribution fit was tested by Chi-square test. Finally the fitted distributions were compared.

The softwares PASW18 as well as @Risk of Palisade were applied for data evaluations.

### Results

We have selected 8 indicators which have significant Pearson correlation with  $(R_t)$ . The indicators are listed in *Table 1*.

**Table 1.** Selected indicators having significant Pearson correlation with  $(R_t)$ . Their  $R$  values together with the significance levels are also shown. The descriptions of the indicators are listed under the table

Indicator	Pearson Correlation R	Sig. (2-tailed)
TXXmt_APR	-0.546	0.003**
TXm(t+1)_FEB	0.442	0.021*
STM(t+1)_i	0.427	0.026*
TXXm(t+1)_MAY	-0.422	0.028*
TNmt_MAR	0.421	0.029*
Pmt_SEP	-0.419	0.029*
TNNm(t+1)_APR	0.392	0.043*
TXXmt_JAN	-0.387	0.046*

\*significant with  $p < 0.05$ ; \*\*significant with  $p < 0.01$

The indicators in *Table 1* are as follows:

- TXX $mt$ \_APR: the maximum of the daily maximum temperatures in April in year  $t$  which is for the temperature condition of the larvae of the parent generation;
- TXM $(t+1)$ \_FEB: the average of the daily maximum temperatures in February in year  $t+1$  which is for the temperature condition of the new generation just before hatching;
- STM $(t+1)$ \_i the average of the daily mean temperatures between 20<sup>th</sup> of July and 15<sup>th</sup> of August in year  $t+1$  which is for the temperature condition of the new generation in their pupal stage;
- TXXM $(t+1)$ \_MAY: the maximum of the daily maximum temperatures in May in year  $t+1$  which is for the temperature condition of the new generation in their late larvae stage;
- TNM $t$ \_MAR the average of the daily minimum temperatures in March in year  $t$  which is for the temperature condition of the parent generation in the hatching period;
- Pmt\_SEP the average of the daily precipitation in September in year  $t$  which is for the fall-time precipitation condition of the parent generation just before their swarming period;
- TNNM $(t+1)$ \_APR: the minimum of the daily minimum temperatures in April in year  $t+1$  for which is for the temperature condition of the new generation in their early larvae stage;
- TXXM $t$ \_JAN: the maximum of the daily maximum temperatures in January in year  $t$  which is for the temperature condition of the parent generation just before hatching.

We extended the basic model step by step with the maximum of the daily maximum temperatures in April in year  $t$  at first, then with the average of the daily maximum temperatures in February in year  $t+1$ , third time with the average of the daily mean temperatures between 20<sup>th</sup> of July and 15<sup>th</sup> of August in year  $t+1$ , fourth time with the maximum of the daily maximum temperatures in May in year  $t+1$ , fifth time with the average of the daily minimum temperatures in March in year  $t$  and finally with the average of the daily precipitation in September in year  $t$ .

In *Table 2* the results of the basic model  $R_t = R_{\max} - R_{\max} \left( \frac{1}{K} \right)^\theta N_t^\theta$  as well as the ones of the extended model  $R_t = R_{\max} - R_{\max} \left( \frac{1}{K} \right)^\theta N_t^\theta + \sum_k C_k I_k$  are presented.

**Table 2.** The results of the basic model  $R_t = R_{\max} - R_{\max} \left( \frac{1}{K} \right)^\theta N_t^\theta$  as well as the ones of the extended model

$R_t = R_{\max} - R_{\max} \left( \frac{1}{K} \right)^\theta N_t^\theta + \sum_k C_k I_k$ : the number of parameters  $k$ , the number of years  $n$ , the three parameters of the basic model ( $K$ ,  $R_{\max}$  and  $\theta$ ), the root mean square error (RMSE), the Akaike Information Criterion with a Bayesian bias-adjustment ( $AIC_B$ ), the explained variance and its square root ( $R^2$ ;  $R$ ). The model with the minimum  $AIC_B$  value is highlighted.

	$R_t = R_{\max} - R_{\max} \left( \frac{1}{K} \right)^\theta N_t^\theta$	TXXmt_APR	TXXmt_APR TXm(t+1)_FEB	TXXmt_APR TXm(t+1)_FEB STM(t+1)_i	TXXmt_APR TXm(t+1)_FEB STM(t+1)_i TXXm(t+1)_MAY	TXXmt_APR TXm(t+1)_FEB STM(t+1)_i TXXm(t+1)_MAY TNmt_MAR	TXXmt_APR TXm(t+1)_FEB STM(t+1)_i TXXm(t+1)_MAY TNmt_MAR Pmt_SEP
$k$ number of parameters	3	4	5	6	7	8	9
$n$ number of years	27	27	27	27	27	27	27
$K$ carrying capacity	5.98	788.89	788.89	788.89	788.89	788.89	788.89
$R_{\max}$ maximal growth rate	800.00	784.25	784.25	784.24	784.24	784.24	784.24
$\theta$ power parameter	4.79E-04	4.86E-04	3.49E-04	2.14E-04	2.00E-04	2.70E-04	2.99E-04
$a = R_{\max} \left( \frac{1}{K} \right)^\theta$	799.31	781.71	782.42	783.12	783.19	782.83	782.68
RMSE	0.94	0.87	0.81	0.75	0.68	0.57	0.53
$AIC_B$	3.60	2.45	1.59	0.98	-0.93	<b>-6.01</b>	-5.23
$R^2$	0.22	0.29	0.39	0.47	0.57	0.69	0.74
$R$	0.46	0.54	0.62	0.69	0.76	0.83	0.86

TXXmt\_APR: the maximum of the daily maximum temperatures in April in year  $t$

TXm(t+1)\_FEB: the average of the daily maximum temperatures in February in year  $t+1$

STM(t+1)\_i: the average of the daily mean temperatures between 20<sup>th</sup> of July and 15<sup>th</sup> of August in year  $t+1$ :

TXXm(t+1)\_MAY: the maximum of the daily maximum temperatures in May in year  $t+1$

TNmt\_MAR: the average of the daily minimum temperatures in March in year  $t$

Pmt\_SEP: the average of the daily precipitation in September in year  $t$

According to the Akaike Information Criterion with a Bayesian bias-adjustment  $AIC_B = -6.01$  the best model was the one with the first five climatic indicators. The coefficients of the best model are listed in *Table 3*.

**Table 3.** The coefficients  $C_k$  of the best model with the lowest  $AIC_B$  value

TXXmt_APR	TXm(t+1)_FEB	STM(t+1)_i	TXXm(t+1)_MAY	TNmt_MAR
-0.111	0.065	0.172	-0.112	0.186

In *Fig. 2* we can see the  $R_t$  values calculated from the observed data as well as the estimated  $R_t$  values of the basic ( $R^2 = 0.22$ ,  $p > 0.1$  nonsignificant) and the extended model ( $R^2 = 0.69$ ,  $p < 0.001$ , highly significant).

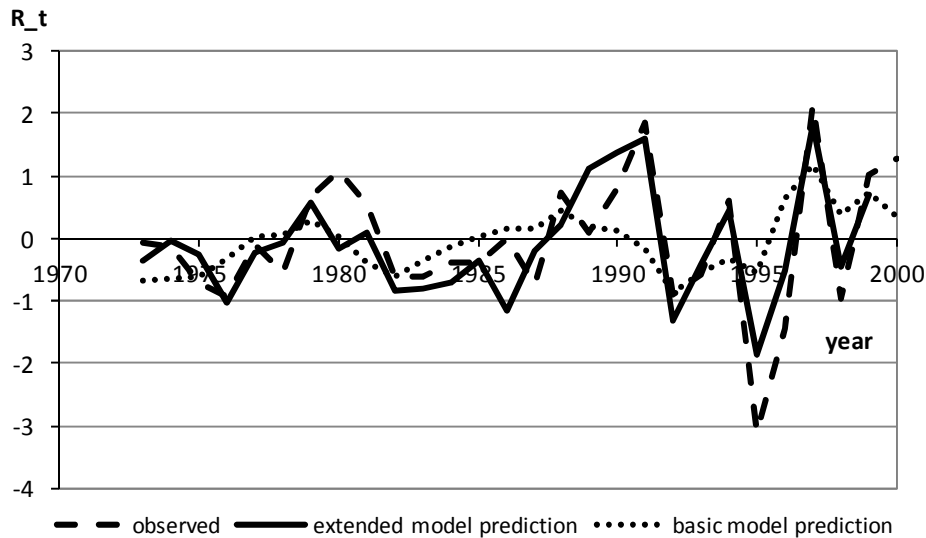


**Figure 2.**  $R_t$  values calculated from the observed data as well as the estimated  $R_t$  values of the basic ( $R^2 = 0.22$ ,  $p > 0.1$  nonsignificant) and the extended model ( $R^2 = 0.69$ ,  $p < 0.001$ , highly significant)

The extended model fits much better which clearly indicates the need of including climatic indicators in the population dynamical model derived by endogenous and exogenous factors, only.

In *Fig. 3* we can observe that in two years the observed values were overestimated by the model. In the remaining years, however, the estimations generated quite low errors.



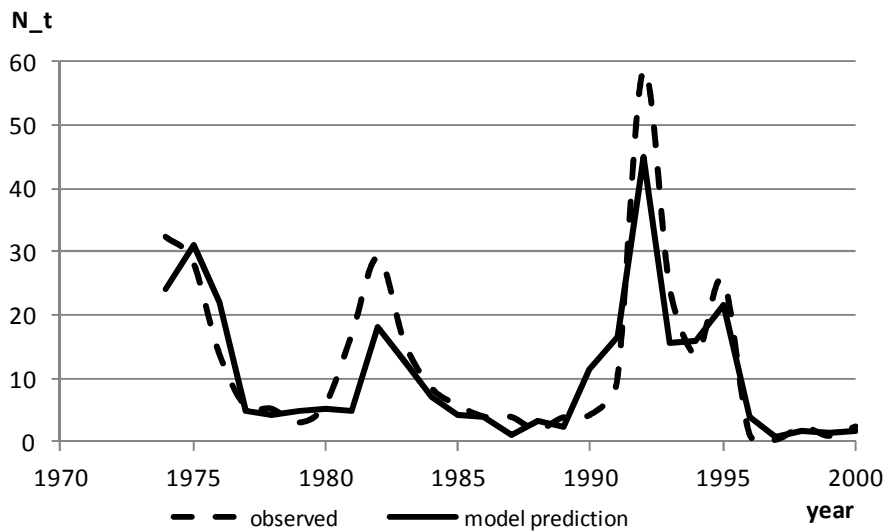


**Figure 3.**  $N_t$  values calculated from the observed data as well as the estimated  $N_t$  values of model extended by five climatic indicators

In Fig. 4 we can see the probability density of the model estimated  $N_t$  values earned by running the extended model with RegCM3.1 daily climatic parameter outputs regarded the reference period 1961-1990 as well as the future predictions for the time intervals 2021-2050 and 2071-2100 (bars) together with their fitted Beta distributions.

We fitted the Beta distributions with fixed minimum and maximum parameters ( $a=0$  and  $b=55$ ) in order to ensure the comparability of the fitted functions. The  $p$  and  $q$  parameters and the result of fitting together with the descriptive statistics of the model outputs can be found in Table 4.

**Table 4.** The  $p$  and  $q$  parameters of the Beta distribution with  $a=0$  and  $b=55$  and the result of distribution fitting together with the descriptive statistics of the model outputs min, max, mean, standard deviation and coefficient of variation (CV) for three time intervals 1961-1990 (as the reference), 2021-2050 and 2071-2100.

	1961-1990	2021-2050	2071-2100
$p$	0.98	0.93	0.60
$q$	9.10	9.43	1.97
Chi-square	1.72	1.00	5.55
Significance level	0.89	0.96	0.35
MIN	0.22	0.16	0.20
MAX	18.93	21.89	54.02
MEAN	5.35	4.92	10.58
St. dev.	5.06	5.10	12.16
CV	0.95	1.04	1.15

Comparing the model predictions of three time intervals 1961-1990 (as the reference), 2021-2050 and 2071-2100 by one-way ANOVA with difference contrast we can state that the intervals 1961-1990 and 2021-2050 do not differ from each other significantly ( $p=0.735$ ). The time scale 2071-2100, however is different from the first two intervals significantly ( $p<0.05$ ).

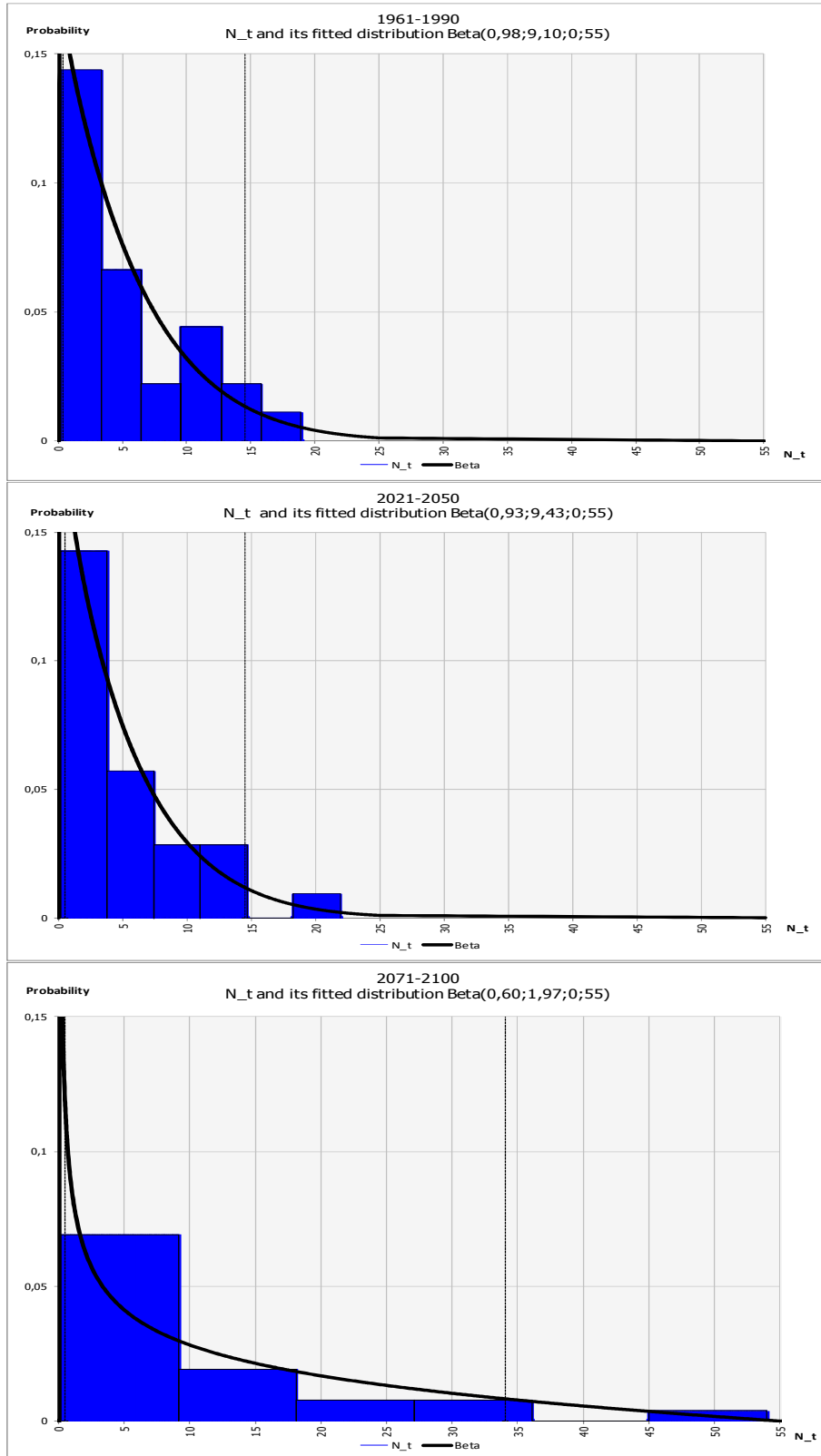


**Figure 4.** Probability density of the model estimated  $N_t$  values earned by running the extended model with RegCM3.1 daily climatic parameter outputs regarded the reference period 1961-1990 as well as the future predictions for the time intervals 2021-2050 and 2071-2100 (bars). The lines are for the estimated Beta distributions

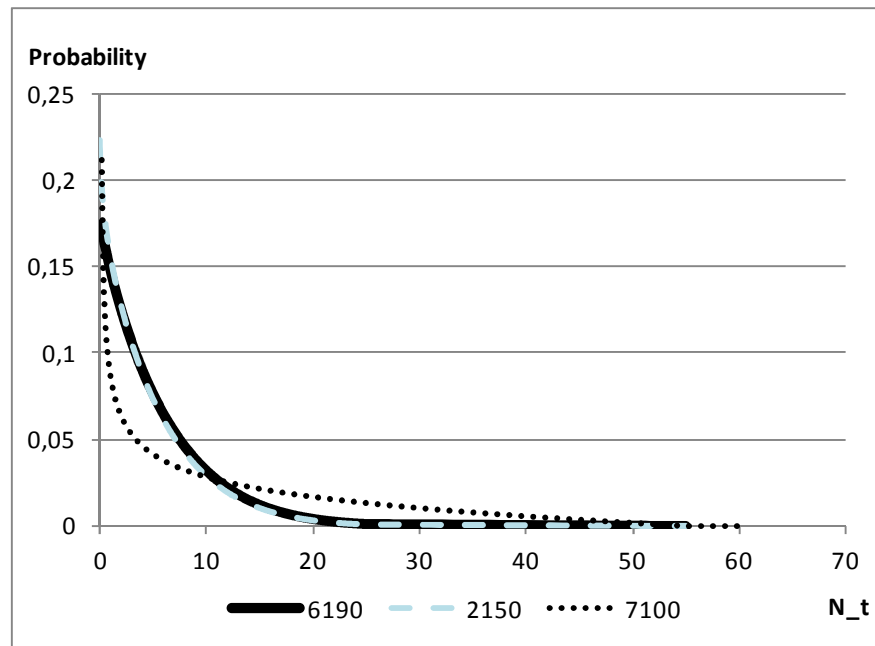


**Figure 5.** The Beta distributions fitted to the extended model predictions run by the RegCM3.1 outputs regarded the reference period 1961-1990 as well as the future time intervals 2021-2050 and 2071-2100.

In Fig. 4 we can see that the probability density functions of the time intervals 1961-1990 and 2021-2050 are very similar. Up to the end of the 21<sup>st</sup> century, however, we can expect some years with a great number of swarming *Operophtera brumata*, L. which can be detected on the probability density function of time interval 2071-2100 shifted to the right. The mean, the maximum and the standard deviation of the results of this late time scale are also much higher than the ones of the earlier time intervals (Table 4). The same can be observed in Fig. 5 in which we can see the fitted Beta distributions. The probability of low number of swarming *Operophtera brumata*, L. is expected to decrease while the one of high-peaked swarming is increasing. It means that we can expect that with the better and better the climatic conditions of swarming of these insects can result a definitely increasing risk of damages as well.

We note that in order to avoid the aggregation of the errors of the two models (the extended population dynamical model and the RegCM3.1 regional climate model) we stressed the expected changes with their direction and magnitude. If we make conclusions based on the differences of the model outputs, than the effect of the systematic model errors are minimal.

**Acknowledgements.** We express our gratitude to professor Zoltán Mészáros D.Sc. for his useful advices. This work was supported by the research project of the National Development Agency TÁMOP 4.2.1/B-09/1/KMR-2010-0005.

## REFERENCES

- [1] Bale, J., Masters, G., Hodkinson, I., Awmack, C., Bezemer, T., Brown, V., Butterfield, J., Buse, A., Coulson, J., Farrar, J., others (2002): Herbivory in global climate change research: direct effects of rising temperature on insect herbivores. – Glob. Chang. Biol. 8: 1-16.

- [2] Bartholy, J., Pngrác, R., Torma, Cs., Pieczka, I., Kardos, P., Hunyady, A. (2009): Analysis of regional climate change modelling experiments for the Carpathian basin. – *International Journal of Global Warming* 1(1-2-3): 238-252.
- [3] Berryman, A.A. (1999): Principles of population dynamics and their application. – Stanley Thornes Publishers, Cheltenham (distributed by Taylor & Francis, London)
- [4] Cammell, M., Knight, J. (1992): Effects of climatic change on the population dynamics of crop pests. – *Adv. Ecol. Res.* 22: 117-162.
- [5] Chinery, M.: Collins Guide to the Insects of Britain and Western Europe, 1986. (Reprinted 1991)
- [6] Diós, N., Szenteleki, K., Ferenczy, A., Petrányi, G., Hufnagel, L. (2009): A Climate profile indicator based comparative analysis of climate change scenarios with regard to maize (*Zea mays* L.) cultures. – *Applied Ecology and Environmental Research* 7(3): 199-214.
- [7] Drégelyi-Kiss, Á., Drégelyi-Kiss, G., Hufnagel, L. (2008): Ecosystems As Climate Controllers – Biotic Feedbacks. – *Applied Ecology And Environmental Research* 6(2): 111-134.
- [8] Drégelyi-Kiss, Á., Hufnagel, L. (2009): Simulations Of Theoretical Ecosystem Growth Model (Tegm) During arious Climate Conditions. – *Applied Ecology And Environmental Research* 7(1): 71-78.
- [9] Estay, S.A., Lima, M., Labra, F.A. (2009): Predicting insect pest status under climate change scenarios: combining experimental data and population dynamics modelling. – *J. Appl. Entomol.* 133: 491-499.
- [10] Gilpin, M.E., Ayala, F.J. (1973): Global models of growth and competition. – *Proc. Natl. Acad. Sci. USA* 70: 3590-3593.
- [11] Gimesi, L., Hufnagel, L. (2010): The possibilities of biodiversity monitoring based on Hungarian light trap networks I. – *Applied Ecology and Environmental Research* 8(3): 223-239.
- [12] Giorgi, F., Marinucci, M.R., Bates, G.T. (1993): Development of a second generation regional climate model (RegCM2): Boundary layer and radiative transfer processes. – *Mon. Wea. Rev.* 121: 2794-2813.
- [13] Heuvelink, G.B.M., Webster, R. (2001): Modelling soil variation: past, present, and future. – *Geoderma* 100: 269-301.
- [14] IPCC (2007): Fourth Assessment Report of the Intergovernmental Panel on Climate Change. ([http://www.ipcc.ch/publications\\_and\\_data/publications\\_ipcc\\_fourth\\_assessment\\_report\\_synthesis\\_report.htm](http://www.ipcc.ch/publications_and_data/publications_ipcc_fourth_assessment_report_synthesis_report.htm))
- [15] Merrill, R., Gutie´rrez, D., Lewis, O., Gutie´rrez, J., Diez, S., Wilson, R., (2008): Combined effects of climate and biotic interactions on the elevational range of a phytophagous insect. – *J. Anim. Ecol.* 77: 145-155.
- [16] Moon, Y., Kim, J. (2007): Efficient moving average transform-based subsequence matching algorithms in time-series databases. – *Information Sciences* 177: 5415-5431.
- [17] Musolin, D. (2007): Insects in a warmer world: ecological, physiological and life-history responses of true bugs (Heteroptera) to climate change. – *Glob. Chang. Biol.* 13: 1565-1585.
- [18] Nelder, J.A. (1961): The fitting of a generalization of the logistic curve. – *Biometrics* 17: 89-110.
- [19] Nowinszky, L., Puskás, J. (1998): Light trapping of winter moth (*Operophtera brumata* L.) at the time of weather fronts. – *Berzsenyi Dániel College, Scientific Papers* 2: 45-51.
- [20] Olfert, O., Weiss, R. (2006): Impact of climate change on potential distributions and relative abundances of *Oulema melanopus*, *Meligethes viridescens* and *Ceutorhynchus obstrictus* in Canada. – *Agric. Ecosyst. Environ.* 113: 295-301.
- [21] Parmesan, C. (2007): Influences of species, latitudes and methodologies on estimates of phenological response to global warming. – *Glob. Chang. Biol.* 13: 1860-1872.

- [22] Porter, J.H., Parry, M.L., Carter, T.R. (1991): The potential effects of climatic change on agricultural insect pest. – *Agric. For. Meteorol.* 57: 221-240.
- [23] Richards, F.J. (1959): A flexible growth function for empirical use. – *J. Exp Bot* 10: 290-300.
- [24] Ricker, W.E. (1954): Stock and recruitment. – *J. Fish. Res. Board Can.* 115: 559-623.
- [25] Robert, D, Childs, Amherst, M.A., Deborah, C., Swanson, Hanson, M.A.: The Winter Moth (*Operophtera brumata* (L.)) – *Umass Extension* 2009: 1-5.
- [26] Royama, T. (1992): *Analytical Population Dynamics*. – Chapman & Hall, New York, 371 p.
- [27] Schwarz, G. (1978): Estimating the dimension of a model. – *Ann. Stat.* 6: 461-464.
- [28] Schwerdtfeger, F. (1969): *Ökologie der Tiere-Demökologie*. – Paul Parey. Hamburg-Berlin.
- [29] Sipkay, Cs., Horváth, L., Nosek, J., Oertel, N., Vadadi-Fülöp, Cs., Farkas, E., Drégelyi-Kiss, Á., Hufnagel, L. (2008): Analysis Of Climate Change Scenarios Based On Modelling Of The Seasonal Dynamics Of A Danubian Copepod Species. – *Applied Ecology And Environmental Research* 6(4): 101-109.
- [30] Sipkay, Cs., Kiss, K.T., Vadadi-Fülöp, Cs., Hufnagel, L. (2009): Trends In Research On The Possible Effects Of Climate Change Concerning Aquatic Ecosystems With Special Emphasis On The Modelling Approach. – *Applied Ecology And Environmental Research* 7(2): 171-198.
- [31] Szontagh, P. (1980): Gradationverhältnisse der eichenschädlicher Geometriden Arten in Ungarn. – *Prace Muzea V, Hradecy Kralove.* 257-259.
- [32] Torma, Cs., Bartholy, J., Pongrácz, R., Barcza, Z., Coppola, E., Giorgi, F. (2008): Adaptation and validation of the RegCM3 climate model for the Carpathian Basin. – *Időjárás* 112(3-4): 233-247.
- [33] Turkheimer, Hinz, Cunningham (2003): On the undecidability among kinetic models: from model selection to model averaging. – *Journal of Cerebral Blood Flow & Metabolism* 23: 490-498.
- [34] Verhulst, P.F. (1838): Notice sur la loi que la population suit dans son accroissement. – *Correspondance Math. Phys.* 10: 113-121.
- [35] Weise, T. (2009): *Global Optimization Algorithms – Theory and Application* – <http://www.it-weise.de/projects/book.pdf>
- [36] Woiwod, I. (1997): Detecting the effects of climate change on Lepidoptera. – *J. Insect Conserv.* 1: 149-158.